CRACK SPACING, CRACK WIDTH AND TENSION STIFFENING EFFECT IN REINFORCED CONCRETE BEAMS AND ONE-WAY SLABS

A thesis submitted in fulfilment of the requirement for
the award of the degree of

Doctor of Philosophy

by

RATNAMUDIGEDARA PIYASENA

B.Sc. (Hons), M.Eng. (Structures), MIEAust

from

School of Engineering
Faculty of Engineering and Information Technology

GRIFFITH UNIVERSITY
GOLD COAST CAMPUS

November 2002

To

Kusum, Anjula and Shilani

for their understanding during the course of this research

DECLARATION

This work has not previously been submitted for a degree or diploma in any university. To the best of my knowledge and belief, the thesis contains no material previously published or written by another person except where due reference is made in the thesis itself.

Ratnamudigedara Piyasena

November 2002

ACKNOWLEDGEMENTS

The author expresses his deepest gratitude and acknowledges his heartfelt indebtedness to his supervisor, Professor Yew-Chaye Loo, Foundation Professor and Head of the School of Engineering, Griffith University, for having provided this research opportunity and for his continuous guidance and encouragement and suggestions throughout the course of the research.

Special gratitude and thanks are due to the author's co-supervisor of the research program, Dr. Sam Fragomeni, Senior Lecturer at the Griffith University, for making available his valuable time to go through the draft thesis thoroughly and making numerous suggestions to enhance the quality of the thesis. The author acknowledges that timely completion of this thesis would not have been possible without Dr. Fragomeni's assistance.

Financial support provided by Griffith University in the form of a Postgraduate Research Scholarship is gratefully acknowledged.

Last, but by no means the least, the author is deeply indebted to his wife, Kusum and two children, Anjula and Shilani, to whom this thesis is dedicated, for their understanding, continuous support and encouragement throughout the course of this research.

LIST OF PUBLICATIONS

During the course of this research work, the following papers have been published or submitted for publications.

1. **Piyasena, R.,** Loo, Y.C. and Fragomeni, S. (2003), *Factors Affecting Spacing and Width of Cracks and New Prediction Formulas*, Accepted for publication in Advances in Structural Engineering – An International Journal.

2. **Piyasena, R.,** Loo, Y.C. and Fragomeni, S. (2003), *Determination of Crack Spacing and Crack Width in Reinforced Concrete Beams*, Structural Engineering and Mechanics- An International Journal, Vol. 15, No. 2, pp 159-180.

3. **Piyasena, R.,** Loo, Y.C. and Fragomeni, S. (2002), *Tension Stiffening Effects in Deflection of Reinforced Concrete Beams*, Proceedings, 17th Australasian Conference on the Mechanics of Structures and Materials (ACMSM17), Southport, Queensland, Australia, pp. 205 - 210.

4. Fragomeni, S., **Piyasena, R**. and Loo, Y. C. (1999), *Spacing and width of cracks in reinforced concrete,* Proceedings of the 16th Australasian Conference on the Mechanics of Structures & Materials, Sydney, Australia, pp 91-96.

5. **Piyasena, R** and Loo, Y.C. (1995), *Effective Moment of Inertia for reinforced Concrete Rectangular and Flanged Beams*, Proceedings of the Fifth East Asia-Pacific Conference on Structural Engineering and Construction (EASEC-5), Gold Coast, Queensland, Australia, Vol. 1, pp 531-536.

SYNOPSIS

An analytical method for determining the crack spacing and crack width in reinforced concrete beams and one-way slabs is presented in this thesis. The locations and the distribution of cracks developed in a loaded member are predicted using the calculated concrete stress distributions near flexural cracks. To determine the stresses, a concrete block bounded by top and bottom faces and two transverse sections of the beam is isolated and analysed by the finite element method. Two types of blocks are analysed. They are: (i) block adjacent to the first flexural crack, and (ii) block in between successive cracks.

The calculated concrete stress distribution adjacent to the first flexural crack is used to predict the locations of primary cracks (cracks formed at sections where the stresses have not been influenced by nearby cracks). The concrete stress distributions in between successive cracks, calculated for various crack spacings and load levels, are used to predict the formation of secondary cracks in between existing cracks.

The maximum, minimum and the average crack spacing at a given load level are determined using the particular crack spacing that would produce a concrete tensile stress equal to the flexural strength of concrete. The resulting crack width at reinforcement level is determined as the relative difference in elastic extensions of steel and surrounding concrete. The accuracy of the present method is verified by comparing the predicted spacing and width of cracks with those measured by others.

The analytical method presented in this thesis is subsequently used to investigate the effects of various variables on the spacing and width of cracks, and the results are presented. These

results are used to select the set of parameters that has the most significant effect. A parametric study is then carried out by re-calculating the spacing and width of cracks for the selected parameters. Based on the results of this parametric study, new formulas are developed for the prediction of spacing and width of cracks. The accuracy of these formulas is ascertained by comparing the predicted values and those measured by other investigators on various types of beams under different load levels.

The calculated stress distributions between successive cracks are also used to develop a new method of incorporating the tension stiffening effect in deflection calculation. First, curvature values at sections between adjacent cracks are determined under different load levels, using the concrete and steel stresses. These results are used to develop an empirical formula to determine the curvature at any section between adjacent cracks. To verify the accuracy of the new method, short-term deflections are calculated using the curvature values evaluated by the proposed formula for a number of beams, and the results are compared with those measured by others.

TABLE OF CONTENTS

4. EVALUATION OF CONCRETE AND STEEL STRESSES NEAR FLEXURAL CRACKS

5. CONCRETE AND STEEL STRESSES NEAR FLEXURAL CRACKS

6. CRACK SPACING AND CRACK WIDTH

7. FACTORS AFFECTING SPACING AND WIDTH OF CRACKS

8. TENSION STIFFENING EFFECT IN DEFLECTION CALCULATION

LIST OF FIGURES

LIST OF TABLES

LIST OF SYMBOLS

A_e	=	effective concrete stretched area
A_{sc}	=	area of compression reinforcement
A_{st}	=	area of tensile reinforcement
a , b, c,…, h	=	polynomial coefficients (Table 7.2)
a_{cr}	=	distance from bar surface to the point where crack width is calculated
b	=	beam width
b_{ef}	=	effective flange width
b_t	=	beam width at reinforcement level
b_w	=	web width
c	=	concrete cover
c_e	=	equivalent concrete cover
c'	=	c/ϕ ratio
d	=	effective depth
d_c	=	depth to compression steel
E_c	=	elastic modulus of concrete
E_{ci}	=	initial tangent modulus of concrete
$E_{c,o}$	=	initial elastic modulus of concrete at time = t_o
E_e	=	age-adjusted elastic modulus of concrete
E_s	=	elastic modulus of steel
E_t	=	gradient of descending branch of Fig. 2.8
e	=	$b/(m\phi)$
e'	=	modified value of e (Eq. 7.1)
e_{co}	=	extension of concrete where peak bond stress occurs
$e_{c,co}$	=	extension of concrete due to compressive force on cracked section
$e_{c,bo}$	=	extension of concrete due to bond force
e_{c1}	=	extension of concrete at the cracked section
e_{so}	=	extension of steel where the peak bond stress occurs
e_{s1}	=	extension of steel at the cracked section
F_b, F'_b	=	total bond force
F_{bx}	=	total bond forces at a distance x from zero-slip point
F_c, F_{c1}, F_{c2}	=	total compressive forces acting on a section
$F_{d,ef}$	=	effective design load per unit width
F_{SP}	=	modification factor for crack spacing
F_t	=	total tensile force acting on a section
F_v	=	transverse shear force
F_{WD}	=	modification factor for crack width
f_b	=	bond stress
f_{bo}, f'_{bo}	=	peak bond stresses
f_{b1}, f_{b2}	=	bond stresses (Fig. 3.8)
f_{bx}	=	bond stress at a distance x from the zero-slip point

f^*_b	=	bond stress determined from Eq. 3.1
f'_c	=	characteristic strength of concrete
f_r	=	flexural strength of concrete
f_{rc}	=	calculated value of flexural stress at the tension face
f_s	=	steel stress at a cracked section
f_{sc}	=	stress in compression steel
f_{sx}	=	steel stress at a distance x from zero-slip section
f_{s1}	=	steel stress at an uncracked section, steel stress at zero-slip point
f_{s2}, f_{s3}	=	steel stresses at cracked sections
f_t	=	concrete tensile stress
f'_t	=	tensile strength of concrete
f_y	=	yield strength of steel
h	=	total height of the member
h_c, h_{cr}	=	height of the crack
h_P, h_S	=	primary and secondary crack heights, respectively
I_{cr}	=	moment of inertia of the cracked section
I_e	=	effective moment of inertia
I_g	=	gross moment of inertia
K_1, K_2	=	coefficients (Eq. 2.6)
K^*	=	a coefficient (Eq. 2.17)
kd	=	depth of compressive stress block
k_cd	=	distance from neutral axis to the centroid of compressive stress block
k_td	=	distance from neutral axis to the centroid of tensile stress block
k_1, k_2	=	coefficients (Eq. 2.27)
L	=	span length
L_{ef}	=	effective span length
L_o	=	distance from the cracked section to zero slip point
l_c	=	critical crack spacing
l_f	=	final value of l_c when steel stress f_s = 400MPa
M	=	applied bending moment at the section
M_a	=	maximum bending moment at mid span
M_{cr}	=	cracking moment
M_s	=	maximum service moment
M_u	=	ultimate strength of the section
M_1, M_3	=	bending moment at the supports in a continuous beam
M_2	=	bending moment at mid span in a continuous beam
m	=	number of bars
n	=	modular ratio
p	=	total perimeter of steel bars divided by beam width
q_{bx}	=	shear force equivalent to bond force at a distance x from zero-slip point
R	=	L_o/d ratio

S	=	crack spacing
S_{ave}	=	average crack spacing
$S_{ave\text{-}pred}$	=	predicted average crack spacing
S_f	=	final value of crack spacing when f_s=400MPa
S_{max}	=	maximum crack spacing
S_{min}	=	minimum crack spacing
S_p	=	primary crack spacing
S_{pm}	=	minimum primary crack spacing
S_{px}	=	maximum primary crack spacing
S_x, S_y	=	distances from the cracked sections to zero slip point
S_o	=	slip length
s	=	bond slip
s_o, s'_o	=	local slips at the points where the peak bond stresses occur
s_1, s_2, s_3	=	slip values (Fig. 3.8)
s_b	=	centre-to-centre spacing between reinforcing bars
t	=	thickness of the concrete block at the level of reinforcement
t	=	time after loading
v	=	average shear stress
W_f	=	final value of W_t when steel stress f_s = 400MPa
W_{lim}	=	part of crack width controlled by crack height
$W_{max\text{-}pred}$	=	predicted maximum crack width
W_s	=	crack width at reinforcement level
$W_{s,ave}$	=	average crack width at reinforcement level
$W_{s,max}$	=	maximum crack width at the reinforcement level
W_t	=	crack width at tension face
$W_{t,ave}$	=	average crack width at the tension face
$W_{t,max}$	=	maximum crack width at tension face
W_o	=	part of crack width controlled by proximity of reinforcement
w_c	=	unit weight of concrete
x	=	depth of compression zone, distance from the nearest crack
y	=	distance from neutral axis to any point in compression zone
z	=	a coefficient (Eq. 2.12)
α	=	a coefficient (Fig. 2.8)
β	=	coefficients (Eq. 2.15 and 2.19)
Δf_{so}	=	steel stress increment due to the formation of a primary crack
δ	=	deflection
$(\delta_{xi})_j$	=	concrete extension at node i due to load case j
ε	=	concrete strain
ε’	=	cracking strain in concrete

ε_c, ε_{c1}	=	concrete strain in the extreme compression fibre
ε_{c2}	=	concrete strain in the tension face of the member
ε_s	=	steel strain
$\varepsilon_{s,ave}$	=	average steel strain
ϕ	=	bar diameter
ϕ_c	=	creep coefficient
ϕ_1, ϕ_2, ϕ_3	=	coefficients (Eq. 2.5)
γ	=	reduction factor for bond stress (Eq. 3.2)
κ	=	curvature
κ_c	=	increase in curvature due to creep
κ_i	=	initial curvature
κ_L, κ_M, κ_R	=	curvature at left support, mid-span and right support, respectively
κ_{sc}	=	increase in curvature due to shrinkage
κ_1	=	curvature at zero-slip section
κ_2, κ_3	=	curvature at cracked sections
λ	=	a parameter (Fig. 7.1)
ρ	=	tension reinforcement ratio
ρ_m, ρ_{mod}	=	modified reinforcement ratios (Eq. 2.4 and 5.4)
ρ_{te}	=	reinforcement ratio based on effective area of tensile concrete
ρ'	=	compression reinforcement ratio
σ	=	concrete stress
$(\sigma_{xi})_j$	=	concrete stress at node *i* due to load case *j*
τ	=	a parameter (Eq. 2.1)
ψ, ν	=	coefficients (Eq. 2.13)
μ	=	long-time deflection multiplier
ζ	=	a coefficient (Eq. 2.22)
χ	=	aging coefficient

CHAPTER 1

INTRODUCTION

1.1 General Remarks

Cracking in reinforced concrete structures is unavoidable due to the low tensile strength of concrete. Wider cracks may not only destroy the aesthetics of the structure, but also expose steel reinforcement to the environment leading to corrosion. To control the crack width at the member surface, designers may use the guidelines prescribed in various building codes. These guidelines are based on certain crack width prediction formulas developed by various researchers.

Inspection of crack width prediction procedures proposed by various investigators indicates that each formula contains a different set of variables. A literature review also suggests that there is no general agreement among various investigators on the relative significance of different variables affecting the crack width, despite the large number of experimental work carried out during the past few decades. This is at least partly due to the differences in the variables incorporated by different investigators in their experimental work. Taking all the parameters in to account in a single experimental program is not normally feasible due to the large number of variables involved, and the interdependency of some of the variables. Analytical methods, on the other hand, can incorporate most of the variables without much difficulty. However, a literature search reveals that different investigators have concentrated on different sets of parameters in their calculation, to simplify the complex phenomenon of cracking in reinforced concrete. A major focus in this research is to incorporate as many parameters as possible in an analytical investigation.

Cracking in a reinforced concrete member also causes a significant increase in deflection. This is a result of the reduction of bending stiffness at cracked sections when the effect of tensile concrete below the neutral axis diminishes. However, at sections between successive cracks, some tensile stress is retained in the concrete around steel bars due to the action of bond, contributing to the bending stiffness of the member. This is called the "tension stiffening" effect. If the tension stiffening effect is neglected, the calculated defection may be overestimated by a large proportion. In simplified methods of deflection calculation, the tension stiffening effect is incorporated in a semi-empirical manner by using the effective moment of inertia method. In analytical methods, the deflection is calculated using the curvature values, evaluated by adopting a non-linear stress-strain relationship for tensile concrete. This relationship allows the concrete to retain some tensile stress beyond the cracking strain. In this thesis, a new method is developed to evaluate the curvature values at sections between successive cracks by incorporating the bond force acting around steel bars in the calculation, instead of the concrete tensile force.

1.2 Objectives and Scope

In the first part of this thesis, an analytical method is developed to determine the concrete stress distribution near flexural cracks in reinforced concrete beams and one-way slabs. To calculate the stresses, a concrete block between two transverse sections is analysed using the finite element method. Forces acting on transverse sections of the block are determined using the equilibrium conditions, while the bond forces are calculated based on the bond slip, using a bond stress-bond slip relationship available in literature.

The maximum, minimum and average crack spacing at a given load level are determined based on the particular spacing that would produce a concrete tensile stress equal to the flexural strength. The resulting crack width is evaluated as the relative difference in elastic extensions of steel and surrounding concrete. The accuracy of the present analytical procedure is verified by comparing the computed spacing and width of cracks with those measured by other investigators.

In the second part of the thesis, the analytical method developed in the first part is used to investigate the effects of various variables on the spacing and width of cracks. For this investigation, crack spacing and crack width are calculated for various members having different material and sectional properties. Based on the results of this investigation, the set of parameters that has the most significant effect on the spacing and width of cracks is selected. A parametric study is then carried out by re-calculating the spacing and width of cracks for different values of the selected parameters. Results of this parametric study are subsequently used to develop simplified formulas for predicting the spacing and width of cracks. The accuracy of the new formulas is verified by comparing the predicted spacing and width of cracks with those measured by other investigators.

In the final part of the thesis, a new method is developed to incorporate the tension stiffening effect in the calculation of deflections of beams and one-way slabs. In this method, the curvature values at sections between adjacent cracks are determined using an empirical formula. This formula is developed using a large number of curvature values calculated from the concrete and steel strains at various sections between adjacent cracks for a number of beams. The present method of incorporating the tension stiffening effect is verified by comparing calculated short-term deflections and those measured by other investigators.

1.3 Layout of the Thesis

Following this introduction chapter, Chapter 2 provides a review of literature on investigations carried out by various researchers aiming to develop crack width prediction procedures together with the different variables incorporated. It also includes a review on different analytical methods used to calculate the concrete stress distribution near flexural cracks. The second part of Chapter 2 provides a literature review on various procedures developed for incorporating the tension stiffening effect in deflection calculation.

Crack spacing, crack width and the tension stiffening effect are greatly influenced and governed by the bond force acting at the interface of steel bars and surrounding concrete. The bond stress can be determined by calculating the associated bond slip and

using a bond stress-bond slip relationship. Chapter 3 describes various methods used by different investigators to measure the bond stress and bond slip, and presents the resulting bond stress-bond slip relationships. Justification of the particular bond stress-bond slip relationship used in this thesis is also described in Chapter 3.

Chapter 4 describes the analytical procedure used to determine the stresses and strains in a concrete block located between two transverse sections of a loaded member. Methods of calculating the forces acting on the two transverse sections, and the bond force acting at reinforcement level are described in detail. Also included are the description of the finite element analytical procedure and different types of concrete blocks considered in the analysis.

Chapter 5 presents the results of calculated concrete stress distribution near flexural cracks in a series of typical beams and one-way slabs. Results are presented for two categories. They are: (*i*) the stress distribution near the first flexural crack, and (*ii*) the stress distribution between adjacent cracks. The effect of load intensity and spacing of adjacent cracks on the maximum concrete tensile stress is also discussed.

The concrete stress distributions presented in Chapter 5 will be utilised in Chapter 6 to predict the locations and width of cracks in a member subjected to a gradually increasing load. Using this prediction procedure, the spacing and width of cracks are calculated and the results are compared with the experimental measurements for a large number of beams and one-way slabs tested by others.

In Chapter 7, the effects of various variables on the spacing and width of cracks are investigated and the results are presented. These results are used to select the particular set of parameters that has the most significant effect. A parametric study is then carried out by re-calculating the spacing and width of cracks for various values of the selected parameters. Based on the results of this parametric study, simplified formulas are developed for the prediction of spacing and width of flexural cracks in beams and on-way slabs. The accuracy of these formulas is verified by comparing the predicted spacing and width of cracks with those measured by other investigators.

Chapter 8 describes the procedure of evaluating the curvature at sections between adjacent cracks, using the calculated concrete and steel strains. An empirical formula is then developed to determine the curvature at any section between cracks. Using the curvature values evaluated by the proposed formula, the short-term deflections are determined for a number of beams and one-way slabs, and the results are compared with those measured by others.

Finally, Chapter 9 summarises the outcomes of this research. It also contains conclusions and makes recommendations for further research.

CHAPTER 2

LITERATURE REVIEW

2.1 General Remarks

This Chapter reviews the most relevant literature on cracking and tension stiffening effect of reinforced concrete flexural members. The first part deals with previous research aiming to develop crack spacing and crack width prediction procedures and their outcomes. Current methods used for controlling crack width in reinforced concrete structures are also included. Literature on various deflection calculation procedures, together with methods of incorporating the tension stiffening effect are discussed later in the Chapter. Current design methods used for controlling deflections in reinforced concrete members are also briefly discussed. Only literature relevant to beams and one-way slabs are included, as two-way slabs are outside the scope of this thesis.

2.2 Cracking in Reinforced Concrete

Cracking in concrete is unavoidable due to its low tensile strength and low extensibility. Reinforced concrete structures having low steel stresses under service loads undergo very limited cracking, except for the cracks that occur due to shrinkage of concrete and temperature changes. However, in cases where service loads cause high steel stresses, particularly when using high-strength steel, some visible cracking may be expected under service loads. If these cracks are too wide they destroy the aesthetics of the structure and may provoke adverse criticism. They also may result in steel reinforcement being exposed to the environment causing corrosion of steel. To minimise these adverse effects, the design of reinforced concrete structures must ensure

that the crack widths under normal service conditions are maintained within acceptable limits. In addition to the aesthetic concerns and possible corrosion of reinforcement, cracking of a reinforced concrete member will cause a significant reduction in the bending stiffness. Therefore, in assessing the deflection of reinforced concrete members, it is necessary to incorporate the effect of cracking in the calculation.

2.2.1 Allowable crack widths in reinforced concrete

The maximum crack width that may be considered not to impair the appearance of a structure depends on various factors including the position, length, and surface texture of the crack as well as the illumination in the surrounding area. According to Park & Paulay (1975), crack widths in the range 0.25 mm to 0.38 mm may be acceptable for aesthetic reasons.

Crack width that will not endanger the corrosion of steel reinforcement depends on the environment surrounding the structure. Table 2.1 shows the maximum allowable crack widths recommended by ACI Committee 224 (1972) for the protection of reinforcement against corrosion. These values are taken as the basis for the development of rules prescribed in ACI 318 (1995) for the distribution of tension steel to limit the crack width.

Table 2.1 Maximum allowable crack widths (ACI Committee 224 (1972))

Exposure condition	Maximum allowable crack width (mm)
Dry air or protective membrane	0.4
Humid, moist air or soil	0.3
De-icing chemicals	0.2
Seawater and seawater spray; wetting and drying	0.15
Water retaining structures	0.1

2.2.2 Causes of cracking

Cracks formed in reinforced concrete members can be classified into two main categories, namely cracks caused by externally applied loads, and those which occur independently of the loads (Leonhardt (1977), Base (1978)). Flexural cracks and inclined shear cracks are the two main types of cracks caused by external loads (Fig. 2.1). Flexural cracks are formed in the tensile zone of the member and have a wedge shape, with the maximum crack width at the tension face and zero width near the neutral axis. Inclined shear cracks usually develop in thin-web beams when subjected to high shear forces (Warner *et al* (1998), Loo (1990)). As this thesis concentrates on flexural cracking in reinforced concrete members, inclined shear cracks are not discussed in this Chapter.

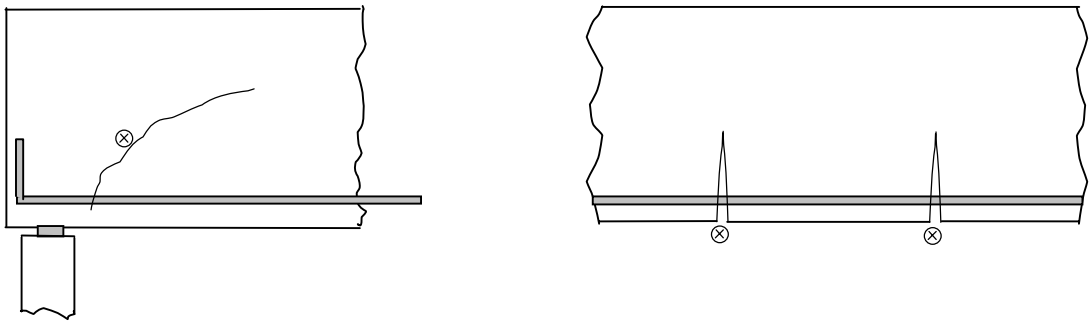

(*a*) inclined shear cracks (*b*) flexural cracks

Note: ⊗ indicates the location of crack initiation

Fig. 2.1 Inclined shear cracks and flexural cracks

Internal micro-cracks fall into the other type of cracks caused by external load. These cracks occur as a result of high concrete stresses near the ribs in deformed bars, and are confined in the immediate neighbourhood of reinforcement without appearing on the concrete surface. These micro-cracks are considered to be part of the bond mechanism and are discussed in the next Chapter.

Cracks developed in restrained members due to concrete shrinkage or temperature change fall into the second category of cracks, which are independent of applied loads. In thin restrained members such as floor slabs these cracks may extend through the entire cross section, usually having an approximately uniform width (Warner *et. al* (1998)). If the width of these cracks is not properly controlled, they may disrupt the integrity of the structure and reduce the bending stiffness considerably resulting in large deflections.

2.2.3 Spacing and width of flexural cracks

Flexural cracks begin to occur when concrete stress in the tension face of a member reaches the flexural strength of concrete. After formation of a crack some elastic recovery takes place in concrete on the member surface, contributing to the crack width. However, some stress and strain is maintained in concrete surrounding the reinforcement due to the action of bond. This contributes to a reduction in the crack width near the bar compared to that at the tension face (Husain & Ferguson (1968), Base *et al*. (1966), (Goto (1971)).

Flexural cracks in a varying moment region of a beam develop at a regular interval; however, in a constant moment region, these cracks develop at discrete intervals. Their locations depend partly on the occurrence and distribution of zones of local weakness in concrete, and therefore cracking is somewhat a random process (Warner *et. al* (1998), Fantilli *et al*. (1998)). As a result, the exact locations of cracks in a constant moment region may not be predicted accurately. However, maximum and minimum spacing of adjacent cracks and the resulting maximum crack width may be predicted with sufficient accuracy by investigating concrete stresses developed in the tensile zone of a member.

2.2.4 Predicting spacing and width of flexural cracks

The development of crack spacing and crack width prediction formulas is usually based on calculated concrete stress distributions within the tensile zone of a member. Different investigators have used various simplified analytical procedures to determine the concrete tensile stress. While some analytical investigations are coupled with

experimental works to verify the new prediction formulas, there are some investigations totally based on test results.

In most investigations, a uniaxial tension member has been used to simulate the conditions around steel bars in the constant moment region of a member. In experimental investigations, a concrete prism with a steel bar embedded along its axis is subjected to a tensile force applied to the two protruding ends of the bar. The resulting tensile cracks are considered to represent flexural cracks in a constant moment region of a beam. In analytical investigations the axial tensile stress distribution, developed in the concrete prism resulting from the bond force transferred from the steel bar, is calculated. This stress distribution is then used to predict the formation of new cracks in between existing cracks. Important aspects of these investigations and the resulting prediction formulas are discussed below.

2.2.4.1 Analytical investigations

(a) Chi & Kirstein method

Cylindrical uniaxial tension members were analysed by Chi & Kirstein (1958) to determine the concrete tensile stresses within the member. The bond force acting around the steel bar was assumed to vary linearly from zero at the mid point of the specimen to the full bond stress at ends. The resulting maximum tensile stress at the mid section was calculated by considering the equilibrium of half-length of the cylinder using elastic analysis. The average crack spacing was taken as the length of the cylinder that produces a concrete tensile stress equal to the tensile strength of concrete. The resulting average crack width was calculated as the extension of steel bar between the two ends of the member, neglecting the concrete extension.

The calculated spacing and width of cracks were found to depend on the diameter of concrete cylinder analysed. A cylinder diameter of 4 times the bar diameter was used in the development of the following prediction formulas.

$$S_{min} = 5\tau\phi \qquad (2.1a)$$

$$W_{s,ave} = \frac{5\tau\phi}{E_s}\left(f_s - \frac{438}{\tau\phi}\right) \qquad (2.1b)$$

where S_{min} = minimum crack spacing (*mm*); $W_{s,ave}$ = average crack width at the level of reinforcement (*mm*), E_s = elastic modulus of steel (*MPa*); f_s = stress in the steel bar (*MPa*); and ϕ = bar diameter (*mm*). In the above equation the coefficient τ relates to the ratio of the assumed effective concrete area in tension to the area of a single bar, which was found to vary between 0.786 and 1 for the 16 members analysed.

(b) Broms method

A slightly different approach was used by Broms (1965*a*) to calculate the tensile stresses developed in concrete due to bond forces. The concrete block between adjacent cracks in a constant moment region of a loaded beam was isolated and the bond force was applied on the two ends of the block. These forces were applied, at the reinforcement level, as surface line loads uniformly distributed across the width of the beam. The magnitude of the bond force was arbitrarily assumed to be one half of the total tensile force carried by reinforcement at the cracked section. Results of the elastic analysis have shown that high longitudinal tensile stresses are developed in the concrete within a circle inscribed between the two adjacent flexural cracks, with its centre located at reinforcement level (see Fig. 2.2).

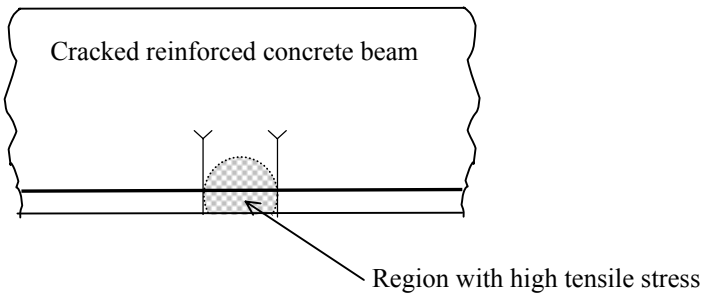

Fig. 2.2 Results of Broms analysis (1965*a*)

Although Raab (1966) has questioned the validity of the assumptions made in the above analysis, Broms (1965*b*) used these findings to argue that a new crack will be formed at

mid way between adjacent cracks only if the crack spacing is larger than twice the concrete cover measured from the centre of the steel bar. This argument was used to predict the maximum crack spacing S_{max} as twice the concrete cover (S_{max}=2c) in a beam reinforced with a single bar. The minimum crack spacing S_{min} was taken to be half the maximum value, which is equal to the concrete cover (S_{min}=c). The theoretical average crack spacing S_{ave} was then predicted as 1.5 times the concrete cover (S_{ave}=1.5c).

However, results of 10 beams tested by Broms (1965*a*) have shown that the average crack spacing was closer to twice the concrete cover (S_{ave}=2c), instead of 1.5c, for steel stresses ranging from 140 to 205 *MPa*. This value of the average crack spacing (S_{ave}=2c) was multiplied by the average strain in steel bar $\varepsilon_{s,ave}$ to predict the average crack width. Thus, for steel stresses ranging from 140 to 205 *MPa* the average crack width at the tension face of members reinforced with a single bar was expressed as

$$W_{t,ave} = 2c\varepsilon_{s,ave} \qquad (2.2)$$

where $W_{t,ave}$ = average crack width at the tension face.

(c) Broms & Lutz method

To investigate the applicability of above findings to members with multiple bars, Broms & Lutz (1965) carried out uniaxial tensile tests on seven concrete specimens reinforced with four steel bars symmetrically placed within the cross section (see Fig. 2.3). Test results have shown that the relationships derived for members with a single bar are also applicable to members with multiple bars if the concrete cover c in Eq. 2.2 is replaced by an equivalent concrete cover c_e. The equivalent concrete cover is related to the distance between adjacent bars and the concrete cover. Assuming that the maximum crack width is twice the average crack width, the following equation was proposed to calculate the maximum crack width for steel stresses from 140 to 205 *MPa*.

$$W_{t,max} = 4c_e\varepsilon_{s,ave} \qquad (2.3)$$

where $W_{t,max}$ = maximum crack width at the tension face.

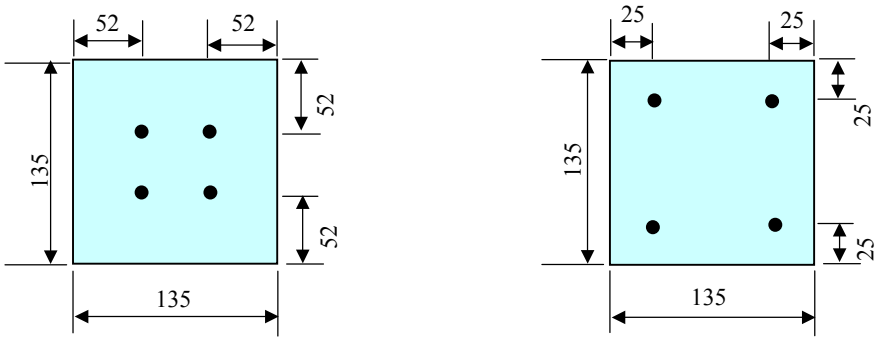

(i) Specimen Type T-RC10 *(ii) Specimen Type T-RC11*

Note: all dimensions are in millimetres

Fig. 2.3 Cross sectional details of tension specimens tested by Broms & Lutz (1965)

(d) Venkateswarlu & Gesund method

Venkateswarlu & Gesund (1972) analysed the portion of a beam between two successive cracks using a two-dimensional finite element method to evaluate the effects of bond force (see Fig. 2.4). Bond force was applied to the concrete block as shear forces at reinforcement level. Three different values have been used for the magnitude of the total bond force, namely 0.1, 0.3 and 0.5 of the total tensile force in reinforcement at the cracked section. Linear, parabolic and sinusoidal bond stress distributions were used in the analysis, with zero bond stress at the mid section and the maximum stress at the cracked sections as shown in Fig. 2.4. Five values were used for the ratio of overall height of the beam to the crack spacing ranging from 1.6 to 7.0.

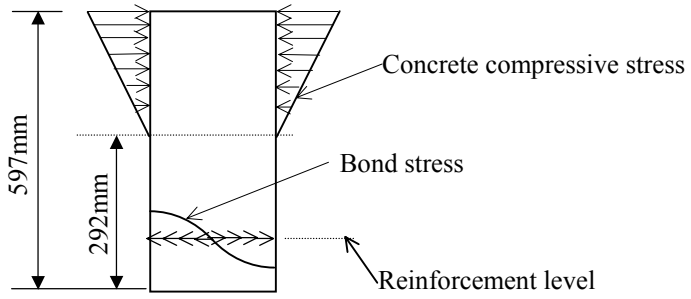

Fig. 2.4 Concrete block analysed by Venkateswarlu & Gesund (1972)

Results have shown that the maximum concrete tensile stress across any section between the cracks occurs at reinforcement level. This maximum stress varied along the length of the bar, with the peak value occurring at the mid-section between the two cracks. Maximum crack spacing was evaluated by comparing the calculated maximum tensile stress and tensile strength of concrete. The maximum crack width at reinforcement level was calculated as the relative difference in extensions of steel and concrete for the length between the two cracks.

Both crack spacing and crack width were first expressed in terms of an unknown parameter called the slip modulus, which relates to the variation of bond stress with slip. The value of slip modulus was indirectly evaluated by comparing predicted crack widths with those measured by other investigators, and the following formula was proposed to calculate the spacing and width of cracks.

$$S_{\max} = \frac{14.5\phi}{1 + n\rho_m} \qquad (2.4a)$$

and,

$$W_{t,\max} = \frac{2.4 \times 10^{-5}\,\phi\,(1462 - f_s)\,f_s}{(1 + n\rho_m)(662 - f_s)} \qquad (2.4b)$$

where S_{max} = maximum crack spacing; $n = E_s/E_c$ = modular ratio in which E_s and E_c are the elastic moduli of steel and concrete respectively, and ρ_m = modified

reinforcement ratio, which relates to the concrete cover. In Eq. 2.4, $W_{t,max}$ and ϕ are in millimetres and f_s is in *MPa*.

(e) Bazant & Oh method

Bazant & Oh (1983) carried out a theoretical study on the spacing and width of cracks, using the energy criterion of fracture mechanics as well as the strength criterion. The strength criterion indicates whether the fracture formation can initiate, while the energy criterion indicates the fracture can actually form. The study suggested that the crack spacing depends mainly on the axial strain of steel bars, bar spacing, bar diameter, fracture energy of concrete and its elastic modulus. Based on the study, Oh & Kang (1987) proposed the following equations for the prediction of average crack spacing and maximum crack width in reinforced concrete members.

$$\frac{S_{ave}}{\phi} = 25.7\left(\phi_1\right)^{4.5} + 1.66\left(\phi_2\right)^{1/3} + \frac{0.236 \times 10^{-6}}{\varepsilon_s^2} \qquad (2.5a)$$

$$\frac{W_{t,\max}}{\phi} = \left\{159\left(\phi_1\right)^{4.5} + 2.83\left(\phi_2\right)^{1/3}\right\}\left(\varepsilon_s - 0.0002\right)\phi_3 \qquad (2.5b)$$

where ε_s = steel strain; ϕ_1 = ratio between concrete cover and distance from neutral axis to tension face; ϕ_2 = ratio between average effective concrete area around steel bar and the area of steel bar; ϕ_3 = ratio between distances from neutral axis to tension face and steel bars.

A comparison with a large number of test results has shown that the spacing and width of cracks predicted by the above formula agree satisfactorily with test data.

(f) Beeby method

A theoretical investigation into the cracking of reinforced concrete members carried out by Beeby (1970, 1971) revealed that the crack width has two components. They are: (*i*) part of the crack width that is controlled by the crack height (W_{lim}), and (*ii*) that part controlled by the proximity of the reinforcement (W_o).

Based on test results of un-reinforced concrete columns subjected to axial force and bending moment (Beaby (1979)), the following relationship was developed for W_{lim}.

$$W_{lim} = K_1 h_{cr} \varepsilon_m \qquad (2.6a)$$

where K_1 = a constant; h_{cr} = crack height; and ε_m = mean strain in the steel bar between adjacent cracks.

To develop a formula for W_o (part of the crack width controlled by the proximity of the reinforcement), it was assumed that the crack width depends on the concrete cover c, bar diameter ϕ and reinforcement ratio ρ. Based on analytical results of axially reinforced tension members, the following formula was proposed.

$$W_o = \left(K_1 c + K_2 \frac{\phi}{\rho} \right) \varepsilon_m \qquad (2.6b)$$

where K_2 = a constant.

The crack width W in a flexural member was then expressed as a combination of W_{lim} and W_o as

$$W = \frac{a_{cr} W_o W_{lim} \varepsilon_m}{c W_{lim} + (a_{cr} - c) W_o} \qquad (2.7)$$

where a_{cr} is the distance from the bar surface to the point where the crack width is calculated.

The constant K_1 (Eqs. 2.6*a* and 2.6*b*) was evaluated using test results of un-reinforced concrete columns subjected to axial force and bending moment, while K_2 was determined empirically for various values of c/h_{cr} ratios. These constants were calculated for various probabilities of the measured crack width exceeding the calculated value. For example, 5% probability of exceedence gave K_1 = 1.86 while K_2 varied from 0.12 to 0.04 for c/h_{cr} ratios between 0.1 and 0.3 (Beeby (1979)). These values have shown to give good correlation between the calculated crack widths and those measured by Base *et. al* (1966) and Beeby (1970).

To develop simplified crack width prediction formulas for practical usage, the equations for W_{lim} and W_o (Eq. 2.6*a* and 2.6*b*) have been modified as shown below.

$$W_{lim} = 1.5(h\text{-}x) \qquad (2.8a)$$

and, $$W_o = 3c\varepsilon_m \qquad (2.8b)$$

where h = overall height of the member; and x = depth of compression zone.

Substitution of Eqs. 2.8*a* and 2.8*b* into Eq. 2.7 leads to the following formula for the crack width in a flexural member.

$$W = \frac{3a_{cr}\varepsilon_m}{\left(1+2\dfrac{(a_{cr}-c)}{(h-x)}\right)} \qquad (2.9)$$

As discussed in Section 2.2.6.3, the above equation has been recommended in BS 8110 : Part 1 (1997) for the calculation of crack width in flexural members.

2.2.4.2 Experimental investigations

(a) Watstein, Parsons & Clark method

Watstein & Parsons (1943) carried out uniaxial tensile tests on axially reinforced concrete cylinders to investigate the formation of cracks. Based on the results, an expression was developed to predict the average crack width of a tension member. To make this prediction procedure applicable to flexural members, Clark (1956) modified two coefficients of the expression based on test results of 56 beams and one-way slabs. Assuming a value of modular ratio n=8, the following formula was proposed by Clark (1956).

$$W_{t,ave} = 1.29x10^{-6}\left(\frac{h-d}{d}\right)\frac{\phi}{\rho}\left[2.56 f_s - \left(\frac{1}{\rho}+8\right)\right] \qquad (2.10)$$

where d = effective depth. In Eq. 2.10, d, h and ϕ are in millimetres and f_s is in *MPa*.

A comparison of predicted and measured crack widths indicated that a good agreement was observed when the measured crack width was based on either (*i*) the average of all cracks in one specimen, or (*ii*) the average of all cracks in specimens of identical design. Test results have also revealed that the maximum crack width ranged from 1.18 to 2.77 times the average crack width for individual specimens, while the average maximum crack width is about 1.64 times the average crack width, at all steel stress levels. Crack width results of 12 beams tested by Mathey & Watstein (1960) have also shown a good agreement with the values predicted by the above expression.

(b) Kaar & Mattock method

Based on test results of 48 beams, Kaar & Mattock (1963) developed the following equation to predict the maximum crack width.

$$W_{s,max} = 1.57x10^{-5} f_s \sqrt[4]{A_e} \qquad (2.11)$$

where $W_{s,max}$ = maximum crack width at reinforcement level (*mm*); and A_e = effective stretched concrete area (mm^2).

(c) Gergely & Lutz method

Gergely & Lutz (1968) proposed the following crack width prediction formula based on a computer statistical analysis of a large number of test results from different sources.

$$W_{t,max} = 0.0132z \tag{2.12a}$$

where $$z = f_s \sqrt[3]{c\,A_e} \times 10^{-3} \tag{2.12b}$$

in which A_e has the same meaning as in Eq. 2.11.

The above equation has been used by ACI 318 (1995) in prescribing the rules for the distribution of tension reinforcement for controlling the crack width, which is described in Section 2.2.6.1.

(d) Lan & Ding method

Lan and Ding (1992) developed an equation to predict the maximum crack spacing based on test results of a large number of reinforced concrete flexural members. Maximum crack spacing was then multiplied by the steel strain ε_s at the cracked section, together with two other coefficients to evaluate the maximum crack width. These two coefficients ψ and υ represent the non-uniformity in steel strain and the bond properties of steel bars, respectively. The proposed prediction formula for the average crack spacing and maximum crack width are as follows:

$$S_{ave} = \left(2.7c + 0.11\phi/\rho_{te}\right)\upsilon \tag{2.13a}$$

$$W_{t,\max} = 1.41 S_{ave}\,\varepsilon_s\,\psi \tag{2.13b}$$

where ρ_{te} = reinforcement ratio based on the effective area of tensile concrete.

(*e*) Chowdhury & Loo method

Based on test results of 18 reinforced and 12 partially prestressed concrete beams, Chowdhury & Loo (2001) developed an equation for predicting the average crack spacing in terms of the concrete cover, bar spacing, bar diameter and the reinforcement ratio. The average crack spacing was then multiplied by the steel strain at the cracked section to determine the average crack width. The resulting maximum crack width was taken as 1.5 times the average crack width. The proposed formulas are as follows:

$$S_{ave} = 0.6(c - s_b) + 0.1(\phi/\rho) \qquad (2.13c)$$

$$W_{t,\max} = 1.5\varepsilon_s S_{ave} \qquad (2.13d)$$

In Eq. 2.13*c*, s_b = centre-to-centre spacing of reinforcing bars; and c = clear concrete cover.

2.2.5 Factors affecting crack width

It is agreed by all investigators that crack width increases with the steel stress at the cracked section. This can be seen by examining the crack width prediction formulas discussed above; in all the above formulas, the steel stress f_s or the steel strain ε_s appears as a multiplier. It is also agreed that the concrete strength has no significant effect on the crack width; only the equation proposed by Venkateswarlu & Gesund (1972) (Eq. 2.4) includes the concrete strength in terms of the modular ratio. However, there is no general agreement among different investigators on the relative significance of other factors influencing the crack width.

As reported by Gergely & Lutz (1968), characteristics of specimens in each investigation and indirect effects of other variables may result in differing conclusions leading to disagreements among investigators. Depending on the conclusions drawn by different investigators, variables such as bar diameter, reinforcement ratio and concrete cover are embedded in prediction formulas differently. (A comparison of the different variables included in various prediction formulas is given in the Summary -Section 2.5). As a result, the influence of each of the above variables on the calculated crack width will vary when different formulas are used. Nevertheless, the following general trend can be seen in every prediction formula: an increase in the bar diameter and concrete cover, as well as a decrease in the reinforcement ratio will increase the crack width, if all other variables are kept constant. Following is a discussion on the effects of various variables on the measured crack width, observed by different investigators.

2.2.5.1 Effect of concrete cover

As mentioned in the previous paragraph, an increase in concrete cover will result in a larger calculated crack width, according to all prediction formulas. In spite of this fact, provision of larger concrete cover is considered as the most practical means of protecting reinforcement against corrosion. To investigate the effect of varying concrete cover, Makhlouf & Malhas (1996) carried out tests on 16 beams and compared the measured and calculated crack widths.

Results of these tests revealed that the measured crack width increased by about 16% when the concrete cover was doubled from 30 mm to 60 mm. However, more than an 80% increase was predicted by the equations recommended in ACI 318 (1995) and BS8110 : Part 2 (1985), which were based on expressions developed by Gegley & Lutz (1968) and Beeby (1979), respectively. It was concluded that, based on the above test results, the equations recommended in both the above building codes are too sensitive to concrete cover.

Further, as reported by Frosch (1999), concrete covers only up to 65mm have been used in experiments considered by Gegely & Lutz (1968) in the development of the prediction formula. As a result, the applicability of ACI 318 (1995) prediction procedure (which is based on Gegely & Lutz formula) is questionable in cases where the concrete cover exceeds 65*mm*.

2.2.5.2 Effect of reinforcement ratio and bar diameter

Individual effects of bar diameter and reinforcement ratio on the crack width have not been investigated separately due to the interdependency of these two variables. It is very difficult to design a series of test specimens where only the bar diameter or the reinforcement ratio is changed one at a time. As reported by Kaar (1968), this difficulty has contributed to large differences in test results of the various investigators. It may also lead to differing conclusions on the relative significance of some of the variables.

The above fact can best be demonstrated by considering another conclusion drawn on the basis of test results. According to the results of test beams mentioned in Section 2.2.5.1, Makhlouf & Malhas (1996) further concluded that the different reinforcement ratios used (0.0031, 0.0056, 0.0087 and 0.0138) had no tangible effect on the measured crack widths. It may be noted however, that different bar diameters (12, 16, 20 and 25 *mm*, respectively), were associated with the above reinforcement ratios. One may argue that a decrease in the crack width caused by using higher reinforcement ratios has been, at least by part, compensated by an increase in the crack width resulted from using larger diameter bars, leading to the net change becoming unnoticeable. This shows the

possibility of producing ambiguous results due to indirect effects of some of the variables, leading to inconsistent conclusions.

2.2.5.3 Effect of beam height

Beam height has not been considered by most investigators as a major variable affecting the spacing and width of cracks; only Clark (1956) has included the beam height and effective depth as variables in the crack width prediction formula (Eq. 2.10). In all other analytical investigations, the resulting tensile stress in the concrete block between adjacent cracks has been determined considering only the bond force, neglecting the compressive force acting above the neutral axis at cracked sections. However it will be shown in Chapter 5 that the compressive force acting above the neutral axis has some influence on the concrete tensile stress developed at reinforcement level, thereby affecting the spacing and width of cracks, especially in shallow members.

2.2.5.4 Effect of loading type

All the available crack spacing and crack width prediction formulas have been based on analytical or experimental investigations in constant moment regions. These formulas are being used for all loading types assuming they are equally valid even for varying moment regions, although this validity has never been proved. It will be shown in Chapter 5 however, that the crack spacing in a varying moment region of a beam is considerably different from that in a constant moment region, making the above assumption questionable.

2.2.6 Current methods of crack control

2.2.6.1 The American Concrete Institute (ACI) approach

For controlling the width of flexural cracks ACI 318 (1995) prescribes rules for the distribution of tension reinforcement. These rules are based on the crack width prediction formula (Eq. 2.12), proposed by Gergely & Lutz (1968). According to these rules, the distance between tension bars should be limited such that the value z in Eq. 2.12*b* does not exceed 30 kN/mm for interior exposure and 25 kN/mm for exterior exposure. These values are equivalent to limiting the maximum crack widths to 0.40 mm for interior exposure and 0.33 mm for exterior exposure, respectively. Although the above rules are widely used in practice, a comparative study has shown that the procedure recommended by ACI 318 (1995) generally underestimates final crack widths in certain cases. In particular, the approach does not model adequately the increase in flexural crack width due to shrinkage of concrete, that occurs in slabs with widely spaced tensile reinforcing bars (Gilbert (1999)).

2.2.6.2. The Standards Association of Australia (AS) approach

To limit the crack width under service loads Standards Association of Australia (AS3600 (2001)) stipulates maximum allowable steel stresses at cracked sections for different bar diameters and bar spacings (see Tables 2.2 and 2.3). Out of the two steel stresses specified in these Tables, the larger value applicable for the particular member may be used as the limiting steel stress. When the calculated steel stress at a cracked section under service loads is less than this limiting value, the resulting crack width of the member is deemed to be acceptable.

Table 2.2 Maximum steel stress for tension or flexure (AS3600 (2001))

Nominal bar diameter (mm)	Maximum steel stress (MPa)
10	360
12	330
16	280
20	240
24	210
28	185
32	160
36	140
40	120

Table 2.3 Maximum steel stress for flexure (AS3600 (2001))

Centre-to-centre spacing (mm)	Maximum steel stress (MPa)
50	360
100	320
150	280
200	240
250	200
300	160

2.2.6.3. The British Standards Institution (BSI) approach

For controlling the crack width under service loads, the British Standards Institution (BS 8110 : Part 1 (1997)) stipulates the maximum clear spacing for tension bars depending on the magnitude of the moment redistribution applied at the section (Table 2.4).

Table 2.4 Maximum distance between bars in *mm* (BS 8110: Part 1 (1997))

f_y *(MPa)*	Redistribution to or from section considered (%)						
	-30%	-20%	-10%	0	+10%	+20%	+30%
250	210	240	270	300	300	300	300
460	115	130	145	160	180	195	210

Note: f_y = yield stress of reinforcing bars.

Instead of using the values shown in Table 2.4, it is also permissible to use the following formula to calculate the maximum spacing between tension reinforcement.

$$\text{clear spacing} \leq \frac{47000}{f_s} \leq 300 \quad mm \tag{2.14}$$

where f_s is in *MPa*.

As an alternative to the use of maximum bar spacing specified above, BS 8110: Part 1 (1997) also recommends the calculation of the crack width using the simplified formula (Eq. 2.9), which was developed by Beeby (1979). The design is considered satisfactory if the calculated crack width is less than 0.3mm, 0.2mm and 0.1mm respectively, in mild, moderate and severe environments.

2.3 Deflection of Flexural Members

Deflection of a flexural member cannot be avoided because it is part of the load carrying mechanism. Excessive deflections of beams and slabs can cause damage to non-structural element such as partitions attached to them. Large deflections may also result in unnecessary ponding of water in exposed areas causing difficulties to the occupants. To avoid these adverse effects, designers need to ensure that the resulting deflections of beams and slabs under service loads are within acceptable limits.

2.3.1 Short-term and long-term deflections and allowable deflection limits

The deflection of a reinforced concrete member increases with time due to the creep of concrete, in cases where the applied load is sustained for a long period of time. Self weight and other superimposed dead loads fall in to the category of sustained loadings. To minimise the adverse effects of deflections mentioned in the previous paragraph, it is necessary to limit the short-term deflection as well as the total deflection including the long-term effects of creep. Various building codes have stipulated deflection limits for different types of members, depending on their intended use. Tables 2.5, 2.6 and 2.7 present these limits prescribed by American Concrete Institute (ACI 318 (1995)), the Standard Association of Australia (AS3600 (2001)) and the British Standards Institution (BS 8110 : Part 1 (1997)), respectively.

Table 2.5 Maximum Allowable Deflections (ACI 318 (1995))

Type of member	Deflection to be considered	Deflec-tion limit
Flat roofs not supporting or attached to non-structural elements likely to be damaged by large deflections	Immediate deflection due to live load	span/180
Floors not supporting or attached to non-structural elements likely to be damaged by large deflections		span/360
Roof or floor construction supporting or attached to non-structural elements likely to be damaged by large deflections	That part of the total deflec-tion occurring after attache-ment of non-structural eleme-nts (sum of the long term def-lection due to all sustained loads and the immediate deflection due to additional live load)	span/480
Roof or floor construction supporting or attached to non-structural elements not likely to be damaged by large deflections		span/240

Table 2.6 Maximum Allowable Deflections (AS3600 (2001)) for spans (For cantilevers different limitations apply)

Type of member	Deflection to be considered	Deflection limit
All members	The total deflection	span/250
Members supporting masonry partitions	The deflection which occurs after the addition or attachment of the partitions	span/500[(1)]
Bridge members	Live load (and impact deflection)	span/800

[(1)] If provision is not made to minimize the effect of movement this deflection limit should be reduced to span/1000

Table 2.7 Maximum Allowable Deflections (BS8100:Part 1 (1997))

Type of member	Deflection to be considered	Deflection limit
All members	The total deflection	span/250
	The deflection which occurs after the addition of finishes and partitions	span/350 or 20mm whichever is less

2.3.2 Calculation of short-term deflection

Almost all reinforced concrete flexural members undergo certain degree of cracking under service loads. After the cracking the bending stiffness along the length of the member varies, which makes the calculation of deflections complicated. In a cracked beam, the bending stiffness is largest at sections within the uncracked region (where the applied moment is less than the cracking moment) while it is smallest at cracked sections. This is because at cracked sections, the concrete below the neutral axis does not contribute to the load carrying mechanism. However at intermediate sections between adjacent cracks, the concrete around reinforcement retains some tensile force due to the action of bond (see Fig. 2.5). These tensile forces cause a reduction in steel stress as well as a movement of the zero-strain plane towards the tension face. As a result, the bending stiffness at sections between adjacent cracks becomes larger than those at the adjacent cracked sections, contributing to an overall increase in the stiffness of the member. This effect is known as "*tension stiffening*". For accurate assessment of deflection, tension stiffening effect needs to be incorporated in the calculation. If this effect is not included, the calculated deflection becomes larger than the actual value, and in certain cases the difference may be as high as 100 percent (Gilbert & Warner 1978).

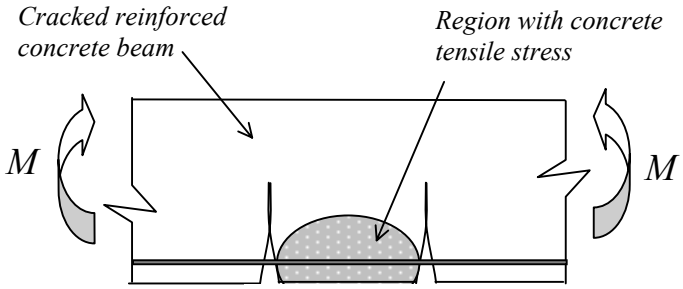

Fig. 2.5 Concrete tensile stresses induced due to the action of bond

Previous investigations have revealed that the tension stiffening effect in a cracked reinforced concrete member decreases with the increase of loading. Other parameters affecting the tension stiffening includes the amount and distribution of reinforcement, bar diameter, bond and tensile strength of concrete, concrete cover and crack spacing (Ouyang *et al* (1997), Kaklauskan & Ghaboussi (2001), Favre & Charif (1994), Prakhya & Morley (1990), Polak & Blackwell (1998)). A direct method of assessing the tension stiffening effect for a particular member is not available at present. Described below are the different procedures of incorporating the tension stiffening effect in deflection calculation proposed by various researchers.

2.3.2.1 Use of effective moment of inertia

In this method the short-term deflection is calculated using an average moment of inertia for the entire beam. Its value is taken, depending on the load intensity, in between the gross moment of inertia I_g for the uncracked section and the moment of inertia I_{cr} for a cracked section. Different investigators have proposed various formulas to calculate the effective moment of inertia I_e, as outlined below.

(a) Branson's method

Based on experimental results, Branson (1963) developed the following equation for computing the effective moment of inertia of cracked reinforced concrete beams and one-way slabs.

$$I_e = I_{cr} + \left(I_g - I_{cr}\right)\left(\frac{M_{cr}}{M_a}\right)^{\beta} \leq I_g \qquad (2.15)$$

where M_a = maximum bending moment *($M_a > M_{cr}$)*; M_{cr} = cracking moment of the member; and $\beta = 3$. This is widely known as Branson's formula. This formula has been recommended in ACI 318(1995) and AS 3600(2001) for the calculation of short term deflections.

It may be noted that the value of I_e calculated using Eq. 2.15 is only slightly smaller than I_g in cases where M_a is marginally larger than M_{cr}. This generally happens in members with low reinforcement ratios, typically $\rho < 0.006$. For these members the calculated I_e is very sensitive to changes of M_{cr}, and therefore, variations in modulus of rupture f'_t, which governs M_{cr} (Gilbert (1999)). This means that Eq.2.15 may overestimate the effective moment of inertia I_e for lightly reinforced members, especially when the estimated f'_t is larger than the actual value.

There have been several attempts by different investigators to modify the Branson's formula aiming to improve the accuracy of the predicted deflection. These are briefly discussed below.

(b) Modification by Al Zaid et al.

Branson's formula has been developed using the results of test beams subjected to uniformly distributed loads. Based on test results, Al Zaid *et al*. (1991) suggested that the value of I_e calculated using Branson's formula may be increased by 20% for beams subjected to central point loads.

(c) Modification by Al Shaik & Al Zaid

Results of experiments carried out by Al Shaik & Al Zaid (1993) indicated that the value of β in Eq. 2.15 decreases with the amount of tensile reinforcement ratio ρ. It was proposed to calculate the value of β using the following equation.

$$\beta = 3 - 0.8\rho \qquad (2.16)$$

(d) Modification by Grossman

Grossman (1981) carried out a parametric study by computing the effective moment of inertia using Branson's equation (Eq. 2.15) for various beams and one-way slabs having different material and sectional properties. Based on the results, Grossman (1981) developed the following formula for calculating I_e, which eliminates the requirement of computing I_{cr}.

$$\frac{I_e}{I_g} = \left(\frac{M_{cr}}{M_a}\right)^2 \le 1.0\,, \qquad \text{if } \frac{M_a}{M_{cr}} \le 1.6\,, \text{ and} \qquad (2.17a)$$

$$\frac{I_e}{I_g} = 0.1\left(\frac{M_a}{M_{cr}}\right) K^*, \qquad \text{if } \frac{M_a}{M_{cr}} > 1.6 \qquad (2.17b)$$

$$\text{with a lower bound of } \frac{I_e}{I_g} = 0.35\,K^*. \qquad (2.17c)$$

K^* in above equations provides adjustments for shape, material properties and the strength of the section, and is determined as follows.

$$K^* = \left(\frac{d/h}{0.9}\right)\left[\frac{\sqrt{2330/w_c}}{0.4 + (1.4\,M_a/M_u)(f_y/690)}\right] \qquad (2.17d)$$

where w_c = unit weight of concrete (kg/m^3) and f_y = yield strength of steel (MPa).

(e) Modification by Rangan

Rangan (1982) computed the effective moment of inertia I_e using Branson's equation (Eq. 2.15), for a number of simply supported rectangular beams and one way slabs under service load. The mid span moment M_a in Eq. 2.15 was replaced by the service moment M_s, which was calculated as the moment of resistance when the steel stress is

equal to 60% of the yield stress. Based on these results following equation was proposed.

If $n\rho > 0.045$,

$$\frac{I_e}{b\,d^3} = 0.1599\sqrt{n\rho}\text{, and} \qquad (2.18a)$$

if $n\rho \leq 0.045$,

$$\frac{I_e}{b\,d^3} = 0.0019/n\rho \qquad (2.18b)$$

where $n = E_s/E_c$ modular ratio.

The above equation for I_e has been used by the Standard Association of Australia (AS 3600 (2001)) in the development of the formula to calculate the span-to-effective depth ratio for controlling deflections of beams and one-way slabs (Section 2.4.2).

2.3.2.2 Use of non-linear stress-strain relationship for tensile concrete

Another way of incorporating the tension stiffening effect in deflection calculations is the use of smeared crack approach, where the concrete tensile stress is averaged over representative lengths to span several cracks. In this method, the concrete tensile stress at a given section is calculated using a non-linear stress-strain relationship that allows the concrete to retain certain amount of tensile stress beyond the cracking strain. The most commonly used non-linear stress-strain relationship comprises of a curvilinear descending branch beyond the cracking strain of concrete (see Fig. 2.6), which is described below.

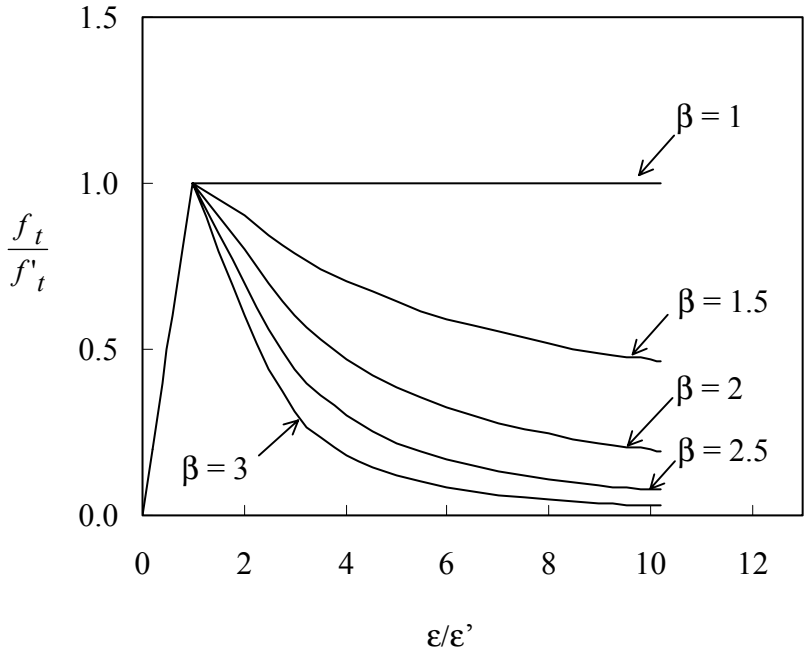

Fig. 2.6 Stress-strain relationship for cracked concrete (curvilinear descending branch)

The relationship shown in Fig. 2.6 can be expressed as

$$f_t = f'_t\left(\frac{\varepsilon}{\varepsilon'}\right) \qquad \text{if } \left(\frac{\varepsilon}{\varepsilon'}\right) \le 1 \tag{2.19a}$$

$$f_t = \frac{\beta f'_t\left(\frac{\varepsilon}{\varepsilon'}\right)}{\beta - 1 + \left(\frac{\varepsilon}{\varepsilon'}\right)^{\beta}} \qquad \text{if } \left(\frac{\varepsilon}{\varepsilon'}\right) > 1 \tag{2.19b}$$

where ε = concrete tensile strain; f_t = corresponding concrete stress; f'_t = tensile strength of concrete; and ε' = cracking strain of concrete. The parameter β, which governs the rate of declining the tension stiffening effect with the increase of applied loading, depends on the sectional properties of the beam.

In using the above constitutive relationship (Eq. 2.19) for calculating the concrete stress, a perfect bond (zero bond slip) between steel reinforcement and surrounding

concrete is assumed. It must be noted however that the bond slip is not ignored in this method; the effect of bond slip is incorporated in the steepness of the descending branch of the stress-strain curve (see Fig. 2.6). For example, a steeper descending branch represents a member that loses most of the tension stiffening effect for smaller slip values.

Fig. 2.7 shows the schematic diagram of the tensile stress distribution obtained by using the above constitutive relationship (Eq. 2.19) for a section within the cracked region (where the applied bending moment exceeds the cracking moment). The neutral axis depth *kd* and the maximum concrete compressive strain ε_c at the section are calculated by satisfying the translational and rotational equilibrium conditions. The resulting curvature κ at the section is then calculated using the following formula.

$$\kappa = \frac{\varepsilon_c}{kd} \qquad (2.20a)$$

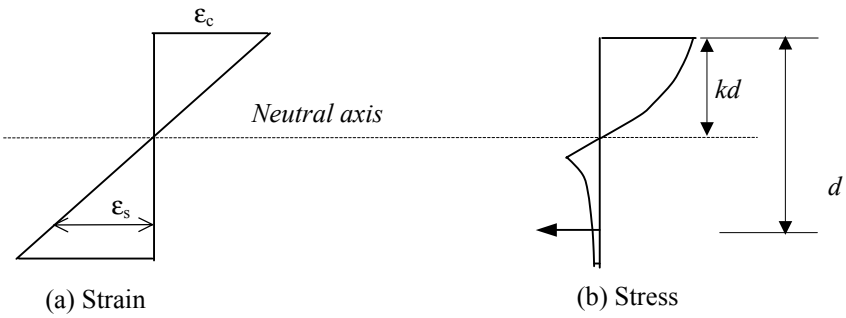

Fig. 2.7 Stress distribution at a section within the cracked region

The deflection is then calculated by double integration of the curvature with respect to the distance along the length of the beam. For example, the use of curvature at the two ends and at mid span of a continuous member leads to the following equation for the mid span deflection, if the curvature is assumed to vary parabolically along the length (Gilbert (1999)).

$$\delta = \frac{L^2}{96}\left(\kappa_L + 10\,\kappa_M + \kappa_R\right) \qquad (2.20b)$$

where δ = mid span deflection; L = span length; and κ_L, κ_R and κ_M are the curvature values at left support, right support and mid span, respectively.

It may be seen that the stress distribution shown in Fig. 2.7*b*, and therefore the calculated deflection, depend on the assumed value of β which governs the shape of the descending branch of the stress-strain relationship (see Fig. 2.6). Prakhya & Morley (1990) have indirectly evaluated the parameter β for 30 flexural members by matching the calculated and measured curvature values. This calculation showed that β for a particular beam depends of various parameters including the reinforcement ratio, diameter and spacing of reinforcing bars, neutral axis depth at the cracked section and the clear concrete cover. It was also seen that the calculated values of β for the above 30 members varied between 1.5 and 3.0. A similar investigation by Carreira & Chu (1986*a*) on four flexural members revealed that the value of β varied from 1.45 to 1.95.

The above non-linear stress-strain relationship (Eq. 2.19) has been successfully used for the calculation of deflection and curvature by many investigators including Carreira & Chu (1986*a*, 1986*b*), Gilbert & Warner (1978), Hand *et al*. (1973), Lin & Scordelis (1975) and Wanchoo & May (1975). Value of the parameter β adopted in each investigation was different because an accepted procedure for the determination of this parameter is not available at present.

Instead of using a curvilinear stress-strain relationship (Fig. 2.19), some investigators have used a linear descending branch beyond the cracking strain of concrete. A typical constitutive relationship of this nature is shown in Fig. 2.8.

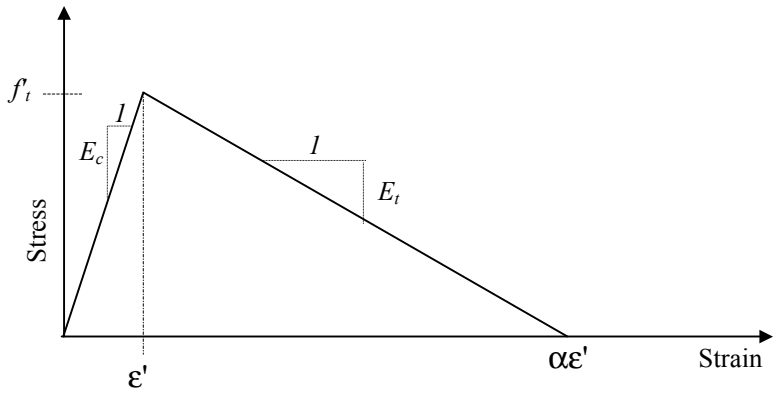

Fig. 2.8 Stress-strain relationship for cracked concrete (linear descending branch)

As seen in Fig. 2.8, for a selected strain, the calculated tensile stress in cracked concrete depends on the steepness of the descending branch of the constitutive relationship. This is represented by the gradient E_t (see Fig. 2.8), or the maximum strain (αε') at which the concrete tensile stress is assumed to be zero. Investigations by Bazant & Oh (1984) have shown that good agreement of calculated and measured deflections are obtained when the gradient E_t is calculated as E_t=-70E_c/(57+f'_t), where E_c is the elastic modulus of concrete and f'_t is the flexural strength. This formula gives α=7.7 for one of the illustrative examples presented by Bazant & Oh (1984). Kaklauskas & Ghaboussi (2001) have evaluated the value of α for 14 beams by matching the calculated and measured deflections. This calculation revealed that α varied from 6 to 28 for the beams considered.

As mentioned previously, the use of non-linear constitutive relationships for tensile concrete (Figs. 2.6 or 2.8) is associated with the assumption of perfect bond between reinforcement and concrete. This assumption makes it possible to use the above constitutive relationships in numerical analysis such as the finite element method; *eg.,* Hand *et al* (1973), Lin & Scordelis (1975), Wanchoo & May (1975), Gilbert and Warner (1978) and Behfarnia *et al*. (1995). It must be mentioned that the parameters β and α (Figs. 2.6 and 2.8) used in these analyses were different, as there are no accepted

procedures to evaluate the values of above parameters applicable for a particular member.

A slightly different smeared crack approach is recommended by BS8110 : Part 2 (1985) to calculate the deflection of reinforced concrete members. In this method, a linearly varying tensile stress distribution, with the maximum stress at the tension face, is assumed (see Fig. 2.9). For short-term deflections the magnitude of concrete tensile stress at reinforcement level is taken as 1*MPa* irrespective of the calculated strain. (This stress is reduced to 0.55*MPa* for long-term deflections, which will be discussed in Section 2.3.3).

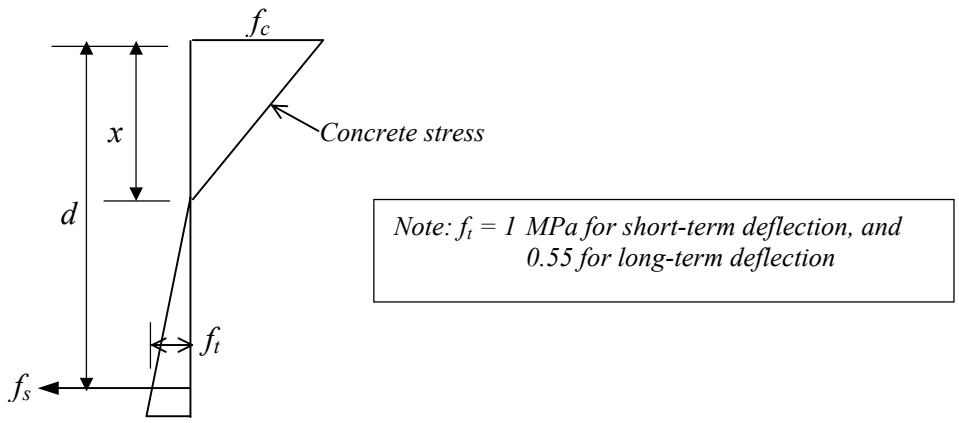

Fig. 2.9 Stress distribution used for deflection calculation (BS 8110: Part 2 (1985))

Using the above concrete stress distribution, the depth of neutral axis x and the steel stress f_s are calculated at certain nominated sections, by considering the equilibrium conditions. The resulting curvature κ at the section is then determined using the following formula.

$$\kappa = \frac{f_s}{(d-x)E_s} \tag{2.21}$$

BS8110 : Part 2 (1985) recommends the calculation of deflection using the κ values evaluated at the mid span for simply-supported and continuous beams, and at the supports for cantilevers.

2.3.2.3 Calculation of curvature using bond force

In calculating the curvature at a section, instead of using the concrete tensile stress, it is also possible to incorporate the bond forces in equilibrium equations. Using this procedure, Fantilli *et al*. (1998) developed a set of differential equations by considering the equilibrium of a portion of the beam of infinitesimal length located between two successive cracks. The bond stress was calculated by using the bond stress-bond slip relationship proposed by CEB (1993). Assuming a linear strain distribution across the depth of the beam, the above equations were solved numerically using the known boundary conditions at the adjacent cracked sections. The *local curvature* was then calculated over a beam length equal to the distance between midway sections of the neighbouring cracked blocks. This investigation showed a good agreement between the calculated and measured curvature values, both in constant and varying moment regions. The results also revealed that the local curvature is significantly affected by the spacing of adjacent cracks, especially in constant moment regions where flexural cracks are found to occur at random locations.

In calculating the curvature, Polak & Blackwell (1998) used a different approach to evaluate the bond force. The bond force was assumed to be totally transferred by the mechanical interlock (bearing of concrete on bar lugs), ignoring the effects of chemical adhesion and friction between bar surface and concrete. It was further assumed that the bearing stress on bar lugs is equal to f'_c at the cracked section, and zero at the mid section between adjacent cracks, with a linear variation in between these two sections. The resulting bond force was calculated by multiplying the lug contact area and the bearing stress, without using a bond stress-bond slip relationship. To determine the curvature, the values of ε_c and *kd* (see Fig. 2.7 and Eq. 2.20*a*) at each section were calculated by assuming a linear strain distribution across the depth of the beam and satisfying the equilibrium conditions. The results showed that the calculated curvature values are in good agreement with the measured values on 14 beam specimens.

The deflection calculation procedure presented in this thesis (Chapter 8) is also based on the curvature values evaluated using equilibrium conditions that incorporate the

bond forces. Unlike in previous investigations, a linear strain distribution across the depth of the beam is not assumed for the calculation of concrete strains. Instead, the concrete strains are computed using a rigorous method involving the finite element analysis. It must be mentioned here that the results of this analysis reveal that the strain distribution at sections between adjacent cracks are in fact non-linear (Chapter 5). In the present method of calculating deflections, a large number of local curvature values are evaluated between each pair of adjacent cracks, as the use of more curvature values generally enhances the accuracy of results (Ghali & Azarnejad (1999)).

2.3.3 Calculation of long-term deflection

The increase in deflection with time depends on various factors including the creep coefficient, elastic modulus and the tensile strength of concrete. The creep coefficient depends on the concrete compressive strength, relative humidity of the environment as well as the age of concrete at the time of loading. Experiments carried out by Washa and Fluck (1952) showed that the deflection measured after two-and-half years varied from 1.63 to 2.27 times the instantaneous deflection for beams without compression reinforcement. It was also revealed that the inclusion of arbitrary amounts of compression steel reduces the long-term deflection by a considerable amount. Swamy & Anand (1974) reported that the deflection measured after one year ranged from 2.07 to 2.75 times the initial deflection. Tests by Nie & Cai (2000) have shown that the deflections measured after three months varied from 1.48 to 1.88 times the initial deflection. Described below are the most commonly used procedures of estimating the increase in deflection of reinforced concrete members when subjected to sustained loading.

2.3.3.1 Long-term deflection multiplier method

The increase in deflection due to a sustained load can be determined by multiplying the initial (short-term) deflection by an appropriate multiplier μ. The value of this multiplier increases with the period of time (t) that the sustained load is acting on the member, and can be reduced according to the amount of compression steel, if provided. The

following formula is recommended by ACI 318 (1995) for calculating the long-term deflection multiplier.

$$\mu = \frac{\xi}{1+50\rho'} \qquad (2.22a)$$

where μ = long term deflection multiplier; ξ = 1.0 and 1.4 for t = 3 months and 1 year respectively; and ξ = 2.0 for periods longer than 5 years (t>5 years). The compression steel ratio ρ' is determined as

$$\rho' = \frac{A_{sc}}{bd} \qquad (2.22b)$$

in which A_{sc} = compression steel area; b = width of the member; and d = effective depth.

Although Eq. 2.22 is widely used to estimate the long-term deflection, this equation is found to exaggerate the role of compression steel in reducing deflections of certain members. This happens particularly in lightly reinforced members with high compression steel ratios (Samra (1997)). In spite of this, the above equation is popular among practising engineers due to the simplicity of its application.

A slightly different formula is recommended for μ by the Standards Association of Australia (AS3600 (2001)) as

$$\mu = \left[2 - 1.2\left(A_{sc}/A_{st}\right)\right] \geq 0.8 \qquad (2.23)$$

where A_{st} = tension steel area.

The British Standards Institution (BS 8110 : Part 1 (1997)) recommends the following multiplier for calculating long-term delections.

$$\mu = 1 + \frac{100\rho'}{\left(3+100\rho'\right)} \leq 1.5 \qquad (2.24)$$

Although the use of a deflection multiplier is simple in practical applications it does not always provide an accurate assessment of the increase in deflection due to long-term

effects. As noted by Ghali & Azarnejad (1999), it is impossible to account for all the factors affecting the long-term deflection with a single multiplier that depends only on time and compression reinforcement ratio. Consequently, several researchers have attempted to develop alternative methods to calculate the long-term deflections, which are briefly described below.

2.3.3.2 Age-adjusted effective modulus method

Long-term deflection of a reinforced concrete member may be evaluated by using an age-adjusted effective modulus for concrete E_e, and adopting any of the methods already described for short-term deflection calculations. The value of E_e can be calculated using the following formula (Bazant (1972)).

$$E_e(t,t_o) = \frac{E_{c,o}(t_o)}{1+\chi(t,t_o).\phi_c(t,t_o)} \qquad (2.25)$$

where E_e = age-adjusted effective modulus for concrete; t_o = age of concrete at loading; t = time when E_e is calculated; $E_{c,o}$= initial modulus of elasticity at time t_o; χ=aging coefficient; and ϕ_c=creep coefficient.

In Eq. 2.25 the aging coefficient χ is taken as 1.0 for constant loading, and if the load is applied intermittently, its value may be reduced down to 0.8 depending on the duration of loading. The creep coefficient, ϕ_c varies from 1.0 for instant loading to 2.5 for loads applied over 20-year period. The above equation has been used by many researchers, including Bazant (1972), Dilger & Ghali (1976), Ghali & Favre (1986) and Nie & Cai (2000) to calculate the long-term deflection.

2.3.3.3 Calculation of long-term deflection using curvature

Long-term deflections may be determined using the curvature values at various sections evaluated by incorporating the creep effects. Gilbert (1999) proposed the following formula to calculate the increase in curvature due to creep of concrete.

$$\kappa_c = \frac{\kappa_i \phi_c}{\alpha} \qquad (2.26a)$$

where κ_c = increase in curvature due to creep; κ_i = initial curvature; and ϕ_c = creep coefficient. In this equation the coefficient α, which accounts for the cracking of concrete, may vary from 1.0 to 1.6 for cracked sections and 4 to 10 for uncracked sections.

In addition to the effects of creep, Gilbert (1999) proposed to include the curvature induced by shrinkage effects κ_{sc}, determined using the following formula.

$$\kappa_{sc} = \left(\frac{\eta \varepsilon_{sc}}{h}\right)\left(1 - \frac{\rho'}{\rho}\right) \qquad (2.26b)$$

where ε_{sc} = free shrinkage strain in concrete, which may be taken as 700 x 10^{-6} for periods over 20 years (AS3600 (2001)); and η = 0.7 for uncracked sections and 1.2 for cracked sections (Gilbert (1999)). The total long-term curvature κ is then calculated as

$$\kappa = \kappa_i + \kappa_c + \kappa_{sc} \qquad (2.26c)$$

To calculate the long-term curvature, the British Standards Institute BS8110 : Part 2 (1997) recommends the use of a smeared crack approach with the concrete tensile stress at reinforcement level taken as $0.55MPa$ (See Fig. 2.9). The long-term deflection is then determined using the curvature values calculated at nominated sections (mid span for simply-supported and continuous beams; support section for cantilevers) using the procedure already described for short-term deflections.

2.4 Control of Deflections in Flexural Members

To ensure that the design of a flexural member complies with the deflection limitations mentioned in Section 2.3.1, the resulting deflection under service loads can be calculated using the procedure described in the previous Section and then compared with the allowable limit. As an alternative to the calculation of deflection, designers may limit the span-to-depth ratio to the values specified in relevant building codes, for a range of members commonly encountered in practice. If the span-to-depth ratio of a particular member is less than the specified value, the resulting deflection is deemed to be within the allowable limit, and the design is considered satisfactory. However, for other members where the span-to-depth ratio limits have not been specified in building codes, the resulting deflection should be calculated to justify the design. Limits on span-to-depth ratios specified by various building codes for the control of deflections in reinforced concrete members are described below.

2.4.1 American Concrete Institute (ACI) approach

Table 2.8 shows the maximum span-to-depth ratios specified in ACI 318 (1995) for beams and one-way slabs, which are not supporting or attached to partitions or other attachments likely to be damaged by large deflections. Larger values of span-to-depth ratios are permitted only if the calculated deflections are shown to be within allowable limits.

Table 2.8 Maximum span-to-depth ratios (ACI 318 (1995))

Member	Support conditions			
	Simply-supported	One end continuous	Both ends continuous	Cantilever
Solid one-way slabs	20	24	28	10
Beams or ribbed one-way slabs	16	18.5	21	8

Values shown in Table 2.8 are applicable for normal weight concrete with density w_c=2325kg/m^3 and high tensile steel with yield stress f_y =410MPa. For other values of w_c and f_y, the span-to-depth ratios shown above should be modified using the procedure described in ACI 318 (1995).

While the span-to-depth ratios given in Table 2.8 are widely used in practice, a comparison of calculated deflections by Scanlon & Choi (1999) has shown that the values specified for one-way slabs are conservative for span lengths typically found in building structures.

2.4.2 Standards Association of Australia (AS) approach

AS3600 (2001) recommends the use of the following equation (Eq. 2.27) to calculate the maximum span-to-effective depth ratio for beams and one-way slabs of uniform cross sections subjected to uniform loading where the live load does not exceed the dead load.

$$\frac{L_{ef}}{d} = \left[\frac{k_1 \left(\Delta / L_{ef} \right) b_{ef} \, E_c}{k_2 \, F_{d.ef}} \right]^{1/3} \tag{2.27}$$

where Δ = maximum allowable deflection; L_{ef} = effective span length; $F_{d.ef}$ = effective design load per unit width; k_1 = 0.045 for rectangular sections; k_1 = 0.045(0.7 + 0.3b_w/b_{ef}) for T- and L-sections; k_2 = 1/185 for end spans; and k_2 = 1/384 for interior spans; b_w = web width; and b_{ef} = effective flange width.

In Eq. 2.27, the value of $F_{d.ef}$ is calculated using the procedure described in AS3600 (2001). Use of this equation for continuous beams is limited to cases where the ratio of adjacent spans does not exceed 1.2 and, where no end span is longer than an interior span. Development of the above equation is based on the effective moment of inertia I_e calculated using the procedure proposed by Rangan (1982), which was already described in Section 2.3.2.1(*e*).

2.4.3 British Standards Institution (BSI) approach

Table 2.9 shows the maximum span-to-effective depth ratios recommended in BS 8110 : Part 1 (1997) for beams and one-way slabs with span lengths less than 10 metres. For flanged beams with b_w/b greater than 0.3, linear interpolation between the values given for rectangular and flanged beams is permitted. For spans exceeding 10 metres, the design should be justified by calculation, in cases where the increase in deflection after the construction of partitions and attachments needs to be limited.

Table 2.9 Maximum span-to-effective depth ratios (BS 8110 : Part 1 (1997))

Support conditions	Cross sectional shape	
	Rectangular	Flanged $b_w/b \leq 0.3$
Cantilever	7	5.6
Simply supported	20	16.0
Continuous	26	20.8

The span-to-effective depth ratios given in Table 2.9 are called the *basic* values. To determine the span-to-effective depth ratio applicable for a particular member, the basic value needs to be multiplied by modification factors, depending on the calculated tensile steel stress, amount of compression reinforcement (if any) and, creep and shrinkage coefficients. The procedure for calculating these modification factors are described in BS8110 : Part 1 (1997).

2.5 Summary

In the first part of this Chapter, details of previous investigations aiming to develop crack spacing and crack width of prediction formulas were described, and their outcomes were presented. Table 2.10 gives a summary of these prediction formulas. Also included in this Chapter are the procedures recommended by different building codes for controlling the crack width in reinforced concrete members.

Table 2.10 Summary of various crack width prediction formulas

Investigator(s)	Variables considered	Eq. No:	Basis of equation
Chi and Kirstein (1958)	f_s, ϕ, E_s	2.1	Analytical
Broms (1965*b*)	ε_s, c	2.2	Analytical
Broms and Lutz (1965)	$\varepsilon_{s\text{-}ave}$, c_e	2.3	Analytical +Experimental
Venkateswarlu and Gesund (1972)	f_s, ϕ, n, ρ_m	2.4	Analytical
Oh & Kang (1987)	ε_s, c, ϕ, h, x	2.5	Analytical
Beaby (1979)	ε_m, c, h, x, a_{cr}	2.9	Analytical +Experimental
Watstein, Parsons and Clark (1956)	f_s, ϕ, h, d, ρ	2.10	Experimental
Kaar and Mattock (1963)	f_s, A_e	2.11	Experimental
Gergely and Lutz (1968)	f_s, c, A_e	2.12	Statistical analysis of experimental data
Chowdhury & Loo (2001)	c, s_b, ϕ, ρ, ε_s		Experimental
Lan and Ding (1992)	ε_s, c, ϕ, ρ_{te}	2.13	Experimental

Definitions of the variables shown in Table 2.10 are given in the respective Sections that described the development of the prediction formulas.

The literature review suggested that there is no general agreement among different investigators on the relative significance of various variables affecting the crack width,

which sometimes leads to differing conclusions. This is at least partly due to the absence of test data that describe the individual effects of each variable. Producing such a data set in the laboratory is expensive and time consuming because of the large number of variables involved, and due to the interdependency of some of the variables. A mathematical model capable of accurately predicting the spacing and width of cracks can be used to overcome this problem if it can include all variables involved in flexural cracking. This is not available at present, and is a main focus in this research.

Various methods of incorporating the tension stiffening effect in deflection calculations are discussed in the second part of this Chapter. For discussion, these methods were divided in to three categories: (*i*) use of effective moment of inertia; (*ii*) curvature evaluated using smeared crack approach with a non-linear stress-strain relationship for tensile concrete, and (*iii*) curvature evaluated using bond forces. It was noted that the first method is simple but may not predict deflections accurately for certain members. In using non-linear stress-strain relationship for tensile concrete, there is no accepted procedure to determine the constitutive relationship applicable for a particular member. Only limited research has been carried out on the use of bond force directly in curvature calculation.

In this thesis, curvature values at sections between adjacent cracks are determined using the bond force in equilibrium conditions. The bond stress at a given section is calculated using a bond stress-bond slip relationship available in literature (Chapter 3). Unlike in previous investigations, a linear strain distribution across the height of the section is not assumed. Instead, the concrete strain and the bond slip are calculated using the analytical procedure developed in this thesis (Chapter 4). The method of calculating the bond force is described in the next Chapter.

CHAPTER 3

BOND STRESS AND BOND SLIP

3.1 General Remarks

As discussed in Chapter 2, the bond force acting at the interface of steel bars and surrounding concrete has a great influence on the initiation and propagation of flexural cracks in reinforced concrete members. Further, the action of bond force is the main contributing factor to the tension stiffening effect in concrete structures. This Chapter will discuss the mechanism of bond force development around a deformed steel bar and the associated bond slip, based on theoretical and experimental investigations carried out by previous researchers. Various bond stress - bond slip relationships proposed by different investigators and the measured bond stress distributions are also described. Finally, the bond stress - bond slip relationship and the bond stress distribution adopted in this thesis will be presented.

3.2 Fundamentals of Bond Stress and Bond Slip

3.2.1 Mechanics of bond force

Bond can be thought of as the shearing force between a reinforcing bar and the surrounding concrete. According to Lutz & Gergely (1967), this force is made up of three components:

(a) Chemical adhesion
(b) Friction
(c) Mechanical interaction between concrete and steel.

Bond of plain bars depends mainly on the first two elements, although there is some mechanical interlocking due to the roughness of the bar surface. Deformed bars on the other hand, depend primarily on the mechanical interlocking for superior bond properties while the contributions from chemical adhesion and friction are secondary. This is evident from the tests by Watstein & Seese (1945), Clark (1949) and Watstein & Mathey (1959) which have indicated that the bonding efficiency of a deformed bar depends mainly on the surface characteristics, especially the bearing area and the spacing and face angle of ribs. Reinforcing bars with larger rib face angles carry higher bond forces than bars with smaller rib face angles, as demonstrated by Esfahani & Rangan (1998) based on experimental results. Also, the tests by Zuo & Darwin (2000) indicated that the bond strength increases with the projected rib area of the reinforcement measured normal to the bar axis.

When a flexural crack is formed in a reinforced concrete member, the strain in the concrete at the crack becomes zero. Subsequently, the concrete near the crack will attempt to regain its original undeformed length resulting in a slip between concrete and the steel bar. For very small slip values (less than 0.003 mm) the movement is achieved by the elastic deformation of the surrounding concrete, and the bond force is entirely dependent on the chemical adhesion of concrete and steel bars (Giuriani *et. al* (1991)). For larger slips values, the chemical adhesion is destroyed and the bond force is provided by the bearing stress acting on the interface of the rib face of deformed bars and concrete.

3.2.2 Bond slip

In a cracked reinforced concrete beam, an increase in loading will result in an increase in steel strain, causing an extension of the reinforcing bar. Consequently, ribs in the bar will tend to move towards the nearest crack relative to the surrounding concrete. This will increase the rib bearing stress on concrete, contributing to a relative slip between steel and surrounding concrete. The slip has the following three components.

(a) crushing of concrete

The rib bearing pressure on concrete may be fairly high causing the porous concrete paste (mortar) to crush. According to Lutz & Gergely (1967), the slip is due almost entirely to this local crushing of the concrete paste, while Giuriani *et. al* (1991) concluded that local crushing contributes only partly to the slip. On the other hand, tests by Mirza & Houde (1979), gave no evidence to indicate that local crushing had taken place in five tensile specimens, which were sawn longitudinally to expose the imprint of the bar.

(b) radial micro-cracking

Experimental results show that radial microcracks occur in concrete adjacent to deformed steel bars resulting in slip due to the relaxation of concrete tensile stress. According to tests by Goto (1971) and Broms (1965*a*), these radial microcracks occur shortly after a flexural crack is formed. They first develop around ribs near the cracks (or ends of specimen) then with increases in steel stress, develop progressively farther from the cracks. Tests by Goto (1971) have shown that these internal microcracks form concrete cones with their apexes near bar ribs and bases directed towards the nearest primary cracks (or ends), as shown in Fig. 3.1.

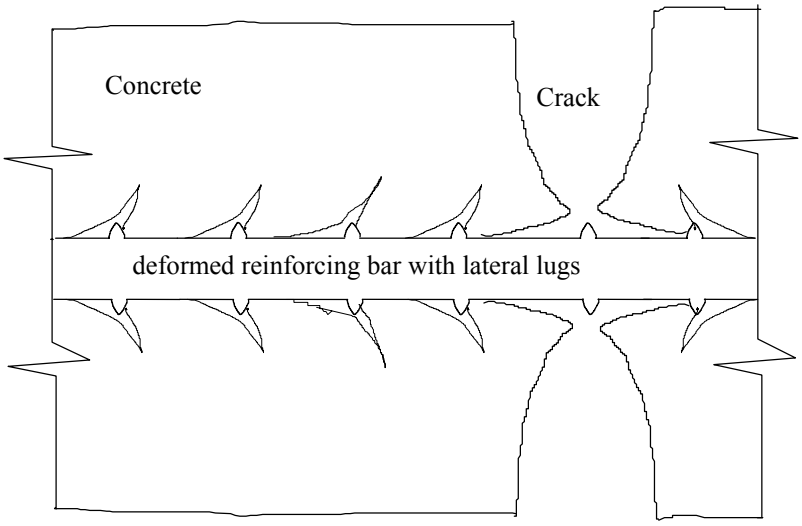

Fig. 3.1 Radial microcracking in concrete around a deformed reinforcing bar (deformations exaggerated for clarity).

In addition to the slip caused by the internal microcracks, they have other implications on cracked reinforced concrete members. Also these internal cracks cause the apparent elongation of the concrete between two flexural cracks along the bar axis to become far greater than the value calculated from the elongation capacity of concrete (Goto (1971)). Due to this elongation the flexural crack faces are not plane, making the crack width at the bar surface smaller than that at the tension face of the beam (see Fig. 3.1).

(c) radial separation of steel and concrete

Lutz & Gergely (1967) reported that an elastic finite element analysis of a concrete cylinder with a concentrically embedded steel bar subjected to a tensile force yields very high radial tensile stresses between the steel and concrete near the crack. Similar results were obtained by Lutz (1970). Since this tensile stress far exceeds the tensile adhesion strength, separation of the bar and the concrete will occur in the vicinity of the crack along a finite length. This separation will not cause the bond force to cease, because the pressure on and the contact with the ribs are not lost. Due to the inclination of the rib faces, the radial separation will result in a longitudinal movement of the concrete adjacent to the steel bar contributing to the slip.

3.2.3 Splitting cracks and effect of stirrups

Wedging action of the bar ribs described above (see Fig. 3.1) may result in splitting the surrounding concrete in cases where the bond slip is relatively high (Gambarova & Karakoc (1982), Gambarova *et al*. (1989), Esfahani & Rangan (1998)). These splitting cracks originate at existing flexural cracks, and propagate longitudinally along the reinforcing bar as shown in Fig. 3.2. These cracks may not always be visible on the member surface, as the splitting crack width is generally smaller than the flexural crack width (Giuriani & Plizzari (1998)).

As revealed by test results of Esfahani & Rangan (1998) and Hwang *et. al* (1996), bond between steel and concrete will be reduced significantly once the splitting crack reaches the outside face of the member. This bond stress reduction is a result of the loss of

radial pressure on the surrounding concrete caused by the formation of splitting cracks. Stirrups placed adjacent to the tension reinforcement can restrict the propagation of splitting cracks, thereby maintaining a higher bond stress. Experimental methods of investigating the effects of stirrups on the measured bond stresses are described in Section 3.3.1, while the results of these experiments are discussed in Section 3.3.2.

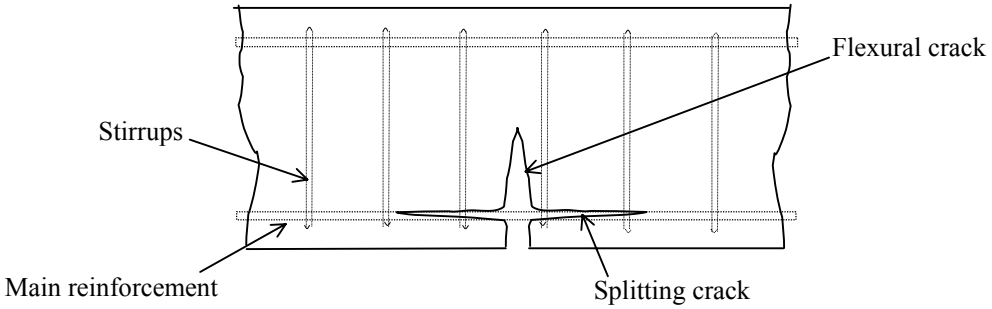

(a) Elevation of a cracked beam

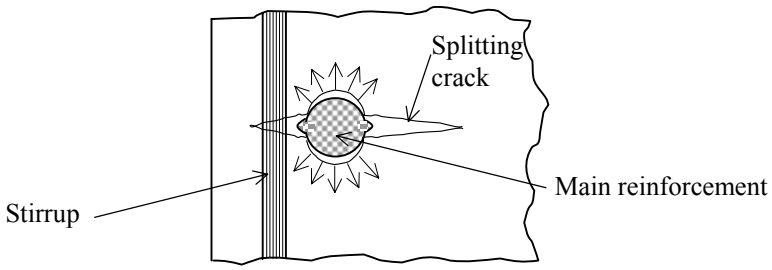

(a) Section through a splitting crack

Fig. 3.2 Development of splitting cracks

3.3 Bond Stress - Bond Slip Relationship

In analytical investigations of cracked reinforced concrete members, the bond stress-bond slip relationship is of fundamental importance. This relationship is directly analogous to the stress-strain law for concrete or steel (Nilson (1972), Edwards & Yannopoulos (1979)). Unlike the constitutive laws for steel or concrete, a unique relationship for bond stress-bond slip is not yet available despite the large number of investigations carried out. Different methods used by various researchers for the measurement of bond stress and bond slip are described below.

3.3.1 Experimental methods of evaluating bond stress and bond slip

Experimental methods used to measure the bond stress and bond slip may be categorised in to the following two groups.

(a) Pull out tests
(b) Uniaxial tensile tests

(a) Pull out tests

In pull out tests, a monotonically increasing tensile force is applied to one end of the steel bar embedded in a rectangular, square or circular concrete prism (see Fig. 3.3). Depending on the length of the specimen used, pull out tests can be categorised in to the following two groups: (i) short pull out tests; and (ii) long pull out tests.

In short pull out tests, the length of the concrete prism is taken as short as practicable (see Table 3.1). Since the specimen length is small, a uniform bond stress distribution can be assumed over the full embedment length. Consequently, the bond stress at a selected load level is calculated by dividing the tensile force in the steel bar by the surface area of the embedded length. The corresponding bond slip is taken as the measured end slip at the loaded end. These results obtained at various load levels are used to develop the bond stress-bond slip relationship, which is described in Section 3.3.2.

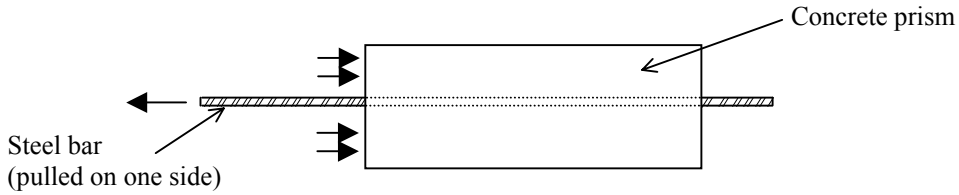

Fig. 3.3 A pull out test specimen

Table 3.1 Details of specimens tested by various investigators

Investigator(s)		Type of test	Cross section (mm)	Specimen length (mm)	Deformed bar diameter (mm)
1	Mirza & Houde (1979)	Pull out	52 x 52 to 152 x 152	410, 835	25, 19, 12
2	Kankam (1997)	Pull out	150 x 150	200	25
3	Perry & Thompson (1966)	Pull out	127 x 110	230	22
4	Edwards & Yannopoulos (1979)	Pull out (#)	148 x 66 and 168 x 86	38	16
5	Esfahani & Rangan (1998)	Pull out (#)	250 x 110 to 250 x 324	55 to 90	20, 24
6	Eligehausen *et. al* (1983)§	Pull out (#)	300 x 135 300 x 225	95, 160	19, 32
7	Soroushian & Choi (1989)§	Pull out (#)	305 x 112 305 x 154 305 x 175	80, 110, 125	16, 22, 25
8	Lahnert *et. al* (1986)	Pull out	152 x 152	225,380	19, 22
		Tension	152 x 152	460	22, 25
9	Mains (1951)	Tension	305 x 200	530	16
10	Nilson (1972)	Tension	152 x 152	460	25
11	Jiang *et. al* (1984)	Tension	76 x 76 to 114 x 114	127	19

(#) Short Pull out tests
(§) Specimens with stirrups

As already described in Section 3.2.3, the confining action of transverse steel (stirrups) placed near the tension reinforcement can restrict the propagation and widening of splitting cracks, thereby maintaining a higher bond stress even at larger slip values. Eligehausen *et. al* (1983) and Soroushian & Choi (1989) have used pull out test

specimens with stirrups placed as shown in Fig. 3.4. The results obtained from these tests are described later in Section 3.3.2.

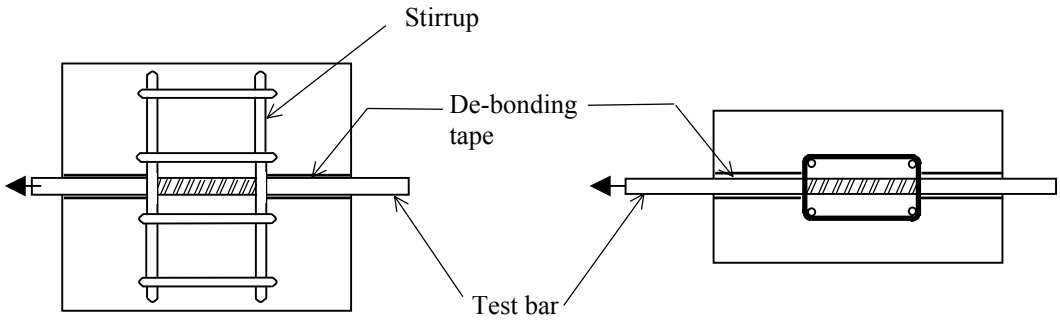

(*a*) Elevation (*b*) Plan

Fig. 3.4 Arrangement of stirrups in test specimens used by Eligehausen et al. (1983) and Soroushian & Choi (1989)

In long pull out test specimens, the bond stress varies along the embedded length of the steel bar. To determine the bond stress along the steel bar, the steel strain is measured using strain gauges attached at various locations. The bond force acting on the steel bar between two strain measurement points is taken as the difference in tensile forces at the two sections. The bond stress is then evaluated by dividing the bond force by the surface area of the steel bar between the two measurement points. Generally the bond slips at respective points are determined indirectly using the measured end slip values corresponding to the steel stress at that point. To measure the bond slip directly, Nilson (1972) used an additional set of internal strain gauges embedded in the concrete 13 mm away from the bar surface. The difference in the measured strain values in steel and concrete was then used to calculate the local slip along the bar surface.

Different methods have been used to attach the strain gauges on the steel bar in the test specimen. In the most common method, the bar is first milled into two equal parts through the diameter, and a longitudinal groove of rectangular cross section is milled on the flat surface along the centre line in each part (see Fig. 3.5*a*). Strain gauges are attached to the inside surface of the groove and then the two parts of the bar are welded

together. In some investigations, the bar is not cut into equal parts. In such cases, the groove is milled only in the larger piece so that the hole in the welded bar is located at the centre (See Fig. 3.5*b*).

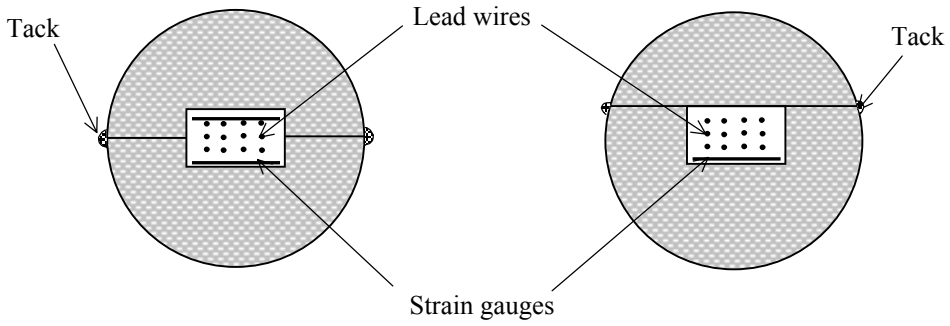

(*a*) Bar milled at centre (*b*) Bar milled off centre

Fig. 3.5 Arrangement of strain gauges in a test bar

A slightly different arrangement was used by Lahnert *et. al* (1986), which enabled the measurement of local slip directly. In this method, a small coil was inserted in a hole made in the steel bar (see Fig. 3.6). This coil produced a magnetic field which was sensed by a target embedded in concrete away from the bar surface. A series of such coils and targets measured the local slip along the length of the specimen. In this experiment, the strain gauges were attached to the steel bar in a way slightly different to the method described in the previous paragraph. They were attached to two grooves milled on the outside surface of the bar, diametrically opposite, without cutting the bar into two parts (Fig. 3.6).

It must be mentioned that a considerable amount of scatter may be expected in the bond stresses measured by the method described above. This is because the bond stress is only a small fraction of the stress in the steel bar; hence a small error in strain measurement can cause a large difference in the calculated bond stress (Jiang *et al*. (1984)).

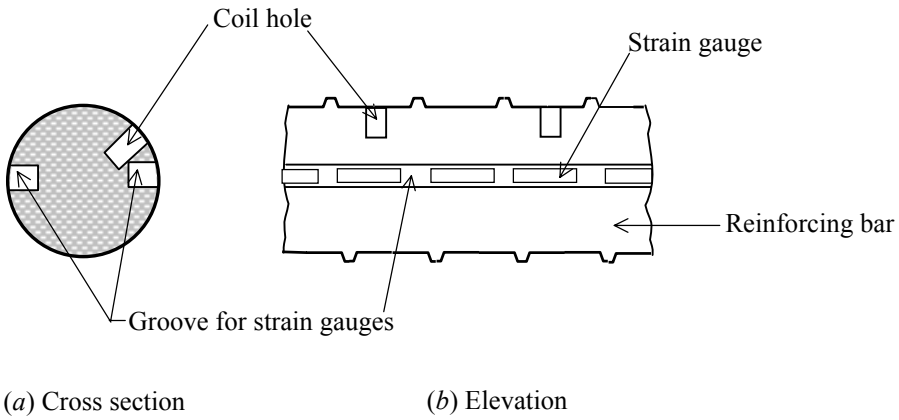

Fig. 3.6 Instrumented reinforcing bar used by Lahnert *et. al* (1986)

(b) Uniaxial tensile tests

In uniaxial tests, a monotonically increasing tensile force is applied to the two protruding ends of the steel bar embedded in the concrete prism as shown in Fig. 3.7. Strain gauges are attached at different locations along the steel bar, using the same procedure described previously for long pull out test specimens. At each load level, strain measurements are recorded, and the bond stress and the corresponding bond slip are determined using the same procedure described previously. In addition to the development of bond stress-bond slip relationships, results of uniaxial tensile tests can also be used to investigate the bond stress distribution along the length of the embedded bar (Section 3.4). Table 3.1 shows the dimensions of uniaxial tensile test specimens and the type of reinforcements used by various investigators. The results obtained from these tests are discussed in the next Section.

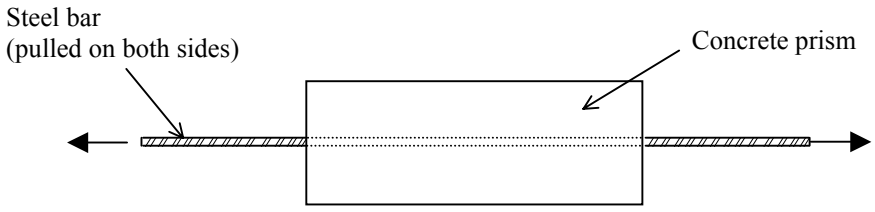

Fig. 3.7 A uniaxial tensile test specimen

3.3.2 Experimental results of bond stress-bond slip relationships

In this Section, bond stress-bond slip relations developed by various researchers based on experimental work outlined previously are discussed. Out of the 11 investigations mentioned in Table 3.1, only 8 researchers have used the results to develop bond stress-bond slip relationships. For the discussion in this thesis, these relationships are categorised in to two groups: They are: (i) bond stress-bond slip relationships involving large slip values (about 10mm), and (ii) those involving small slip values (less than 0.1mm).

(a) bond stress for large slip values

Fig. 3.8 shows the bond stress-bond slip relationship developed by Eligehausen *et al*. (1983) using the results of short pull out tests, involving large slip values. Transverse steel (stirrups) have been used in these test specimens to provide the confinement, which facilitates the specimen to undergo a relatively large slip before the bond failure. These test specimens closely simulate the conditions in anchorage zones and splices with lapped bars where relatively large bond slips take place (Soroushian & Choi (1989)).

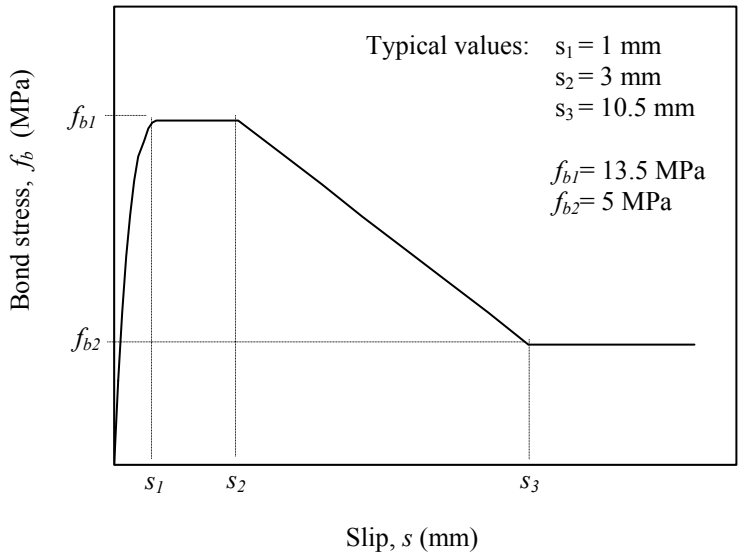

Fig. 3.8 Bond stress-bond slip relationship for large slip values (Eligehausen *et al*. (1983))

Values of s_1, s_2, s_3, f_{b1} and f_{b2} shown in Figure 3.8 depend on various parameters including the bar diameter, concrete strength and the distance between lugs of the reinforcing bar (Soroushian & Choi (1989), Youssef & Ghobarah (1999)). By adopting appropriate values for the variables shown in Fig. 3.8, this relationship has been used in many analytical investigations for calculating the concrete and steel stress distributions in anchorage zones (Soroushian & Choi (1991), Monti *et. al*. (1997), Gravina & Warner (1999), Ayoub & Filippou (1999), Youssef & Ghobarah (1999), Spacone & Limkatanyu (2000) and Limkatanyu & Spacone (2002)). Unlike in anchorage zones, the slip values encountered near flexural cracks are much smaller than those shown in Fig. 3.8 (in the range of 0.1mm). As this thesis concentrates on flexural cracks, the above bond stress-bond slip relationship, which is more relevant to large slip values, is not discussed any further.

(b) bond stress for small slip values

Figure 3.9 shows bond stress-bond slip relations proposed by various investigators based on the results of tests involving small slip values. Bond stress in this figure has been expressed as a function of the square root of the concrete strength, $\sqrt{f'_c}$ to account for the differences in concrete strengths used in various tests.

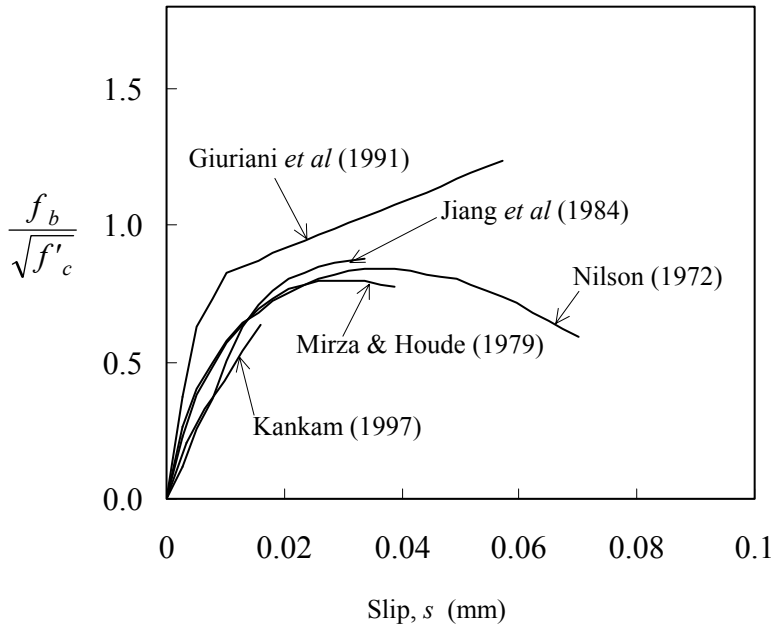

Fig. 3.9 Bond stress-bond slip relationships for small slip values

Considering the large scatter normally encountered in bond stress and bond slip measurements, the difference between various relationships shown in Fig. 3.9 can be considered to be small, for slip values less than 0.03mm. For larger slip values this difference tends to rise as the bond stress curves proposed by Jiang *et al.* (1984), Nilson (1972) and Mirza & Houde (1979) have descending branches for slip values larger than 0.03mm (Fig. 3.9). This decline in bond stress for large slip values may be attributed to the reduction in radial pressure on the reinforcement due to the formation of internal splitting cracks (Section 3.2.3), as the specimens used did not contain stirrups. It may be noted that the relationship proposed by Giuriani *et. al* (1991) is based on the results of test specimens containing stirrups (tested by Eligehausen *et.al* (1983)), and does not show a decline in bond stress for the range of slip values shown in Fig. 3.9. It is worth mentioning here that a decline in bond stress is not observed until the slip reaches about 3mm for test specimens containing stirrups (see Fig. 3.8).

3.3.3 Bond stress-bond slip relationship used in the thesis

As described in the previous paragraph, the relationship proposed by Giuriani *et. al* (1991) shown in Fig. 3.9 can be considered to be the most appropriate for using in this thesis. This is because all practical beams contain stirrups while one-way slabs are provided with transverse steel, which offer the confinement against splitting cracks. The bond stress-bond slip relationship proposed by Giuriani *et. al* (1991) can be expressed mathematically as

$$\frac{f^*_b}{\sqrt{f'_c}} = 150s \qquad \text{if } s \le 0.004 \qquad (3.1a)$$

$$\frac{f^*_b}{\sqrt{f'_c}} = 0.47 + 33s \qquad \text{if } 0.010 \ge s \ge 0.004 \qquad (3.1b)$$

$$\frac{f^*_b}{\sqrt{f'_c}} = 0.71 + 9s \qquad \text{if } s > 0.010 \qquad (3.1c)$$

where the bond stress f^*_b and the concrete strength f'_c are in *MPa* and the slip s is in *mm*.

3.3.4 Effect of the distance from the crack

Experiments by Nilson (1972) have shown that different bond stress-bond slip relationships exist for different points along the steel bar depending on the distance from the free end of a specimen (distance from the crack in a beam). Tests by Tassios & Koroneos (1984), Jiang *et. al* (1984) and Kankam (1997) have also indicated that different constitutive relationships exist for different points along the steel bar. Out of the many bond stress-bond slip relationships proposed by Nilson (1972) for various points along the steel bar, only the curve applicable for points more than 153mm away from the free end of the specimen is included in Fig. 3.9. Similarly, Kankam's curve shown in this figure is only applicable for points more than 75mm away from the free end of the specimen.

Fig. 3.10 shows various bond stress-bond slip relationships proposed by Nilson (1972) for different points along the steel bar in a uniaxial tensile test specimen. It can be seen that the bond stress developed at a point near the end of the specimen is smaller compared to the corresponding bond stress developed for the same slip value at a point near the mid-section. Further, the magnitude of the bond stress developed for a particular slip value can be approximated to be a linear function of the distance from the end of the specimen, up to a distance of 153 mm.

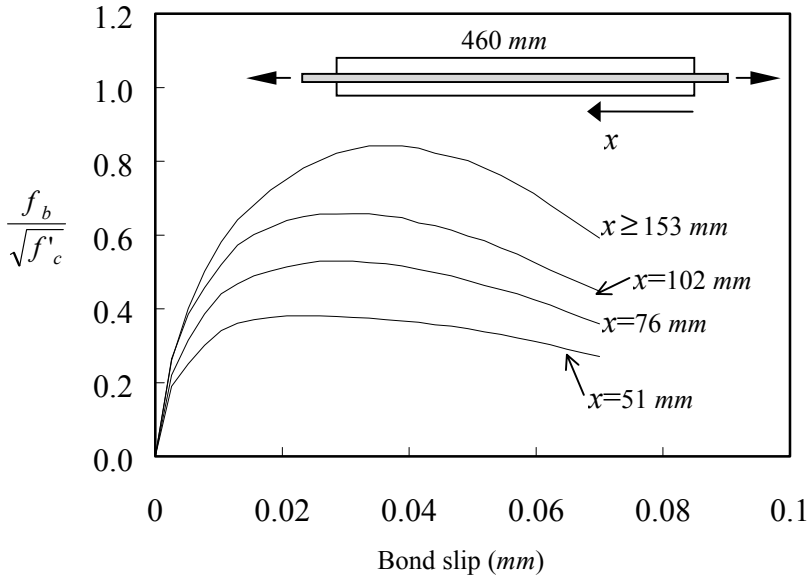

Fig. 3.10 Bond stress-bond slip relationships for various points along a bar (Nilson (1972))

The above decline in bond stress at the ends of the specimen can be related to the radial separation between the bar surface and concrete, which was already described in Section 3.2.2*c*. This separation has the same effect as splitting cracks in reducing the radial pressure around reinforcing bars, resulting in a reduction of the bond stress.

According to the test results of Nilson (1972), the bond stress-bond slip relationship varies only for a distance up to 153mm from the free end. For points beyond this distance, the bond stress-bond slip relationship remained unchanged. This limiting distance of 153mm was observed in a single bar size of 25.4 mm. It is reasonable to assume that this limiting distance depends on the bar diameter ϕ, when different bar sizes are used. According to the test results of Nilson (1972), this limiting distance is equal to 6ϕ, while the test results of Kankam (1997) suggested a distance of 3ϕ. For the calculation of bond stress in this thesis, this limiting distance is taken as 4ϕ, which is close to the mean of the two values mentioned above.

Consequently for the use in this thesis, the bond stress obtained from the relationship proposed by Giuriani, *et. al* (1991) is used without any modification, if the bond stress is calculated at a distance larger than 4ϕ measured from the nearest crack. For points that are closer than 4ϕ, the bond stress obtained from the above relationship is reduced proportionately according to the distance from the nearest crack. Thus, the bond stress f_b calculated at any point can be expressed as

$$f_b = \gamma f^*_b \tag{3.2}$$

where f_b = bond stress at the point; and f^*_b = bond stress obtained using Eq. 3.1. In this equation, γ is the reduction factor that depends on the distance from the nearest crack to the point where f_b is calculated. Using the linear variation assumption mentioned previously, the value of this reduction factor is determined as

$$\gamma = \frac{x}{4\phi} \leq 1 \tag{3.3}$$

in which x is the distance from the nearest crack to the point where the bond stress f_b is calculated.

3.4 Bond Stress Distribution

In a tensile test specimen, before any cracks are formed, the slip and the bond stress at the mid point between the two ends will be zero due to symmetry. The bond stress at the two free ends of the specimen will also be zero, although the slip is the largest at these points. The same arguments are valid for a concrete section between two successive cracks in a tensile test specimen, *i.e*., zero bond stresses at the two cracked sections and at the mid point. Variation of the bond stress between these two *zero-points* (between the mid point and the nearest cracked section) established by previous investigators based on experimental results is described below.

3.4.1 Experimental results of bond stress distribution

The results of uniaxial tension tests carried out by Jiang *et al* (1984) for developing bond stress-bond slip relationship (Section 3.3.1) were also used to investigate the bond stress distribution between adjacent flexural cracks. In this experiment, two types of specimens *Type A* and *Type B* were tested. For the preparation of *Type A* specimen, a deformed reinforcing bar was split into two halves and the two parts were embedded on opposite faces of the concrete prism as shown in Fig. 3.11(*a*). The strain gauges were then attached on to the exposed sides of the half-steel bars. In *Type B* specimen, the reinforcing bar was embedded at the centre of the cross section as shown in Fig. 3.11*b*. (Before the embedment of this steel bar, it was split in to two halves and welded together after attaching the strain gauges, as shown in Fig. 3.5*a*.)

In *Type A* specimens, the two half-bars were connected together by welding a steel plate at each end, as shown in Fig. 3.11(*a*). A gradually increasing load was then applied to these plates through a pin connection. To prevent any movement of the two half-bars away from each other, a steel bar of 3mm diameter was welded at the centre of the specimen as shown.

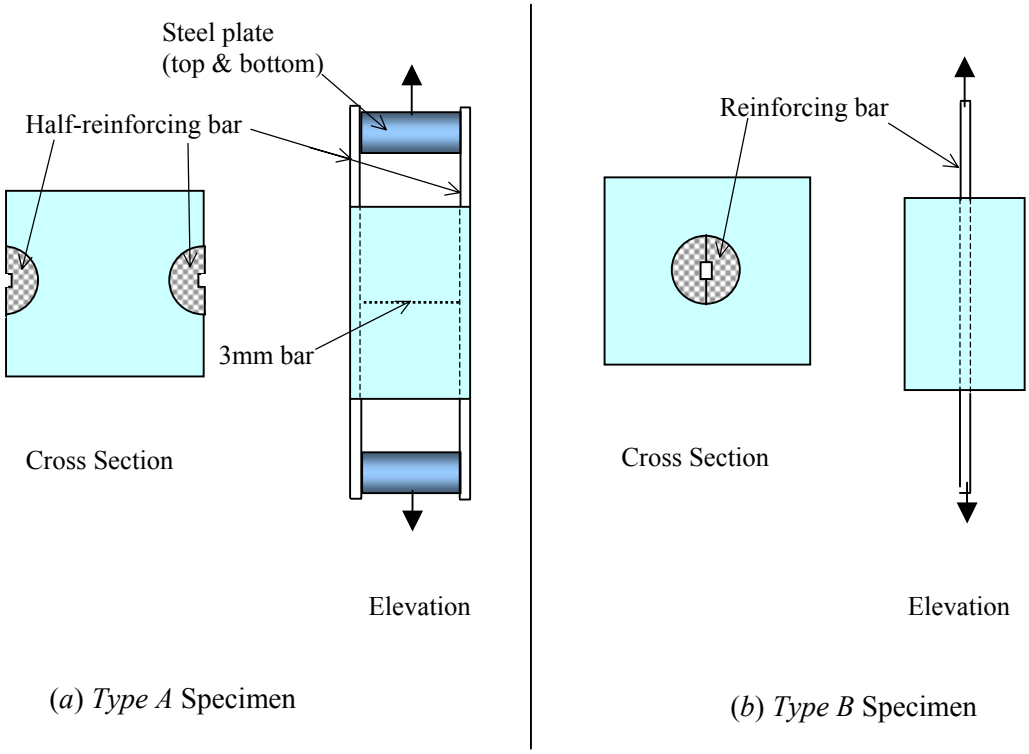

Fig. 3.11 Uniaxial tension specimens tested by Jiang *et. al* (1984)

Altogether eight specimens (four from each type) were tested, and the resulting bond stress along the length of the specimen was calculated at various load levels, using the measured strains. The bond stress distributions obtained from these tests are reproduced in Fig. 3.12(*b*).

A Similar experiment was carried out by Kankam (1997) using 200mm long 150mm x 150mm square specimens with a 25mm diameter reinforcing bar embedded at the centre (see Table 3.1). Both plain round bars and hot-rolled deformed bars were used in this experiment. Strain gauges were attached to the centre of the bar by splitting the reinforcement in to two halves as shown in Fig. 3.5(*a*). The bond stress distributions obtained from these tests are reproduced in Fig. 3.12(*c*). Note that only the results of deformed bars are included, because the use of plain round bars as main reinforcement is not very common in practice at present, and therefore, not considered in this thesis.

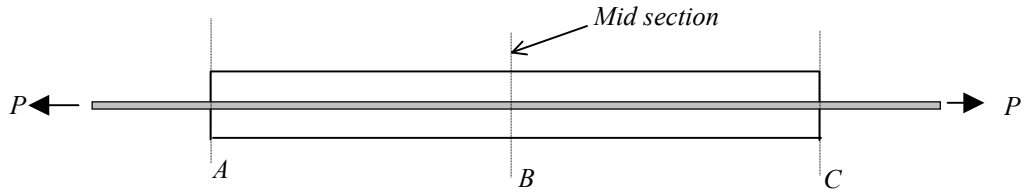

(a) Uniaxial tensile specimen

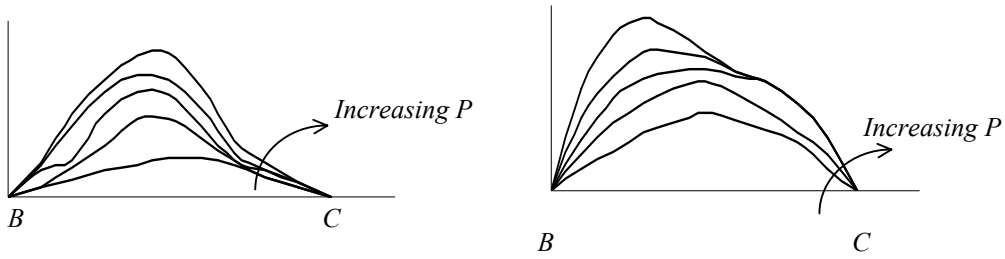

(b) Experimental results of Jiang et al (1984)

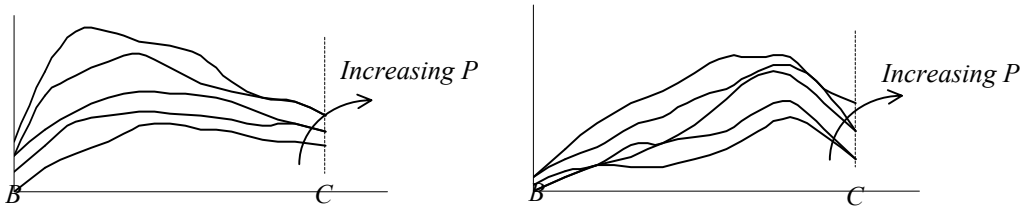

(c) Experimental results of Kankam(1997)

Fig. 3.12 Experimental results of bond stress distribution

Inspection of Fig. 3.12 indicates that the bond stress at mid point of the specimen (section *B*) is zero as expected due to symmetry. According to Fig. 3.12(*b*), the bond stress is also zero at the free end (section *C*), while Fig. 3.12(*c*) gives non-zero values at this section. In all cases, the peak value of the bond stress occurs in between the free end and the mid point of the specimen. Further, Fig. 3.12(*b*) shows that the peak bond stress at moderate load levels occurs close to the mid-way between the two zero points (sections *B* and *C*).

3.4.2 Bond stress distribution used in the thesis

While Fig. 3.12*b* and 3.12*c* do not totally agree with regards to the bond stress at the free end, it is considered more appropriate to assume a zero bond stress at section *C*, as seen in Fig. 3.12(*b*). For the calculation of bond stress in this thesis, it is further assumed that the peak bond stress occurs at the mid section between the two zero points, with a parabolic variation. These two assumptions greatly simplify the mathematical formulation in calculating the bond stress, while the resulting bond stress distribution closely agrees with the experimental observations discussed above. The resulting parabolic bond stress distribution between two successive flexural cracks is shown in Fig. 3.13. Note that points *A, B* and *C* in this figure correspond to the same points shown in Fig. 3.12(*a*).

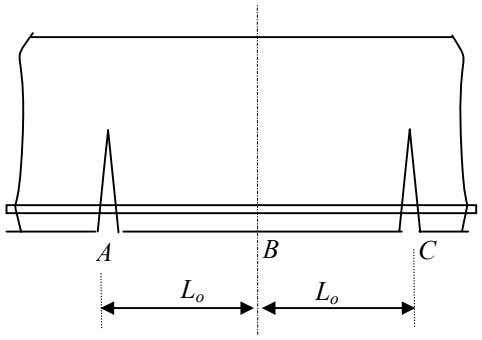

Beam section between two successive flexural cracks

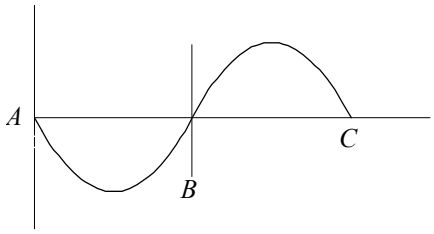

Assumed bond stress distribution

Fig. 3.13 Assumed bond stress distribution between adjacent flexural cracks

Using the parabolic variation, the bond stress at any point x away from the zero-slip section can be expressed in terms of the peak bond stress as

$$f_{bx} = 4 f_{bo} \frac{x}{L_o}\left(1 - \frac{x}{L_o}\right) \qquad x \le L_o \qquad (3.4)$$

where f_{bo} = peak bond stress that occurs at the mid section between the two zero stress points (see Fig. 3.14); f_{bx} = bond stress at a distance x away from the zero-slip section; and $2L_o$ is the distance between adjacent cracks.

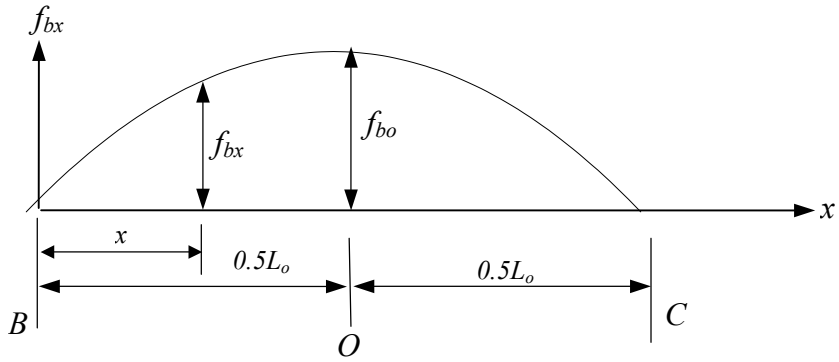

Fig. 3.14 Variation of bond stress between zero-slip section and cracked section (B: zero-slip section; C: cracked section; $2L_o$=crack spacing)

It may be noted that the entire bond stress distribution between the two *zero stress* points can be established once the peak bond stress f_{bo} is calculated. Its value is determined by calculating the slip s_o at point O (see Fig. 3.14), and using the bond stress-bond slip relationship given in Eq. 3.1. The bond stress f^*_{bo} obtained from this relationship is modified using Eqs. 3.2 and 3.3 to account for the effect of distance from the nearest crack as already described in Section 3.3.4. It must be noted that the variable x in Eq. 3.3 is replaced by $0.5L_o$ (see Fig. 3.14) where $0.5L_o$ is the distance from the nearest crack to the point where f_{bo} is calculated.

3.5 Summary

The mechanism for the development of bond stress and bond slip together with the experimental methods used by previous researchers to measure their values are discussed in this Chapter. Constitutive relationships for bond stress and bond slip developed by different investigators using experimental results are also presented. It was noted that the bond stress-bond slip relationship for different points along the steel bar varies, depending on the distance from the nearest crack. While several constitutive relationships are available in literature, no one has attempted a comparative study on the validity of the different proposals. It was noted that only the constitutive relationship proposed by Giuriani *et al* (1991) has incorporated the effects of stirrups. Therefore, this relationship is considered to be the most appropriate one for using in this thesis.

To be consistent with experimental results, a parabolic bond stress distribution is assumed between the cracked section and the zero-slip point (where the bond slip is zero). The peak value of the parabolic bond stress distribution is determined by calculating the local slip at that point and using the above bond stress-bond slip relationship. The bond stress obtained by this relationship is then modified according to the distance from the nearest crack to the point where the peak bond stress occurs. This modification is required as the constitutive relationship varies with the distance from the nearest crack to the point under consideration.

CHAPTER 4

EVALUATION OF CONCRETE AND STEEL STRESSES NEAR FLEXURAL CRACKS

4.1 General Remarks

In this Chapter, equations are derived for the determination of forces acting on a free-body concrete block located between two transverse sections of a loaded reinforced concrete member. Axial and bending forces acting on transverse sections and bond forces acting at reinforcement level are calculated using equilibrium conditions. Iterative procedures are used in these calculations because of the non-linear nature of the constitutive relationships used for concrete and bond stress. Also included is the finite element analytical procedure used to calculate the concrete stress distribution between two transverse sections of a beam. Finite element mesh, boundary conditions and the element type used in the analysis are also described.

4.2 Assumptions Made in the Evaluation of Stresses

The following assumptions are made in the calculations:

(*a*) Steel and concrete are assumed to be homogeneous and isotropic;

(*b*) Concrete stresses due to shrinkage and temperature changes are negligible;

(*c*) Stress-strain relationships for concrete and steel are governed by the constitutive laws described in Section 4.3;

(*d*) The bond stress varies parabolically along steel bars, as described in Section 3.4.2;

(*e*) The peak bond stress is related to the local slip via the constitutive relationship described in Section 3.3.3;

(*f*) The total bond force acting around steel bars at a particular section can be replaced by a shear force uniformly distributed across the width of the beam;

(*g*) Plane sections remain plane in bending at all sections before the development of the first crack, and only at cracked sections afterwards.

4.3 Constitutive Relationships for Concrete and Steel

The non-linear stress-strain relationship, consisting of a parabolic ascending part and a linear descending part used by Park & Paulay (1975) is adopted for the concrete in compression. This constitutive relationship, which has been originally developed by Hognestad (1951) can be expressed as

$$\sigma = f'_c \left[\frac{2\varepsilon}{\varepsilon_o} - \left(\frac{\varepsilon}{\varepsilon_o} \right)^2 \right] \qquad \text{if } \varepsilon \le \varepsilon_o \qquad (4.1a)$$

and $$\sigma = f'_c - 83 f'_c (\varepsilon - \varepsilon_o) \qquad \text{if } \varepsilon_1 \ge \varepsilon > \varepsilon_o \quad (4.1b)$$

where σ = concrete stress; ε = concrete strain; f'_c = characteristic strength of concrete; $\varepsilon_o = 0.002$; and $\varepsilon_1 = 0.0038$.

For concrete in tension, a linear stress-strain relationship is used up to the cracking strain of concrete (see Fig. 4.1). The elastic modulus of concrete in tension is taken as the initial tangent modulus of concrete in compression, which is equal to 1000 f'_c for the relationship defined by Eq. 4.1*a*. The stress strain relationship used for steel is shown in Fig. 4.2.

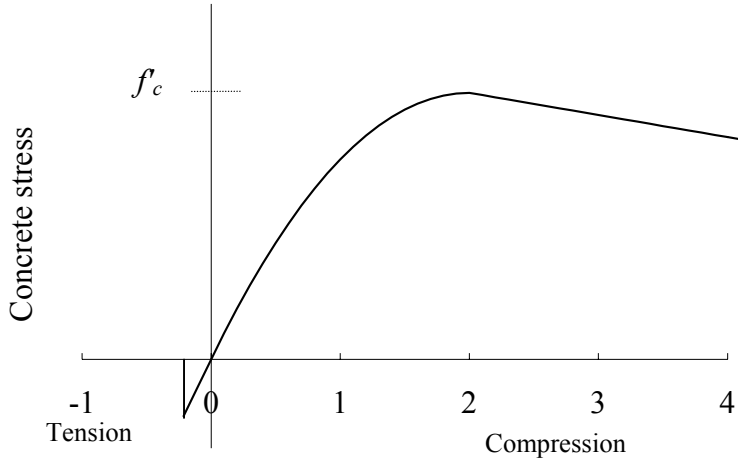

Fig. 4.1 Constitutive relationship for concrete

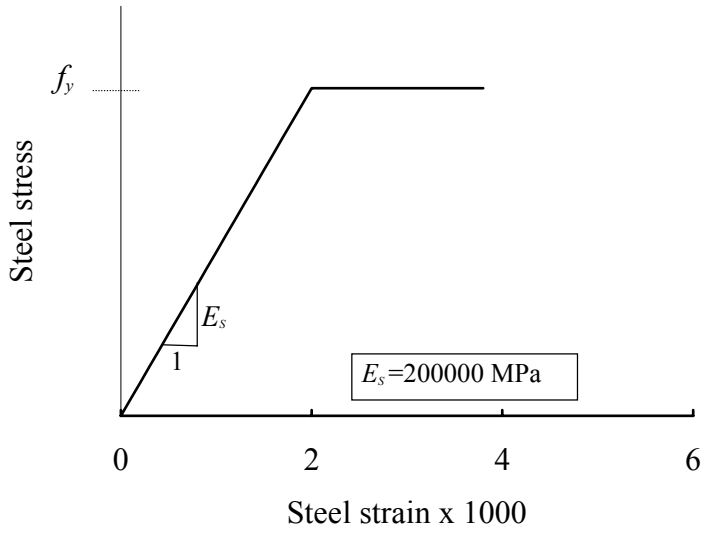

Fig. 4.2 Constitutive relationship for steel

4.4 Forces Acting on Transverse Sections in an Uncracked Beam

Fig. 4.3 shows the strain and stress distributions at a transverse section of a beam where the maximum bending moment is less than that is required to form a flexural crack. According to assumption (*g*) in Section 4.2, the strain distribution is taken to be varying linearly across the depth of the beam. The resulting stress distribution is determined using the stress-strain relationship given by Eq. 4.1. Note that the concrete stress f_t at the tension face has not reached f_r anywhere in the beam, where f_r is the flexural strength of concrete.

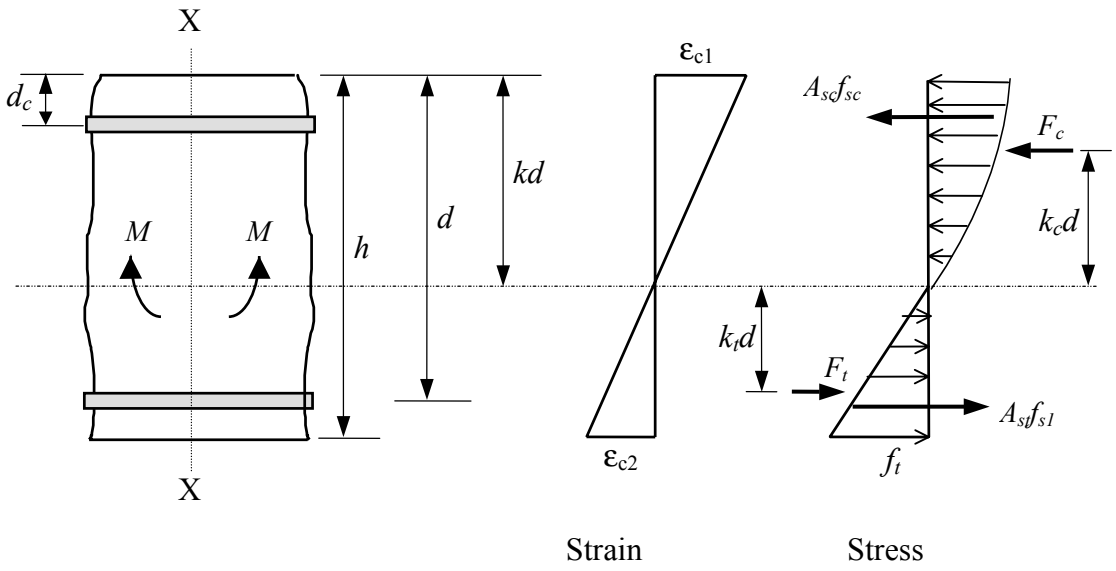

(*a*) Part of uncracked beam (*b*) Strain and stress distributions at section X-X

Fig. 4.3 Stress and strain distributions at a transverse section in an uncracked beam

For a given bending moment *M* at the section, the stress distribution shown in Fig 4.3(*b*) can be evaluated if the maximum concrete strain, ε_{c1} and the depth of compression zone, *kd* are known. These two unknowns can be determined by solving the following two simultaneous equations (Eqs. 42*a* and 4.2*b*), derived from the conditions of translational and rotational equilibrium of the section.

For translational equilibrium,

$$F_c + A_{sc}f_{sc} = F_t + A_{st}f_{s1} \qquad (4.2a)$$

and for rotational equilibrium,

$$M = F_c\, k_c d + A_{sc}f_{sc}(kd-d_c) + F_t k_t d + A_{st}f_{s1}(d-kd) \qquad (4.2b)$$

where F_c and F_t = total compressive and tensile forces offered by concrete, respectively; A_{st} = total tensile steel area; f_{s1} = tensile steel stress; $k_c d$ and $k_t d$ = distances from the neutral axis to the centroids of compressive and tensile stress blocks, respectively (see Fig. 4.3); A_{sc} = compression steel area (if any); f_{sc} = stress in compression steel; and d_c = depth to compression steel from the extreme face as shown.

To solve for the maximum concrete strain and the depth of compression zone, all the unknown quantities appearing in Eq. 4.2 need to be expressed in terms of ε_{c1} and kd as indicated below.

The total compressive force, F_c acting on the section is obtained by the following integral.

$$F_c = \int_{y=0}^{y=kd} b\Phi(\varepsilon)dy \qquad (4.3)$$

where b and ε are the width and strain at a distance y above the neutral axis respectively, and $\Phi(\varepsilon)$ is the compressive stress computed using the constitutive relationship given in Eq. 4.1. Note that for flanged beams, the width b is expressed in terms of y as $b=\psi(y)$. The strain ε at any distance y can be expressed as a linear proportion of ε_{c1} using Fig. 4.3(b) as follows.

$$\varepsilon = \frac{y}{kd}\varepsilon_{c1}\,. \qquad (4.4)$$

The distance from the neutral axis to the centroid of the compression stress block $k_c d$ can be obtained from the following equation.

$$F_c . k_c d = \int_{y=0}^{y=kd} b\Phi(\varepsilon) y dy \tag{4.5}$$

The total tensile force F_t can be calculated by the following integral.

$$F_t = \int_{y_1=0}^{y_1=h-kd} b\left(E_{ci} \frac{\varepsilon_{c1}}{\mathrm{kd}} y_1 \right) dy_1 \tag{4.6}$$

where y_1 is measured from the neutral axis towards the tension face, E_{ci} is the elastic modulus of concrete in tension and h is the total height of the beam.

The tensile and compressive stresses in reinforcing bars f_{s1} and f_{sc} respectively, are calculated using corresponding strains as follows.

$$f_{s1} = E_s \left[\frac{d - kd}{kd} \right] \varepsilon_{c1} \tag{4.7}$$

$$f_{sc} = E_s \left[\frac{kd - d_c}{kd} \right] \varepsilon_{c1} \tag{4.8}$$

where E_S is the elastic modulus of steel. To determine the concrete and steel stresses for a given bending moment M ($<M_{cr}$ the cracking moment of the beam), Eqs. 4.2 to 4.8 are solved simultaneously. Due to the non-linear nature of the constitutive relationship for concrete, a trial and error procedure is used for this calculation. Note that in Fig. 4.3*b*, $k_t d = \frac{2}{3}(h - kd)$, due to the linear variation of concrete tensile stress.

The step-by-step procedure adopted for solving these equations is as follows:

(*a*) select a trial value for ε_{c1}

(*b*) select a trial value for kd

(*c*) calculate F_c, F_t, f_{s1}, f_{sc} and $k_c d$ using Eq. 4.3 to 4.8

(*d*) check whether Eq. 4.2*a* is satisfied with a pre-selected tolerance (Section 4.8). If not, change the value of *kd* and go to step (*c*). Once the equation (4.2*a*) is satisfied go to step (*e*).

(*e*) check whether Eq. 4.2*b* is satisfied with a pre-selected tolerance. If not, change the value of ε_{c1} and go to step (*b*). If Eq. 4.2*b* is satisfied, then the selected values of ε_{c1} and *kd*, and the calculated values of F_c, F_t, f_{s1}, f_{sc}, $k_c d$, and $k_t d$ are acceptable.

A computer program written in BASIC language (program name = *FORCES.BAS*) is used for the above calculation (see *Appendix E1* to *E15* for the source program of *FORCES.BAS*). Flowchart that describes the steps used in the calculation is shown in Fig. 4.4, and the structure of the computer program is described later in Section 4.8. This program is used to calculate the concrete and steel stresses at cracked and uncracked sections as well as the bond stress at reinforcement level, as described in relevant Sections in this Chapter. Once the concrete and bond stresses are calculated, they are converted to equivalent nodal forces and stored in computer data files for subsequent use in the finite element analysis, which is described in Section 4.11. These stored data are later retrieved using *Microsoft Excel* and the nodal forces are input into the finite element mesh manually. Manual input was selected as the number of nodal forces involved is not very large. There are only 11 nodes associated with the bond force. On transverse sections in cracked beams, non-zero forces exist only at a small number of nodes, mostly less than 10 depending on the depth of compression zone. Only for uncracked beams, the force on the transverse section needs to be applied on the full height of the beam (25 nodes). More details on the finite element mesh are given in Section 4.11.

As an example, the nodal forces calculated by the program *FORCES.BAS* on uncracked sections of two typical beams are shown in *Appendix A*. *Appendix A1* shows the sectional properties of the two beams, and the calculated nodal forces are given in *Appendix A2* and *A3*. *Appendix C1* shows the locations of the nodes at which these nodal forces are applied on the finite element mesh.

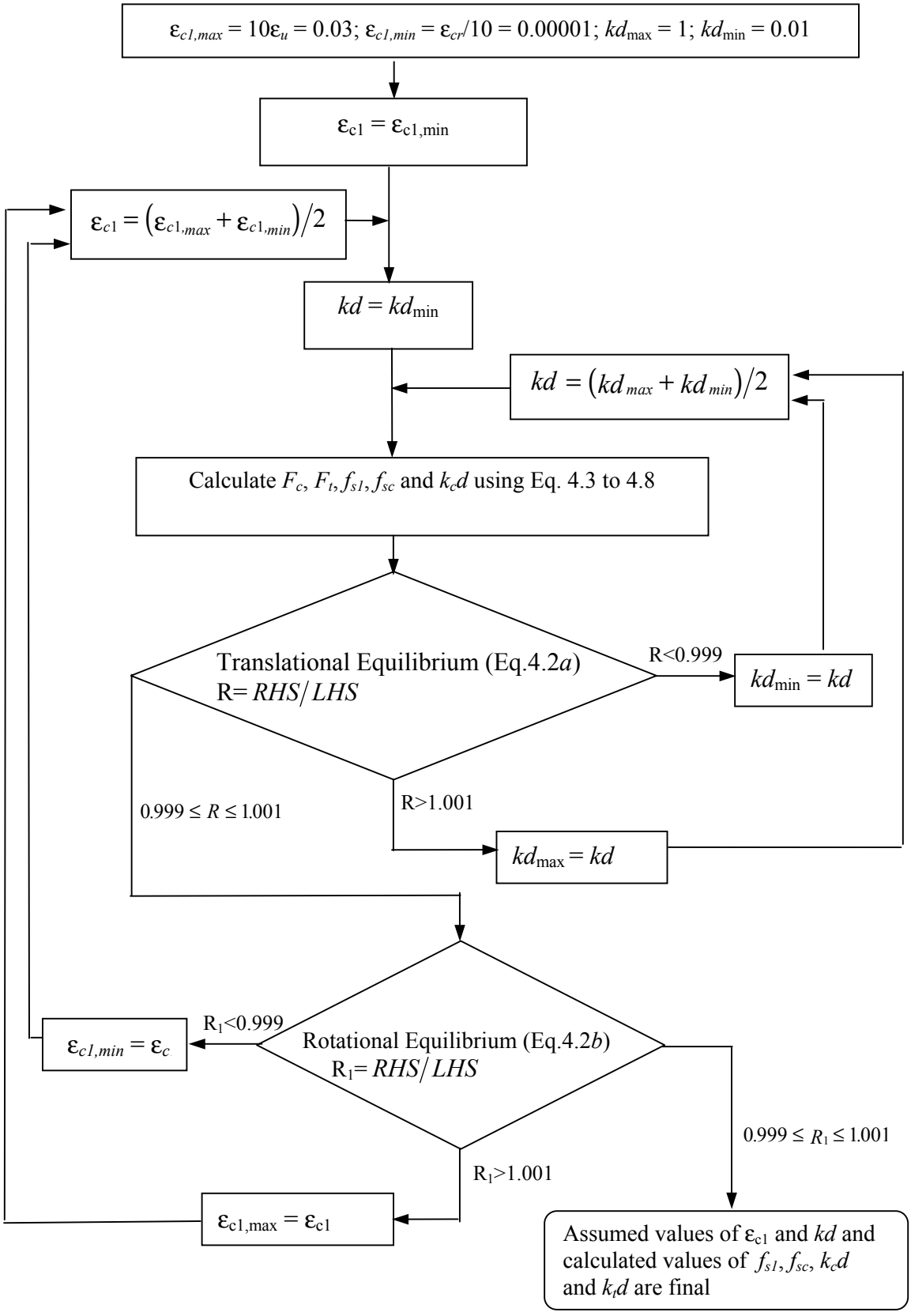

Fig. 4.4 Flowchart for calculating forces in an uncracked section

4.5 Cracking Moment of the Beam M_{cr}

The cracking moment of a beam is calculated using the trial and error procedure described in the previous Section with slight modifications. At the onset of cracking, the maximum tensile strain ε_{c2} is known (Fig. 4.3), and therefore, the depth of compression zone *kd* can be calculated for a selected trial value of ε_{c1} using the following expression.

$$kd = \left[\frac{\varepsilon_{c1}}{\varepsilon_{c1} + \varepsilon_{c2}}\right] h \tag{4.9}$$

where the maximum tensile strain ε_{c2} at the onset of cracking is given by

$$\varepsilon_{c2} = \frac{f_r}{E_{ci}}. \tag{4.10}$$

In Eq. 4.10, f_r is the flexural strength of concrete determined using the following relationship recommended by Standards Association of Australia (AS3600 (2001)).

$$f_r = 0.62\sqrt{f'_c}\ MPa \tag{4.11}$$

where f'_c is the characteristic strength of concrete in *MPa*. To calculate M_{cr}, a trial value is selected for ε_{c1} and the values of F_c, F_t, f_{s1}, f_{sc} $k_c d$ and $k_t d$ are calculated using Eq. 4.3 to 4.8. The validity of the translational equilibrium condition given by Eq. 4.2*a* is then checked (with a pre-selected tolerance), and the trial value is modified until the equilibrium condition is satisfied. Once this is achieved, the cracking moment M_{cr} of the beam is calculated using the following equation.

$$M_{cr} = F_c\, k_c d + A_{sc} f_{sc}(kd - d_c) + F_t k_t d + A_{st} f_{s1}(d - kd). \tag{4.12}$$

Fig. 4.5 shows the flowchart that describes the procedure used in the computer program *FORCES.BAS* for calculating M_{cr}.

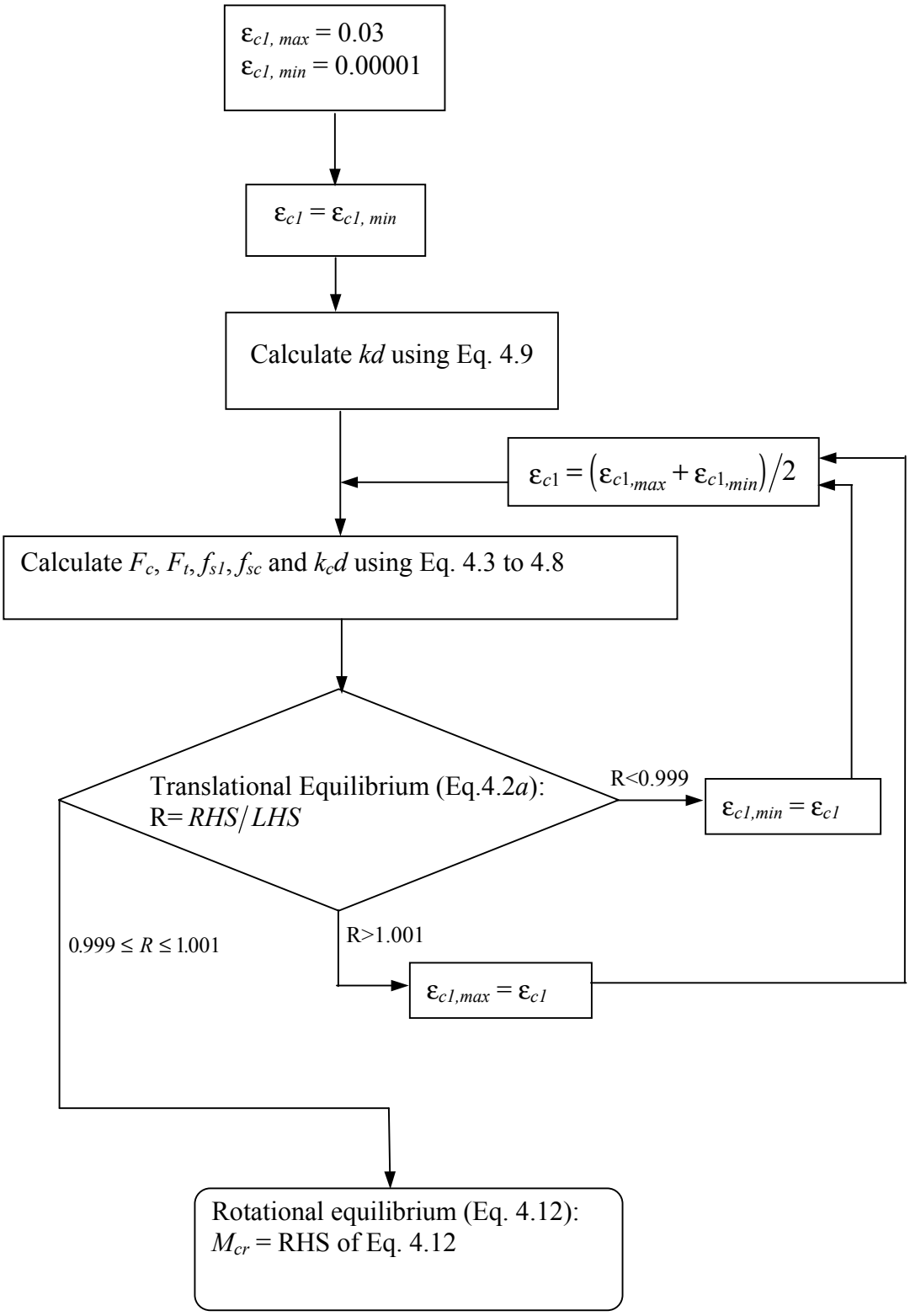

Fig. 4.5 Flowchart for calculating the cracking moment M_{cr}

4.6 Forces Acting on a Cracked Section

4.6.1 Forces for selected bending moment

A cracked section of a beam and the associated strain and stress distributions are shown in Fig. 4.6. The applied bending moment at this section is greater than or equal to the cracking moment of the beam ($M \geq M_{cr}$). The strain distribution is assumed to be linear across the height, as in the case of an uncracked section. Forces acting on this section are calculated by the program *FORCES.BAS* using the same procedure described in Section 4.4 for an uncracked section, with the upper limit of integration in Eq. 4.6 changed from $y_1 = h\text{-}kd$ to $y_1 = k_1 d$ (see Fig. 4.6). As an example, equivalent nodal forces calculated for selected values of bending moments M ($M_{cr} < M < M_u$, where M_u = ultimate moment capacity) in the two typical beams (rectangular and flanged) mentioned previously are given in *Appendix A4*.

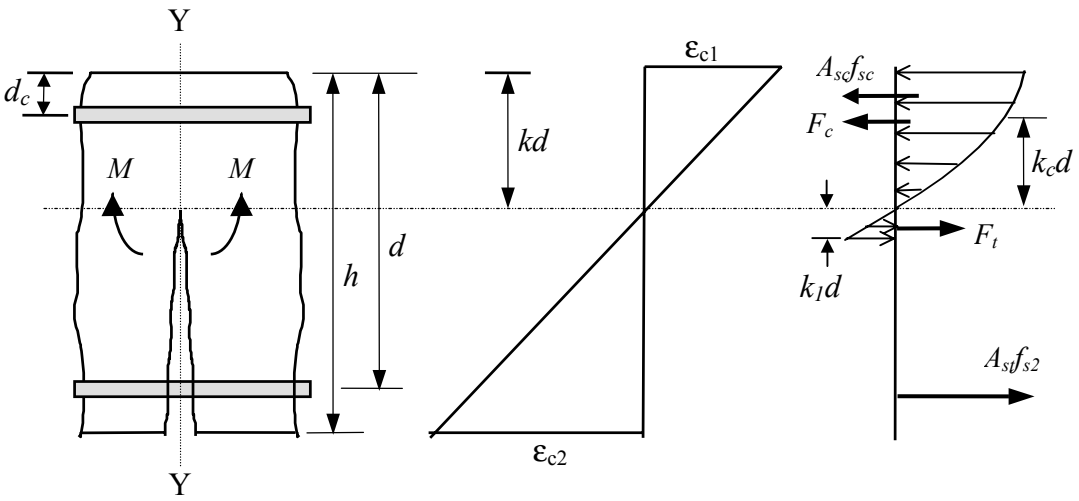

(*a*) Cracked section (*b*) Strain and stress distributions at section Y-Y

Fig. 4.6 Strain and stress distributions at a cracked section

4.6.2 Forces for selected steel stress

Some of the crack spacing and crack width measurements of test programs have been reported at various steel stress values calculated at the cracked section. This method has been adopted because the steel stress at the cracked section is considered to be the most significant parameter affecting the spacing and width of cracks (Section 2.2.5). To compare the results of the present analytical method with such measurements, it is necessary to calculate the forces acting on the cracked section corresponding to a given steel stress. This procedure is described below.

In calculating the concrete stress distribution at a cracked section corresponding to a given steel stress, only the translational equilibrium condition needs to be satisfied. This is because when the steel stress is specified, the bending moment at the section is already defined. To determine the forces acting on the section, a trial value is selected for the depth of compression zone *kd* and the concrete strain ε_{c1} is calculated using Eq. 4.7 for the given steel stress f_{s1}. The value of *kd* is changed until the translational equilibrium condition given in Eq. 4.2*a* is satisfied. The step-by-step procedure is as follows.

(*a*) select a trial value for *kd*

(*b*) calculate F_c, F_t, f_{s1}, f_{sc} and $k_c d$ using Eq. 4.3 to 4.8

(*c*) check whether the Eq. 4.2*a* is satisfied with a pre-selected tolerance (Section 4.8). If not, change the value of *kd* and go to step (*b*).

Fig. 4.7 shows the flowchart that describes the steps used in the program *FPRCES.BAS* in calculating the forces on the cracked section using the above iterative procedure. As an example, the calculated nodal forces at cracked sections for selected steel stress values are given in *Appendix A5* and *A6* for two typical beams.

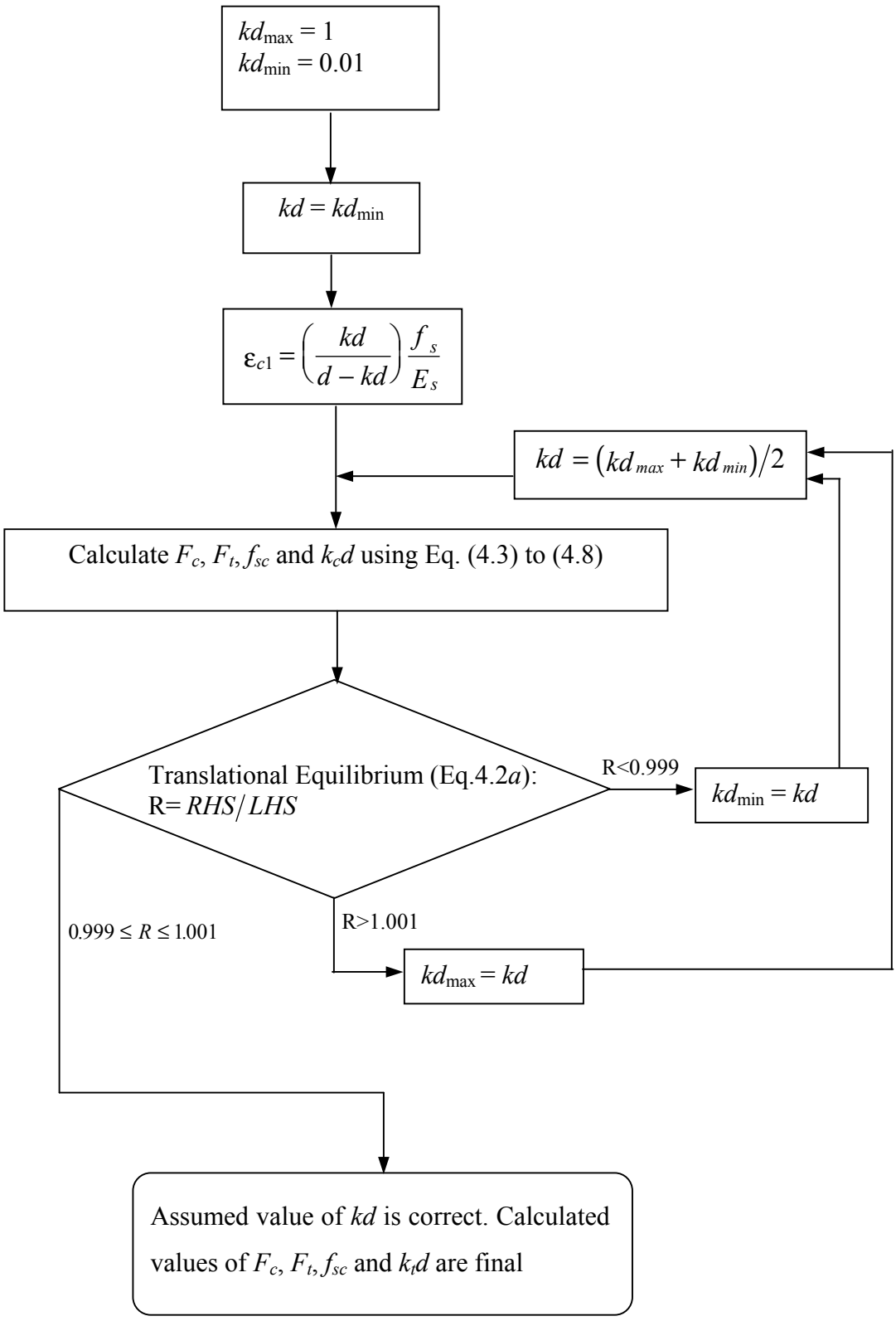

Fig. 4.7 Flowchart for calculating the forces on a cracked section for selected steel stress

4.7 Bond Forces Near Flexural Cracks

4.7.1 Bond force near the first flexural crack

When the first flexural crack is developed in a loaded beam, the steel stress at the cracked section increases as the tensile force carried by concrete is transferred to the steel bars. This steel stress increment is resisted by bond forces developed along a certain length of the steel bars on either side of the crack. The bond force is associated with bond slip, and the length along which the bond slip takes place depends on the steel stress increment as well as the bond stress-bond slip relationship and bar diameter. Described below is the method of calculating the distance for which the bond slip takes place near the first flexural crack, and the associated bond force.

Fig. 4.8*a* shows part of a beam soon after the formation of the first flexural crack at section *A*. The steel stress increment due to the formation of the crack has resulted in a slip for a distance S_o as shown. The distance S_o is herein referred to as the *slip length*. Tensile stresses at the two ends of a steel bar between the cracked section and the end of slip length, together with the associated bond force are shown in Fig. 4.8*b*. Variation of the bond stress and steel stress along the slip length, and the extension of the steel bar measured from the end of slip length are shown in Fig 4.8*c* to 4.8*e*. (Note that the bond stress is assumed to be varying parabolically as described in Section 3.4.2.)

Stress and strain conditions at sections where the slip has not taken place (beyond a distance S_o away from the crack) are assumed to be unchanged due to the formation of the first crack. Consequently, the steel stresses f_{s1} at section *X* (end of slip length) can be calculated using the procedure described for an uncracked section (Section 4.4). The steel stress f_{s2} at the cracked section *A* (Fig. 4.8*b*) is evaluated as described in Section 4.6. As already mentioned, the computer program *FORCES.BAS* is used for the above calculations.

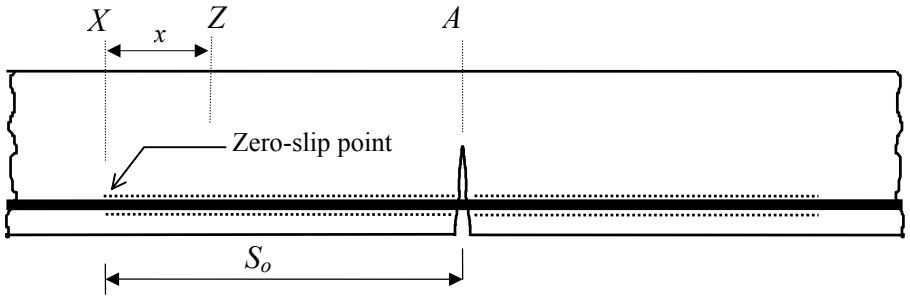

(*a*) First crack in a beam

(*b*) Bond forces acting on a steel bar

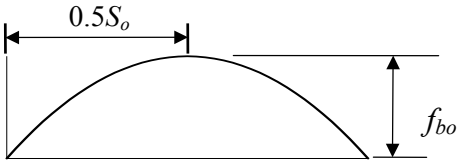

(*c*) Bond stress distribution along the slip length

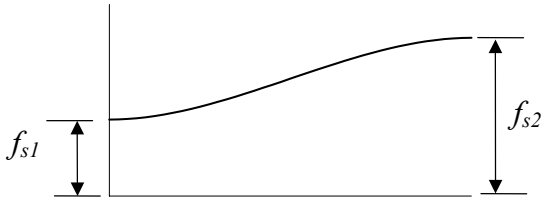

(*d)* Variation of steel stress along the slip length

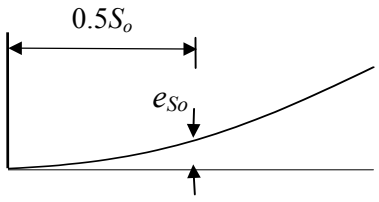

(*e*) Extension of steel bar measured from zero-slip point

Fig. 4.8 The first flexural crack formed in a beam

After calculating the values of f_{s1} and f_{s2}, the slip length S_o and the associated peak bond stress f_{bo} are determined by solving the following two equations (Eqs. 4.13 and 4.14) simultaneously.

The condition of equilibrium of forces acting on part of the steel bar between the cracked section and the zero-slip point (between sections *A* and *X* in Fig. 4.8*b*) gives

$$\frac{\pi \phi^2}{4}\left(f_{s2} - f_{s1}\right) = \frac{2}{3}\pi\phi f_{bo} S_o \qquad (4.13)$$

The peak bond stress f_{bo} and the local slip s_o at that point should satisfy the constitutive relationship

$$f_{bo} = \Phi'(s_o) \qquad (4.14)$$

where $\Phi'(s_o)$ is the constitutive relationship given in Eq. 3.1. The slip s_o at the point where f_{bo} occurs (at a distance $0.5S_o$ from the zero-slip point as shown in Fig. 4.8) can be calculated as

$$s_o = e_{so} - e_{co} \qquad (4.15)$$

in which e_{so} and e_{co} are the extensions of steel and concrete respectively, at the point $0.5S_o$ away from section *X* (zero-slip point). Note that both extensions are measured from the same reference point at section *X*. The elastic extension of steel, e_{so}, is calculated by integrating the strain function as the steel stress varies non-linearly due to the parabolic bond stress distribution. This procedure is described below.

The bond stress f_{bx} at a distance x from the zero-slip section (section *Z* in Fig. 4.8*a*) can be calculated by replacing the variable L_o in Eq. 3.4 with S_o (see Figs. 3.14 and 4.8). The resulting equation is as follows.

$$f_{bx} = 4 f_{bo} \frac{x}{S_o}\left(1 - \frac{x}{S_o}\right) \qquad (x \le S_o) \qquad (4.16a)$$

The total bond force F_{bx} acting on the bar surface between sections X and Z in Fig. 4.8 can then be calculated using the following integral.

$$F_{bx} = \int \pi\phi f_{bx}\, dx = \frac{4 f_{bo} \pi\phi}{S_o}\left(\frac{x^2}{2} - \frac{x^3}{3 S_o}\right) \qquad (x \le S_o) \qquad (4.16b)$$

The resulting steel stress f_{sx} at section Z can be calculated using the following equation, which is derived by equating the difference in tensile forces acting at sections X and Z of the steel bar, and the total bond force acting on the bar surface between those two sections.

$$\frac{\pi \phi^2}{4}\left(f_{sx} - f_{s1}\right) = F_{bx} \qquad (4.16c)$$

Substitution of Eq. 4.16*c* into Eq. 4.16*b* leads to the following equation for f_{sx}.

$$f_{sx} = f_{s1} + \frac{16 f_{bo}}{S_o \phi}\left(\frac{x^2}{2} - \frac{x^3}{3 S_o}\right) \qquad (x \le S_o) \qquad (4.16d)$$

The corresponding steel strain ε_{sx} at section Z is then calculated as $\varepsilon_{sx} = f_{sx}/E_s$. The resulting extension of the steel bar e_{so}, at a distance $0.5S_o$ from the zero-slip section is calculated by integrating the steel strain function ε_{sx} as follows.

$$e_{so} = \int_{x=o}^{x=0.5S_o} \varepsilon_{sx}\, dx = \int_{x=o}^{x=0.5S_o} \left\{\frac{f_{s1}}{E_s} + \frac{16 f_{bo}}{S_o \phi E_s}\left(\frac{x^2}{2} - \frac{x^3}{3 S_o}\right)\right\} dx = \frac{f_{s1} S_o}{2 E_s} + \frac{f_{bo} {S_o}^2}{4 E_s \phi} \qquad (4.16e)$$

In calculating e_{so}, the use of f_{s2} (steel stress at the cracked section) is considered more appropriate than the use of f_{s1} (steel stress at the zero-slip section), because the crack spacing and crack width are usually expressed as a function of f_{s2}. Therefore, the variable f_{s1} in Eq. 4.16*e* is changed to f_{s2} using the following relationship, which is derived by re-arranging Eq. 4.13.

$$f_{s1} = f_{s2} - \frac{8 f_{bo} S_o}{3\phi} \qquad (4.16f)$$

Substitution of Eq. 4.16*f* into Eq. 4.16*e* yields the following formula for the calculation of e_{so}.

$$e_{so} = \frac{f_{s2} S_o}{2 E_s} - \frac{13 f_{bo} S_o^{\,2}}{12 E_s \phi} \qquad (4.16g)$$

In calculating the slip s_o (see Eq. 4.15), the concrete extension e_{co} is determined using Eqs. 5.6 to 5.8, which are developed in Chapter 5. (It must be noted that in this calculation the variable L_o in Eqs. 5.6 to 5.8 are replaced by S_o).

In solving for f_{bo} and S_o using Eqs. 4.13 to 4.16*g*, a trial and error procedure is adopted because of the non-linear nature of the constitutive relationship $f_{bo} = \Phi'(s_o)$. The procedure is as follows:

(*a*) select a trial value for f_{bo}

(*b*)calculate S_o using Eq. 4.13

(*c*) determine s_o using Eq. 4.15, 4.16*g* together with Eqs. 5.6 to 5.8

(*d*) calculate f_{bo} using Eq. 4.14. If the difference between the calculated f_{bo} and the selected trial value is less than the pre-selected tolerance (see Section 4.8), then the calculated values of f_{bo} and S_o are acceptable. If not, select another trial value for f_{bo} and go to step (*b*).

The program *FORCES.BAS* calculates the slip length S_o and the corresponding peak bond stress f_{bo} for a given beam, using the above iterative procedure. Fig. 4.9 shows the flowchart that describes the steps used in the program. The calculated bond force acting between sections *X* and *A* (Fig. 4.8) is then converted into equivalent nodal forces for subsequent use in the finite element analysis. Calculated values of f_{bo} and the equivalent nodal bond forces for the two typical beams (rectangular and flanged) mentioned earlier are shown in *Appendix A11* and *A12*.

As mentioned earlier in this Chapter, stress and strain conditions at sections beyond a distance S_o away from the first crack are not influenced by the formation of the first crack. If a second crack is developed in this unaffected region, the stress conditions near the new crack will be identical to that near the first crack just discussed. If however, a new crack is formed at a relatively smaller distance from the first crack, the slip lengths for the two cracks may overlap. The resulting bond stress distribution between the two cracks will be different from that already described. The procedure of evaluating the bond stress distribution between two successive cracks is described in the next Section.

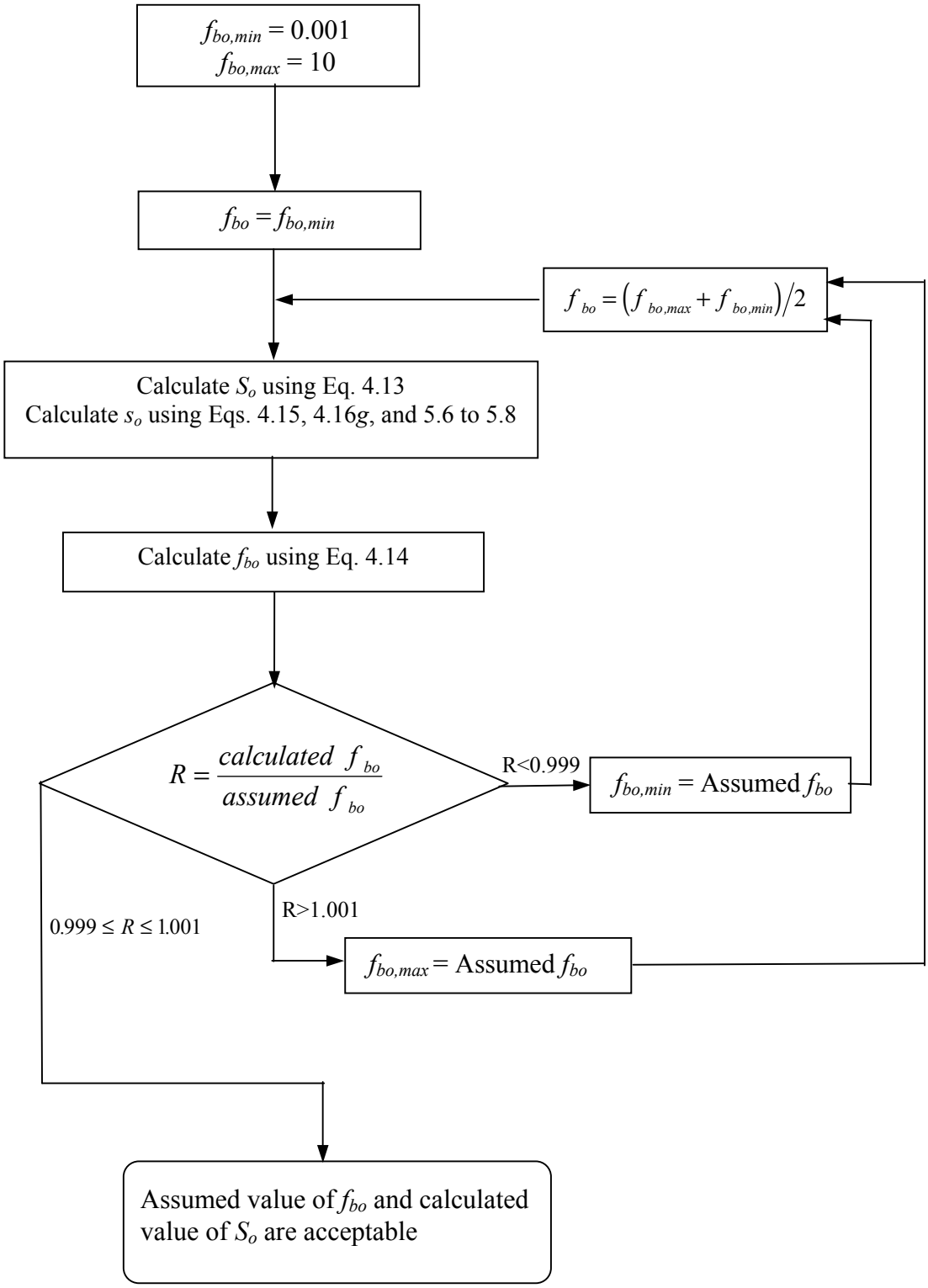

Fig. 4.9 Flowchart for calculating slip length S_o and peak bond stress f_{bo}

4.7.2 Bond stress between adjacent cracks

(*a*) *Constant moment region*

Fig. 4.10 shows two cracks developed at sections *A* and *B* in a constant moment region of a beam such that their slip lengths overlap. This occurs when the crack spacing *S* is less than $2S_o$.

In a constant moment region, the tensile stresses at both cracked sections are equal because the bending moments are the same. Therefore, the stresses and strains within the concrete block between the two cracks are symmetrical about the mid section *C*. As a result, the slip and the bond stress at the mid section are zero.

The bond force acting on a steel bar, bond stress and steel stress distributions and the extension of the steel bar measured from the zero-slip point are shown in Fig. 4.10*b* to 4.10*e*. For a known bending moment (known steel stress at the cracked section f_{s2}), and selected crack spacing *S*, the peak bond stress f_{bo} is determined using the following procedure.

The peak bond stress f_{bo} and the slip s_o at a point $0.25S$ away from the cracked section (Fig. 4.10) are related via the constitutive relationship given in Eq. 4.14. The slip s_o is calculated as the relative difference in elastic extensions of steel and surrounding concrete, using Eq. 4.15 also discussed previously. These equations are repeated below for easy reference.

$$f_{bo} = \Phi'(s_o) \tag{4.17}$$

$$s_o = e_{so} - e_{co} \tag{4.18}$$

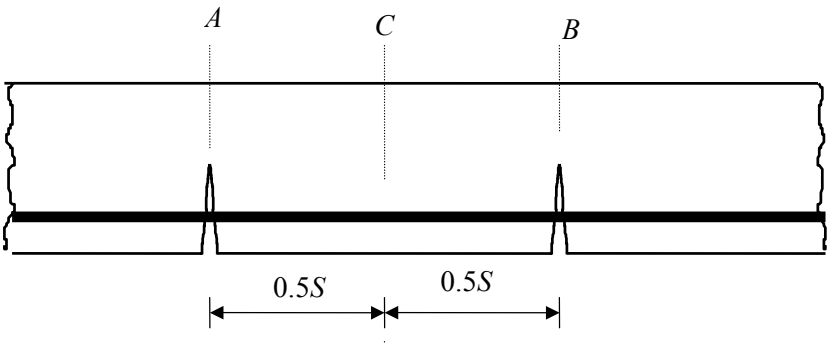

(*a*) Adjacent flexural cracks in a beam

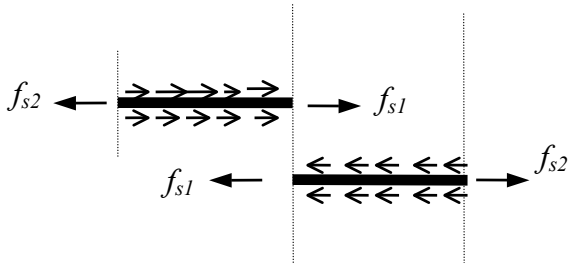

(*b*) Bond forces acting on a steel bar

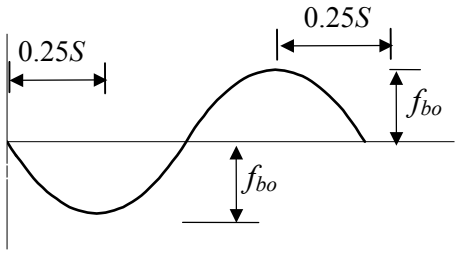

(*c*) Bond stress distribution between the two cracks

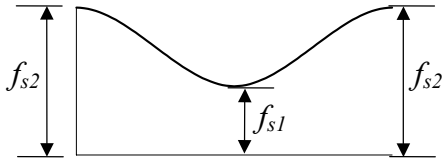

(*d*) Variation of steel stress between the two cracks

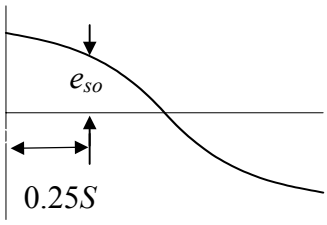

(*e*) Extension of steel bar measured from the mid section between cracks

Fig. 4.10 Adjacent cracks in a constant moment region of a beam ($S < 2S_o$)

For the concrete block shown in Fig. 4.10, e_{so} and e_{co} are measured in relation to the mid point between the two cracks where the slip is zero. The equation for e_{so} at a distance 0.25S away from the mid section is obtained by substituting 0.5S into S_o in Eq. 4.16g. The resulting equation is as follows.

$$e_{so} = \frac{f_{s2} S}{4 E_s} - \frac{13 f_{bo} S^2}{48 E_s \phi} \tag{4.19}$$

The expression for e_{co} is derived in Chapter 5 (Eqs. 5.6 to 5.8 with L_o replaced with 0.5S). In solving for f_{bo} using Eqs. 4.17 to 4.19, the following trial and error procedure is adopted.

(*a*) select a trial value for f_{bo}

(*b*) calculate s_o using Eqs. 4.18 and 4.19 together with Eqs. 5.6 to 5.8

(*c*) calculate f_{bo} using Eq. 4.17. If the difference between the calculated f_{bo} and the selected trial value is less than the pre-selected tolerance, then the selected value of f_{bo} is acceptable. If not, select another trial value for f_{bo} and go to step (*b*).

The program *FORCES.BAS* calculates the peak bond stress f_{bo} using the above iterative procedure, for given values of steel stress f_{s2} and crack spacing S. Fig. 4.11 shows the flowchart that describes the steps used in the program. Note that the steel stress f_{s2} corresponding to a given bending moment is calculated as described in Section 4.6.1 while S is the crack spacing selected for finite element analysis. As an example, calculated values of f_{bo} and the corresponding equivalent nodal forces for the two beams (rectangular and flanged) mentioned earlier in this Chapter are given in *Appendix A13* and *A14*, for selected typical values of f_{s2} and S.

Once the peak bond stress f_{bo} is determined, the steel stress f_{s1} at the zero-slip section (at mid section C) can be calculated using Eq. 4.16f, with the variable S_o replaced with 0.5S. The resulting equation is as follows.

$$f_{s1} = f_{s2} - \frac{4 f_{bo} S}{3\phi}. \tag{4.20}$$

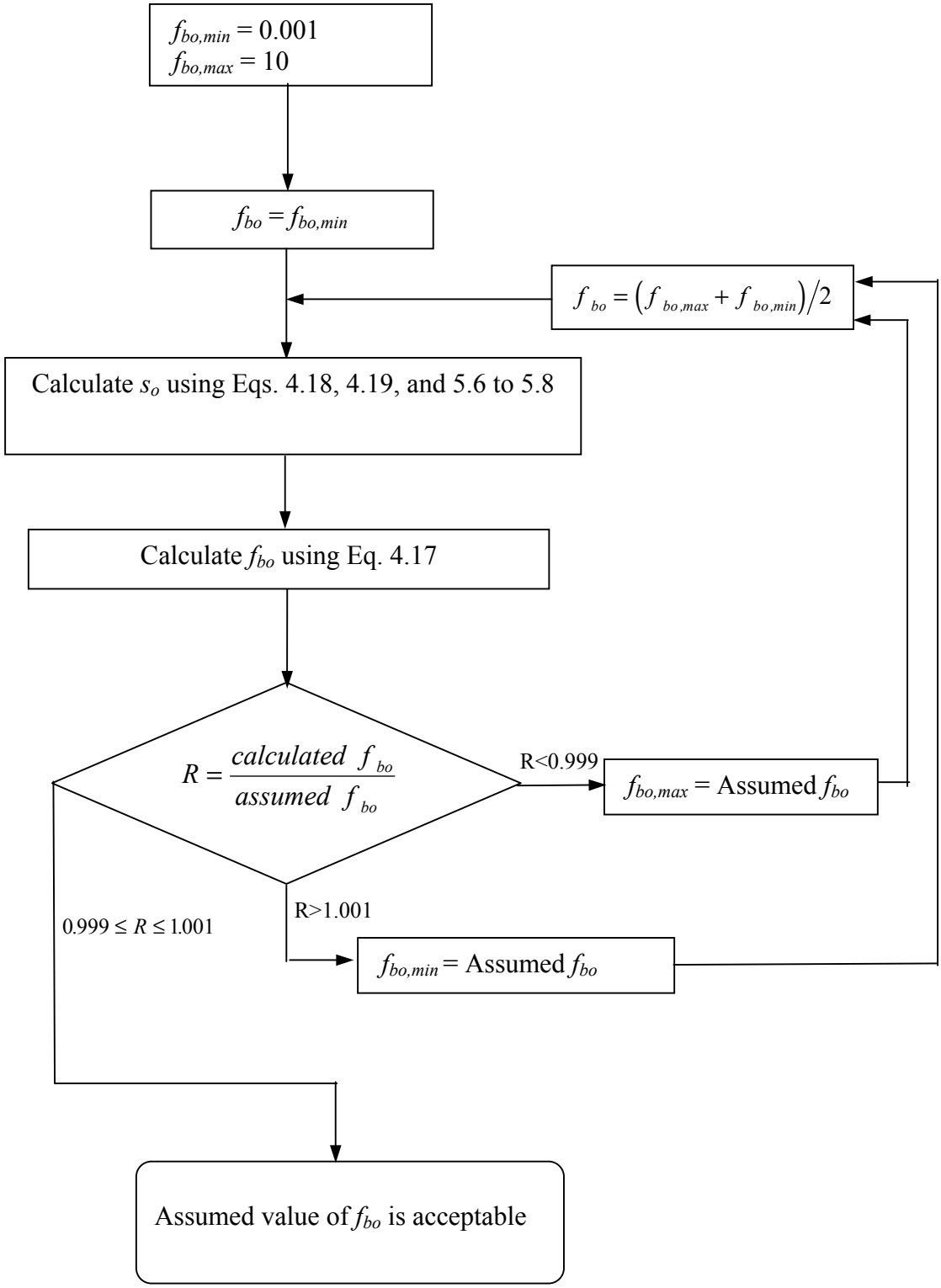

Fig. 4.11 Flowchart for calculating the peak bond stress f_{bo} between adjacent cracks in constant moment region

(*b*) *Varying moment region*

Bond stress and steel stress distributions as well as the slip and extension of steel bars between two cracks in a varying moment region are different to those described above for a constant moment region. This is because the bending moments at the two cracked sections are different, and consequently, the stress and strain fields within the concrete block between the cracks are not symmetrical about the mid section. The zero-slip point therefore does not lie at the mid section.

Fig. 4.12 shows the bond stress and steel stress distributions in between two cracks in a varying moment region of a loaded beam. The distance between the cracks is S, and the zero-slip section lies at a distance S_x away from the crack having the lower bending moment. Steel stresses at the two cracked sections are f_{s2} and f_{s3}, while that at the zero-slip section is f_{s1} ($f_{s1} < f_{s2} < f_{s3}$). The peak bond stresses on either side of the zero-slip section are designated as f_{bo} and f'_{bo}, as shown in Fig. 4.12. To determine the location of the zero-slip section, the resulting peak bond stresses, and the minimum steel stress f_{s1} the following equations are derived.

The constitutive relationships for the peak bond stresses should satisfy the equations

$$f_{bo} = \Phi'(s_o) \qquad (4.21a)$$

$$f'_{bo} = \Phi'(s'_o) \qquad (4.21b)$$

where $\Phi'(s_o)$ is the constitutive relationship given in Eq. 3.1. In Eq. 4.21, s_o and s'_o are the slips at locations where the peak bond stresses occur, as shown in Fig. 4.12. Also note that $S_y = S - S_x$.

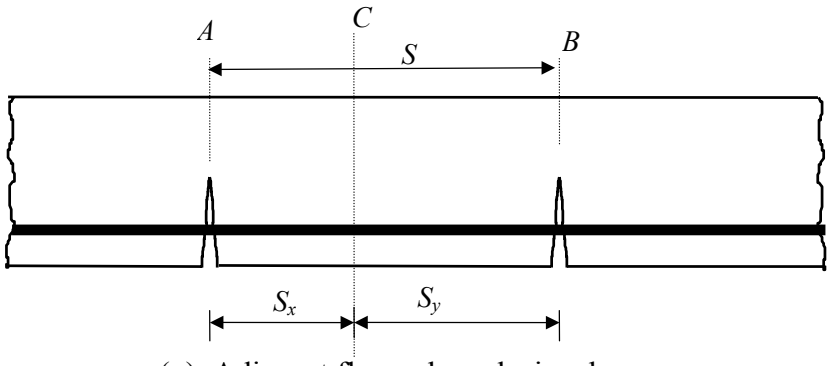

(*a*) Adjacent flexural cracks in a beam

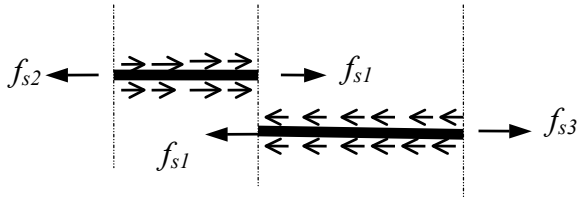

(*b*) Bond forces acting on a steel bar

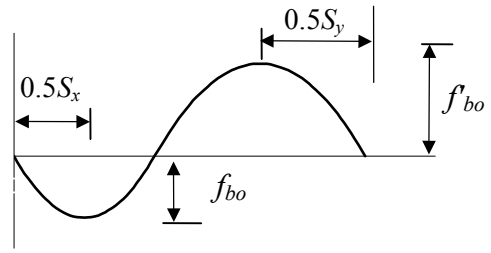

(*c*) Bond stress distribution between the cracks

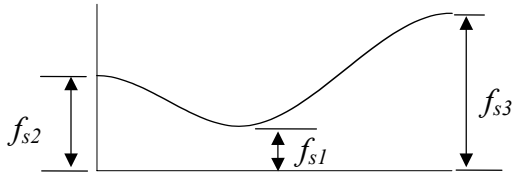

(*d*) Steel stress distribution between the cracks

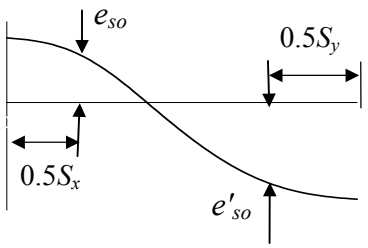

(*e*) Extension of steel bar measured from the zero-slip point

Fig. 4.12 Adjacent cracks in a varying moment region of a loaded beam

The slips s_o and s'_o are calculated as the relative difference in elastic extensions of steel and surrounding concrete as

$$s_o = e_{so} - e_{co} \tag{4.22a}$$

$$s'_o = e'_{so} - e'_{co} \tag{4.22b}$$

in which e_{so} and e_{co} are the extensions of steel and concrete respectively, at the location where the peak bond stress f_{bo} occurs. e'_{so} and e'_{co} are those values corresponding to the peak bond stress f'_{bo}. Note that all the extensions are measured from the zero-slip point at section *C*. The steel extensions e_{so} and e'_{so} are calculated using the following equations, which were derived by substituting $0.5S_x$ and $0.5S_y$ into S_o in Eq. 4.16*g*.

$$e_{so} = \frac{f_{s2} S_x}{4 E_s} - \frac{13 f_{bo} S_x^{\,2}}{48 E_s \phi} \tag{4.23a}$$

$$e'_{so} = \frac{f_{s3} S_y}{4 E_s} - \frac{13 f'_{bo} S_y^{\,2}}{48 E_s \phi} \tag{4.23b}$$

The concrete extensions e_{co} and e'_{co} are calculated using the procedure described in Chapter 5 (using Eqs. 5.6 to 5.8 with L_o replaced by S_x and S_y respectively).

The final set of equations is derived by considering the equilibrium of the two parts of the steel bar between each cracked section and the zero-slip point. The resulting equations are as follows.

$$f_{s1} = f_{s2} - \frac{8 f_{bo} S_x}{3\phi} \tag{4.24a}$$

and

$$f_{s1} = f_{s3} - \frac{8 f'_{bo} S_y}{3\phi} \tag{4.24b}$$

It may be noted that for an arbitrary value of S_x, Eqs. 4.24*a* and 4.24*b* will generally yield two different f_{s1} values for the steel stress at the zero-slip section. In solving for the unknowns S_x, f_{bo}, f'_{bo} and f_{s1}, a trial distance is first selected for S_x and the values of f_{s1} obtained from Eqs. 4.24*a* and 4.24*b* are compared after solving Eqs. 4.21 to 4.24. If Eqs. 4.24*a* and 4.24*b* give different f_{s1} values, the trial value of S_x is changed and the solution process is repeated until the same f_{s1} value is obtained from these two equations. The step-by-step procedure is as follows.

(*a*) select a trial value for S_x

(*b*) select a trial value for f_{bo}

(*c*) calculate s_o using Eq. 4.22*a* and 4.23*a*, together with Eqs. 5.6 to 5.8

(*d*) substitute s_o into Eq. 4.21*a* and determine a new value for f_{bo}. If the difference between the calculated f_{bo} and selected trial value of f_{bo} is less than the pre-selected tolerance, the calculated values of f_{bo} and s_o are acceptable and go to step (*e*). If not change the value of f_{bo} and go to step (*c*).

(*e*) select a trial value for f'_{bo}

(*f*) calculate s'_o using Eq. 4.22*b* and 4.23*b*, together with Eqs. 5.6 to 5.8

(*g*) substitute s'_o into Eq. 4.21*b* and determine a new value for f'_{bo}. If the difference between the calculated f'_{bo} and selected trial value of f'_{bo} is less than the pre-selected tolerance, the calculated values of f'_{bo} and s'_o are acceptable and go to step (*h*). If not change the value of f'_{bo} and go to step (*f*).

(*h*) use Eq. 4.24*a* to calculate f_{s1}

(*i*) use Eq. 4.24*b* to calculate f_{s1}

(*j*) if the difference between the two f_{s1} values calculated from steps (*h*) and (*i*) is less than the pre-selected tolerance, then the selected value of S_x and the calculated values of f_{bo}, f'_{bo} and f_{s1} are acceptable. If not, change the value of S_x and go to step (*b*).

The program *FORCES.BAS* calculates the values of f_{bo}, f'_{bo}, f_{s1} and S_x for given values of f_{s2}, f_{s3} and S using the above iterative procedure. Fig. 4.13 shows the flowchart that describes the steps used in the program. Note that f_{s2} and f_{s3} corresponding to the bending moments at the two cracked sections are determined as described in Section

4.6.1, while S is the crack spacing selected for the finite element analysis. Typical results of f'_{bo}, f_{bo}, f_{s1} and S_x for the two beams (rectangular and flanged) mentioned earlier in this Chapter are presented in *Appendix A15* and *A16*. As seen in these appendices, the calculated bond forces have been converted into equivalent nodal forces, for the use in finite element analysis.

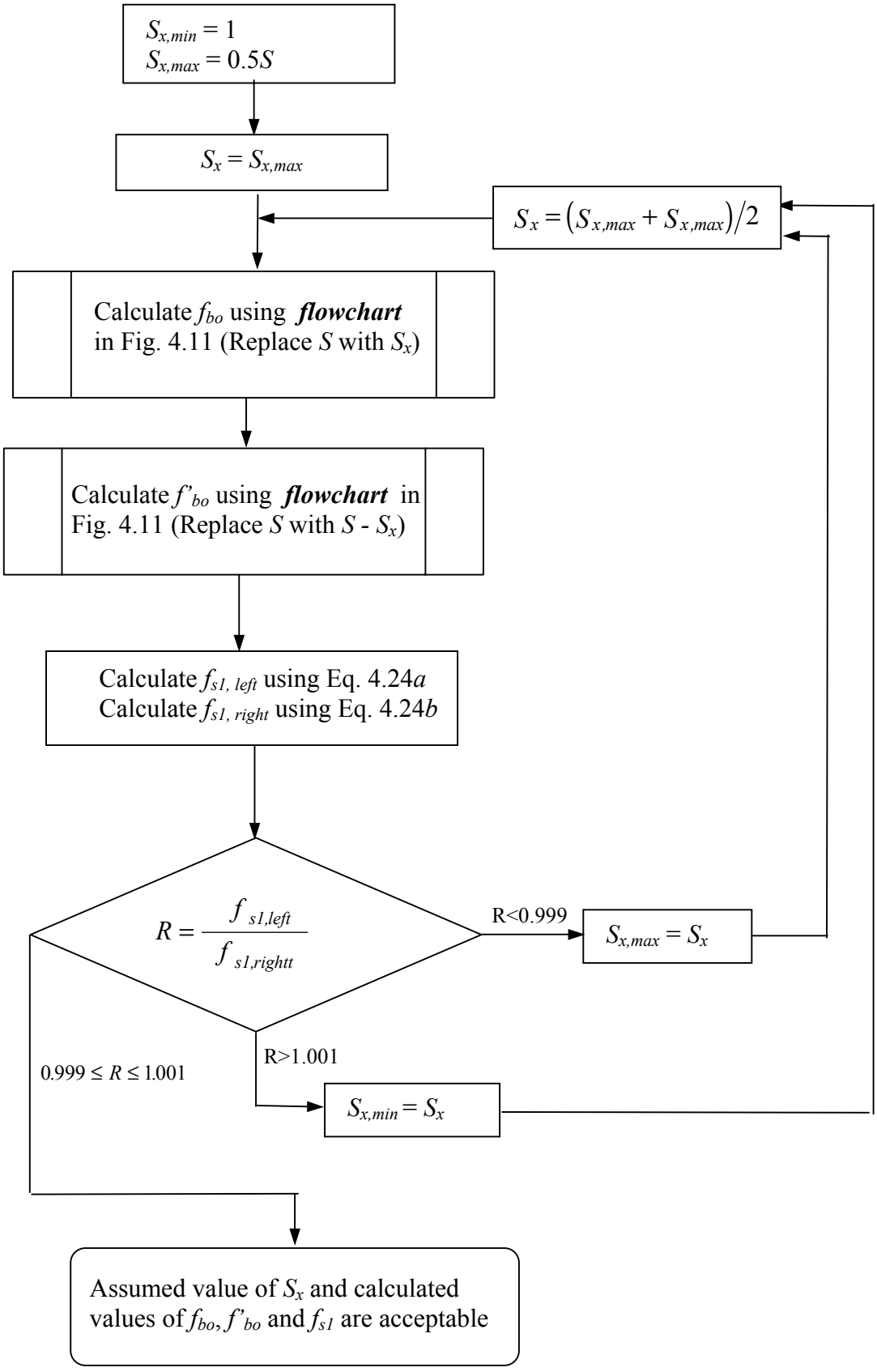

Fig. 4.13 Flowchart for calculating bond stress between cracks in a varying moment region

4.8 Computer Program to Calculate the Forces

As described in Sections 4.4 to 4.7, a considerable amount of repetitive calculations are required for the determination of forces acting on a concrete block between two transverse sections. As a large number of beam sections are considered in the present finite element analysis, a computer program written in *BASIC* language is utilised for the determination of above forces. The structure of this program is briefly outlined below.

The program requires the input of sectional properties of the member at the beginning of execution. Rectangular, T-shaped as well as Box-shaped sections are acceptable, with or without compression reinforcement. Once the sectional properties are input, they are stored in a data file for future use.

After the sectional properties are input (or read from an existing data file), the program calculates the following parameters:

(*a*) Cracking moment of the section, M_{cr};
(*b*) Tensile steel stress just before cracking, f_{s1};
(*c*) Tensile steel stress just after cracking, f_{s2}; and
(*d*) Ultimate moment, M_u.

The values of M_{cr}, f_{s2} and f_{s1} are calculated using the procedure already described in Sections 4.5, 4.4 and 4.6 respectively. The ultimate moment M_u is calculated using the procedure described for M_{cr} with the concrete strain at the extreme compression fibre ε_{c1} taken as 0.003.

The program then prompts for the selection of any of the following six Solution Modes. Some of these solution modes require additional inputs as outlined below.

Solution Mode 1: *(calculates concrete and steel stress just before cracking)*
Additional inputs: None.

Solution Mode 2: *(calculates concrete and steel stress just after cracking)*
Additional inputs: None.

Solution Mode 3: *(calculates concrete and steel stress for any bending moment)*
Additional input: Bending moment at the section.

Solution Mode 4: *(calculates slip length and bond stress near the first flexural crack)*
Additional inputs: None.

Solution Mode 5: *(calculates bond stress between cracks – constant moment region)*
Additional inputs: Steel stress at the cracked section and crack spacing.

Solution Mode 6: *(calculates bond stress between cracks – varying moment region)*
Additional inputs: Steel stresses at two adjacent cracked sections and crack spacing.

Solution Mode 7: *(calculates concrete stresses for a given steel stress at cracked section)* - Additional inputs: Steel stress at the cracked section.

In Solution Mode 1, the iterative procedure described in Section 4.4 is used for the calculation of concrete and steel stresses, while in Solution Modes 2 and 3, the procedure described in Section 4.6.1 is adopted. Iterative procedures described in Sections 4.7.1, 4.7.2(*a*) and 4.7.2(*b*) respectively are used in Solution modes 4, 5 and 6 for the calculation of bond force and the corresponding steel stress at the zero-slip section. For Solution Mode 7, the iterative procedure described in Section 4.6.2 is used.

Once the concrete compressive and/or tensile forces acting on the transverse section and the bond force acting at reinforcement level are computed, they are converted by the program into equivalent nodal forces. The arrangement of the finite element mesh (see Section 4.11) has been already incorporated into the program for this purpose. At the end of the conversion, a further equilibrium check is performed to verify that the nodal forces are accurate (see *Appendix A1* to *A16*).

The calculated steel stress, nodal forces and the accompanying node numbers are stored in individual data files by the name *FILE.ixy*, where *FILE* is the file name initially selected for storing the sectional properties, *i* is the Solution Mode number and *xy* is the file identification number selected for the particular data set. Note that a file identification number *i* is not required for Solution Modes 1, 2, and 4 because no additional inputs are required for these modes, and the output results depend only on the sectional properties. The program selects *i*=1 for storing output data in these Solution Modes. The stored data are later retrieved by *Microsoft Excel* for the input into the finite element mesh manually.

The flowcharts that describe the steps used in the program for various iterative procedures have been already presented in respective Sections (Section 4.4 to 4.7). The overall flowchart that describes the structure of the program *FORCES.BAS* is given in Fig. 4.14. (As already mentioned previously, the source program of *FORCES.BAS* is given in *Appendix E1* to *E15*).

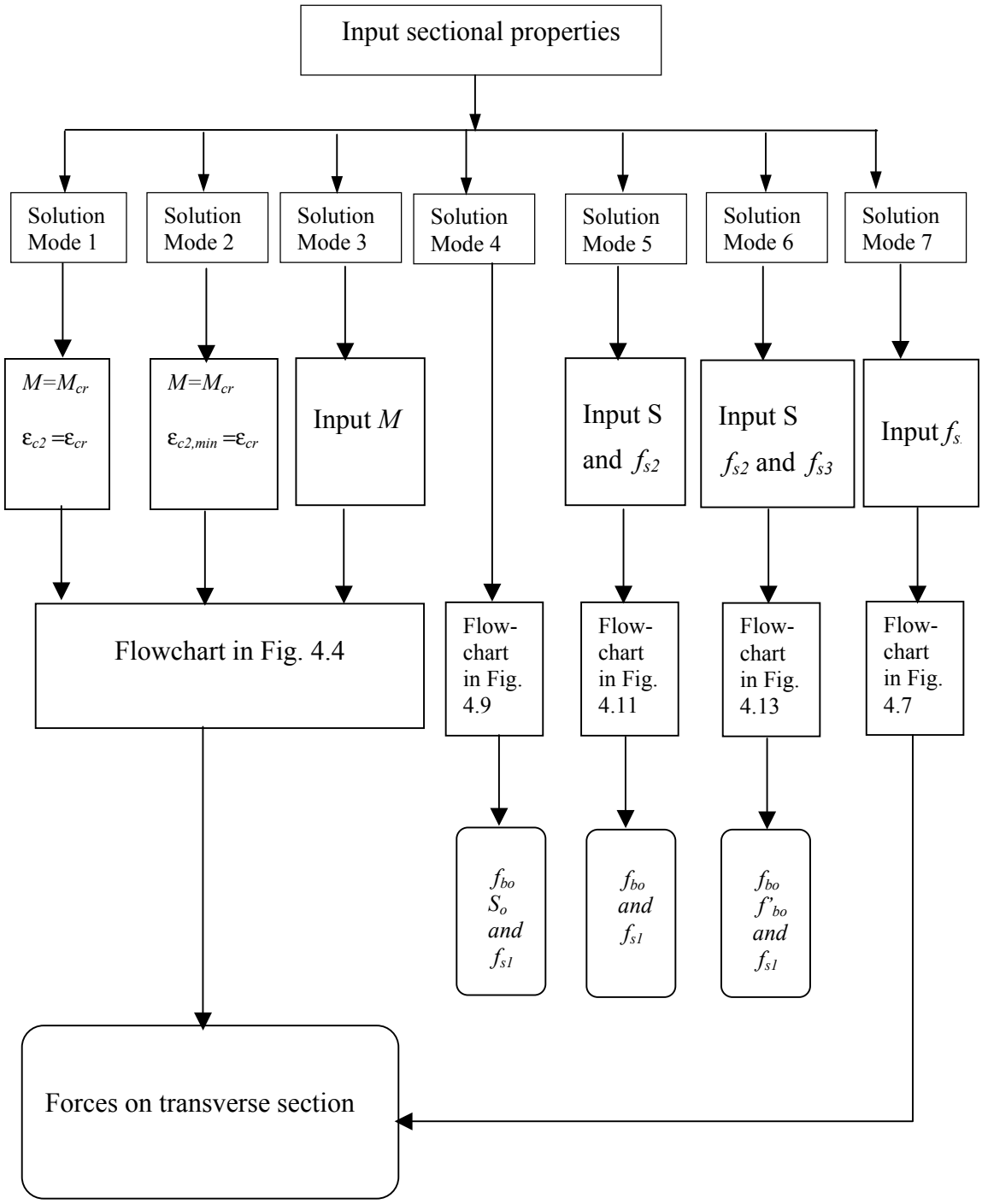

Fig. 4.14 Structure of the program *FORCES.BAS*

Convergence of iteration

As described in Sections 4.4 to 4.7, each Solution Mode in the program *FORCES.BAS* requires iterative procedures for satisfying equilibrium conditions (translational and rotational equilibrium for Solution Modes 1 to 3 and only translational equilibrium for Solution Modes 4 to 7). In the present computation, the convergence is checked at the end of each iteration by calculating the ratio of the trial value and the computed value for the selected parameter (see Section 4.4 to 4.7). Convergence is assumed if this ratio lies between 0.999 and 1.001. The procedure for varying the trial value in the iteration process is shown in the flowcharts presented in Sections 4.4 to 4.7 (Figs. 4.4, 4.5, 4.7, 4.9, 4.11 and 4.13).

4.9 Shear Force Equivalent to Bond Forces

In the present analysis, the total bond force exerted by all steel bars on the concrete section is replaced by an equivalent shear force uniformly distributed across the width of the beam (see Fig. 4.15). The intensity of this shear force at any section is calculated as follows.

The bond stress f_{bx} at any section x away from the zero-slip section has been already expressed in terms of the peak bond stress f_{bo} in Eq. 3.4, which is repeated below for easy reference.

$$f_{bx} = 4 f_{bo} \frac{x}{L_o}\left(1 - \frac{x}{L_o}\right) \qquad (x \le L_o) \tag{4.25}$$

where L_o is the distance from the zero-slip point to the nearest crack. Note that $L_o = S_o$ for the concrete block near the first flexural crack (Fig. 4.8); $L_o = 0.5S$ for the concrete block between two adjacent cracks in a constant moment region (Fig. 4.10) and $L_o = S_x$ or $L_o = S_y$ in a varying moment region (Fig. 4.12).

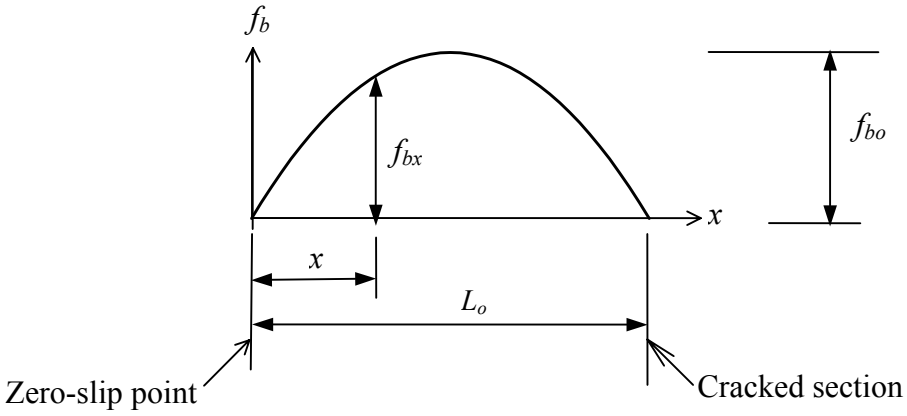

(*a*) Bond stress distributions

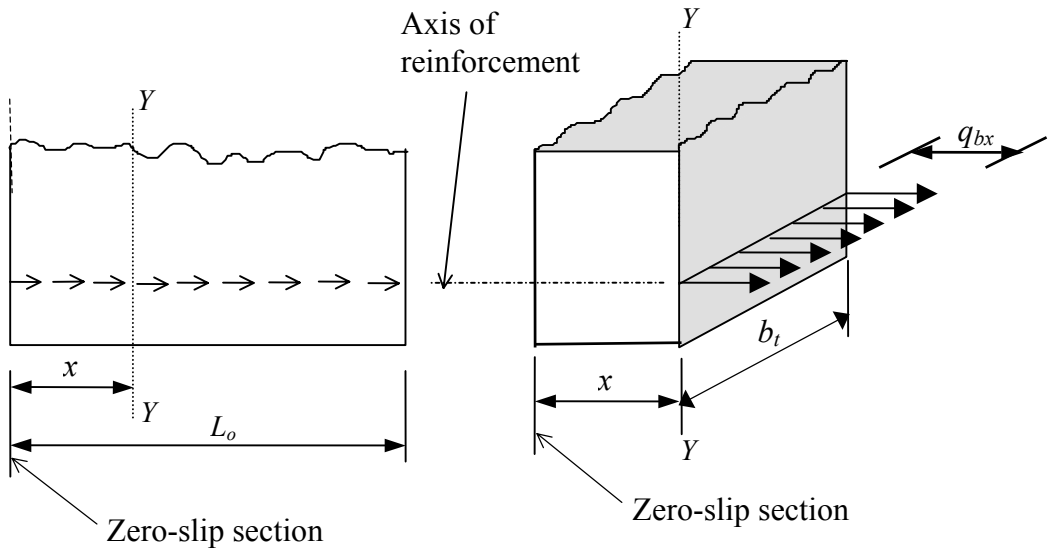

(*b*) Equivalent shear force

Fig. 4.15 Approximation of bond forces by an equivalent shear force

The intensity of the equivalent shear force q_{bx} at section *YY* in Fig. 4.15, uniformly distributed across the beam width, can be calculated as

$$q_{bx} = \frac{m\pi\phi f_{bx}}{b_t} \tag{4.26a}$$

where m is the number of bars, b_t is the width of the beam at reinforcement level and f_{bx} is the bond stress at section *YY* . Also the total steel area A_{st} can be expressed as

$$A_{st} = \frac{m\pi\phi^2}{4} = \rho bd \, . \tag{4.26b}$$

Substituting Eq. 4.26*b* for m into Eq. 4.26*a*, q_{bx} can be expressed as

$$q_{bx} = \frac{b}{b_t}\left(\frac{4\rho d}{\phi}\right) f_{bx} \tag{4.27}$$

in which $\rho = A_{st}/bd$ is the reinforcement ratio.

4.10 Transverse Shear Force in Varying Moment Regions

The total transverse shear force at a cracked section is carried by the combination of the shear in concrete compression zone, the dowel action of longitudinal tensile reinforcement and the shear due to the aggregate interlock in the cracked zone. According to Taylor (1974), the approximate proportions of the above components are 20-40%, 15-25%, and 35-50%, respectively. The effect of aggregate interlock, which makes the largest component of the shear carrying mechanism, becomes less effective when the crack widens (Kong and Evans (1987)).

According to Evans & Kong (1967) and ACI-ASCE Committee 426 (1973), beams with shear span-to-depth ratio less than 6 tend to fail in shear before reaching the ultimate flexural strength. However, this research is concerned with members that have shear

span-to-depth ratio larger than this value and fail in flexure rather than in shear. Shear force at transverse sections in such members are usually small in magnitude. Consequently, for the purpose of present calculation, it is assumed that the shear force at a cracked section is totally carried by the web area of the concrete compression zone. It is further assumed that the resulting shear stress is uniformly distributed along the height of the concrete compression zone at the cracked section. Using these assumptions, the average shear stress v due to a transverse shear force F_v acting at a cracked section is calculated as

$$v = \frac{F_v}{b_w kd} \tag{4.28a}$$

where b_w = web width. Using the same assumption that the shear force is uniformly distributed along the height of the member the shear stress at an uncracked section is calculated as

$$v = \frac{F_v}{b_w h} \tag{4.28b}$$

4.11 Finite Element Analysis

To determine the concrete stress distribution near flexural cracks a free body concrete block is analysed, with the forces acting on the block calculated as described previously. This concrete block is bounded by top and bottom faces and two transverse sections of a loaded member. Locations of transverse sections are selected as described later in Section 4.11.4. The analysis is carried out by the finite element method using the standard software package STAND6 (1993). A brief description of this software package and the model used in the analysis are detailed below. (A more recent version of this software – *STRAND7*- is now available with more user-friendly input and output modes including more versatile graphical presentations; however, the analytical procedures remain unchanged)

4.11.1 STRAND6 (1993) software package

STRAND6 (1993) has the capability of analysing one, two and three-dimensional models using various types of elements available in the library. These elements include truss, beam, plate/shell and 3D-bricks which can be used for analysing trusses, frames, plane stress, plane strain, axi-symmetric plate/shell structures and full three dimensional continua. The analytical capabilities of this software package include linear and non-linear analysis of structures (both geometric and material non-linearity), dynamic analysis, harmonic response to periodic loads, buckling analysis, potential flow analysis, and linear and non-linear heat flow analysis.

For the present analysis, QUAD4-CST quadrilateral element available in the element library is used. This element can be used for two-dimensional plane stress/plane strain analysis, axisymmetric analysis and three-dimensional thin plate/shell analysis. QUAD4-CST element is generated by the software package by combining four Constant Strain Triangular (CST) elements with the internal fifth node condensed out (see Fig. 4.16). The in-plane behaviour of this CST element has been formulated using the theory described by Zienkiewicz (1977) and Cook *et.al* (1989). The bending behaviour applicable for thin plates has been included into the element using the theory described by Clough & Felippa (1968).

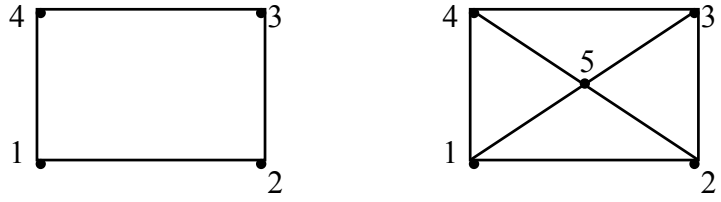

Fig. 4.16 Automatic assembly of a quadrilateral from four CST elements

4.11.2 Finite element mesh

Fig. 4.17*a* shows a free body of concrete block *PQRS* bounded by top and bottom faces of the member and two transverse sections. A slice of this block having unit thickness is considered for the finite element analysis. This block is divided by 10 transverse and 24

longitudinal divisions into 240 elements consisting of 275 nodes, as shown in Fig. 4.17*b* and 4.17*c*. The spacings of longitudinal divisions are made closer near reinforcement level to have a finer mesh as the stress in this region is found to vary rapidly in the transverses direction. The spacing of longitudinal divisions are further changed depending on the relative magnitudes of the concrete cover and the bar diameter. As seen in the figure, all transverse divisions are taken at equal spacing.

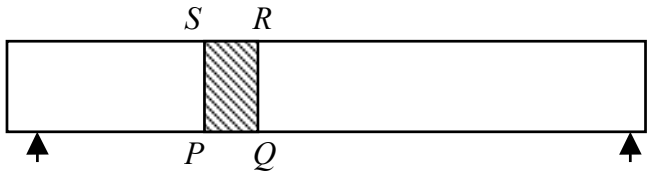

(*a*) Concrete block isolated for the analysis

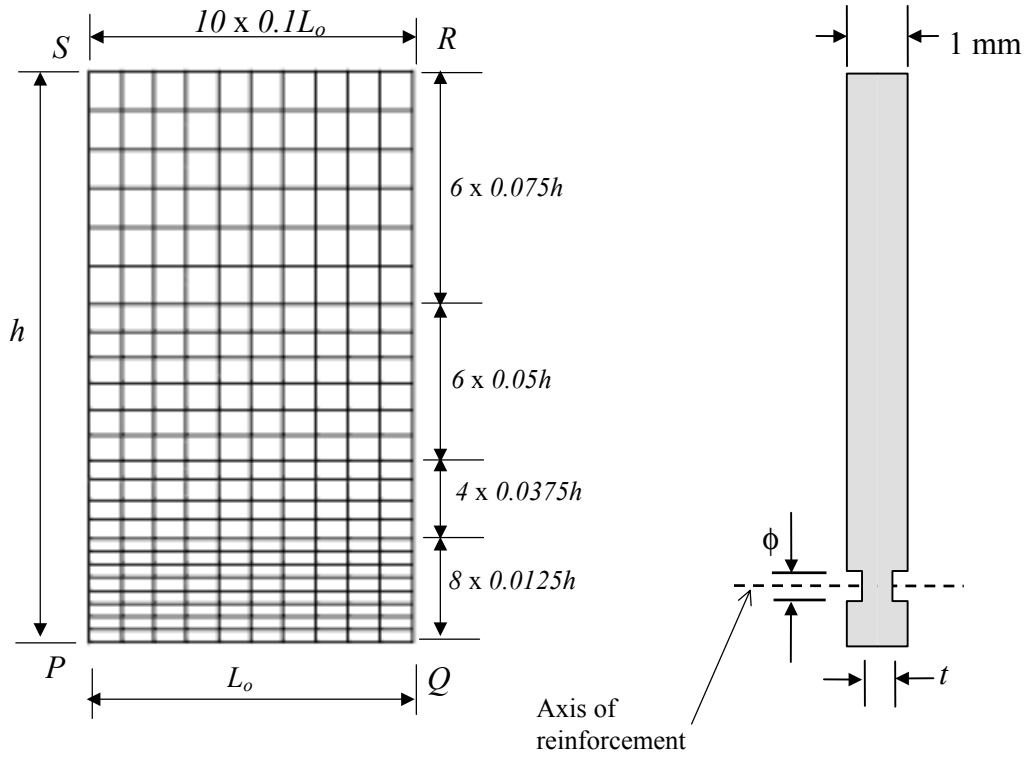

(*b*) Finite element mesh

(*c*) Cross section

Fig. 4.17 Finite element idealisation (See *Appendix C1* for the locations of node numbers at which the calculated forces are applied)

4.11.3 Reduction of the concrete area due to reinforcement

Steel bars normally occupy a substantial fraction of the beam width. To account for the reduction of the concrete area due to reinforcement, the thickness of the concrete slice is modified at reinforcement level as shown in Fig. 4.17*c*. The modified thickness *t* at the level of reinforcement is calculated to be

$$t = 1 - \frac{\rho d}{\phi} \tag{4.29}$$

A Similar approach was used by Nilson (1968) to account for the reduction in the concrete area due to reinforcement.

4.11.4 Types of concrete blocks analysed

Three types of concrete blocks are used in the present analysis with different locations selected for the transverse sections bounding the concrete block. Fig. 4.18 shows the forces acting on each type of the free bodies and corresponding boundary conditions. These three types of concrete blocks are described below.

(a) Free body near the first flexural crack (Type A)

Fig. 4.18*a* shows the concrete block analysed to determine the stress distribution near the first flexural crack in a loaded beam. One transverse section bounding this concrete block is taken through the first flexural crack in the beam (at *A*), while the other section is taken through the zero-slip point (at *X*). Note that these two sections correspond to sections *A* and *X* respectively, in Fig. 4.8. Nodal forces equivalent to the compressive forces F_{c1}, F_{c2}, tensile force F_t and bond force F_b are determined using the program *FORCES.BAS* as described previously. It may be noted that this free body is in a state of self-equilibrium (both translational and rotational) under the forces indicated. As the mathematical model requires certain boundary restraints for the analysis, two supports arbitrarily located at Z_1 and Z_2 as shown are introduced. All the calculated reactions on these supports will become zero, and therefore, these supports have no effect on the computed stress distribution. The exact locations of these arbitrary supports are shown in *Appendix C1*.

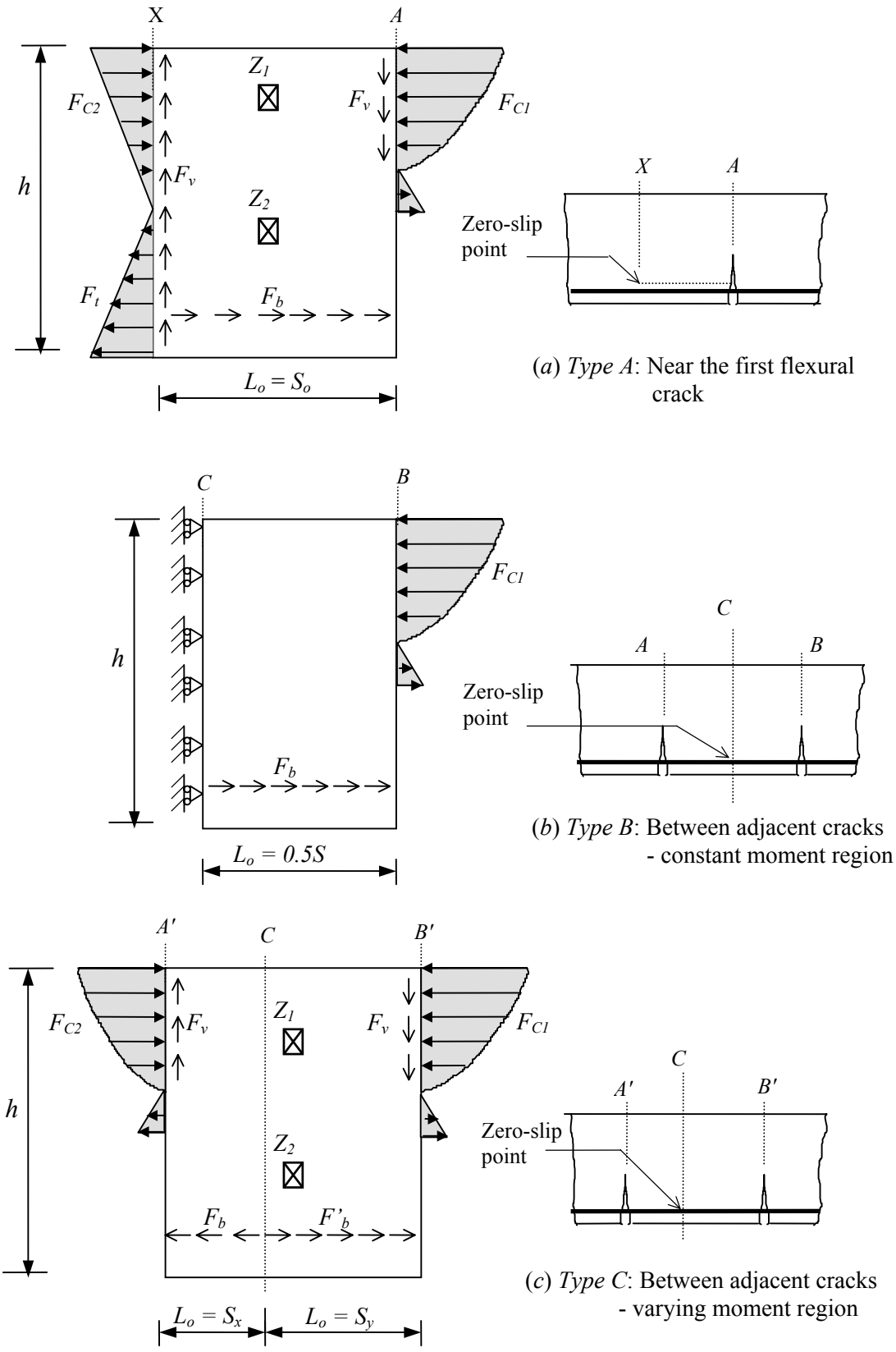

Fig. 4.18 Three different types of free bodies used in the analysis (Note: all forces shown are nodal forces computed using the program *FORCES.BAS*)

(b) Free body between two flexural cracks in a constant moment region (Type B)

To evaluate the stress distribution between adjacent cracks in a constant moment region, the free body shown in Fig. 4.18*b* is analysed. Since the forces acting on two transverse sections at *A* and *B* as well as the bond forces are symmetrical about the mid section at *C*, only one half of the block is analysed. The boundary conditions along the line of symmetry are taken as having only a displacement in the transverse direction.

(c) Free body between two flexural cracks in a varying moment region (Type C)

Fig. 4.18*c* shows the free body of concrete block analysed to determine the concrete stress distribution between adjacent flexural cracks in a varying moment region. It may be seen that the forces acting on the two transverse sections are different, and consequently, the zero-slip point is not located at the mid section between the cracks. Therefore, the full free body between the two cracks is analysed. As in the *Type A* concrete block described previously, two supports Z_1 and Z_2 are introduced in the finite element mesh (Fig. 4.18*c*) for mathematical reasons. This free body is in a state of self-equilibrium under the forces indicated in Fig. 4.18*c*, and therefore the stress field within the concrete block is not affected by the introduction of these supports.

4.11.5 Elastic modulus of concrete

In the compression zone of the finite element mesh, different rows of elements are assigned different values for the elastic modulus, depending on the distance from the neutral axis. The elastic modulus applicable for a particular row of elements is taken as the instantaneous modulus of elasticity, corresponding to the strain at the cracked section at the level of the centroid of elements in that row. The instantaneous modulus of elasticity is calculated using the constitutive relationship for concrete, which is shown in Fig. 4.1. This relationship is reproduced in Fig. 4.19 for easy reference. If the compressive strain at the cracked section at the level of the centroid of elements in a particular row (Fig. 4.11) is equal to ε_{cx}, all the elements in that row are assigned the elastic modulus E_{cx}, calculated using the following equation.

$$E_{cx} = \frac{f'_{cx}}{\varepsilon_{cx}} \tag{4.30}$$

where f'_{cx} is the concrete stress corresponding to the strain ε_{cx}.

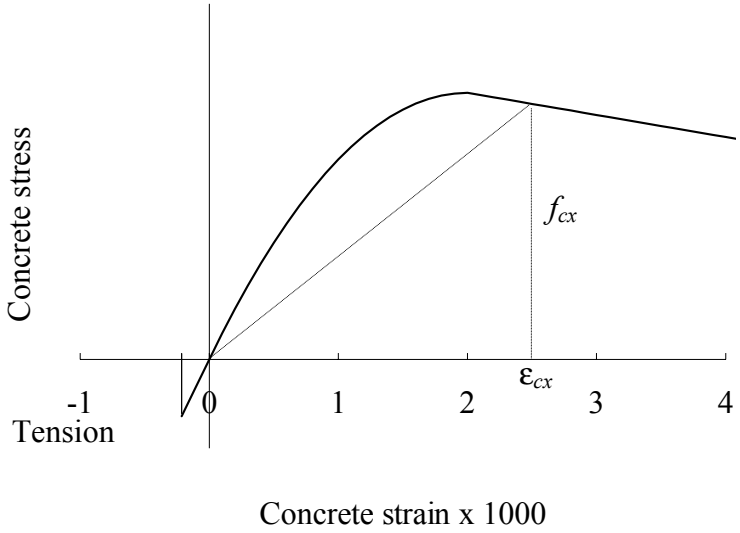

Fig. 4.19 Calculation of elastic modulus for compression zone

The elastic moduli for all elements below the neutral axis (tensile zone) are taken as the tangent modulus of concrete in compression, which is equal to $1000f'_c$ as already mentioned in Section 4.3.

The program *FORCES.BASIC* mentioned previously determines the elastic modulus values applicable for each row of elements in the finite element mesh, at the end of Solution Modes 3 and 7 after calculating the compressive force distribution at the cracked section. *Appendix A5* shows the values of elastic modulus applicable for different rows of the finite element mesh calculated for a typical case.

4.12 Summary

This Chapter described the methods of calculating the forces acting on a free body concrete block, for incorporating in the finite element analysis. Forces on cracked and uncracked sections of a loaded beam are determined by considering the equilibrium conditions and the constitutive relationships for steel and concrete. Bond forces acting

around reinforcing bars are determined based on the local slip and the bond stress-bond slip relationship. Iterative procedures are used for the above calculations because of the non-linear nature of the constitutive relationship for concrete and the bond stress-bond slip relationship. Step-by-step procedures used in the iterative methods of calculating the concrete and bond forces are described in detail. A computer program written in *BASIC* language is used for carrying out the above calculations. A description of the structure of this computer program is also given. Finally, the finite element model and the standard software package used for the analysis are described, together with the details of different types of concrete blocks analysed.

CHAPTER 5

CONCRETE AND STEEL STRESSES NEAR FLEXURAL CRACKS

5.1 General remarks

The three types of concrete blocks described in Chapter 4 (*Types A, B* and *C* shown in Fig. 4.18) are analysed using the finite element method and the results are presented in this Chapter. Concrete stresses near the first flexural crack are investigated by using the results of *Type A* block. *Type B* and *Type C* blocks are analysed for various load levels and crack spacing values, to investigate their effects on the concrete stress distribution between adjacent cracks, and the results are discussed.

It is assumed that a new secondary crack is formed in between two existing cracks when the maximum concrete tensile stress between the cracks reaches the flexural strength of concrete. The height of this new crack is determined by repetitive analysis of the finite element mesh, with discontinuities introduced at locations where the concrete tensile stress has exceeded the flexural strength.

In the later part of this Chapter, an empirical formula is developed to determine the slip length (S_o in Fig. 4.8) for a given beam, based on the results of a parametric study carried out using the calculation procedure described in Chapter 4. The slip length and the concrete stress distributions near flexural cracks described in this Chapter are used in Chapter 6 to predict the locations of cracks that are formed at various stages of loading, when the beam is subjected to a gradually increasing load.

5.2 Concrete Stresses Near Flexural Cracks in Constant Moment Region

Concrete stresses calculated near flexural cracks in constant moment regions are described in this Section. The results obtained from the finite element analysis are used to develop two-dimensional stress contours for typical cases of beams and slabs, as described below.

It is noted that the contours for major and minor principal stresses in constant moment regions are almost identical to the longitudinal tensile and compressive stress contours, respectively. Therefore, contours are developed for the longitudinal stress, instead of the principal stress, to avoid the production of two diagrams (major and minor principal stresses) for each case. In varying moment regions however, major principal stress diagrams are also presented in addition to the longitudinal stress contours, because they are found to be different.

5.2.1 Stresses near the first flexural crack

When the first flexural crack is formed in a member, there is a sudden increase in the steel stress at the cracked section, as already discussed in Chapter 4. This stress increment, Δf_{so} is resisted by the bond forces acting for a certain length of the steel bar, called the slip length S_o (see Fig. 4.8), which depends on Δf_{so} and the bond characteristics of reinforcement. At the end of the slip length (at a point S_o away from the crack – section *X* in Fig. 4.8), the slip between the steel bar and surrounding concrete is zero. This point is called the zero-slip point. As already mentioned in Chapter 4, the steel and concrete stresses beyond the zero-slip point are not influenced by the formation of the first crack.

To investigate the stresses near the first flexural crack, a concrete block of length S_o located between the first flexural crack and the zero slip point (block between sections *X* and *A* in Fig. 4.8) is analysed by the finite element method (block *Type A* in Fig. 4.18). Results obtained from this analysis on four typical members are presented in this Section. These members include two one-way slabs and two beams with low and moderate reinforcement ratios, as detailed in Table 5.1 (See *Appendix B1* for typical cross sections). Note that the slip length S_o shown in Table 5.1 is calculated using the Solution Mode 4 in the program *FORCES.BAS* as already described in Chapter 4. Results of this Solution

Mode on the four members analysed are given in *Appendix B2 to B5*. As seen in these Appendices, the above Solution Mode also calculates the equivalent nodal bond forces that will be input into the finite element model.

Table 5.1. Details of members analysed (first crack in constant moment region; f'_c =32 MPa).

Member	Width b (mm)	Effective depth d (mm)	Total height h (mm)	Tensile reinforcements	Tensile reinforcement Ratio	S_o (mm)
Slab -5.1	1000	170	200	6ϕ12	0.004	184
Slab -5.2	1000	170	200	6ϕ16	0.0071	151
Beam-5.1	200	400	450	3 ϕ16	0.0075	126
Beam-5.2	325	400	450	4 ϕ25	0.015	136

Forces acting on the two transverse sections of this concrete block are determined using the Solution Modes 1 and 2 of the program *FORCES.BAS* as described in Chapter 4. Note that these Solution Modes calculate the forces on uncracked and cracked sections respectively, for an applied bending moment of M_{cr} at each section (see Fig. 4.8 and 4.18*a*). *Appendix B6* to *B13* present the calculated nodal forces on the two transverse sections of the four members analysed.

The calculated nodal forces are applied to the finite element mesh at the respective nodes in transverse sections and reinforcement level (see Fig. 4.17, 4.18*a* and Appendix *C1*). To prepare a finite element mesh of different size for each member, a '*master mesh*' is first prepared with overall height h = 100mm and block length L_o=100mm (Fig. 4.17). The *SCALE* command available in *STRAND6* software package is used to change the size of the block as required, with the mesh arrangement remained unchanged as shown in Fig. 4.17. After analysing the finite element model, the *PLOT* command available in *STRAND6* software package is used to produce the stress contours.

Fig. 5.1 shows the resulting longitudinal stress contours for the four members analysed. It can be seen that the stress contours at section *X* (zero-slip section) in all cases occur at a regular interval, suggesting the variation of stress from compression face to the tension face is linear, as expected. It is also seen that the concrete stress at the tension face of the member increases gradually, from zero at the crack to the maximum at section *X* (zero slip section). Stress distributions shown in this figure indicate that there is no significant effect of the reinforcement ratio on the stresses near the first flexural crack.

Variation of the concrete stress at the tension face along the slip length is shown in Fig. 5.2 for the four members analysed. These stresses have been obtained from the finite element analytical results at the nodes in the tension face (nodes 1 to 11 in *Appendix C1*). As seen in this figure, the variation of the concrete tensile stress along the slip length is identical for all the members considered. This property is used in the next Chapter to predict the formation of subsequent cracks when the load on the member is gradually increased.

The resulting tensile stress in the reinforcement along the slip length is shown in Fig. 5.3 for all the four members analysed. These steel stress values have been calculated using the procedure described in Section 4.7.1 (Eqs. 4.16*d* and 4.16*f*). As seen in this figure, the variation of the steel stress along the slip length is identical for all the members considered. This property will be utilised in Chapter 8 in evaluating the curvature at sections between adjacent cracks for the calculation of deflections.

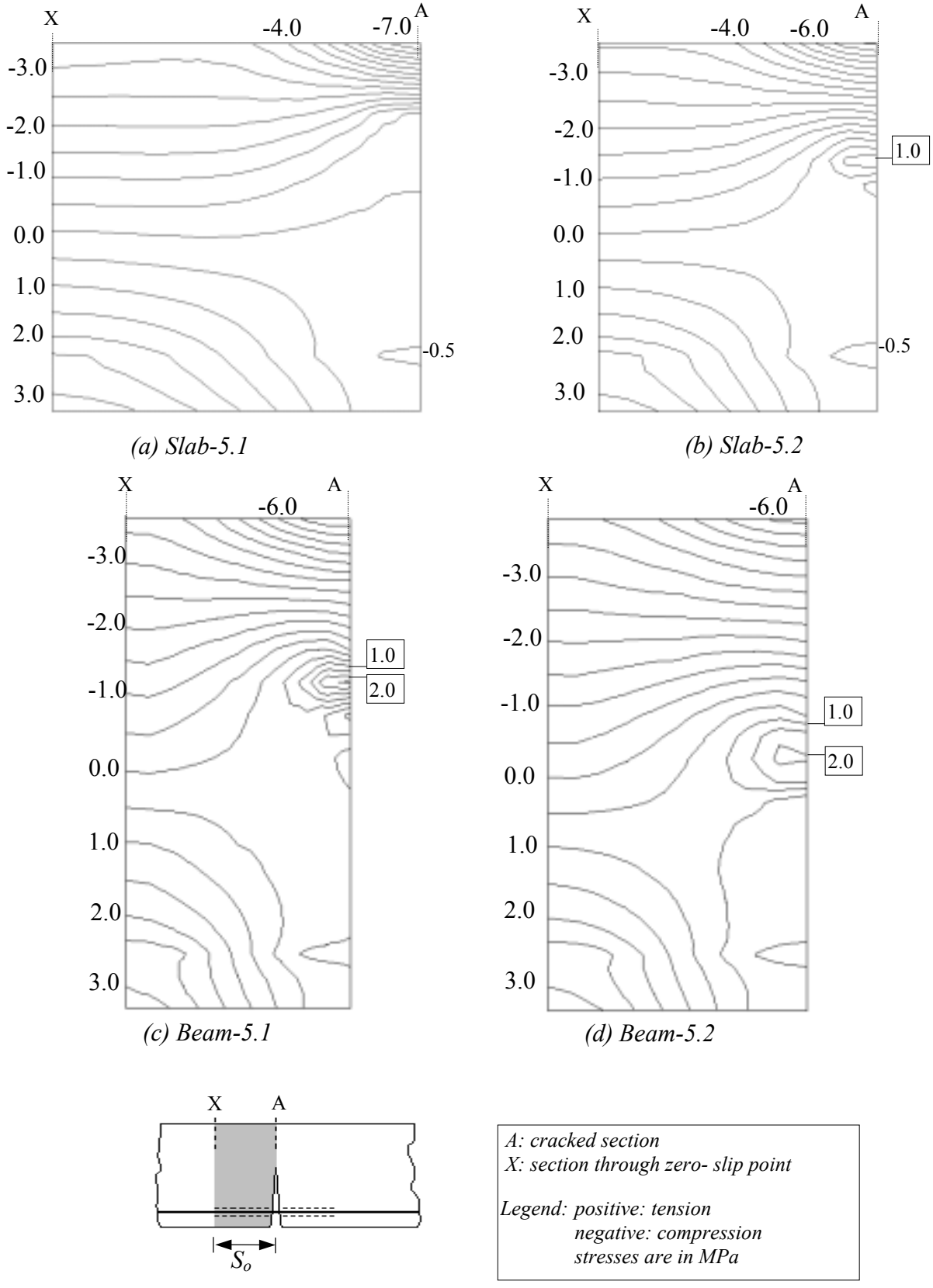

Fig. 5.1 Longitudinal concrete stress contours near the first flexural crack in constant moment region (see Table 5.1 for details of slabs and beams)

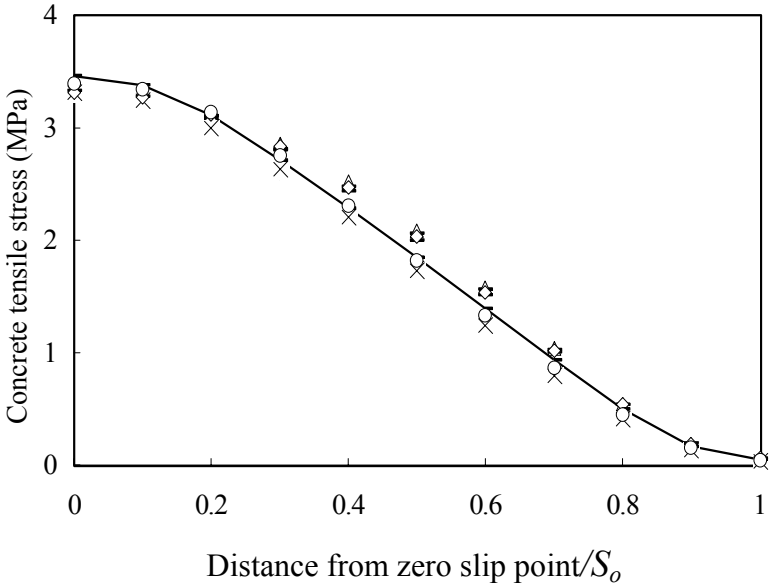

Fig. 5.2 Variation of concrete stress at the tension face along the slip length S_o (constant moment region in *Slab-5.1, Slab-5.2, Beam 5.1* and *Beam -5.2*; see Table 5.1 for details)

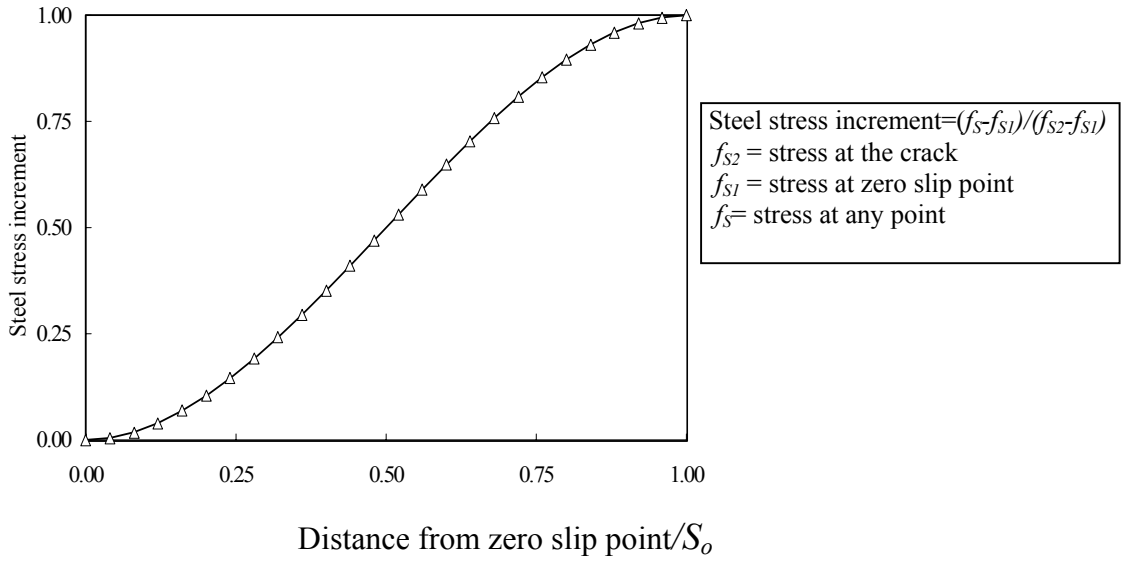

Fig. 5.3 Variation of steel stress along the slip length S_o (constant moment region in *Slab-5.1, Slab-5.2, Beam 5.1* and *Beam -5.2*; see Table 5.1 for details)

5.2.2 Definition of primary cracks

Prior to the formation of the first crack, the stress distribution at all sections in a beam has a similar pattern as shown in Fig. 4.3 for an uncracked section. After the first crack is developed, the stress distribution at any other section beyond a distance S_o away from the crack is also identical to that of an uncracked section. Therefore, the subsequent cracks formed at a distance larger than S_o away will be identical to the first crack. Such cracks developed at sections where the concrete and steel stresses have not been altered by the formation of previous cracks are defined as *primary cracks*.

5.2.3 Stresses in between adjacent cracks

If a second crack is formed at a distance less than $2S_o$ away from the first crack then the slip lengths for the two cracks will overlap with each other. When this happens, a redistribution of concrete and bond stresses will take place in the region between the two cracks. The resulting stress distribution depends on the distance between the two cracks as well as the steel stresses at the cracked sections. To develop longitudinal stress contours in between two such cracks, the concrete block between adjacent cracks is analysed by the finite element method, for two typical flexural members. (Note that the free body *Type B* shown in Fig.4.18*b* is used for this analysis). These two members comprise of a one-way slab and a beam with moderate reinforcement ratios, as shown in Table 5.2. The cross sectional details of these members are similar to those shown in *Appendix B1*. The slip length S_o shown in Table 5.2 has been calculated using the procedure described in Chapter 4.

Table 5.2. Details of members analysed (adjacent cracks in constant moment region

Member	Width *b* (mm)	Effective depth *d* (mm)	Total height *h* (mm)	Span (m)	Tensile reinforce-ments	Tensile Reinforce-ment Ratio	S_o (mm)
Slab -5.3	1000	170	200	3.3	9ϕ12	0.006	133
Beam-5.3	315	400	450	7.2	4 ϕ20	0.010	137

Note: For all beams f'_c = 32MPa.

Both these members are simply supported with the slab (*Slab 5.3*) and the beam (*Beam 5.3*) having a clear span of 3.3m and 7.2m, respectively. Each member is loaded with two equal point loads at third points (Fig. 5.4) so that the bending moment within the middle third is constant. For each member, two sets of concrete blocks between adjacent cracks in the constant moment region are analysed. They are: *set 1*: constant load level with different crack spacings, and *set 2*: constant crack spacing with different load levels. Note that in all cases, the selected crack spacings are less than $2S_o$ so that the two slip lengths overlap, and the loading causes a bending moment M in the constant moment region, such that $M_{cr}<M<M_u$.

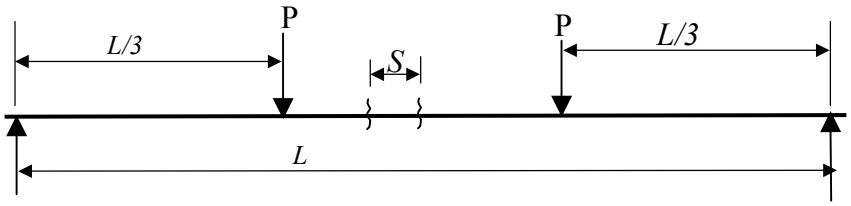

Fig. 5.4 Loading arrangement on *Slab 5.3* and *Beam 5.3*

Table 5.3 shows the different load levels and crack spacings selected for *set 1* and *set 2* concrete blocks in each member. The resulting stress contours obtained from the finite element analysis are shown in Figs. 5.5 and 5.6, for *slab 5.3* and *Beam 5.3* respectively. (Note that for clarity, only the contours in the tensile zone are shown for *Beam 5.3*). The nodal forces applied on the finite element mesh for the above two sets of concrete blocks in *slab 5.3* and *Beam 5.3* are shown in *Appendix B14 to B31*.

Table 5.3 Load levels and crack spacings used for analysis (constant moment region - *Slab 5.3* and *Beam 5.3*)

Category	P (kN)	Bending Moment (kNm) (Constant moment region)	Steel stress at cracked section f_s (MPa)	Crack spacing *S (mm)*
Slab 5.3 Set 1	29.5	32.5	200	120
				160
				220
Slab 5.3 Set 2	22.73	25	150	180
	29.5	32.5	200	
	43.64	43.64	300	
Beam 5.3 Set 1	38.21	91.7	200	80
				120
				160
Beam 5.3 Set 2	18.75	45	90	140
	38.21	91.7	200	
	56.25	135.65	300	

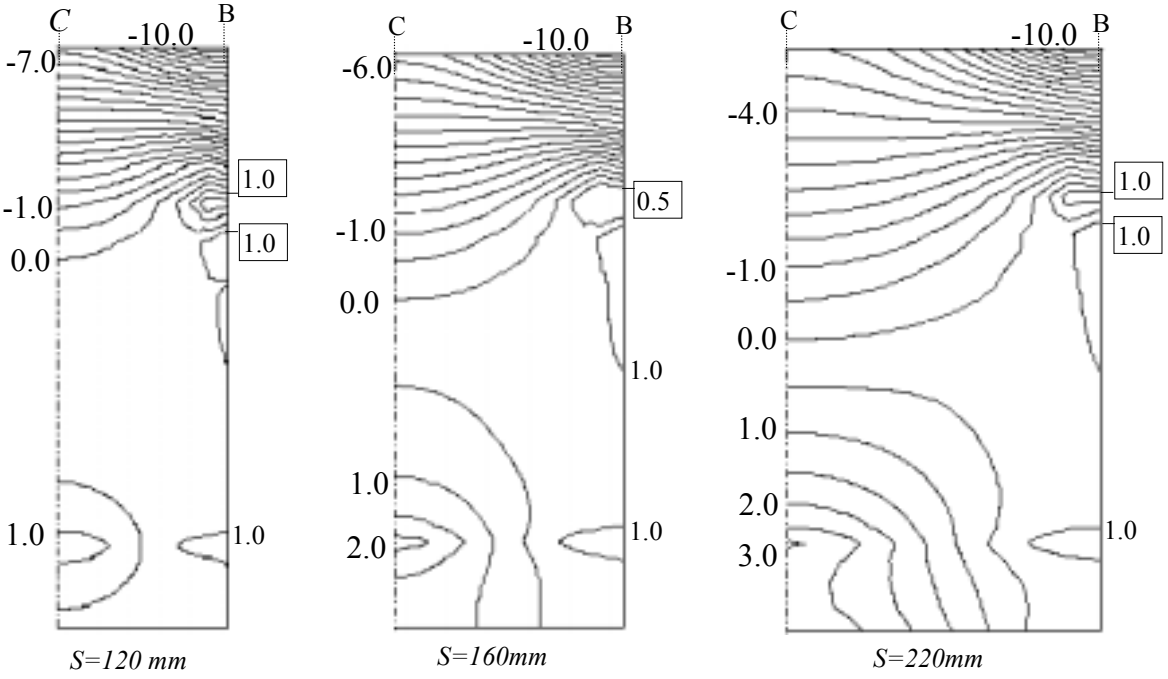

(a) Variation of concrete stress with crack spacing (f_s=200 MPa)

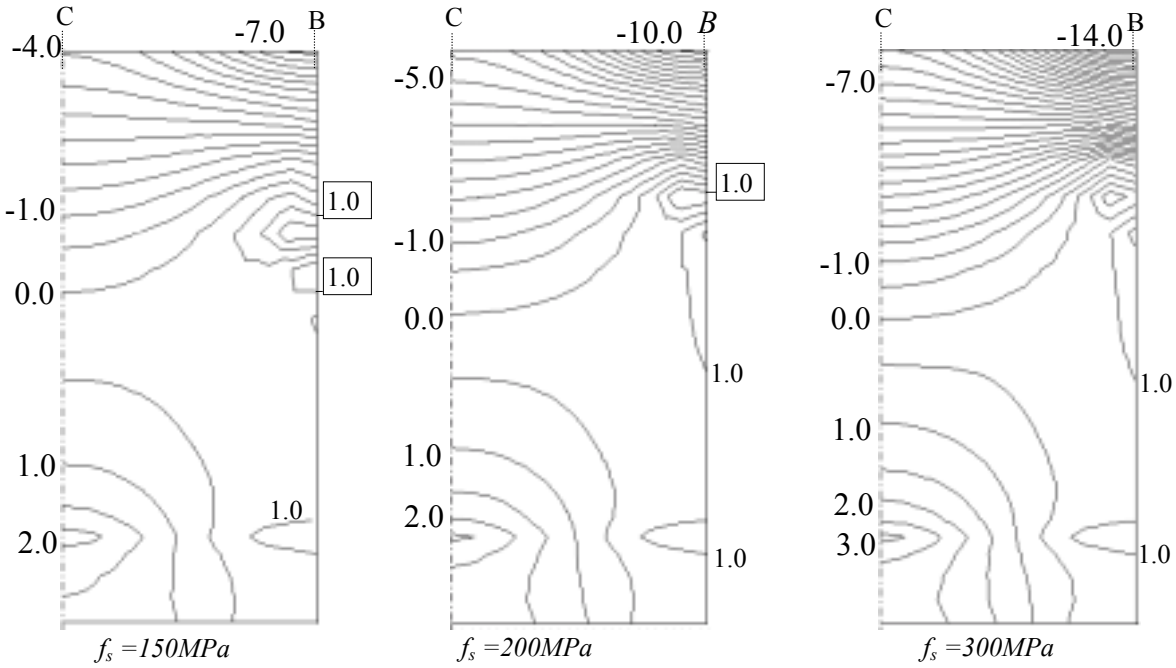

(b) Variation of concrete stress with steel stress at the crack (S=180 mm)

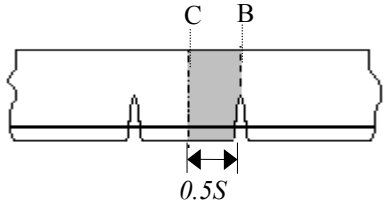

f_s = steel stress at the cracked section
S =crack spacing

Legend: positive: tension
negative: compression
stresses are in MPa

Fig. 5.5 Longitudinal concrete stress contours between adjacent cracks in constant moment region for *Slab-5.3* (see Table 5.2 for details of *Slab-5.3*)

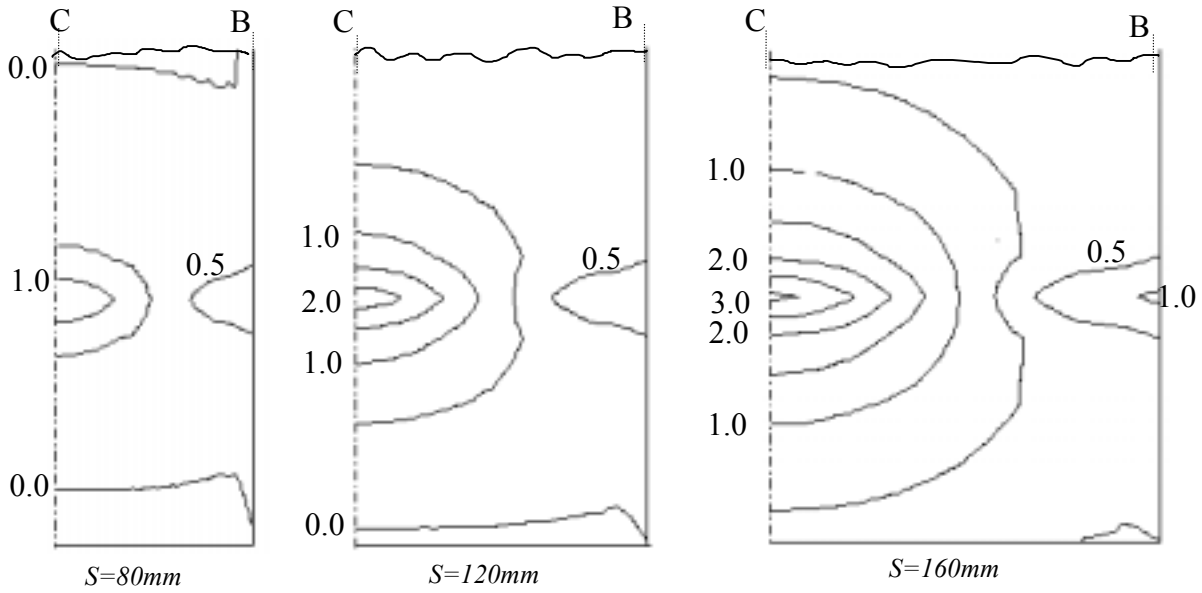

(a) Variation of concrete stress with crack spacing (f_s=200 MPa)

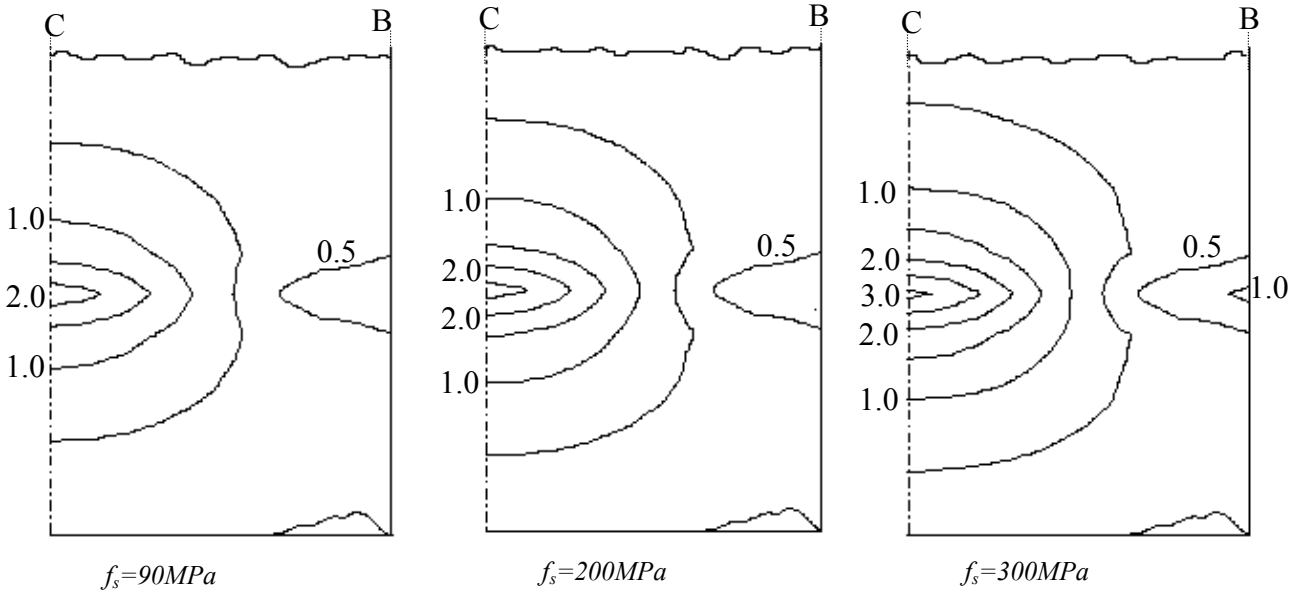

(b) Variation of concrete stress with steel stress at the crack (S=140mm)

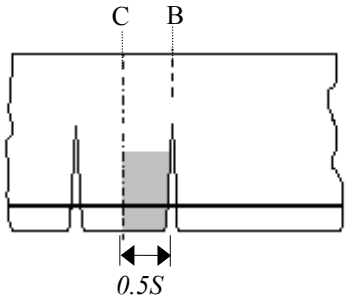

f_s = steel stress at the cracked section
S =crack spacing

Legend: positive: tension
negative: compression
stresses are in MPa

Fig. 5.6 Longitudinal stress near reinforcement between cracks in constant moment region for *Beam-5.3* (see Table 5.2 for details of *Beam-5.3*). Stresses are in *MPa*.

5.2.4 Critical crack spacing

Inspection of Figs. 5.5(*a*) and 5.6(*a*) indicates that, at a given loading on the beam, concrete tensile stress at reinforcement level increases with the spacing between adjacent cracks. This suggests that, at any given load level, there is a particular crack spacing which produces a concrete tensile stress equal to the flexural strength of concrete. This spacing is herein referred to as the *critical crack spacing* (l_c) for the given load level. At this load level, crack spacings larger than l_c cannot exist, because for such crack spacings the resulting concrete tensile stress exceeds the flexural strength, causing a new crack to form.

Critical crack spacing for a given load level is determined by analysing the finite element mesh with different trial crack spacing values. The analysis is repeated until the calculated maximum concrete tensile stress is equal to the flexural strength. When this condition is achieved the trial crack spacing is taken as the critical crack spacing l_c for the given load level. A detailed description of this procedure is presented in Chapter 6 (section 6.5.1).

5.2.5 Definition of secondary cracks

Figs. 5.5(*b*) and 5.6(*b*) show that the concrete tensile stress at reinforcement level increases with the loading on the beam, if the crack spacing is kept constant. Therefore, if the load on the beam is increased gradually, at a certain load level, the concrete tensile stress between a particular pair of adjacent cracks may reach the flexural strength. When this happens, a new crack will develop at the location where the concrete tensile stress has reached the flexural strength. Such cracks developed in between existing cracks at higher load levels are defined as *secondary cracks.*

It is also seen in Figs. 5.5 and 5.6 that, in constant moment regions, the maximum concrete tensile stress occurs at the mid section (Section *C*) between the two cracks. This means that the formation of *secondary cracks* in constant moment regions divides the existing crack spacings into two halves.

It may be noted that the *primary cracks* are initiated at the tension face as evident from the stress distribution across the height of the member shown in Fig. 4.3. On the other hand, *Secondary cracks* are initiated at reinforcement level as seen in the stress contours given in Figs. 5.5 and 5.6. Once these cracks are initiated, they propagate in the transverse direction to form a fully grown flexural crack. The propagation of cracks in the transverse direction is investigated below.

5.2.5.1 Height of primary cracks

When a primary crack is initiated, the stress in the adjacent uncracked concrete at that section increases to compensate for the loss of concrete tensile force due to cracking. When the increased concrete stress reaches the flexural strength, the crack propagates further upwards. This propagation of the crack is also associated with an increase in the tensile strain at the section, resulting in an increase of the steel stress by a large proportion due to the high elastic modulus compared to that in concrete. The upward propagation of the crack continues until the increased tensile force in the reinforcement is sufficient to maintain the equilibrium of the section. This final height of the primary crack h_c ($h_c=h-kd-k_1d$; see Fig. 4.6) can be calculated once the values of kd and k_1d are evaluated using the procedure described in Section 4.6 for a cracked section.

It must be noted that the upward propagation of primary cracks is not progressive, but instant because any height of the crack that is less than the final one does not satisfy the equilibrium. This can be seen in Fig. 5.7 where the moment of resistance of the section is plotted against the crack height for a typical beam. The moment of resistance corresponding to a selected crack height was calculated using Eq. 4.2*b* after evaluating the heights of compression and tensile zones, kd and k_1d (see Fig. 4.6) to satisfy the translational equilibrium (Eq. 4.2*a*).

Inspection of Fig. 5.7 indicates that there is a minimum crack height which can provide a moment of resistance equal to the cracking moment M_{cr}. This means that once the primary crack is initiated, (on reaching the bending moment $M=M_{cr}$) the crack will immediately grow to the minimum crack height required to satisfy the equilibrium condition. As seen in Fig. 5.7, this minimum height is 0.69h for the beam considered, if the reinforcement ratio is 0.008. It is also seen in this figure that there is only a slight

increase in the primary crack height, when the applied bending moment is increased beyond the cracking moment M_{cr}.

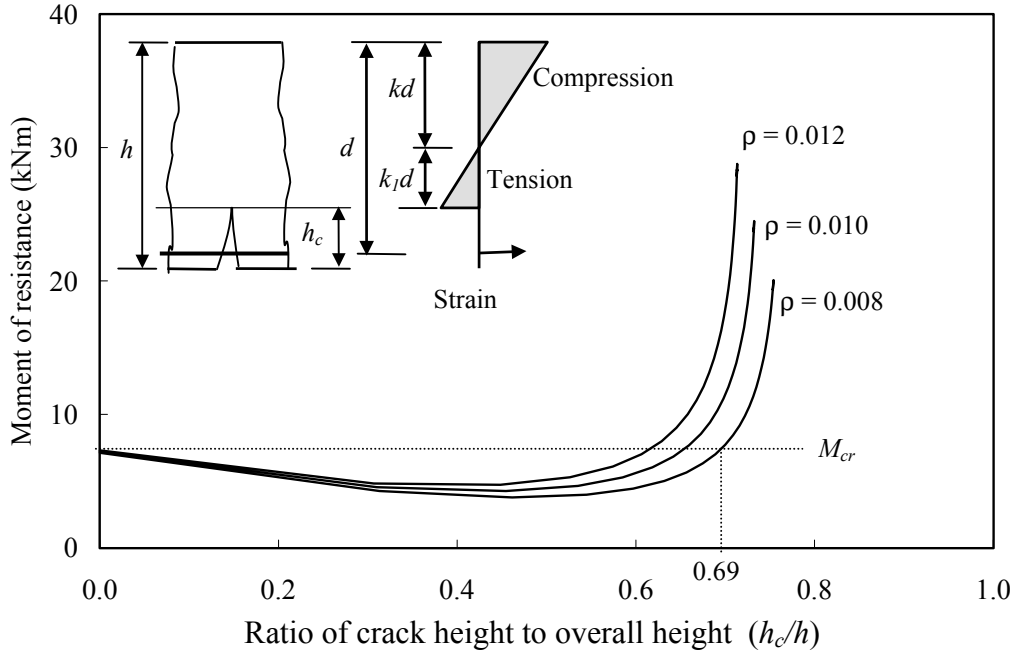

Fig. 5.7 Variation of moment of resistance with the primary crack height (b=200 mm, d=188 mm, h=240 mm, f'_c=32 MPa)

5.2.5.2 Height of secondary cracks

(a) stress distribution prior to cracking

Calculation of the primary crack height described above is based on the assumption that plane sections remain plane before and after the formation of the crack. This assumption is valid for all primary cracks in a beam, as they are developed at sections where the stress conditions have not been affected by the formation of nearby cracks. However, results of finite element analyses indicated that the concrete stress distributions are non-linear at sections where secondary cracks occur (in between adjacent cracks). This can be seen in Fig. 5.8 where the concrete stresses along the mid section between adjacent cracks are plotted for two typical members. Details of these members are shown in Table 5.4, while the nodal forces applied on the finite element mesh are given in *Appendix B19*, *B22, B23* and *B26*. Because of the non-linearity of the concrete stress distribution at sections between adjacent cracks, the height of secondary cracks are determined using the results of finite element analyses, as described below.

Table 5.4 Members analysed to calculate concrete stresses at the mid-section

Member	Effective depth (mm)	Overall height (mm)	Reinforce-ment ratio	Steel stress at the primary crack (MPa)	Primary crack spacing (mm)
Slab-5.3	170	200	0.006	300	180
Beam-5.3	400	450	0.01	200	160

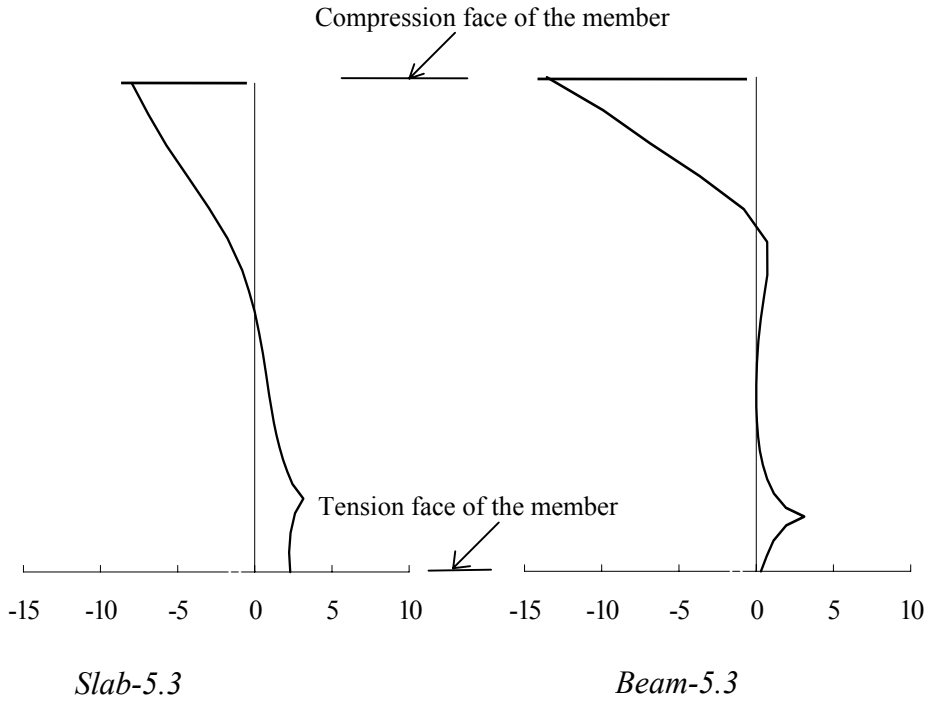

Fig. 5.8 Stress distribution across the mid section between two primary cracks (constant moment region - Note: all stresses are in MPa)

(*b*) *propagation of secondary cracks*

The height of a secondary crack is determined by progressively introducing discontinuities at nodes in the finite element mesh, where the concrete tensile stress has reached the flexural strength. The analysis is repeated until the calculated maximum concrete tensile stress becomes less than the flexural strength. The step-by-step procedure is as follows (refer to Fig. 5.9).

(*a*) Determine the critical crack spacing l_c for the given load level (see Section 5.2.4). The length of the concrete block $L_o = 0.5l_c$ (see Fig. 4.18*b*);

(*b*) Introduce a crack at reinforcement level (node *A* in Fig. 5.9) by releasing the boundary restraint;

(*c*) Analyse the finite element mesh and compare the concrete stresses with flexural strength, at the top and bottom ends of the crack (nodes *B*', *B*", *C', C''* etc. in Fig. 5.9);

(*d*) If the stress at the end(s) of the crack exceeds the flexural strength, enlarge the crack by releasing the boundary restraints at respective node(s), and go to step (c). If the stresses are lower, the height of the crack is final.

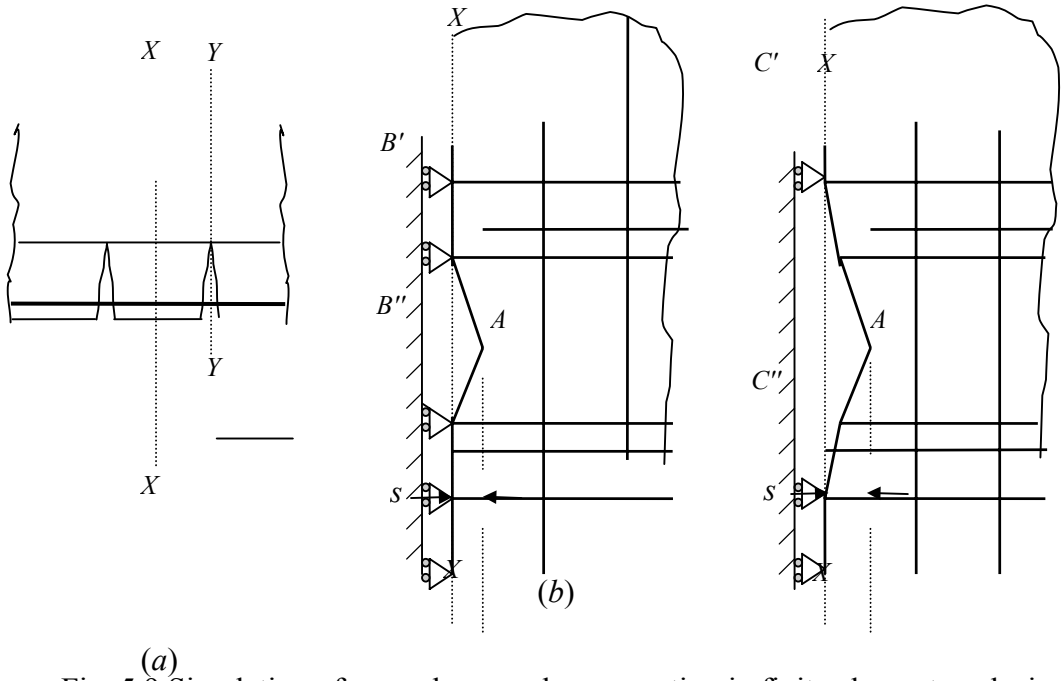

Fig. 5.9 Simulation of secondary crack propagation in finite element analysis (Line *X*-*X* indicates the mid-section between the two primary cracks)

It must be pointed out that the bond forces acting between the existing primary crack and the new secondary crack are different at each stage of analysis described above. This is because the gradual increase in the slip that occurs at the secondary crack (shown as *s* in Fig. 5.9) results in a movement of the zero-slip point away from the new crack, causing a reversal of bond stresses. The resulting variation of the bond stress distribution during the propagation of the secondary crack is schematically shown in Fig. 5.10. In this figure, *Curve-1* and *Curve-2* represent the bond stress distributions before and after the formation of the secondary crack, respectively. The other two curves show two intermediate stages. f_{bo} and f'_{bo} represent the positive and negative peak bond stresses respectively, after the propagation of the secondary crack is completed. Corresponding distances from the final zero-slip point to the secondary and primary cracks are S_x and S_y, respectively, as shown in Fig. 5.10.

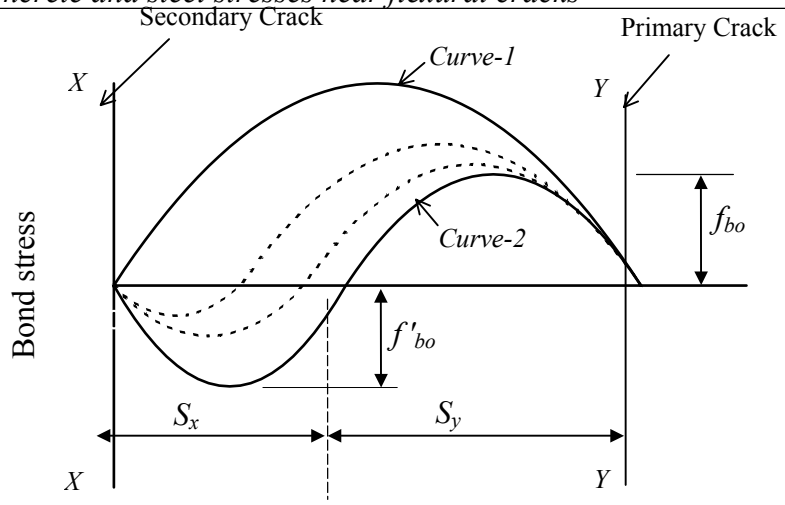

Fig. 5.10 Redistribution of bond stress during the propagation of a secondary crack (*Curve -1*: before, *Curve -2*: after)

Bond stress distribution

The position of the zero-slip point, which determines the bonds stress distribution at each stage of analysis described above, depends on the magnitude of the slip at the new secondary crack indicated as *s* in Fig. 5.9. On the other hand, *s* depends on the bond force acting on the concrete block. Therefore, at each stage of analysis, the bond stress distribution between the primary crack and the secondary crack is determined using the following trial-and-error procedure. Refer to Figs. 5.9 and 5.10.

(*a*) select a trial value for S_x

(*b*) calculate f_{bo} and f'_{bo} using the trial and error procedure described in Chapter 4 for determining bond stresses in a varying moment region (Section 4.7.2*b*).

(*c*) determine the extensions of steel and concrete at section *X* with respect to the zero-slip point as described in Chapter 4, and then calculate the value of *s*.

(*d*) carry out the finite element analysis and determine the displacement at point *A* in Fig. 5.9. If this value is larger (or smaller) than *s* obtained in step (*c*), increase (or decrease) the trial value of S_x and go to step (*b*). If they are equal then the selected value of S_x, and calculated values of f_{bo} and f'_{bo} are acceptable.

(*c*) *results of secondary crack height*

The analytical procedure described above is used to determine the secondary crack heights for three typical beams, which have moderate reinforcement ratios. Details of these beams are given in Table 5.5. For each beam, the secondary crack height is determined under four different load levels. Calculated values of the steel stress at the primary crack f_{s2} and the critical crack spacing l_c for the selected load levels are shown in Table 5.6. The secondary crack heights obtained from the analysis and the corresponding primary crack heights for each case are given in Table 5.7 (total 12 cases). These crack heights together with their spacings are graphically presented in Fig. 5.11.

The calculated values of crack heights shown in Table 5.7 and Fig. 5.11 indicate that the primary and secondary cracks have nearly the same height for beams with effective depth of 300 mm. For larger values of the effective depth, the height of secondary crack is considerably smaller than the height of adjacent primary cracks. This prediction is consistent with experimental results including the observations by Broms (1965 and 1965*a*).

Table 5.5. Beams analysed to calculate secondary crack height (f'_c=32 MPa)

Beam No	Effective Depth (mm)	Width (mm)	Overall height (mm)	Number of bars and diameter (mm)	Reinfor-cement ratio
Beam 5.4	300	200	340	3 ϕ 16	0.01
Beam 5.5	400	315	440	4 ϕ 20	0.01
Beam 5.6	500	315	540	4 ϕ 25	0.0125

Table 5.6. Calculated values of the steel stress at cracked section and critical crack spacing

Beam No.	CASE -1		CASE -2		CASE -3		CASE -4	
	f_{s2}	l_c	f_{s2}	l_c	f_{s2}	l_c	f_{s2}	l_c
Beam 5.4	90	200	170	160	200	150	260	140
Beam 5.5	100	200	150	180	220	160	320	140
Beam 5.6	95	200	140	180	210	160	310	140

Note: f_{s2} is the steel stress at the primary crack in MPa

l_c is the critical crack spacing in mm.

Table 5.7. Calculated primary and secondary crack heights

Beam No.	CASE -1		CASE -2		CASE -3		CASE -4	
	h_P	h_S	h_P	h_S	h_P	h_S	h_P	h_S
Beam 5.4	190	155	220	220	225	225	225	225
Beam 5.5	261	170	285	190	300	210	305	210
Beam 5.6	314	212	340	240	360	260	365	260

Note: h_P is the primary crack height in mm
h_S is the secondary crack height in mm.

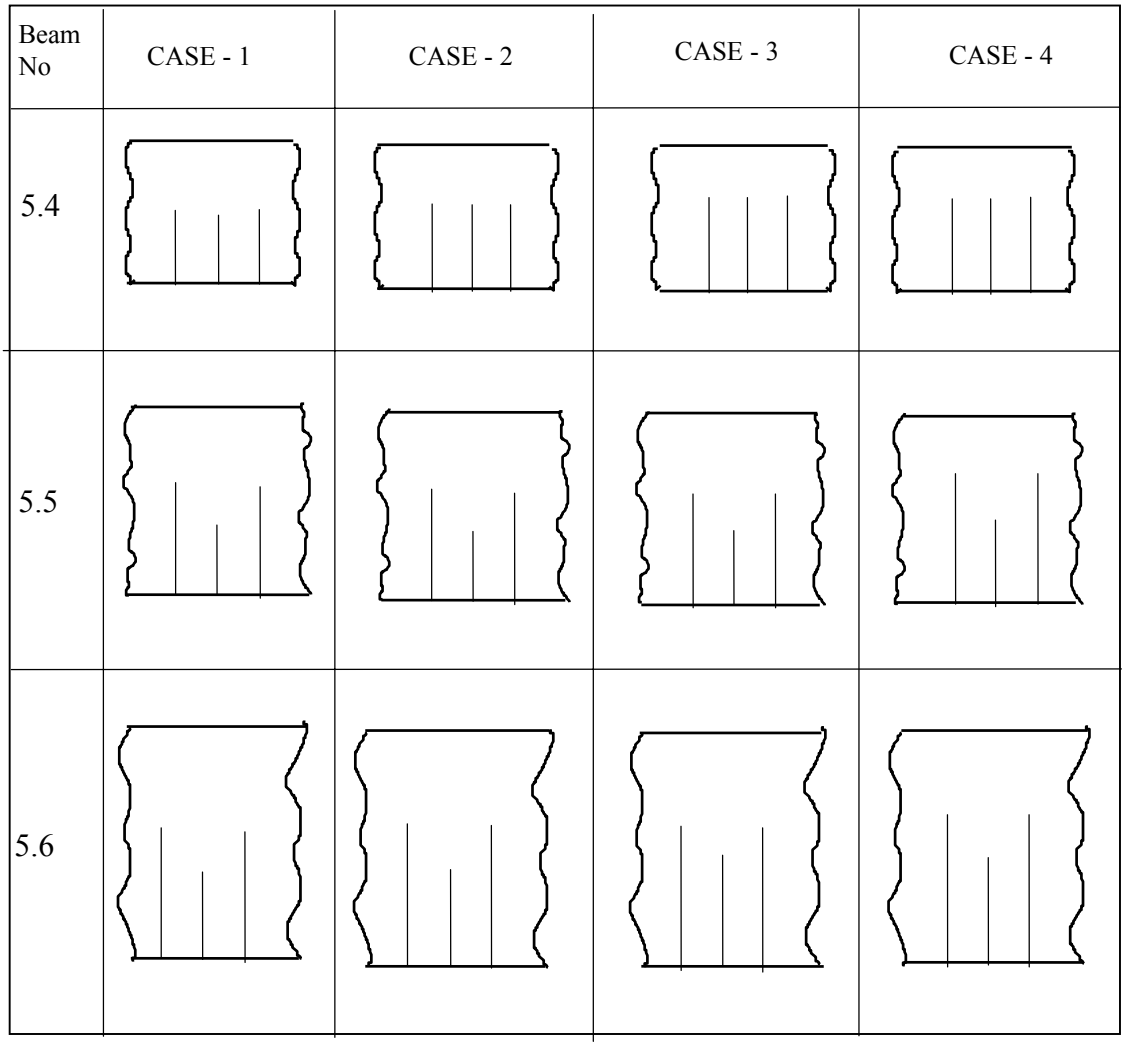

Note: See Tables 5.5, 5.6 and 5.7 for details of beams, selected values of crack spacing and steel stress at primary cracks, and the calculated crack heights.

Fig. 5.11 Illustration of primary and secondary crack heights (constant moment region)

5.2.5.3 Effect of concrete cover on the propagation of secondary cracks

As already mentioned, secondary cracks originate at the level of reinforcement, where the maximum concrete tensile stress occurs (Fig. 5.5 and 5.6). The step-by-step procedure of calculating the secondary crack heights described in the previous Section has shown that the secondary cracks reached the tensile face of the member for all the 12 cases considered.

It is seen however, that there are situations where the secondary cracks do not reach the tensile face of the member. The calculation procedure described in the previous Section shows that this happens if the concrete cover is relatively large. For such beams, the maximum concrete tensile stress remains below the flexural strength, after propagating the crack for a certain distance, but before reaching the tension face. In these cases, the secondary crack is confined to the immediate neighbourhood of the reinforcement, and is not visible on the tension face of the member. Occurrence of such cracks has been observed in laboratory experiments by many investigators, including Broms (1965*b*) and Warner *et al* (1998).

It must be noted that the propagation of secondary cracks on to the tension face is desirable in practice, as it facilitates a reduction in the crack width at the tension face. This is because when the secondary crack reaches the tension face, it can divide the primary crack spacing into two halves, making the individual crack spacings smaller. As seen in the next Chapter, smaller crack spacings will result in smaller crack widths. Therefore, the concrete cover in flexural members should not be too excessive as to confine the secondary cracks in the immediate neighbourhood of the reinforcement without propagating on to the member surface.

5.2.5.4 Limiting value of concrete cover

The limiting value of the concrete cover that will prevent the propagation of secondary cracks on to the tension face depends largely on the concrete strength. This limiting concrete cover is determined using the repetitive analytical procedure described in Section 5.2.5.2, for beams with effective depths ranging from 300 to 500 mm and bar diameters from 16 to 25 mm. Results obtained from this analysis are presented in Fig. 5.12. A concrete cover which lies above the line shown in this figure will prevent the propagation of secondary cracks on to the tension face of the member.

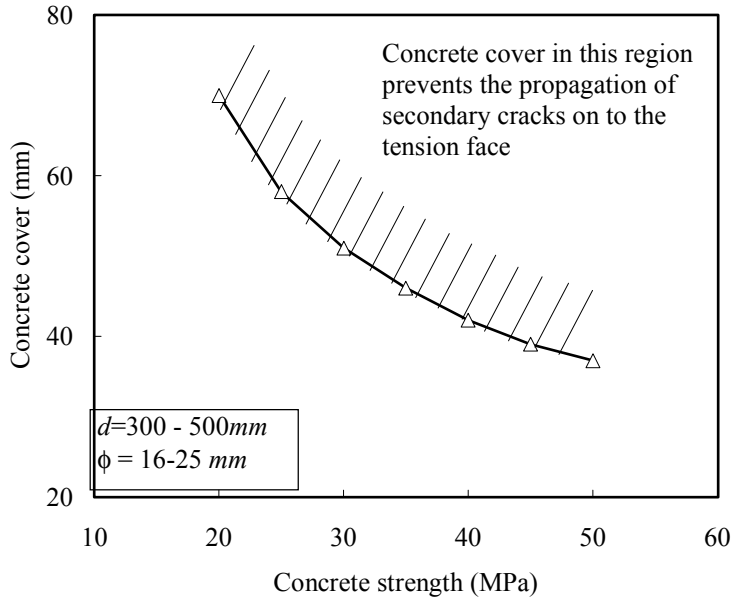

Fig. 5.12 Limiting value of the concrete cover

5.2.6 Determination of crack width

5.2.6.1 Crack width at the level of reinforcement

Crack width at the level of reinforcement is determined as the relative difference in elastic extensions of steel and surrounding concrete. Both extensions are measured with respect to the zero-slip point. The extension of steel at the cracked section ε_{s1} is evaluated by integrating the strain function using the same procedure described in Chapter 4 for the calculation of ε_{so} (see Eq. 4.16*e*). To determine ε_{s1}, the upper limit of integration in Eq. 4.16*e* is changed from $0.5S_o$ to $0.5S$ (see Figs. 4.8 and 4.10). The resulting equation for ε_{s1} is as follows.

$$e_{s1} = \frac{f_{s2} S_o}{2E_s} - \frac{f_{bo} S^2}{4 E_s \phi} \qquad (5.1a)$$

The corresponding extension of concrete ε_{c1} at the cracked section is determined from the results of the finite element analysis (Section 5.5). Assuming that there exist two cracks on either side, equally distant from a particular crack, the width at the middle crack is calculated using the following equation.

$$W_S = 2(e_{s1} - e_{c1}). \qquad (5.1b)$$

where W_s is the crack width at the level of reinforcement.

5.2.6.2 Crack width at the tension face of the member

The crack width at the tension face of the member W_t is calculated assuming that the two concrete faces of the crack are plane as shown in Fig. 5.13. W_t can then be expressed in terms of the crack width at reinforcement level W_S, using the following relationship.

$$W_t = \frac{h - kd}{d - kd} W_s \qquad (5.2a)$$

The depth of the compression zone *kd* varies with the amount of reinforcement and the concrete strength. However, the ratio (*h-kd*)/(*d-kd*) included in Eq. 5.2*a* does not vary significantly with the value of *k*, in the range encountered in practice (0.3 to 0.4), for moderately reinforced beams and slabs. Therefore, in this thesis a constant value of k=0.3 is used for all the beams in calculating the crack width at the tension face. This will eliminate the necessity for calculating the depth of compression zone for each case. Eq. 5.2*a* can then be simplified as

$$W_t = \{1.43(h/d) - 0.43\} W_S \qquad (5.2b)$$

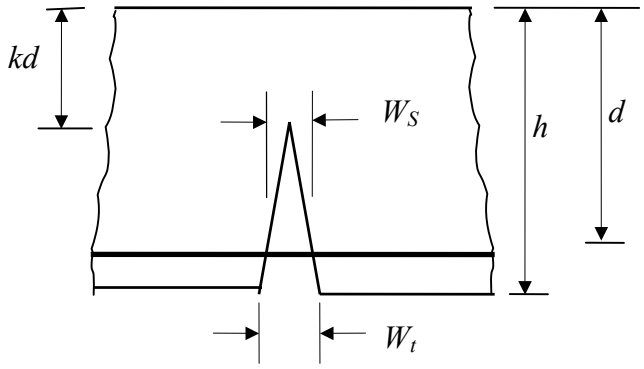

Fig. 5.13 Crack width at the tension face

5.3 Concrete Stresses Near Flexural Cracks in Varying Moment Regions

In this Section, concrete stresses near flexural cracks in varying moment regions are determined and compared with corresponding stress distributions in constant moment regions. *Slab-5.1* and *Beam-5.2* (see Table 5.1) analysed in the previous Section are taken as typical cases for this comparison.

5.3.1 Stresses near primary cracks in varying moment regions

When a simply supported beam is subjected to a gradually increasing point load at the mid span, the first crack will appear under the loading point where the bending moment is largest. This occurs when the maximum bending moment reaches the cracking moment of the beam M_{cr}. The applied load at this stage is significantly smaller than the ultimate load for moderately reinforced beams. Therefore, at the time when primary cracks occur near the mid span, the corresponding shear stress at cracked sections is considerably small. These are called *low-shear* primary cracks.

On the other hand, within the region close to the supports of a beam, new primary cracks may occur at very high load levels. For example, in *Beam-5.2* (see Table 5.1) with a clear span length 4000 *mm*, the first primary crack occurs at the mid-span when the central point load is only 46 kN, while new primary cracks may occur at sections 1600 *mm* away from centre when the load reaches 230 kN. (Note that the ultimate load

for this beam is 281 kN). These primary cracks occurring near the supports under higher load levels are called *high-shear* primary cracks.

Concrete stresses are investigated in this Section for both types of primary cracks, *low-shear* and *high-shear*. However, as already mentioned in Chapter 4, beams with small shear span to depth ratio, that tend to fail in shear are not considered. Primary cracks formed near the mid spans in *Slab-5.1*, (see Table 5.1) and those formed near the supports in *Beam-5.2* are considered as typical cases in the present calculation.

(a) Primary cracks near mid span of Slab-5.1 (low-shear stress)

When this slab is simply supported with a clear span of 4000 *mm* and subjected to an increasing central point load, the first crack will appear near the mid span when the load reaches 24*kN*. The average shear stress at the section before the formation of the crack is very small (0.06 *MPa*), and the corresponding concrete stress distribution near the first crack is almost identical to that in a constant moment region, as seen in Fig. 5.14. Note that the stress contours shown in Fig. 5.1 for *Slab-5.1* in constant moment region is also reproduced here for easy comparison.

Propagation of the crack in transverse direction

As evident from the stress distributions shown in Fig. 5.14, primary cracks near the mid span of a beam subjected to a central point load should be formed in a manner similar to that in a constant moment region *i.e*., perpendicular to the tension face. This prediction agrees with the experimental observations by Warner *et al* (1998), Park & Paulay (1975).

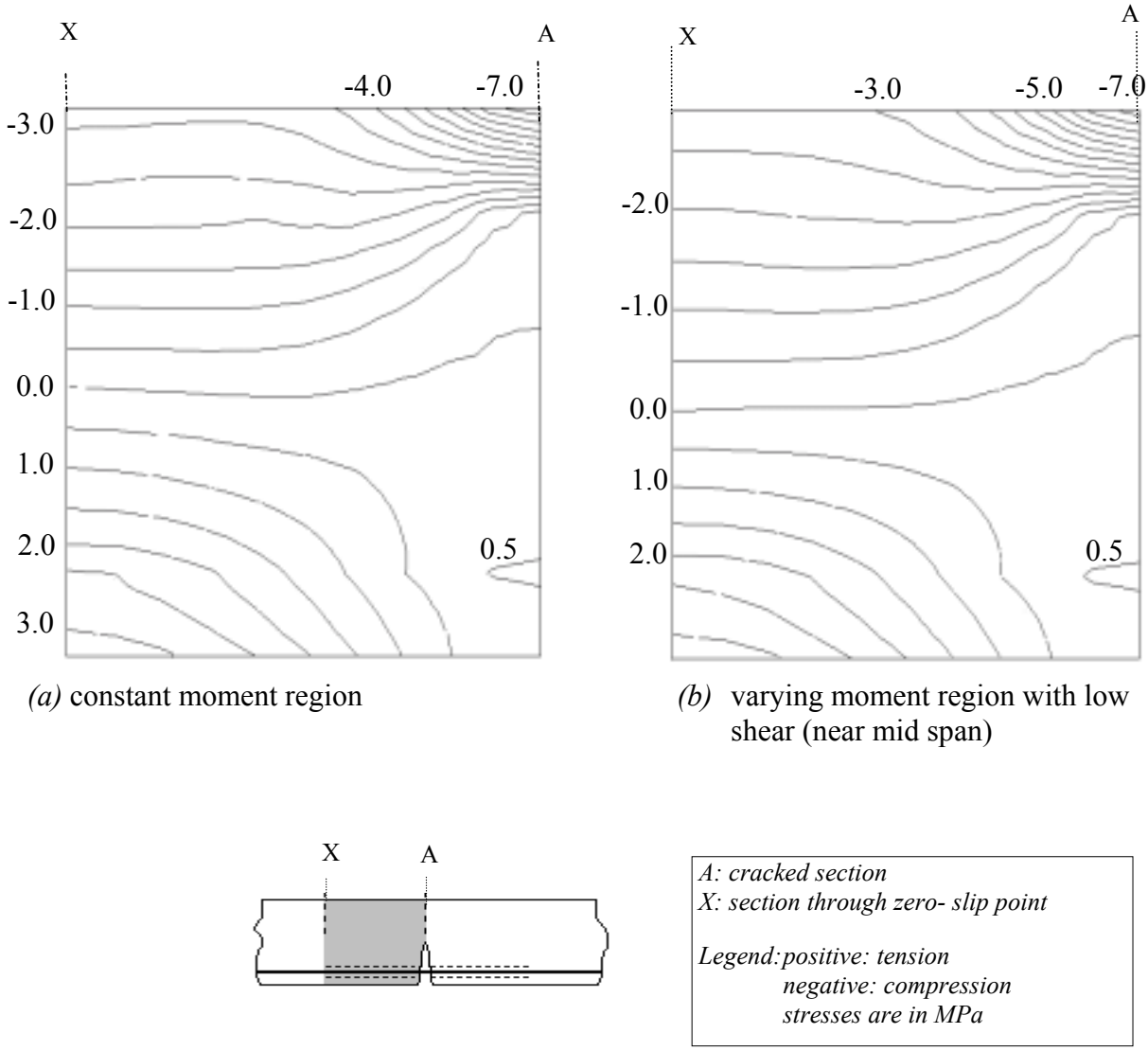

(a) constant moment region

(b) varying moment region with low shear (near mid span)

Fig. 5.14 Longitudinal concrete stress contours adjacent to a primary crack in *Slab-5.1* (see Table 5.1 for details of *Slab-5.1*).

(b) Primary cracks near supports in Beam-5.2 (high-shear stress)

Concrete stresses are also determined near the primary crack formed 1600 *mm* away from the mid span (400 *mm* from the support) in *Beam-5.2* when it is simply supported with a clear span of 4000 *mm* and subjected to a central point load. This crack was formed when the applied load reached 230 *kN*, and the crack is subjected to high shear stresses (average shear stress before the formation of the crack is 0.79 *MPa*). The resulting longitudinal concrete stress distribution adjacent to the cracked section is shown in Fig. 5.15, together with the stress distribution obtained for the constant moment region, for comparison.

Comparison of Figs. 5.15*a* and 5.15*b* indicates that there is only a small difference between the stress distributions, in the region where the maximum tensile stress occurs (variations in compression stress is not considered). In particular, the gradual increase of the concrete stress at the tension face, from zero at the cracked section to the maximum at the zero slip section, is nearly the same for both cases. This property is used in the next Chapter to predict the locations of cracks formed in a member subjected to a gradually increasing load.

Although the longitudinal tensile stress distributions in the above two cases are nearly the same, there is a remarkable difference in the directions of principal stresses in the region where the maximum tensile stress occurs. As seen in Fig. 5.16(*a*), in a constant moment region, the direction of major principal stress at the zero slip section is parallel to the tension face. However, it is not so in the case of the high-shear primary crack considered, as evident in Fig. 5.16(*b*). It can be seen that at the zero-slip section, major principal stress near the tension face is slightly inclined to the longitudinal direction, while its inclination increases with the distance from the tension face, for the high-shear primary crack.

Propagation of the crack in transverse direction

The directions of the principal stresses shown in Fig. 5.16(*b*) suggest that primary cracks closer to a support may originate nearly perpendicular to the tension face. After it originates, it should propagate in a direction that is perpendicular to the major principal stress. According to the stress pattern shown in Fig. 5.16(*b*), the primary crack propagates in a curved direction towards the existing crack. This prediction also agrees with experimental observations by Warner *et al* (1998), Paulay & Park(1975).

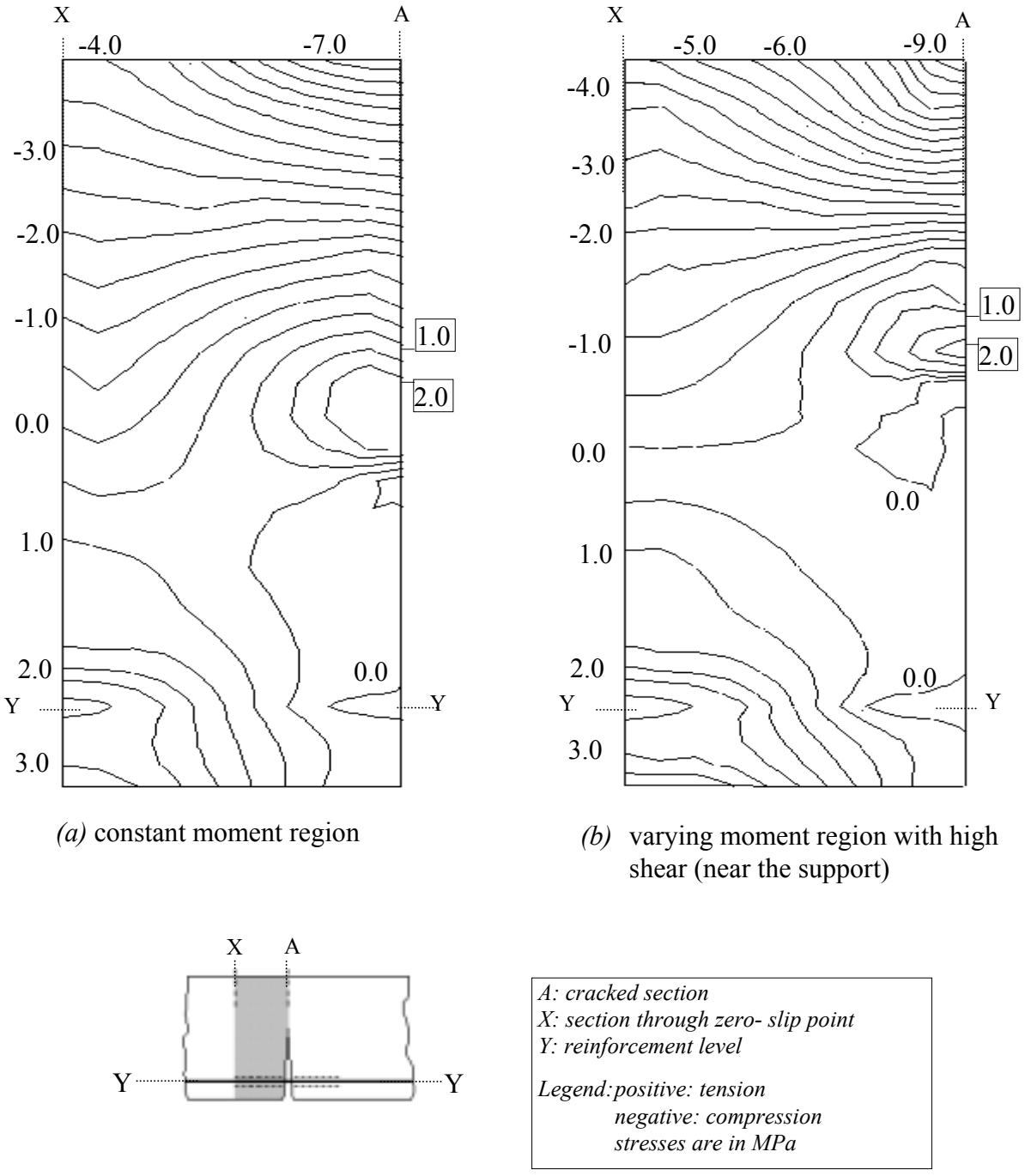

(a) constant moment region

(b) varying moment region with high shear (near the support)

Fig. 5.15 Longitudinal concrete stress contours near primary cracks in *Beam-5.2* (see Table 5.1 for details of *Beam-5.2*)

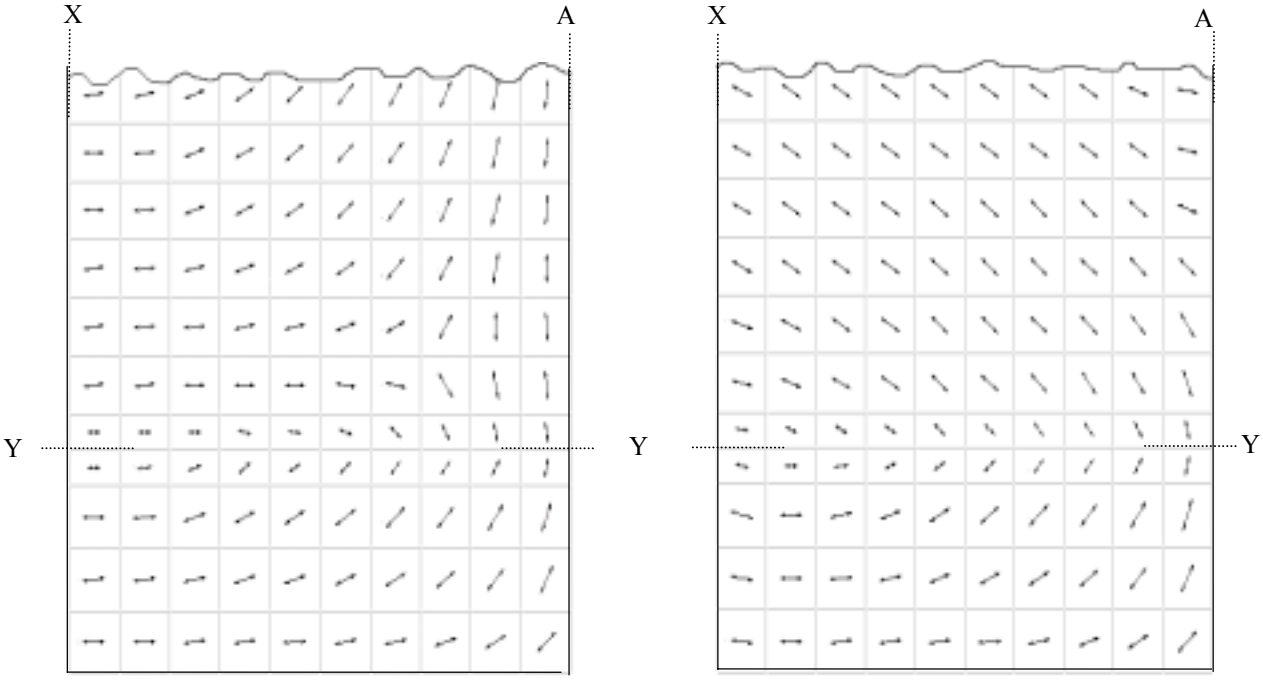

(a) constant moment region

(b) varying moment region with high shear (near the support)

A: cracked section
X: section through zero- slip point
Y: reinforcement level

Fig. 5.16 Directions of major principal stress in concrete near primary cracks in *Beam-5.2* (see Table 5.1 for details of *Beam-5.2*)

5.3.2. Stresses in between cracks in varying moment regions

Fig. 5.17 shows the longitudinal concrete stress distribution around reinforcement between adjacent primary cracks in a varying moment region of *Beam 5.2* considered earlier. A comparison of this figure with Fig. 5.6 indicates that the longitudinal tensile stress patterns in constant moment and varying moment regions are nearly the same. However, there is a remarkable difference in the directions of major principal stresses at the zero-slip section (where the maximum stress occurs) as described below.

In a constant moment region, the major principal stress at the zero-slip section (where the maximum stress occurs) is parallel to the longitudinal direction of the beam, due to symmetry. However, in a varying moment region this is not the case, as seen in Fig. 5.17*b*. The major principal stress near the tension face is slightly inclined to the longitudinal axis, and at other locations, this inclination increases with the distance from the tension face.

Propagation of secondary cracks

Because of the inclination of major principal stress described above, secondary cracks that originate between existing cracks in a varying moment region are not perpendicular to the tension face. When a secondary crack originates, it will propagate in a direction perpendicular to the major principal stress. According to the stress pattern shown in Fig. 5.17*b*, the crack propagates in a curved direction towards the existing crack that has the higher moment. Inspection of Fig. 5.17 also indicates that the maximum concrete tensile stress between adjacent cracks in a varying moment region occurs at a section closer to the crack that has the lower bending moment.

The determination of the actual shape of secondary cracks requires the repetitive analysis of the concrete block between adjacent cracks, by introducing discontinuities at locations where the principal stress exceeds the tensile strength of concrete. This procedure was already described in detail under Section 5.2.5.2 for constant moment regions. However, the investigation of the propagation of inclined secondary cracks developed in regions with high shear stresses is beyond the scope of this thesis.

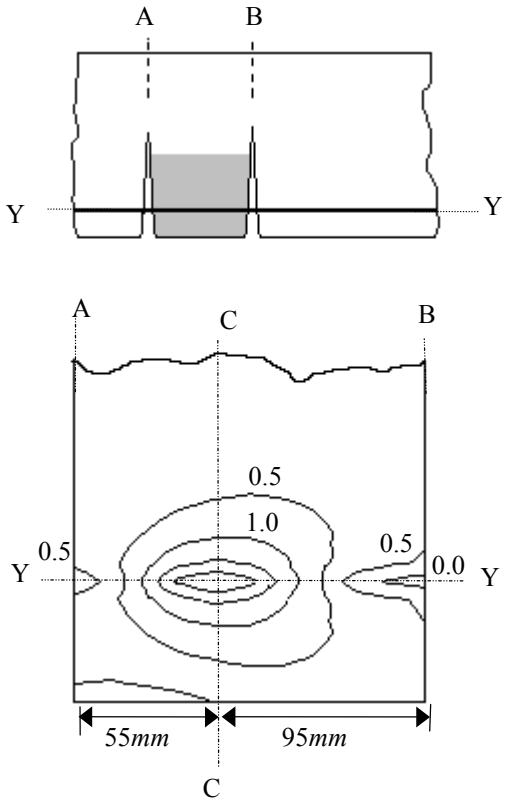

(a) Longitudinal stress contours

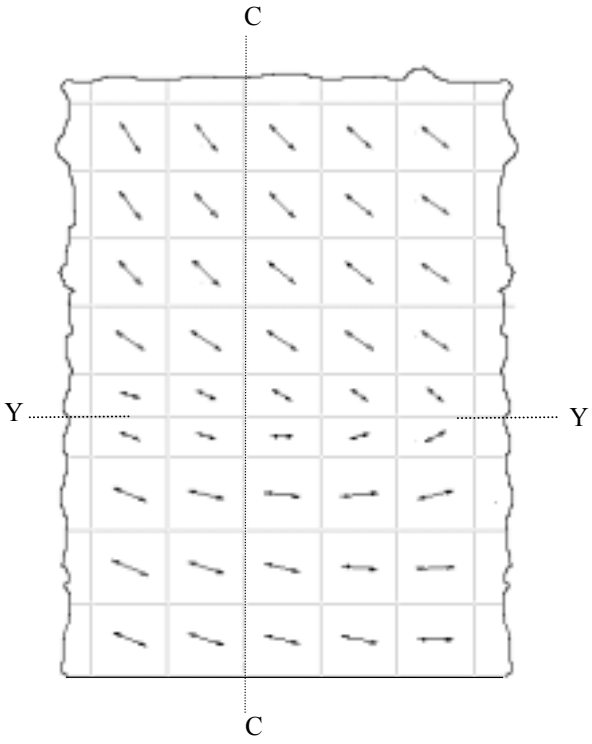

(b) Direction of major principal stress

A, B: cracked sections
C: section through zero- slip point
Y: reinforcement level

Fig. 5.17 Concrete stress distribution in tensile zone between two primary cracks in a varying moment region for *Beam-5.2*. *Note: at B: M=207kNm and f_s =303MPa; at A: M=190kNm and f_s=277MPa; at C: f_s =267MPa (M = bending moment and f_s = steel stress)*

5.4 Approximate Formula for the Slip Length S_o

The slip length S_o is a major parameter that governs the spacing of cracks in reinforced concrete flexural members as described in the next Chapter. In this Section, an empirical formula is developed for the calculation of slip length, using the results of a parametric study.

The slip length S_o depends primarily on the steel stress increment Δf_{so} that occurs at the formation of a primary crack, and bond characteristics of reinforcements. Therefore, an empirical formula is first developed for the calculation of Δf_{so}, and the slip length is expressed in terms of Δf_{so}, as described below.

5.4.1 Parametric study

The steel stress increment Δf_{so} is calculated as $\Delta f_{so} = f_{s2} - f_{s1}$ where f_{s1} and f_{s2} are the steel stresses just before and just after the formation of the first flexural crack. Both steel stresses, f_{s1} and f_{s2}, are calculated under the same applied bending moment M_{cr}, the cracking moment of the section. For a given beam, the values of f_{s1} and f_{s2} are determined using the computer program *FORCES.BAS* as already described in Chapter 4.

The value of Δf_{so} for a given beam depends on the amount of reinforcement, cross sectional dimensions and concrete strength. To develop an empirical formula, Δf_{so} is calculated for a large number of beams having different values for the above parameters. Ranges of the parameters used in the present calculation are shown in Table 5.8. Note that a constant value is assumed for h/d =1.15, which is close to most practical situations. Three types of cross sections, rectangular, T-shaped and Box-shaped are considered in this calculation. Notation used for different cross sectional dimensions are shown in Fig. 5.18.

Table 5.8 Variables used in the parametric study and their ranges

Parameter	Range
Concrete strength, f'_c	20 - 50 MPa
Reinforcement ratio, ρ	0.003 - 0.033
Flange width/web width, b/b_w	1.5 - 3.0
Flange thickness/effective depth, h_f/d	0.2 - 0.4

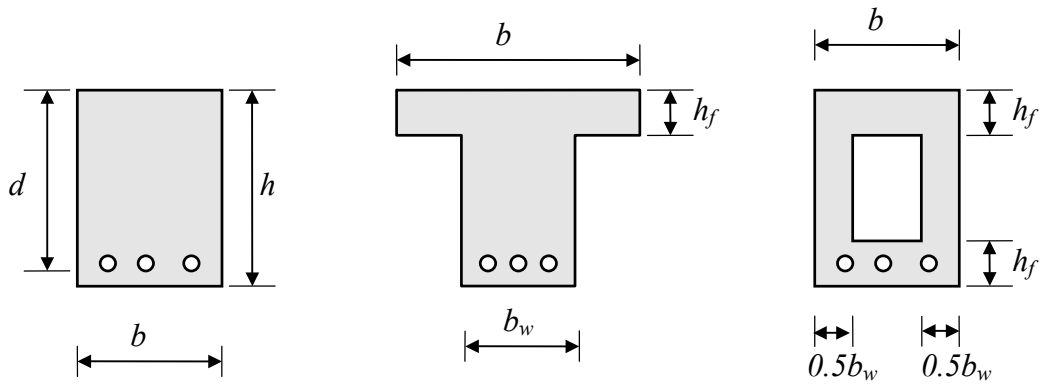

(*a*) Rectangular (*b*) T- beam (*c*) Box-beam

Fig. 5.18 Types of cross sections considered in the parametric study

For the calculation of f_{s1} and f_{s2} in the parametric study, the computer program *FORCES.BAS* described in Chapter 4 is slightly modified. Once the ranges for the above parameters are input in to the modified program, it calculates f_{s1} and f_{s2} for all the combinations of the parameters. For each combination, the calculated value of Δf_{so} and the accompanying parameters are then stored in a computer data file.

5.4.2 Formula for steel stress increment in rectangular sections

Results of the parametric study show that the steel stress increment Δf_{so} for a rectangular section increases if the concrete strength is increased or if the reinforcement ratio is decreased. This variation can be seen in Fig. 5.19 where the calculated values of Δf_{so} are plotted against $1/\rho$ for various concrete strengths. This figure also suggests that Δf_{so} increases with $1/\rho$ almost linearly.

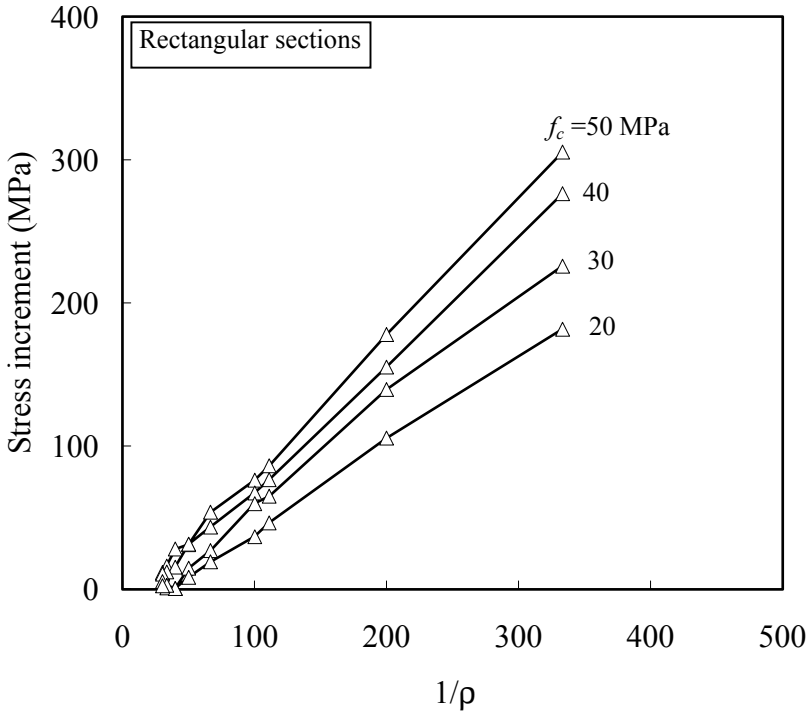

Fig. 5.19 Variation of steel stress increment Δf_{so} for rectangular sections

The calculated values of Δf_{so} are subsequently used in a linear regression analysis to develop the following empirical formula.

$$\Delta f_{so} = \frac{\left(0.4 + 0.012\, f'_c\right)}{\rho} \qquad (5.3)$$

where Δf_{So} is the steel stress increment on the formation of a primary crack in a rectangular section (*MPa*), f'_c is the concrete strength (*MPa*) and ρ is the reinforcement ratio.

Values of Δf_{so} calculated using the rigorous method (using the computer program *FORCES.BAS*) are plotted against those obtained from the above empirical formula in Fig. 5.20. This comparison indicates that the proposed empirical formula (Eq. 5.3) is acceptable.

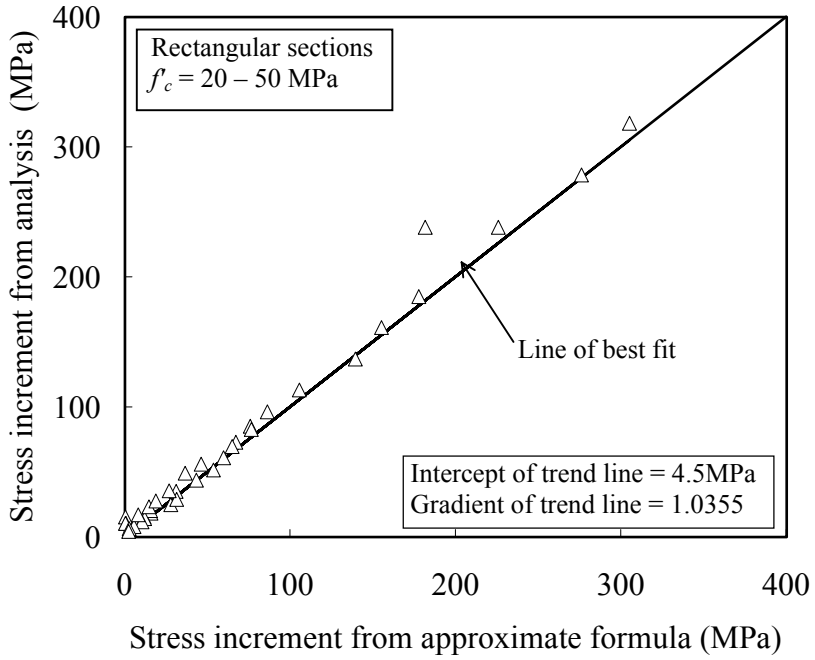

Fig. 5.20 Comparison of Δf_{so} calculated using rigorous analysis and empirical formula for rectangular sections (Eq. 5.3)

5.4.3 Formula for steel stress increment in T-sections and Box-sections

Results of the parametric study indicate that the steel stress increment at a primary crack in a flanged beam can be calculated with sufficient accuracy using the empirical formula developed for rectangular beams, with a slight modification. In using Eq. 5.3 for flanged beams, a modified reinforcement ratio, ρ_{mod} computed using the following equation should be used in place of ρ.

For T- beams, $$\rho_{mod} = \rho\left(1.067 - 0.067\frac{b}{b_w}\right)\frac{b}{b_w} \qquad (5.4a)$$

and for Box-beams, $$\rho_{mod} = \rho\left(1.3 - 0.3\frac{b}{b_w}\right)\frac{b}{b_w} \qquad (5.4b)$$

The above equations have been derived based on a linear regression analysis of Δf_{so} values determined using the computer program *FORCES.BAS*. A comparison of "exact"

values of Δf_{so} and those calculated using Eqs. 5.3 and 5.4 is shown in Fig. 5.21. This comparison indicates that the proposed empirical formulas can predict the steel stress increment in flanged beams accurately.

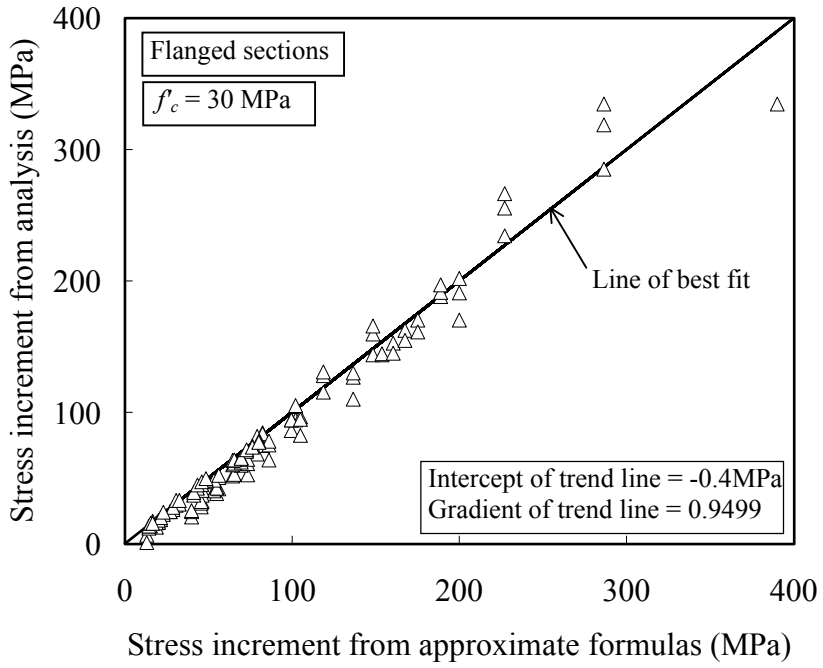

Fig. 5.21 Comparison of Δf_{so} calculated using rigorous analysis and empirical formula for flanged sections (Eqs. 5.3 and 5.4)

5.4.4 Formula for slip length S_o

It was already mentioned that the slip length S_o depends on the steel stress increment at the primary crack and the bond characteristics of reinforcement. As the magnitude of the bond force depends on the total perimeter of bars, the bar diameter has a significant effect on S_o. Therefore, in the development of an empirical formula for S_o, the bar diameter (ranging from 10mm to 30mm) is also included in the parametric study, in addition to those given in Table 5.8. For each case, the steel stress increment Δf_{so}, and the corresponding slip length are determined using computer program *FORCES.BAS* already described. Results of the parametric study show that the slip length increases almost linearly with the steel stress increment while it decreases with concrete strength, as shown in Fig. 5.22.

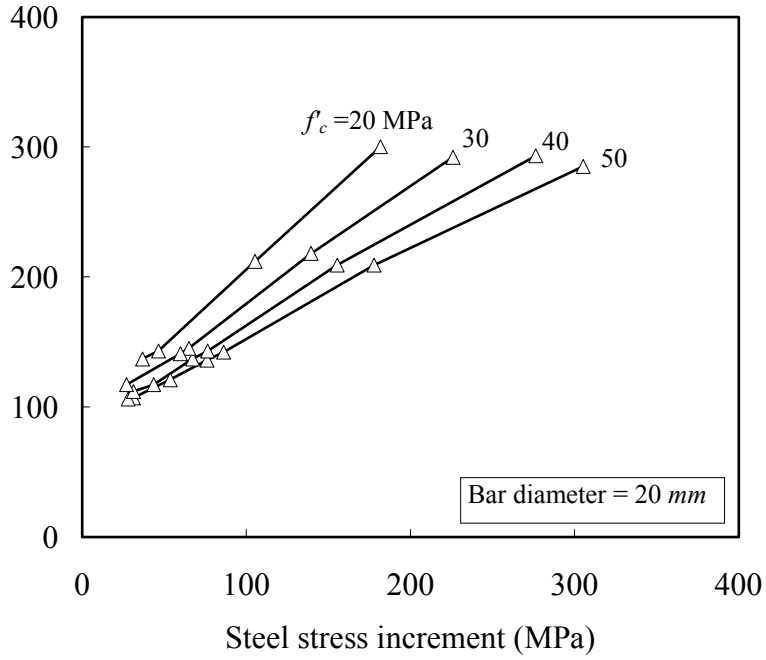

Fig. 5.22 Variation of slip length S_o with steel stress increment

The calculated values of the slip length S_o and the steel stress increment Δf_{so} are used in a linear regression analysis to develop the following relationship.

$$S_o = 90 + \left(1.3 - \frac{f'_c}{80}\right)\left(0.28 + \frac{\phi}{28}\right)\Delta f_{so} \qquad (5.5)$$

where S_o and ϕ are in millimetres, and f'_c and Δf_{so} are in *MPa*.

A comparison of "exact" values of the slip lengths determined by the rigorous method (computer program *FORCES.BAS*), and those calculated by using Eq. 5.5 together with Eqs. 5.3 and 5.4 is shown in Fig. 5.23. This comparison indicates that the proposed formulas can predict the slip length accurately.

Validity of Eq. 5.5 is verified in the next Chapter when the primary crack spacings are predicted in terms of S_o and compared with measured values for various types of beams.

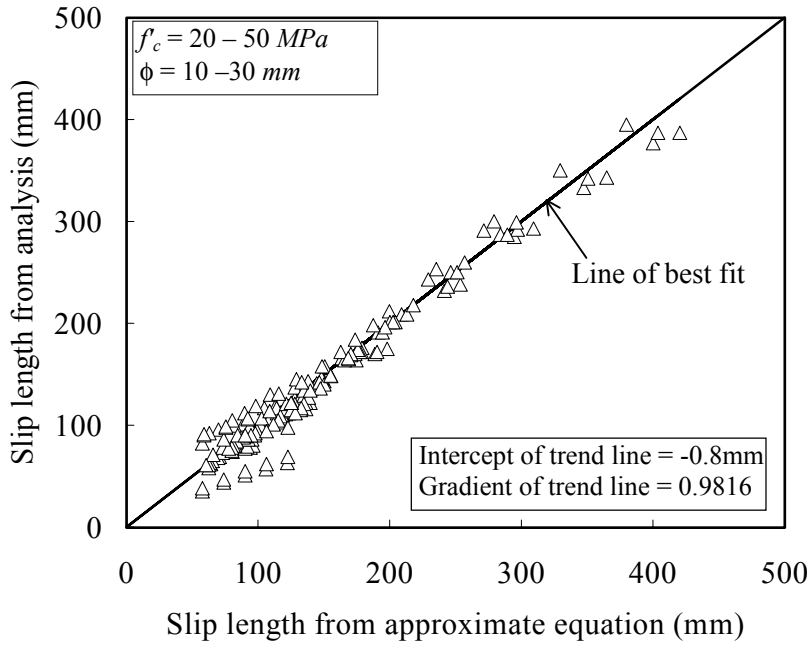

Fig. 5.23 Comparison of S_o calculated using rigorous method and empirical formulas

It may be noted from the discussion in Section 4.7.1 that the slip length depends only on the condition of equilibrium of the steel bar, with no reference to the sectional properties. Shape of the cross section is reflected in the slip length via Eq. 5.4 in the evaluation of Δf_{so}. Therefore, Eq. 5.5 can be considered as a general formula relating the steel stress increment to the slip length for all types of cross sections.

5.5 Concrete Extension for Computing the Slip

As already mentioned in Chapter 4, the slip s_o is calculated as the relative difference in elastic extensions of steel e_{so} and surrounding concrete e_{co}. The extension of steel e_{so} can be readily calculated by integrating the stain function as already described in Section 4.7 (see Eq. 4.16*e*). However, the extension of concrete adjacent to the reinforcement depends on the bond force, while the bond stress in turn depends on the slip (extension of concrete). Therefore, the extension of concrete e_{co} needs to be calculated using an iterative procedure. An iterative procedure for computing the concrete extension in constant moment region (block *Type B* in Fig. 4.18*b*) can be easily developed because the length of the block and the location of the zero-slip point are known. (Such a procedure is developed in Chapter 6, using the displacement results calculated by the finite element analysis – Section 6.5).

However, the above iterative procedure becomes too time consuming for the concrete block adjacent to the first flexural crack (*Free body Type A* in Fig. 4.18*a*), because the length of the block S_o is unknown before analysing the block. Similarly for the concrete block in a varying moment region (*Free body Type C* in Fig. 4.18*c*), this iterative procedure becomes too long, as the location of the zero-slip point is unknown before analysing. Therefore, an empirical formula is developed for calculating the concrete extension e_{co}, as described below.

To derive an expression for e_{co}, the concrete block between a cracked section and the adjacent zero-slip section is analysed by the finite element method (Free body *Type B* in Fig. 4.18*b*). The component of the extension due to the compressive force at the cracked section and, that due to the bond force at reinforcement level are calculated separately.

(a) extension of concrete due to compressive force at the cracked section

Results of the finite element analyses show that the extension of concrete at reinforcement level, caused by the compressive force acting at the cracked section does not vary significantly with the reinforcement ratio ρ or the steel stress at the crack, f_s. Therefore, constant values (ρ =0.01 and f_s =200 MPa) are used for these variables in the derivation of the expression for the extension of concrete. The ratio of overall height to effective depth is taken as h/d = 1.15 for all beams, as already mentioned in Section 5.4.1.

The results show that the ratio of displacement at any point to the effective depth (Δ/d) remains constant for all the beams, as long as the aspect ratio of the block (ratio of L_o/h in Fig. 4.18) remains the same. The results also reveal that for different aspect ratios, the calculated value of (Δ/d) increases with L_o/d almost linearly (see Fig. 5.24). Consequently, the concrete extension due to the compressive force $e_{c,co}$ (in millimetres), midway between the zero slip section and the cracked section at reinforcement level, can be approximated as

$$1000e_{c,co} = \left(2.5\frac{L_o}{d} + 0.5\right)\frac{d}{100} \geq 0 \qquad (5.6)$$

Note that Fig. 5.24(*a*) represents the graph of $e_{c,co}$ for the case where d=100 mm, and therefore the values shown in this figure need to be multiplied by $d/100$ for other cases, as seen in Eq. 5.6.

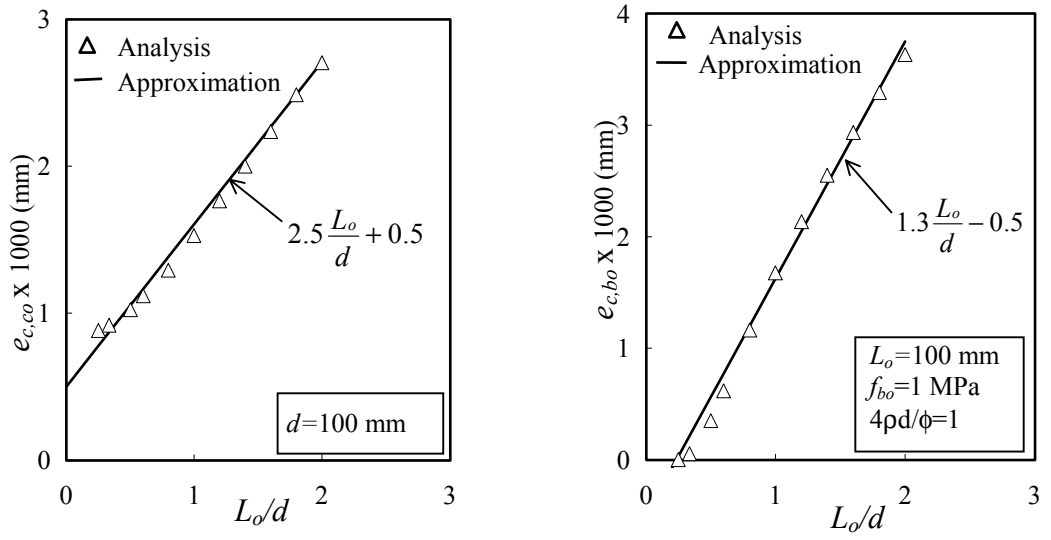

(*a*) Due to compressive forces (*b*) due to bond forces

Fig. 5.24 Approximation for concrete extension for calculating the slip

(b) extension of concrete due to bond force at reinforcement level

While the extension of concrete depends on the bond force, the bond stress is unknown before computing the concrete extension. Therefore, the expression for the concrete extension due to bond force is developed for a unit bond stress (f_{bo}=1 MPa). In addition, the *total perimeter of steel bars/beam width* is assumed to be unity (*i.e.*, $4\rho d/\phi = 1$) in the development of this expression. The calculated concrete extension is later multiplied by $4\rho d/\phi$ and f_{bo} to determine the actual extension.

Results of the analysis show that the ratio of the displacement at any particular point to the length of the concrete block (Δ/L_o) remains constant for all beam sizes, if the aspect ratio L_o/h of the concrete block remains the same. The results also reveal that for different aspect ratios, the value of (Δ/L_o) increases almost linearly with L_o/h, as seen in Fig. 5.24(*b*). Consequently, the concrete extension due to bond force $e_{c,bo}$ (in millimetres) midway between the zero slip section and the cracked section at reinforcement level, can be approximated as

$$1000e_{c,bo} = \left(1.3\frac{L_o}{d} - 0.5\right)\left(\frac{L_o}{100}\right) f_{bo}\left(\frac{4\rho d}{\phi}\right) \geq 0 \qquad (5.7)$$

Note that the Fig. 5.24(*b*) represents the graph of $e_{c,bo}$ for the case where L_o =100 mm, f_{bo} =1 MPa and the total perimeter per unit width of the beam equal to unity ($4\rho d/\phi = 1$). Therefore, the values shown in Fig. 5.24(*b*) are multiplied by the actual values of $L_o/100$, f_{bo} and $4\rho d/\phi$, as seen in Eq. 5.7.

Finally, the total extension in concrete e_{co} at the mid section between the crack and zero-slip point is determined as

$$e_{co} = e_{c,co} + e_{c,bo} \qquad (5.8)$$

Concrete extension calculated by this formula is used by the computer program *FORCES.BAS* for the determination of the peak bond stress f_{bo} and the associated slip length S_o. Validity of this formula can be verified in Chapter 6 when the primary crack spacings are predicted in terms of S_o and compared with measured values for various types of beams.

5.6 Summary

This Chapter presents some of the most important results obtained from the finite element analysis of concrete blocks adjacent to flexural cracks in loaded reinforced concrete beams and one-way slabs. The calculated concrete stress distributions near the first flexural crack, and in between two successive cracks are presented for various types of flexural members.

These stress distributions show that the longitudinal concrete tensile stress between adjacent cracks increases with the loading on the beam (steel stress at the cracked section) as well as the crack spacing. The maximum tensile stress within the concrete block occurs at the zero-slip section (section where there is no slip between concrete and reinforcement). In a constant moment region, this section lies at the mid point between the two cracks, while in a varying moment region it is closer to the crack having the lower bending moment. These stress distributions are used in the next Chapter to predict the formation of new *secondary cracks* in between existing *primary cracks*.

The finite element analytical results also reveal that for beams with effective depth larger than 300 mm, the height of *secondary cracks* are smaller than the height of nearest *primary cracks*. This difference increases with the beam depth.

The results also show that the secondary cracks that originate at the level of reinforcement may not propagate on to the tension face of the member if the concrete cover is relatively large. For such cases, the secondary crack is confined in the immediate neighbourhood of the reinforcement.

It is also shown that the cracks formed at sections with low shear stress (near mid span of a beam under central point load) are perpendicular to the tension face, similar to those formed in constant moment regions. In contrast, the new cracks formed near the supports at higher load levels are inclined towards the nearest existing crack (towards the centre of the beam). This prediction and those given in the previous two paragraphs agree with the numerous laboratory observations (Warner *et al* (1998), Park & Paulay (1972), Loo (1990)).

Empirical formulas are developed in this Chapter to calculate the increase in the steel stress on the formation of a *primary crack* in rectangular as well as flanged members. A second formula is developed to predict the corresponding *slip length* (the bond length required to resist the increase in steel stress). Accuracy of these formulas is verified by comparing the predicted values with the "exact" values obtained by the analytical procedure described in Chapter 4. The *slip length* calculated by the above empirical formula will be utilised in the next Chapter to predict the locations and spacing of cracks that are formed in beams subjected to gradually increasing loads.

CHAPTER 6

CRACK SPACING AND CRACK WIDTH

6.1 General Remarks

Concrete stress distribution patterns determined in Chapter 5 are utilised in this Chapter to predict the locations of cracks formed in a member when it is subjected to a gradually increasing load. In the first part of this Chapter, locations of primary cracks are determined based on the concrete stress distribution evaluated near the first flexural crack of the member. It is shown that the *primary crack spacings* in both constant and varying moment regions are governed by the *slip length* (bond length required to resist the steel stress increment at the first flexural crack). This prediction is verified by comparing the calculated and measured values of primary crack spacings in constant and varying moment regions. The effect of stirrups on crack spacing is also discussed.

Average crack spacings at higher load levels are determined by calculating the *critical crack spacing* l_c described in Chapter 5 (Section 5.2.4). To evaluate the critical crack spacing for a given load level, the concrete tensile stresses between two primary cracks are determined using the finite element method. The length of the concrete block (primary crack spacing) is varied and the analysis is repeated until the resulting maximum concrete tensile stress equals the flexural strength of concrete. Assuming that a secondary crack is formed when the maximum concrete stress reaches the flexural strength, the maximum crack spacing is taken as the critical crack spacing for the given load level.

In a constant moment region, the minimum crack spacing for a given load level is taken as one half of the *critical crack spacing*, because the secondary cracks are developed at the mid section between primary cracks (Section 5.2.5). The corresponding average

crack spacing is taken as the arithmetic mean of the maximum and the minimum crack spacings.

The maximum crack width at a given load level is determined using the elastic extensions of steel and surrounding concrete as already described in Chapter 5. Using the present analytical procedure, the average crack spacings and maximum crack widths within constant moment regions are computed for 70 flexural members, tested by other investigators at various load levels. The accuracy of the proposed calculation method is verified by comparing the calculated spacing and width of cracks with the measured values.

6.2 Location of Primary Cracks

When a member is subjected to a gradually increasing load, the first flexural crack is developed at the location where the applied bending moment is equal to the cracking moment. Even in a prismatic member, the cracking moment may vary slightly along the length of the span due to the non-homogeneity of concrete and due to the presence of micro-cracks that may have occurred before the application of loading. Since the cracking moment M_{cr} is proportional to the flexural strength of concrete f_r, the possible variation of M_{cr} along the length of the beam is treated as a variation of f_r for convenience, in the following discussion. Consequently, it is assumed that a primary crack is formed when the calculated tensile stress f_{rc} at the tension face of the member reaches the flexural strength of concrete f_r.

6.2.1 Primary cracks in a constant moment region

Fig. 6.1(*a*) shows a beam *AB* subjected to two equal point loads at *C* and *D* such that the bending moment along the length *CD* is constant. Line *A′C′D′B′* in Fig. 6.1(*b*) represents the calculated tensile stress at the tension face of the beam, before the first flexural crack is developed. The line *A″B″* indicates the flexural strength of the member that varies slightly above and below a mean value along the length of the beam.

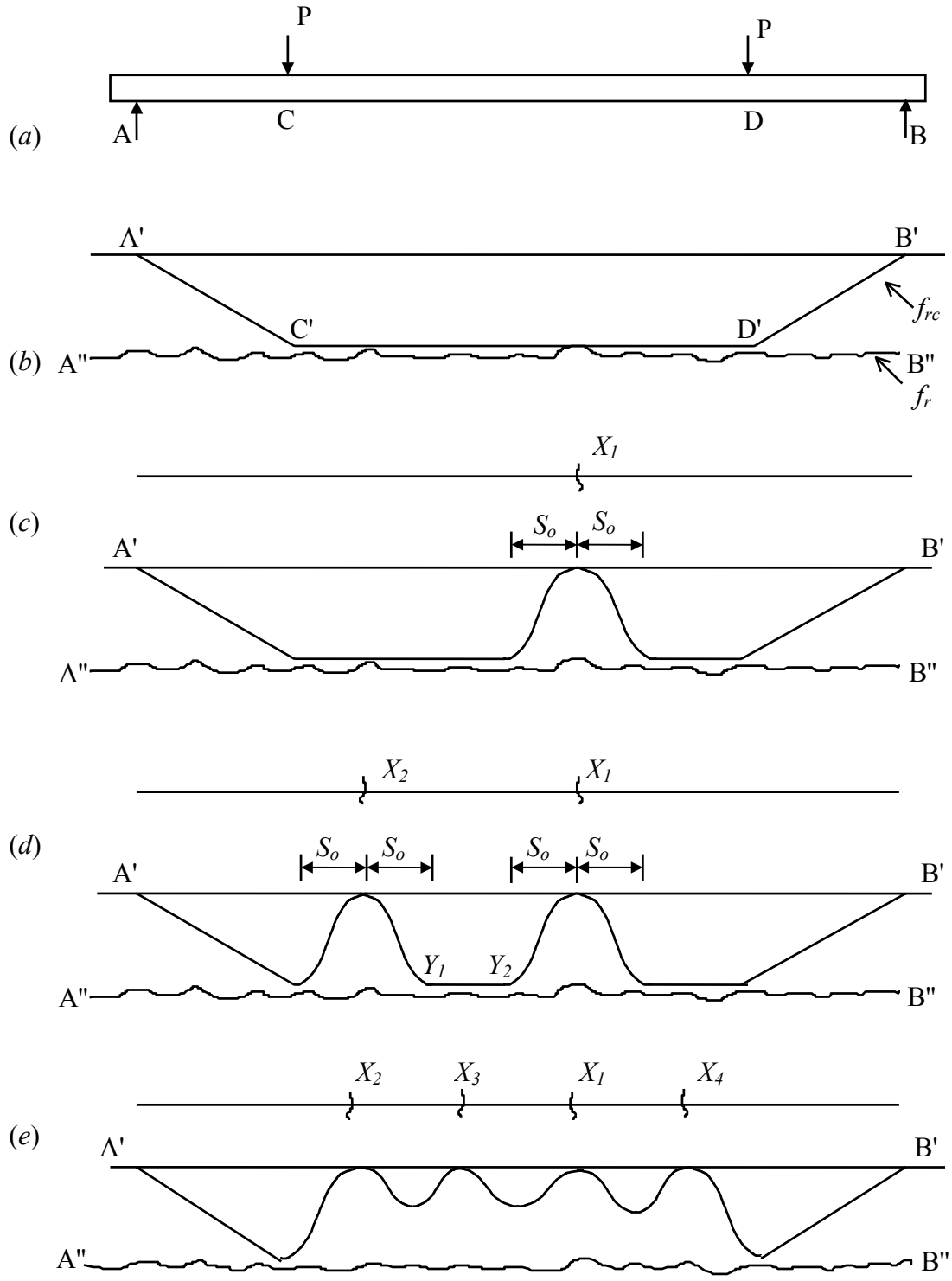

Note: f_{rc} = calculated concrete stress, f_r= flexural strength

Fig. 6.1 Progressive development of primary cracks in a constant moment region

Since the concrete stress at the tension face between *C* and *D* is constant, the first crack would occur at the point which has the lowest flexural strength between *C* and *D*. This point is shown as X_1 in Fig. 6.1(*c*). Once this crack is developed, the concrete stress at the tension face will be redistributed within a distance of S_o on either side of the crack, as described in Chapter 5 (see Fig. 5.2). Fig. 6.1(*c*) shows the concrete stress at the tension face, after this redistribution. It is clear in this figure that an increase in the load may develop flexural cracks only in the region more than a distance S_o away on either side of the crack at X_1, because the concrete stress within this region is much lower than the rest. Therefore, the minimum primary crack spacing S_{pm} in a constant moment region can be expressed as

$$S_{pm} = S_o \tag{6.1}$$

where S_o is the slip length associated with the first flexural crack described in Chapters 4 and 5.

According to Fig. 6.1(*c*), the second crack occurs at the point X_2 that has the next lowest flexural strength within the constant moment region, and beyond a distance S_o away from the first crack. When this crack is developed, stress redistribution will again take place within a distance S_o on either side of the new crack. The concrete stress at the tension face after this redistribution is schematically shown in Fig. 6.1(*d*). It can be seen in this figure that the concrete stresses in between Y_1 and Y_2 are not affected by the formation of the two cracks at X_1 and X_2. As a result, more cracks can be developed between Y_1 and Y_2 when the load is increased further. This condition is achieved as long as the distance X_1X_2 is greater than $2S_o$. This means that if two primary cracks are more than $2S_o$ apart, then intermediate cracks can be developed in between them. Therefore, the maximum primary crack spacing S_{px} in a constant moment region can be expressed as

$$S_{px} = 2S_o \tag{6.2}$$

Fig. 6.1(*e*) depicts the concrete stress distribution at the tension face of the member after the formation of two more primary cracks at X_3 and X_4 within the constant moment region. The distances between adjacent cracks are less than $2S_o$ so that their slip lengths overlap. As already described in the Chapter 5, the tensile stresses between the cracks

are now much lower than the flexural strength. As a result, further increase in loading will not cause any more *primary* cracks to occur in the constant moment region. When the load is increased further, primary cracks will spread in to the adjoining varying moment regions while new *secondary* cracks are developed between existing primary cracks in the constant moment region.

It may be noted that the formation of primary cracks in the constant moment region is completed within a small loading increment that depends on the variation of cracking moment along the beam. In Fig. 6.1, the first and the last cracks occur at X_1 and X_4, respectively. The difference in the cracking moments at these two sections (which is generally small in practical situations) determines the load increment between the formation of the first and the last primary cracks in the constant moment region.

It can be seen that the locations of the four primary cracks developed in the above beam depend on the shape of the line *A″B″* or the variation of the cracking moment along the beam. As described earlier in this Section, the cracking moment at any section may be affected by the non-homogeneity of concrete as well as the presence of microcracks that are formed before the load is applied. As such, even two beams of identical design may not have the same variation of the flexural strength along the beam. This suggests that the locations of primary cracks in the constant moment region may vary randomly such that the spacing of adjacent primary cracks S_p is in between $2S_o$ and S_o. *i.e.,* in a constant moment region,

$$S_o \le S_p \le 2S_o \tag{6.3}$$

6.2.2 Primary cracks in a varying moment region

Progressive cracking in a beam *AB* subjected to a central point load is shown in Fig. 6.2. The calculated tensile stress at the tension face of the beam is shown by the line *A′C′B′* in Fig. 6.2(*b*), which has the same shape as the bending moment diagram. Line *A″B″* indicates the variation of the flexural strength along the beam. It can be seen that the first crack will occur near the centre of the beam (at X_1) where the tensile stress is highest.

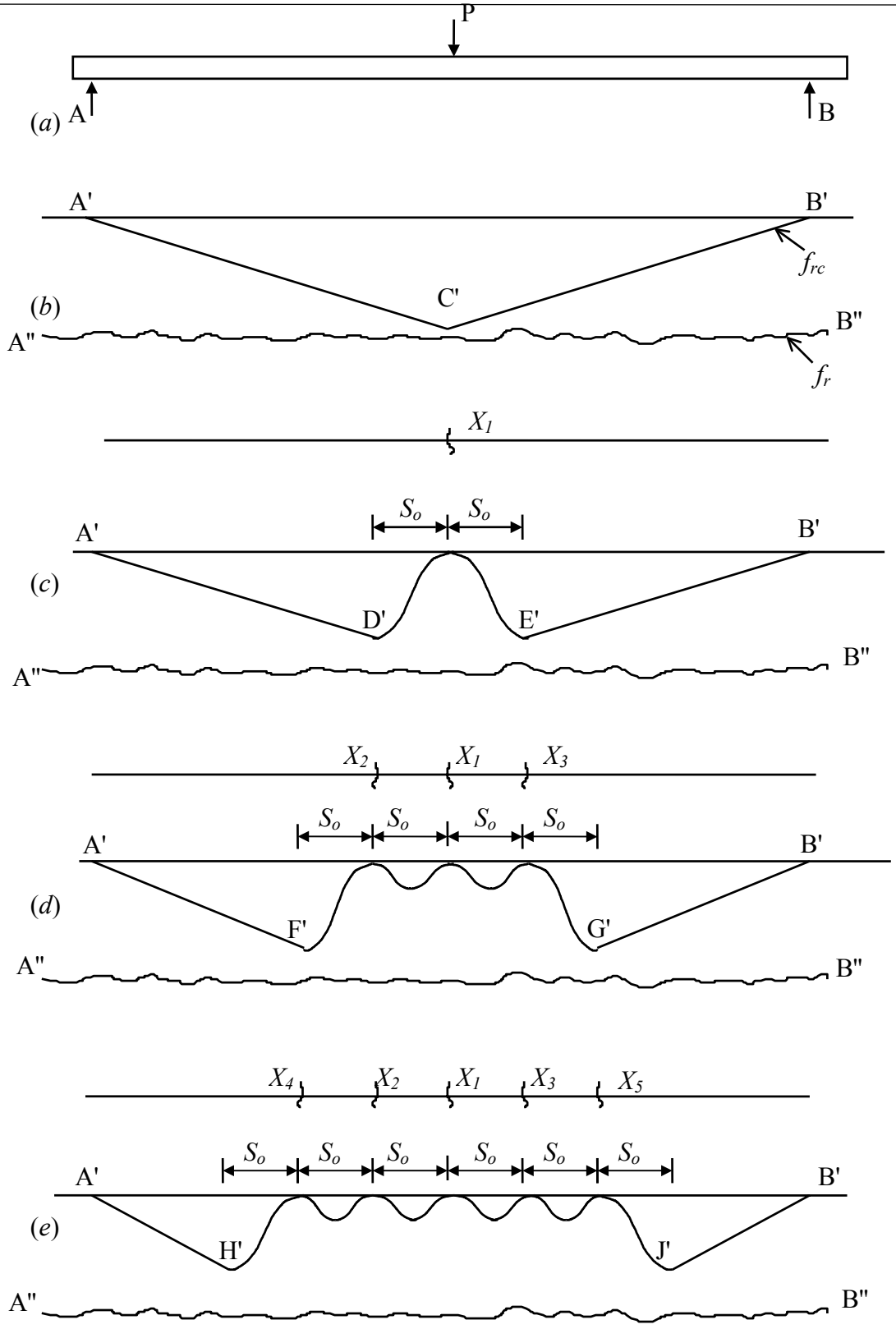

Note: f_{rc} = calculated concrete stress, f_r= flexural strength

Fig. 6.2 Progressive development of primary cracks in a varying moment region

Once this crack is formed, the concrete stress at the tension face of the member will be redistributed for a length of S_o on either side of the crack. The modified stress pattern at the tension face is shown by the line *A'D'E'B'*. It is evident in this figure that the maximum tensile stress at the tension face will now occur at points S_o away on either side of the first crack. When the load is increased further tensile stresses at these two points will reach the flexural strength resulting in two new cracks (at X_2 and X_3) equally distant from the first crack. The modified concrete stress distribution at the tension face after the formation of these two new cracks is shown by *A'F'G'B'* in Fig. 6.2(*d*). It is clear that if the load is increased further, two more new cracks will be formed at X_4 and X_5 such that the spacings between all adjacent cracks are equal to S_o as shown in Fig. 6.2(*e*). Similar results can be obtained by considering a beam subjected to a uniform load where the bending moment varies parabolically along the length. Therefore, it is concluded that the primary cracks in a varying moment region are equally spaced at a distance S_o. *i.e.,* in a varying moment region,

$$S_p = S_o \tag{6.4}$$

6.2.3 Effects of stirrups

Occurrence of flexural cracks at constant spacings in varying moment regions, as concluded in the previous paragraph, has been observed by many investigators (Makhoulf & Malhas (1996), Fantilli *et al* (1998)). This fact is often correlated to the spacing of stirrups, assuming that the presence of a stirrup makes the section 'weak'. However, the stress distributions shown in Fig. 6.2 clearly indicates that the primary crack spacing in a varying moment region is constant and equal to S_o even if the strength along the member is unchanged. This can be easily verified by considering the line *A"B"* in Fig. 6.2 as a straight line.

In a constant moment region, on the other hand, all primary cracks appear in 'weak' sections, because the concrete stress at the tension face is constant throughout. This means that even a slight reduction in strength at a section should cause a crack to form providing that the closest cracks are more than a distance S_o away. This can be seen in Fig. 6.1 where the strengths at crack locations X_3 and X_4 are only marginally lower than the surrounding region. This indicates that the cracks in a constant moment region has a more tendency to form at a constant spacing, if the stirrups act as crack inducers.

However, numerous laboratory tests have shown that the cracks in constant moment regions appear at random locations (Park & Paulay (1975), Warner *et al* (1998)), suggesting that stirrups may not form 'weak' sections.

It may be noted that in many beams with moderate reinforcement ratios, the slip length S_o varies from about 120mm to 150mm. Therefore, the regular crack spacing in varying moment regions falls within this range. When the stirrup spacing is also used in this range, the regular crack spacing is mistakenly correlated to the stirrup spacing. This will be clarified in Section 6.2.4, where the calculated crack spacing is compared with measured values for a beam that has a stirrup spacing much larger than S_o.

6.2.4 Experimental results on primary crack spacing

Although many investigations have been carried out on cracking of reinforced concrete flexural members, results of individual crack spacings are rarely available; only the average crack spacings are reported most of the times. Stewart (1997) has reported the results of individual crack spacings on two simply supported and three continuous box beams. These measurements are compared with the predictions made in the previous Section on primary crack spacings in constant and varying moment regions. Properties of the five beams tested by Stewart (1997) are summarised in Table 6.1. Notations of the beam dimensions shown in this Table are same as those given in Chapter 5 (Fig. 5.18).

Both simply supported beams, *SSB1* and *SSB2* having a clear span of 5.3 metres were subjected to two equal point loads, each 1 metre away from the beam centre so that the constant moment region is 2 metres long. Crack spacing measurements between the two point loads are considered for the constant moment region while the rest is considered for the varying moment region.

Two-span continuous beams *CB1*, *CB2* and *CB3* were supported at the centre and two ends with two equal clear spans of 5.9 metres. Each span is loaded with two equal point loads, 2 metres and 4 metres away from the central support. All the primary cracks developed on the tension face are considered in the comparison for varying moment region.

As described in the previous Section (Eqs. 6.3 and 6.4), the predicted primary crack spacing S_p is expressed in terms of the slip length S_o (*viz.* constant moment region: $S_o \le S_p \le 2S_o$, and varying moment region: $S_p = S_o$). The slip length S_o is determined (based on the calculated steel stress increment Δf_{So}) using the empirical formulas (Eqs. 5.3 to 5.5) developed in Chapter 5. Values of Δf_{So} and S_o calculated for the above five beams are given in the last two columns of Table 6.2.

Table 6.1 Summary of beam details tested by Stewart (1997)

Beam No[(1)]	b (mm)	$0.5b_w$ (mm)	h (mm)	h_f (mm)	d (mm)	Tensile reinforcement[(2)]	
						Main	Stirrups
SSB1	300	60	300	60	270	3ϕ20	ϕ6@300
SSB2	300	60	300	60	270	6ϕ20	ϕ6@125
CB1	300	60	300	60	266	3ϕ20	ϕ6@125
CB2	300	60	300	60	266	6ϕ20	ϕ10@130
CB3	300	60	300	60	264	4ϕ24	ϕ10@125

Table 6.2 Calculated steel stress increments and slip lengths

Beam No	Reinforcement ratio, ρ	Concrete compressive Strength, f'_c [(3)] (MPa)	Calculated Steel Stress Increment, Δf_{So} (MPa)	Calculated Slip length, S_o (mm)
SSB1	0.0116	32.0	49	134
SSB2	0.0232	27.6	23	112
CB1	0.0118	28.9	46	133
CB2	0.0236	29.1	23	112
CB3	0.0228	26.0	23	115

Notes:

(1) SSB1 and SSB2 are simply supported; CB1, CB2 and CB3 are continuous.

(2) Span reinforcements are shown for continuous beams.

(3) As reported by Stewart (1997), concrete samples of two diameters namely, the standard 100 mm and 70 mm have been tested for the compressive strength in continuous beams. Results showed that the smaller diameter samples gave an average of 15% reduction in compressive strength compared to the standard size sample. Because the wall thickness of all box beams is 60 mm, the compressive strength determined by using a 70 mm diameter sample is considered more appropriate. Therefore, for all box beams compressive strength is taken as 85% of the values determined by standard method.

For this comparison, primary cracks are selected from the above five beams as follows:

constant moment regions - all the cracks developed within the constant moment region before the formation of any crack on the adjoining varying moment regions

varying moment regions- all cracks developed, except those formed in between existing cracks.

Measured primary crack spacings in constant moment and varying moment regions are separately arranged in ascending order and plotted as bar graphs, for comparison. These graphs shown in Fig. 6.3 for beams *SSB1*, *SSB2*, *CB1* and *CB3* reveal the following important facts.

(*a*) *Constant moment region - beams SSB1 and SSB2:*

The primary crack spacing in a constant moment region varies between a minimum and a maximum value. These two values are close to S_o and $2S_o$ as predicted. Comparison of the stirrup spacings and crack spacings of these two beams clearly indicates that there is no relationship between them. Note that the distributions of primary crack spacings in these two beams are nearly identical while the stirrup spacings are entirely different (300 and 125 *mm*).

(*b*) *Varying moment region - beams SSB1, SSB2, CB1 and CB3:*

The primary crack spacing in a varying moment region varies above and below a mean value. This mean spacing is close to the calculated value of S_o, as predicted. Comparison of the stirrup spacing and crack spacings in beam *SSB1* clearly shows that there is no relationship between them. Coincidentally the stirrup spacing and the slip length S_o are nearly the same in beams *CB1* and *CB3* (see Tables 6.1 and 6.2). Therefore, it is not clear whether the regular crack spacings in these two beams are related to the stirrup spacing or to the slip length S_o. However, considering the large difference between the stirrup spacing and the crack spacing in beam *SSB1*, it can be concluded that the regular crack spacings in *CB1* and *CB3* are in fact related to S_o.

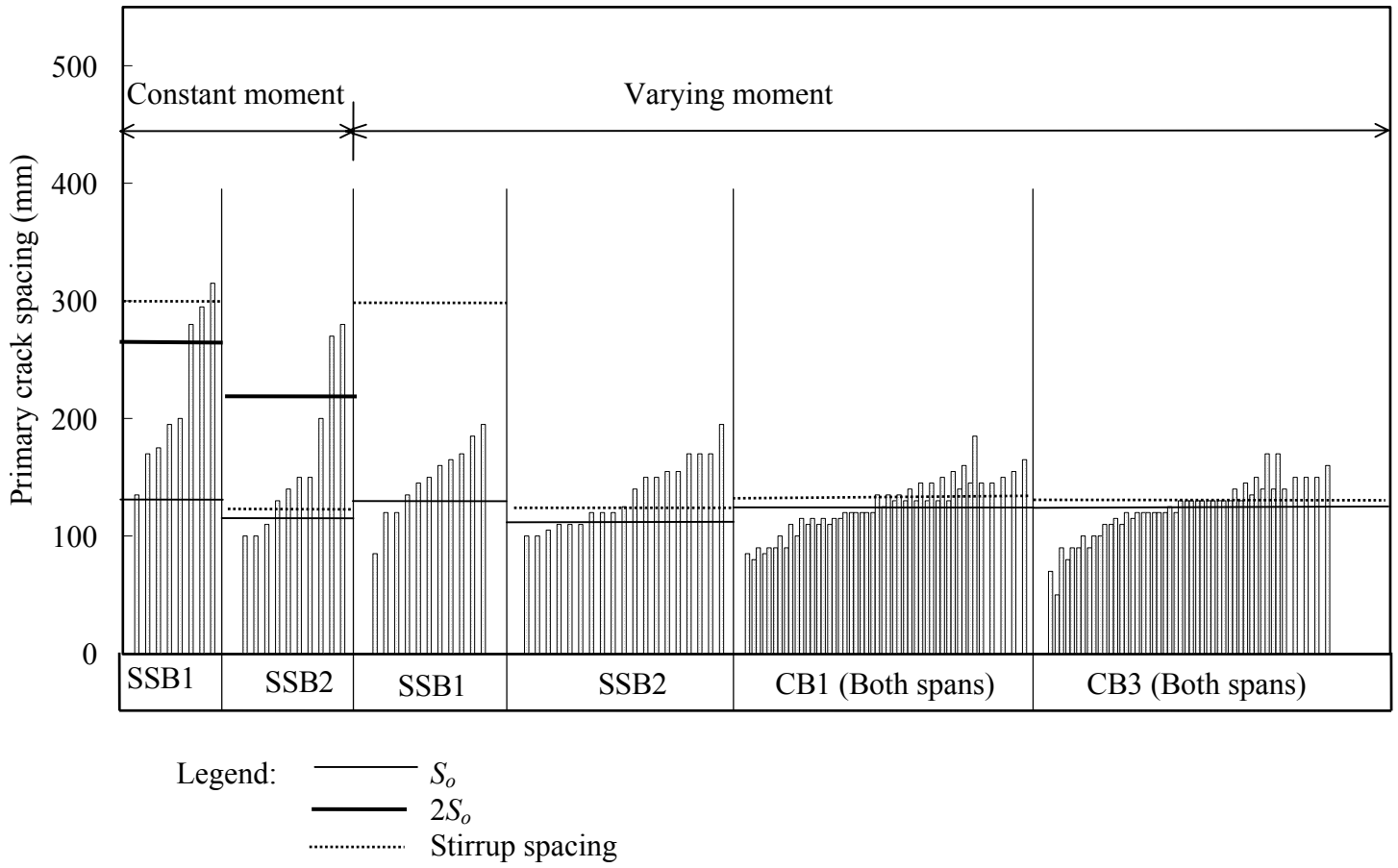

Fig. 6.3 Comparison of calculated primary crack spacings with measured values in constant moment and varying moment regions (data from tests reported by Stewart (1997). Note: Primary crack spacings for CB2 not available.)

6.3 Secondary Cracking

6.3.1. Secondary cracking in a constant moment region

As described in Section 6.2.1, primary cracks in a constant moment region are developed such that their spacings fall between S_o and $2S_o$ (see Eq. 6.3). If the load is increased after the completion of primary cracking, at a certain load, the largest crack spacing will be divided into two halves by the formation of a new secondary crack, when the maximum tensile stress reaches the flexural strength of concrete. This follows from the fact that the maximum concrete tensile stress between adjacent cracks increases with the crack spacing as well as the loading (steel stress), as seen in Figs. 5.5 and 5.6. As such, the load at which the first secondary crack occurs depends on the magnitude of the largest crack spacing. If the load is increased further, another secondary crack is formed at a certain load within the next largest crack spacing. This process continues until the maximum tensile stress within the largest crack spacing becomes less than the flexural strength of concrete.

6.3.2. Secondary cracking in a varying moment region

In a varying moment region, spacings of primary cracks are generally small (S_p=S_o) compared to that in a constant moment region ($S_o \leq S_p \leq 2S_o$), (see Eqs. 6.3 and 6.4). Therefore, the occurrence of secondary cracks in a varying moment region is rare. This is because for small crack spacings, the concrete tensile stress can reach the flexural strength only at very high steel stresses (see Figs 5.5 and 5.6). Another contributing factor for this rare occurrence of secondary cracks is that high steel stresses occur only within a small length of the beam in varying moment regions (near the mid span), in contrary to a constant moment region.

6.4 Average Crack Spacing

Average crack spacing at a given load level is defined as the mean value of all the distances between adjacent cracks. Because of the formation of secondary cracks, the average crack spacing in a constant moment region reduces with the increase of the

load. However, in a varying moment region, the occurrence of secondary cracks is rare (see Section 6.3.2) and the average crack spacing remains nearly constant at all load levels. This constant value is approximately equal to the primary crack spacing (S_o), as only a few secondary cracks are formed. This difference can be seen in Fig. 6.4, where the measured average crack spacings at various load levels are plotted for the four box beams mentioned previously. It is seen that the average crack spacing in a constant moment region reduces considerably with the increase of the load. This reduction of the average crack spacing in a constant moment region is discussed below.

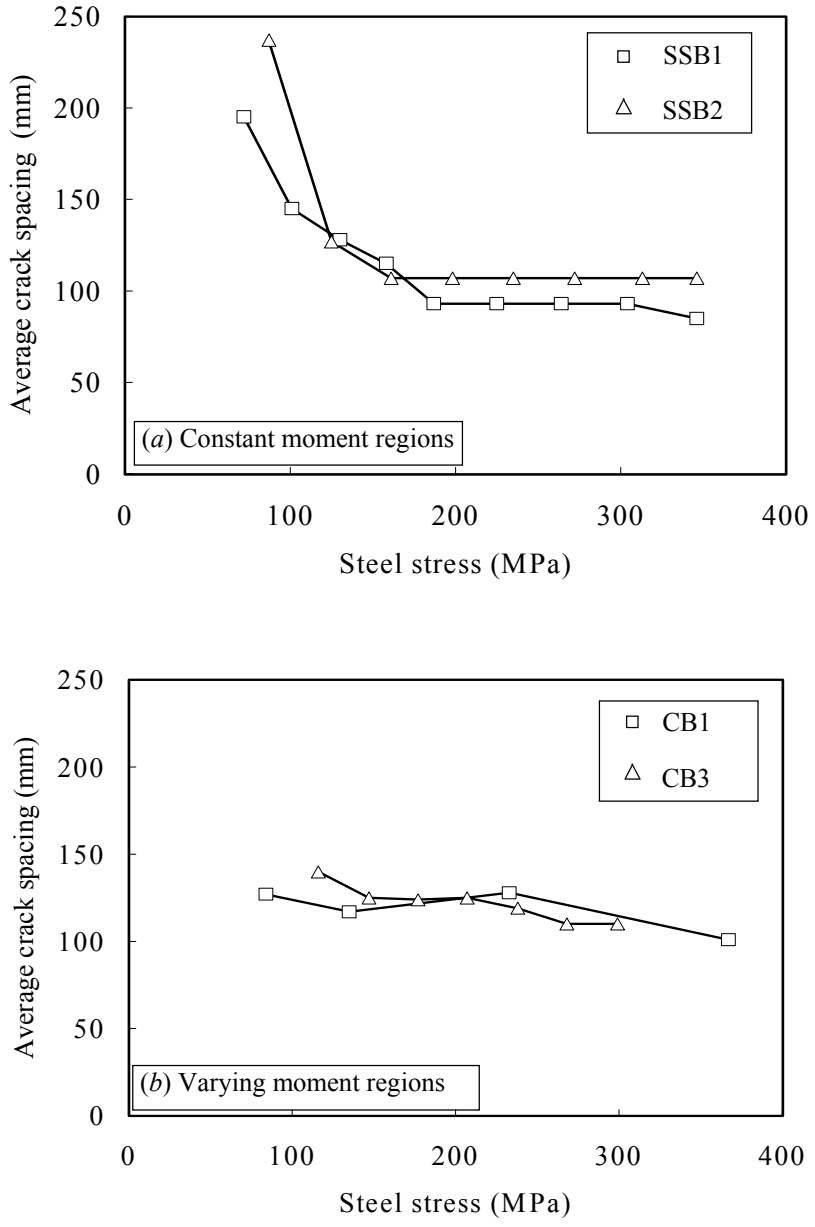

Fig. 6.4 Variation of average crack spacing with loading (constant and varying moment regions- measured by Stewart (1997) for Beam Nos. SSB1, SSB2 CB1 and CB3).

6.4.1 Average crack spacing in constant moment regions

6.4.1.1 Average crack spacing immediately after primary cracking

As described in Section 6.2.1, primary cracking in a constant moment region will be completed within a small load increment after formation of the first crack. It was also pointed out that at this stage the locations of primary cracks may vary randomly such that the distance between any pair of adjacent cracks is in between S_o and $2S_o$ (Eq. 6.3). Therefore, the average crack spacing immediately after the completion of primary cracking can be any value between the two limits S_o and $2S_o$ depending on the distribution of primary cracks, as demonstrated by the following example.

Beam number 30 in Clark's (1956) test series is considered in this example to investigate the average crack spacing. Properties of this beam are:

effective depth, d	= 330 mm
beam width, b	= 300 mm
overall height, h	= 381 mm
concrete strength, f'_c	= 26 MPa
tensile reinforcement ratio, ρ	= 0.01
bar diameter, ϕ	= 25 mm
length of constant moment region	= 1372 mm

Using Eqs. 5.3 to 5.5, the slip length S_o for this beam is calculated to be 167 *mm*. The maximum number of primary cracks that can be formed within the constant moment region of the above beam is 9, with all eight crack spacings equal to the minimum value of S_o =167 mm. This distribution of primary cracks gives an average crack spacing 167mm. The other extreme is the formation of only 5 cracks with all four crack spacings equal to the maximum value of $2S_o$ =334mm, giving an average crack spacing of 334mm. In practice, the average crack spacing falls between S_o and $2S_o$ with the individual crack spacings taking certain values between the two limits 167 and 334mm. In such cases, the number of primary cracks will be in between 9 and 5.

As described in Section 6.2, the distribution of primary cracks in a constant moment region is a random occurrence that depends on the variation of the strength along the beam. Therefore, even two specimens of identical design may have entirely different distribution of primary cracks. Table 6.3 presents five sets of primary crack spacings applicable for the above constant moment region, randomly generated by computer such that each spacing is in between 167 mm and 334 mm. As expected, the average crack spacing for each set falls between the two limits S_o and $2S_o$.

Table 6.3 Primary crack spacings randomly generated by computer (Beam No. 30 in Clark's test series)

	Spacing of Primary Cracks (mm)				
	Set 1 6 cracks	Set 2 7 cracks	Set 3 6 cracks	Set 4 6 cracks	Set 5 5 cracks
	298	332	328	331	321
	239	268	249	272	313
	214	209	244	252	308
	209	189	231	247	200
	181	183	213	234	
		171			
Average spacing	228	225	253	267	285

The mean value of the average crack spacings for the above five sets is found to be 252 *mm*. This is very close to the mean of the two limits S_o and $2S_o$ ($1.5S_o$=251 mm). This suggests that the average primary crack spacing for a single beam may vary between S_o and $2S_o$ while the mean of average crack spacing in a number of identical beams is equal to $1.5S_o$.

6.4.1.2 Average crack spacing at higher load levels

The average crack spacing in a constant moment region will gradually decrease with the increase of the load due to the formation of new (secondary) cracks in between existing cracks. The load at which a new crack is formed depends on the individual values of the distances between adjacent cracks. This is because the concrete tensile stress, that initiates a new crack, increases with the crack spacing (see Figs. 5.5 and 5.6). This means that the average crack spacing at a given load level depends mainly on the distribution of primary cracks, which is a random occurrence. This fact is demonstrated by considering the five sets of different primary crack spacings selected (see Table 6.3), for Beam No. 30 of Clark's (1956) test series.

Results of a finite element analysis on this beam indicate that the concrete tensile stress between adjacent cracks reaches the flexural strength if the crack spacing is 300 mm when the steel stress is 103 MPa. Therefore, when the steel stress reaches this value, all the crack spacings larger than or equal to 300 mm would have been divided into two halves by the formation of secondary cracks. After this happens, the new average crack spacings for the above five sets of primary cracks are calculated as 228, 193, 211, 223 and 163 mm, respectively. Note that no new cracks are developed in the first set because the largest crack spacing is less than 300 mm. One new crack each is developed in the second, third and fourth sets while three new cracks are developed in the fifth set.

The above example demonstrates that the average crack spacing in a constant moment region at a given load level varies largely with the spacings of primary cracks. Since the primary cracks are formed at random locations, the average crack spacing at a given load level cannot be predicted accurately. Only the upper and lower limits for the average crack spacing can be predicted. The procedure for the determination of upper and lower limits of average crack spacing at a given load level is described in the next Section.

6.4.1.3 Upper and lower limits of average crack spacing

The particular crack spacing that produces a concrete tensile stress equal to the flexural strength (*critical crack spacing* l_c) is the maximum crack spacing S_{max} for the given load level. This is because a slight increase in the load will cause the concrete tensile stress to exceed the flexural strength resulting in a new crack in between existing ones. Therefore, the maximum crack spacing S_{max} at a given load level can be expressed as

$$S_{max} = l_c. \tag{6.5a}$$

The formation of a new secondary crack at the mid section between the two cracks divides the crack spacing l_c in to two halves. Therefore, the lower limit of the average crack spacing S_{min} at this load level should be equal to $0.5l_c$. This is because the crack spacings previously divided in to two halves at lower load levels are larger than l_c. *i.e.,*

$$S_{min} = 0.5l_c. \tag{6.5b}$$

The predicted average crack spacing at this load level can be taken as the arithmetic mean of the upper limit and the lower limits as

$$S_{ave\text{-}pred} = 0.75l_c. \tag{6.5c}$$

6.5 Determination of Critical Crack Spacing l_c and Crack Width W_s

6.5.1 Critical crack spacing l_c

Critical crack spacing l_c for a given load level is determined by analysing the concrete block *Type B* (see Fig. 4.18*b*) for various crack spacing values S (various block lengths L_o=0.5S) until the computed maximum concrete tensile stress equals the flexural strength of concrete. It may be seen that for each selected crack spacing, different bond forces develop along the steel bars, as the concrete and steel extensions depend on the crack spacings. To avoid repetitive changes to the applied bond force on the finite element mesh, the following procedure is adopted. This procedure can best be demonstrated by considering the total bond force acting on the concrete block between the cracked section and the zero-slip section (between sections *C* and *B* in Fig. 4.18*b*).

The total bond force acting on a unit width of the concrete block is equal to

$$F_b = \frac{2}{3} f_{bo} p L_o \tag{6.6}$$

where p is the total perimeter of steel bars divided by the beam width. It can be seen from Eq. 6.6 that the total bond force acting on the concrete block varies linearly with f_{bo}, L_o and p. For this reason, the finite element analysis can be carried out for a certain bond force corresponding to selected values of f_{bo}, L_o and p, and the computed stresses subsequently multiplied by the appropriate proportions. For convenience, the following values are used in the present analysis: f_{bo} =1 MPa, L_o =100 mm and p =1. The computed concrete stresses are later multiplied by the values of f_{bo}, L_o/100 and p to obtain the final stresses. When this procedure is adopted, loading on the mesh can be kept unchanged in repetitive analyses; only the length of the block needs to be changed for different crack spacing values selected. The *SCALE* command available in STRAND6 software package is conveniently used to modify the length of the block, and the mesh is re-analysed for the new crack spacing, using the same loading (Note that forces on transverse sections do not change with crack spacing).

It must be mentioned that the stress within the concrete block has two components; (*a*) stress resulted from the compressive force acting on transverse section; and (*b*) stress caused by bond forces acting at reinforcement level. Note that only the component of the stress due to bond force needs to be multiplied by f_{bo}, L_o/100 and p as described in the previous paragraph. To separate the resulting stress components, the analysis is carried out using two load cases, namely, (*i*) compressive force on the transverse section, and (*ii*) bond forces. After analysing the finite element mesh for each trial crack spacing, the results of the second load case are multiplied by f_{bo}, L_o/100 and p, and added to the results of the first load case to obtain the final stresses.

The peak bond stresses f_{bo} for each selected crack spacing is calculated using the trial and error procedure described in Chapter 4 (Section 4.7.2*a*). It must be noted that in step (*b*) of the above trial and error procedure, the concrete extension e_{co} is not computed by using the empirical formulas (Eqs. 5.6 to 5.8) as mentioned. This is because Eqs. 5.6 to 5.8 have been derived to calculate the concrete extensions for

blocks *Type A* and *Type C*, due to the unknowns involved (S_o and S_x), as already described in the derivation of these formulas (Section 5.5). In the present calculation (block *Type B*), the concrete extension e_{co} for each trial crack spacing can be obtained from the results of the finite element analysis. To calculate e_{co}, the component of the displacement due to the bond force needs to be multiplied by f_{bo}, $L_o/100$ and p and added to the displacement due to load case 1, as in the case of the stresses described earlier.

The procedure for calculating the maximum concrete tensile stress within the mesh is described below.

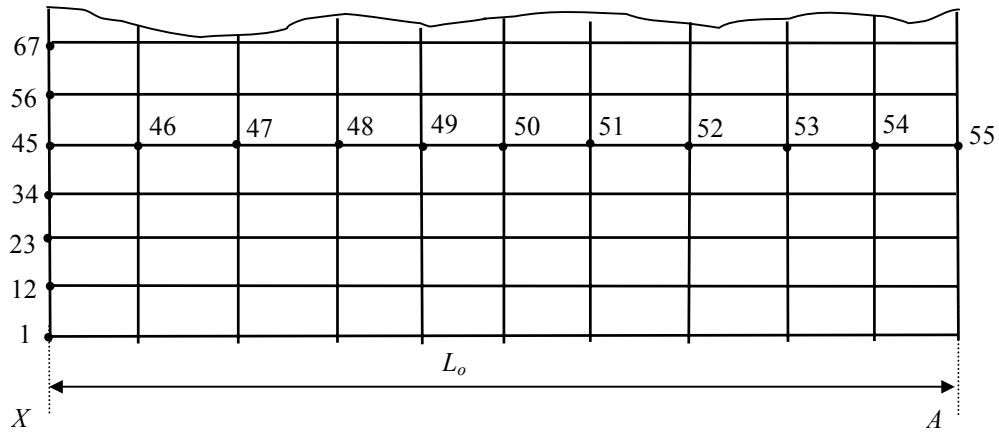

Fig. 6.5 Part of the finite element mesh

Fig. 6.5 shows part of the mesh (L_o = 0.5S) used in the finite element analysis for a selected trial value of the crack spacing S. This mesh is prepared by modifying the '*master mesh*' (developed for L_o =100mm and h = 100mm), using the command *SCALE* available in STRAND6 software package, as described in Chapter 5 (Section 5.2.1). The non-zero nodal forces calculated using the program *FORCES.BAS* are then applied at the respective nodes along the cracked section at *A* (load case 1). The nodal bond forces calculated based on f_{bo}=1MPa, L_o=100mm and p=1, as described earlier, are applied at the nodes 45 to 55 in Fig. 6.5 (load case 2). As shown in Fig. 4.18*b*, nodal restraints are applied at nodes along the section at *X*, such that only transverse displacement is allowed. The mesh is then analysed for the selected crack spacing, and the following results are stored in data files, for load cases 1 and 2 separately.

(a) longitudinal stresses σ_x at nodes 1, 12, 23,…,67 (7 nodes)
(File name: *stres*)
(These nodes are selected because the results have shown that the maximum stress occurs in the vicinity of Node 45 (see Fig. 6.5)

(b) longitudinal displacement δ_x at nodes 50 and 55
(File name: *displ*)

The final stresses at nodes 1, 12, 23, ….67 are then calculated as follows.

$$\sigma_{xi} = (\sigma_{xi})_1 + (p f_{bo} \ L_o/100) (\sigma_{xi})_2 \qquad (6.7)$$

where $(\sigma_{xi})_1$ is the longitudinal stress at node *i* due to load case 1 (compressive force on transverse section) and $(\sigma_{xi})_2$ is the longitudinal stress at the same node due to load case 2 (bond force), which is based on p=1; f_{bo} =1MPa and L_o = 100 mm, and *i* is the node number (*i* = 1, 12, 23,…., or 67).

The corresponding extension of concrete e_{co} is calculated as

$$e_{co} = (\delta_{x50})_1 + (p f_{bo} \ L_o/100) (\delta_{x50})_2 \qquad (6.8)$$

where $(\delta_{x50})_1$ is the displacement at node 50 due to load case 1 (compressive force on transverse section) and $(\delta_{x50})_2$ is the displacement at the same node due to load case 2 (bond force), which is based on p=1; f_{bo} =1MPa and L_o = 100 mm.

It can be seen in Eq. 6.8 that the extension e_{co} varies with the bond stress f_{bo}, while f_{bo} depends on the slip s_o, which in turn varies with e_{co} (Eq. 4.15). Therefore, the peak bond stress f_{bo} is calculated using a trial and error procedure. The calculated f_{bo} is then used in Eq. 6.7 to evaluate the concrete stresses σ_{xi} at Nodes 1, 12, 23,…., and 67.

A computer program written in *BASIC* language (program name = *STRESS.BAS*) is used for the above calculation (See *Appendix E16* and *E17* for the source program). The flowchart for the calculation procedure is shown in Fig. 6.6.

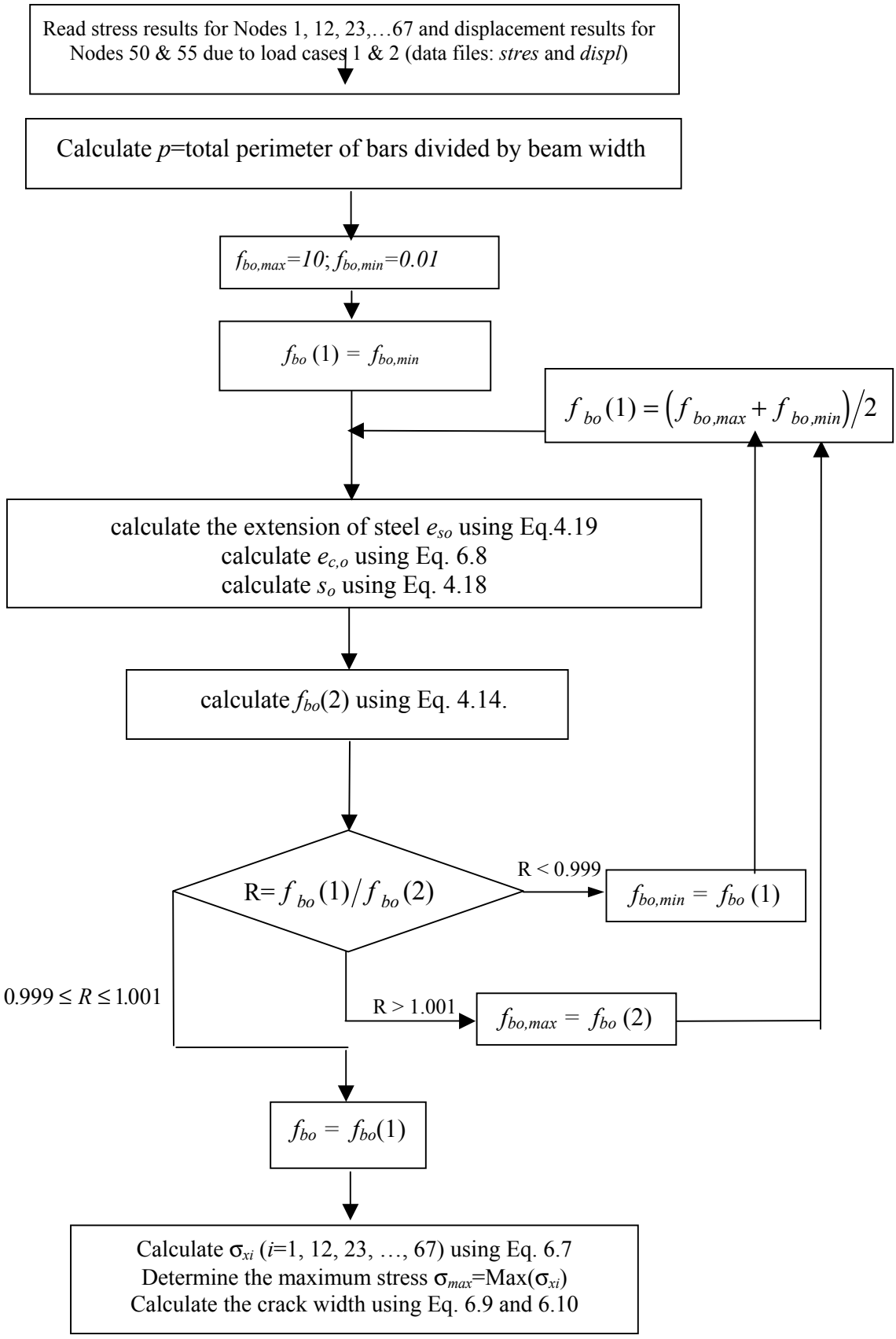

Fig. 6.6 Flowchart for calculating f_{bo} and maximum concrete tensile stress

After the peak bond stress f_{bo} is computed, the program *STRESS.BAS* calculates the concrete stresses at the seven nodes (1, 12, 23, ….67) using Eq. 6.7. The maximum concrete tensile stress among these seven stress values are then evaluated and displayed on computer screen. Appendix *E17* shows a sample output of the results displayed on the computer screen for Beam No. 30 in Clark's (1956) test series. If the computed maximum tensile stress is less (or more) than the flexural strength of concrete, the crack spacing is increased (or decreased), and the finite element analysis is repeated. When the calculated maximum concrete tensile stress equals the flexural strength, the selected crack spacing S, (S=2L_o) is taken as the *critical crack spacing* l_c.

6.5.2 Calculation of the crack width

For each trial crack spacing value, the program *STRESS.BAS* calculates the resulting crack width using the displacements at the Node number 55 (see Fig. 6.5), as follows.

The crack width at the reinforcement level W_s is calculated using Eq. 5.1*b*, as described in Chapter 5. This equation is repeated below for easy reference.

$$W_S = 2(e_{s1} - e_{c1}). \tag{6.9}$$

The extension of steel e_{s1} is calculated using Eq. 5.1*a*. The corresponding extension of concrete e_{c1} at the cracked section is evaluated using the results of finite element analysis as

$$e_{c1} = (\delta_{x55})_1 + (\, p\, f_{bo}\ \ L_o/100)\ (\delta_{x55})_2 \tag{6.10}$$

where $(\delta_{x55})_1$ is the displacement at node 55 due to load case 1 (compressive force on transverse section) and $(\delta_{x55})_2$ is the displacement at the same node due to load case 2 (bond force), which is based on p=1; f_{bo} =1MPa and L_o = 100 mm. The crack width at the tension face of the member is then calculated using Eq. 5.2*b*.

6.5.3 Variation of crack width with crack spacing

Crack width values calculated for various trial crack spacings may be used to investigate the variation of crack width with the crack spacing. Fig. 6.7 shows the relationship between the crack width and crack spacing calculated for a typical beam.

The properties of the beam used are as follows:

overall height, h	= 450mm
effective depth, d	= 400mm
beam width, b	= 315 mm
bar diameter, ϕ	= 20mm
number of bars, m	= 4
reinforcement ratio, ρ	= 0.01

As seen in Fig. 6.7, the crack width increases with the spacing of adjacent cracks at all three steel stress levels, f_s = 200, 250 and 300 MPa, considered for the above beam.

It may be seen in Fig. 6.7 that 9 to 10 trial crack spacing values have been used at 10mm intervals to evaluate the critical crack spacing. In actual calculation, the critical crack spacing can be determined using a lesser number of trials. However, more trial crack spacings have been used for this beam purposely to produce data for Fig. 6.7.

A similar trend of increasing the crack width with crack spacings has been observed in all beams considered in this Chapter (70 beams as described in Section 6.6).

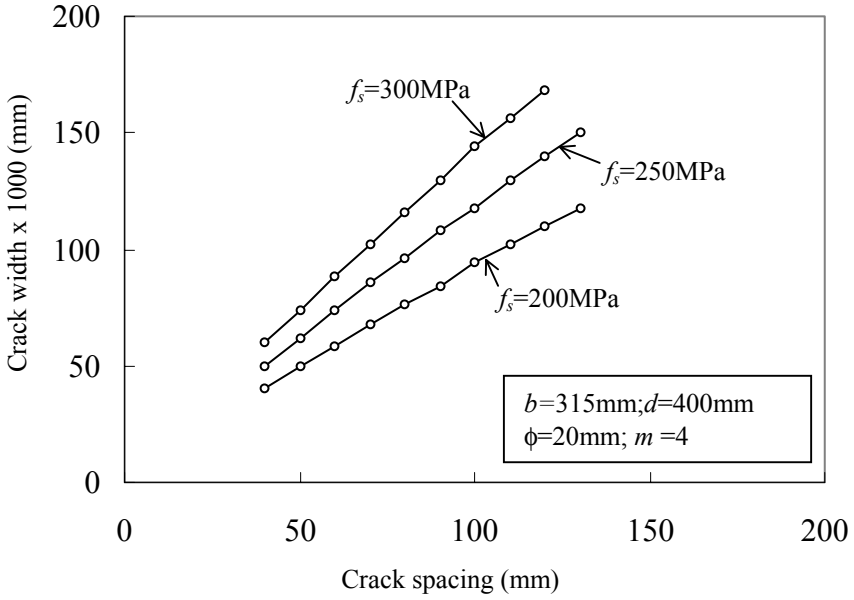

Fig. 6.7 Variation of crack width with crack spacing

6.5.4 Effect of loading type on the crack width

As already mentioned, the crack spacing in a varying moment region remains constant (Section 6.4) as S=S_o at all load levels. In contrast, the individual crack spacings in a constant moment region initially varies between S_o and $2S_o$, and with the increase of the applied loading, larger crack spacings divide in to two halves. Therefore, the individual crack spacings in a constant moment region will be generally larger than in a varying moment region at all load levels. As the crack width increases with crack spacing (Fig. 6.7), the resulting maximum crack width in a constant moment region is larger than that in a varying moment region, when compared at the same load level. Therefore, crack widths in constant moment regions have more practical significance. In addition, in most practical beams the largest crack widths occur near the mid span where the bending moment is highest. In this region, the shear forces are generally small and the stress conditions closely resemble that in a constant moment region. Due to these reasons, new crack width prediction formulas are developed in this thesis for a constant moment region only (Chapter 7).

6.6 Comparison of Results

6.6.1 Average crack spacing

Critical crack spacing l_c is determined using the procedure described in Section 6.5.1 for 70 flexural members tested by Clark (1956) and Chi & Kirstein (1958), and the results are compared with measured values at various load levels. These test members consist of 152mm thick slabs, and 381mm and 584mm deep rectangular beams with various bar diameters and reinforcement ratios (Table 6.4). The width of slab specimens varied between 152mm and 304mm, while all beams had a constant width of 152mm. All members were simply supported and loaded at quarter span points so that the bending moment within the middle half of the span is constant. Crack spacing and crack width measurements have been taken within the constant moment region at seven steel stress levels, namely, 103, 138, 172, 207, 241, 276 and 310 MPa.

Table 6.4 Ranges of variables used in specimens tested by Clark (1956) and Chi & Kirstein (1958)

Member	Height (mm)	Range of bar diameter (mm)	Range of reinforcement ratio	Span (mm)
Slab	152	10 to 25	0.0035 to 0.025	1830
Beam	381	22 to 32	0.010 to 0.0258	2740
Beam	584	28 to 35	0.010 to 0.025	3350

For each of the above members, the value of l_c is calculated using the procedure described in Section 6.5.1 at the seven steel stress levels for which the measurements are available. As a typical example, the critical crack spacing calculated for Beam No. 30 of Clark's (1956) test series and the measured average crack spacings are plotted against the steel stress in Fig. 6.8.

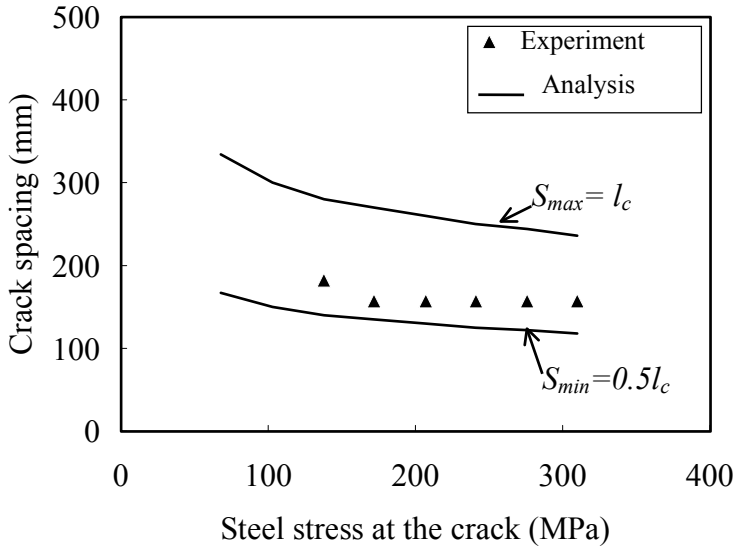

Fig. 6.8 Comparison of calculated and measured crack spacing (Beam No. 30 of Clark's (1956) Test Series)

Comparison of measured and predicted average crack spacings for the above 70 flexural members is shown in Fig. 6.9. The *x*-axis in this figure represents the predicted average crack spacing which is calculated as $S_{ave\text{-}pred} = 0.75l_c$, as described in Section 6.4.1.3 (Eq. 6.5*c*). Note that this figure contains 420 data points, which is less than the expected number of 490, because measurements are not available for certain members at lower steel stress values.

Inspection of Fig 6.9 indicates that most of the measured average crack spacings for all the beams fall within the upper and lower limits of l_c and $0.5l_c$, as predicted by Eqs. 6.5*a* and (6.5*b*). It may be seen that only two measurements are larger than the predicted S_{max}, while 27 measurements are smaller than the predicted S_{min}. This means that 391 measurements (94%) lie within the predicted range of $05.l_c$ and l_c.

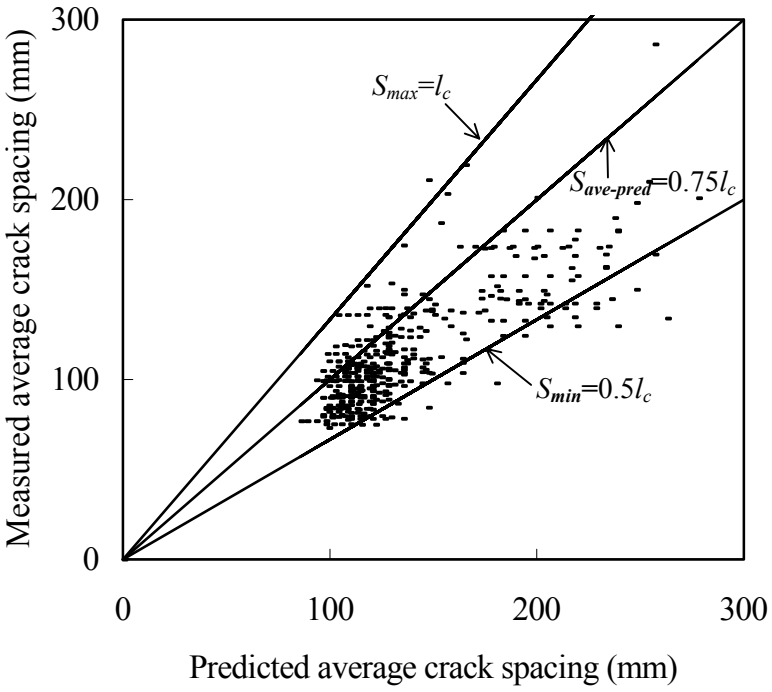

Fig. 6.9 Comparison of predicted and measured average crack spacings for 70 Beams tested by Clark (1956) and Chi & Kirstein (1958)

6.6.2 Maximum Crack Width

The maximum crack width at the tensile face of the member $W_{t\text{-}pred}$ is determined using the procedure described in Section 6.5.2, for the 70 test beams mentioned previously. As a typical example, the calculated and measured maximum cracks widths are plotted against the steel stress in Fig. 6.10, for Beam No 30 in Clark's (1956) test series.

Measured maximum crack widths for all the 70 flexural members are plotted against the corresponding predicted values at all steel stress levels, in Fig. 6.11. The *x*-axis in this figure represents the predicted maximum crack width, which is calculated as described in Section 6.5.2. As seen in this figure, most of the measured values lie within ±50% of the predicted maximum crack width. Only 15 measurements exceed 150% of the predicted crack width, while 27 measurements are less than 50% of the predicted value. This means that 388 measurements (92%) lie within ±50% of the predicted maximum crack width. Considering the large scatter normally encountered in crack width measurements, this correlation is considered acceptable.

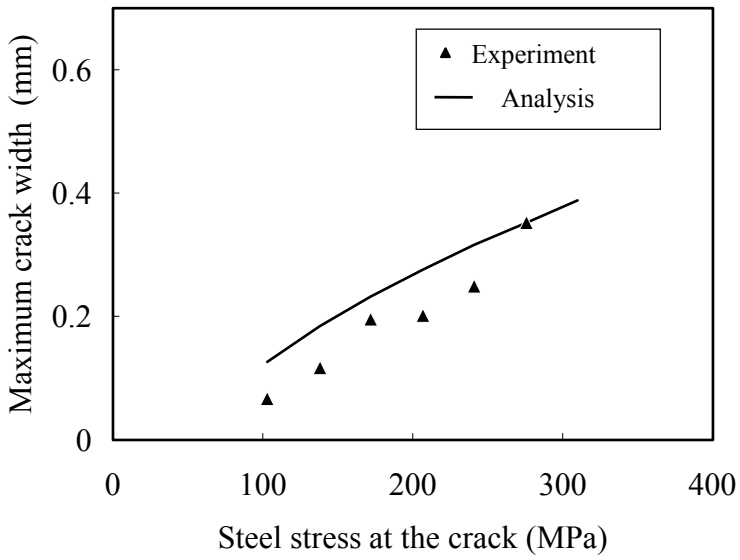

Fig. 6.10 Comparison of calculated and measured crack width (Beam No. 30 of Clark's Test Series)

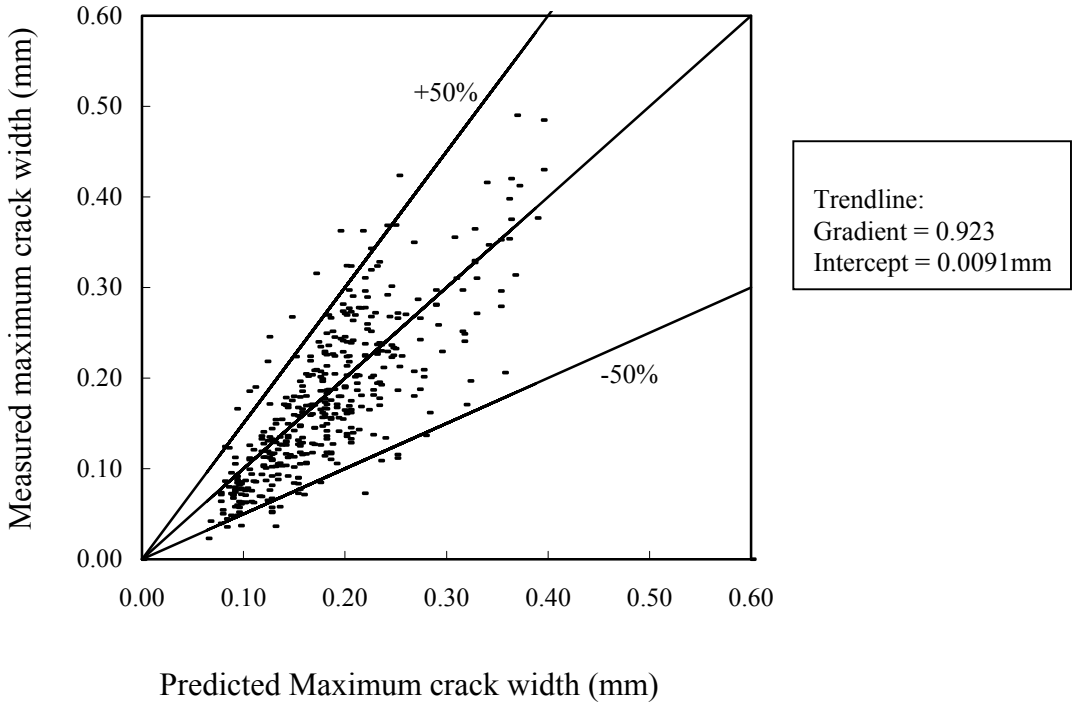

Fig. 6.11 Comparison of measured and predicted maximum crack widths for 70 Beams tested by Clark (1956) and Chi & Kirstein (1958)

6.7 Summary

Concrete stress distributions determined in Chapter 5 are used in this Chapter to predict the locations of flexural cracks. Two different types of cracks are identified, namely, (*a*) cracks that are developed at sections where the concrete and steel stresses have not been influenced by nearby cracks (*primary cracks*), and (*b*) the cracks formed in between two existing cracks (*secondary cracks*). Concrete stress distributions presented in Chapter 5 are used to establish the following important facts in relation to the formation of these two types of cracks.

(a) Primary cracks

(i) In a constant moment region, the primary cracks are formed at random locations such that the spacings of adjacent cracks fall between a maximum and a minimum value. The formation of primary cracks will be completed within a short interval of load increment.

(ii) In a varying moment region, cracks are formed at a constant spacing. Primary cracks will continue to develop towards the supports during the full loading stage.

(iii) Maximum and minimum crack spacings in a constant moment region as well as the regular crack spacing in a varying moment region are related to the *slip length* (bond length required to resist the steel stress increment at the first flexural crack). They have no relation to the stirrup spacings.

(a) Secondary cracks

(i) When the load increases, the average crack spacing in a constant moment region decreases due to the formation of secondary cracks in between existing primary cracks. The average crack spacing at any load level falls between a maximum and a minimum value, which are related to the *critical crack spacing*.

(ii) In a varying moment region, the occurrence of secondary cracks is rare and therefore, the average crack spacing remains nearly constant at all load levels.

Experimental results are used in this Chapter to verify the accuracy of the above predictions on crack spacing.

Crack width at reinforcement level is calculated as the relative difference in elastic extensions of steel and surrounding concrete. The extension of steel is determined by integrating the strain function, while the concrete extension is evaluated using the results of the finite element analysis. The resulting crack width at the tension face of the member is evaluated using an empirical formula. Comparison of the calculated crack widths and those measured by other investigators on 70 flexural members indicates that the above calculation procedure is acceptable.

Chapter 7

FACTORS AFFECTING SPACING AND WIDTH OF CRACKS - A Parametric Study and New Prediction Formulas

7.1 General Remarks

In Chapter 6, a rigorous analytical method was presented for the determination of spacing and width of cracks. In this method, stresses and extensions within a concrete block between adjacent cracks were determined using the results of finite element analysis. As this method is time consuming, a simplified procedure is developed in this Chapter to determine the concrete stresses and extensions at selected nodes of the finite element mesh. Using the stresses and extensions calculated by this simplified method, the critical crack spacing and crack width are determined for a large number of beams and slabs having various material and sectional properties. These results are used to investigate the relative significance of the effects of individual variables on the spacing and width of cracks.

The above investigation reveals that the spacing and width of cracks at a given load level are governed by only a small number of variables; however, there are many choices to select a particular set because some of the variables involving sectional properties are interrelated. Bar diameter, effective width of the member per one bar, and the concrete cover are shown to be the most convenient variables to represent the spacing and width of cracks at a given load level. The effective depth has shown to influence the spacing and width of cracks only if its value is less than 300 mm.

The crack spacing and crack width data calculated by using the simplified method are subsequently used in a parametric study to develop new prediction formulas in terms of

the above significant variables. Accuracy of these formulas is verified by comparing the measured and predicted values of spacing and width of cracks for the same 70 test beams considered in Chapter 6.

As mentioned in Chapter 6 (Section 6.5.4), crack widths in constant moment regions have more practical significance, as they are larger than the crack widths in varying moment regions, when compared at the same load level. Therefore, cracking only in constant moment regions of beams and one-way slabs are considered in this Chapter.

7.2 Simplified Method of Calculating Concrete Stress and Extension

In this Section, a simplified method is developed to calculate the concrete stresses and extensions at certain selected nodes of the finite element mesh used in Chapter 6. The basis for the development of this simplified method is the equivalence of stress and strain fields in two geometrically *similar* concrete blocks (of different sizes) subjected to *similar* loads. This means that two concrete blocks of different sizes will have identical internal stresses and strains at corresponding locations, when they are subjected to the same external stress patterns. This is described below.

7.2.1 Stress and strain fields in 'similar' concrete blocks of different sizes

Fig. 7.1 shows two geometrically *similar* concrete blocks subjected to *similar* external stress patterns. These two concrete blocks, which have the same length to height ratio are subjected to two types of *similar* loads. They are: (*i*) the concrete compressive force acting at transverse section (load case 1); and (*ii*) the unit bond force acting at reinforcement level (load case 2), with the peak bond stress f_{bo} =1 MPa and total perimeter of bars divided by beam width p=1. Results of the finite element analyses show that the internal stress and strain fields in the above two blocks are identical for both the load cases.

The above identities are used in the simplified method presented in this Chapter to determine the concrete stresses and extensions in beams of various sizes. First, a beam of a particular size called the *base model* is analysed by the finite element method for

various sectional and material properties (Section 7.3), and the stress and extension results are stored in a computer data file. These stored data are subsequently used to determine the resulting concrete stresses and extensions in beams of various sizes.

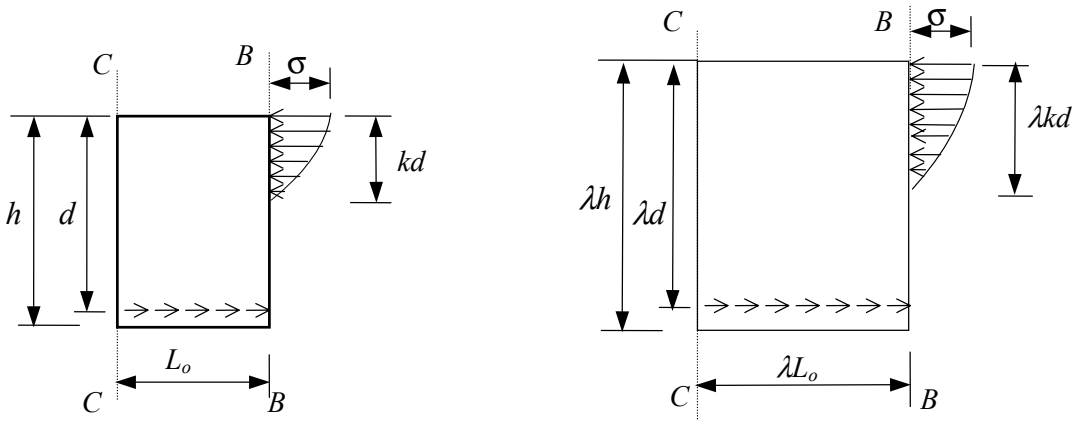

Block -1 *Block -2*

(a) Concrete compressive stress at the cracked section (load case 1)

(b) Bond stress at reinforcement level (load case 2)

BB : Cracked section
CC : Mid section between cracks (zero-slip section)

Fig. 7.1 Forces acting on two geometrically *similar* concrete blocks (same reinforcement ratio, cross sectional shape and steel stress at the cracked section)

Two types of *base models* are considered for the two load cases described previously. For load case 1, a base model with constant effective depth (d=100mm) is used (*base model*-1). When d is constant, the resulting loading on the transverse section of the finite element mesh remains unchanged for selected values of reinforcement ratio and the steel stress at the cracked section. Therefore, only the geometry of the mesh needs to be modified for subsequent analysis when other parameters are changed.

A base model with constant block length L_o (L_o =100mm) is analysed to calculate the concrete stresses and extensions for load case 2 (*base model*-2). When L_o is constant, the loading due to unit bond force (f_{bo}=1MPa and p=1) applied on the finite element mesh remains unchanged, and only the geometry of the mesh needs to be modified for subsequent analysis. After the analyses of base models, the concrete stress and extension results are stored only for four selected nodes of the finite element mesh, as described below.

The concrete stress results are stored for Nodes 1 and 45 while the concrete extension results are stored for Nodes 50 and 55 (see Figs. 7.2 and 6.5). Nodes 1 and 45 were selected based on the rigorous analytical results (Chapter 6), which showed that the maximum concrete stress always occurred at reinforcement level for the 70 beams considered, while the stress at the tension face was also considerably high occasionally (for beams with small heights and large critical crack spacing values). The concrete extension at Node 50 is required to determine the peak bond stress f_{bo} while the extension at Node 55 is used to calculate the crack width.

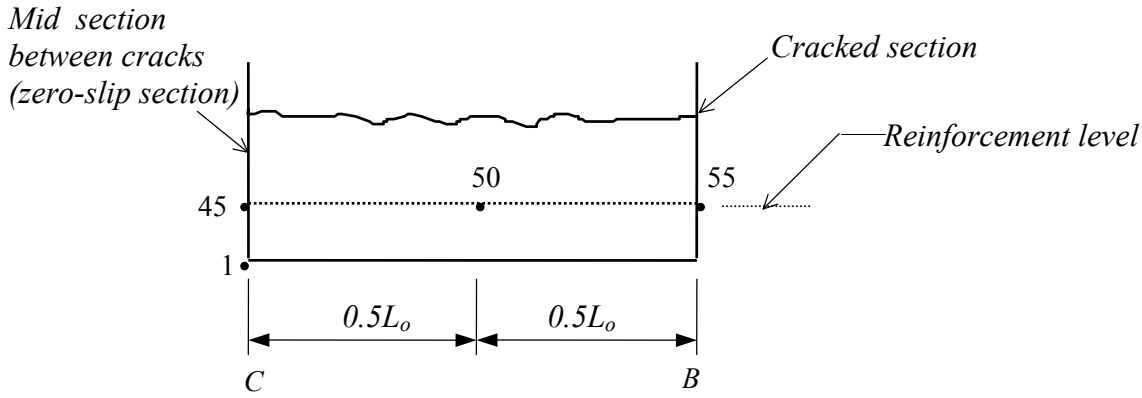

Fig. 7.2 Nodes for which concrete stress and extension results are stored
(Node 1 & 45: stresses; Node 50 & 55: extensions)

7.2.2 Calculation of stresses and extension in base models

(*a*) *Analysis of the base model*-1 *(load case 1)*

The externally applied concrete compressive stress distribution at the cracked section (Fig. 7.1) usually depends on the steel stress at the cracked section f_s, reinforcement ratio ρ and the concrete strength f'_c. The effects of concrete strength and reinforcement ratio on the calculated concrete compressive stress at the cracked section were found to be small. As a result, concrete stresses at Nodes 1 and 45 (Fig. 7.2) are not significantly affected by different ρ and f'_c used. Therefore, constant values ρ = 0.01 and f'_c = 32MPa were used in the analysis of *base model*-1. Table 7.1 shows the different f_s values used in the analysis. Also concrete stresses at Nodes 1 and 45 varied with the concrete cover, so the use of *h/d* ratio was adopted to account for this. For different combinations of f_s and *h/d* ratios given in Table 7.1, the base model is analysed with different L_o/d ratios shown.

Table 7.1. Variables used to analyse *base model*-1

Variable	Values
Steel stress at the cracked section (f_s)	100, 150, 200, 250, 300, 350, and 400 MPa
Overall height to effective depth ratio (*h/d*)	1.10, 1.15, 1.20 and 1.25
Ratio of the length of concrete block to effective depth (L_o/d)	0.2, 0.3, 0.4, 0.6, 0.8, 1.2 and 2.0

It will be seen in Section 7.3 that the spacing and width of cracks are calculated for different beams having various values for the effective depth *d*, beam width *b*, number of bars *m*, bar diameter ϕ, and concrete cover *c*, to investigate their effects. In this

calculation, concrete stresses and extensions for various values of *h/d* ratios other than those given in Table 7.1 are obtained by linear interpolation.

As described in Chapter 6, the critical crack spacing is determined by calculating the maximum concrete tensile stress within the concrete block and comparing with the flexural strength, for various trial crack spacing values (L_o values). For a selected trial crack spacing, the resulting L_o/d ratio generally lies in between the selected values shown in Table 7.1. In computing the concrete stress for a particular L_o/d ratio, the linear interpolation method (described in the previous paragraph) is not considered satisfactory because the variation of stress with L_o/d is found to be large, especially when $L_o/d < 1$ (see Fig. 7.3). Therefore, to determine the concrete stress for any value of L_o, a polynomial function is developed by matching the calculated concrete stresses corresponding to the selected L_o/d ratios given in Table 7.1. This procedure is described below.

Fig. 7.3 shows the calculated concrete tensile stresses at nodes 1 and 45 in the *base mode*-1 (d=100mm), for the seven L_o/d ratios given in Table 7.1. These stresses have been calculated for a typical case f_S =200 MPa and h/d=1.1. It can be seen that a smooth curve can be fitted to match the calculated stresses. This curve comprises of the following four segments of polynomials:

$0.2 \leq L_o/d < 0.4$,	3rd order polynomial ($aR^3 + bR^2 + cR$)
$0.4 \leq L_o/d < 0.6$,	linear function (dR)
$0.6 \leq L_o/d < 1.2$,	4th order polynomial ($eR^4 + fR^3 + gR^2 + hR$)
$1.2 \leq L_o/d < 2.0$,	constant

where a to h are the polynomial coefficients to be determined and R is the length to effective depth ratio of the concrete block analysed $R=L_o/d$ (see Fig. 7.1). Once the above eight coefficients (a to h) are determined, the concrete stress for any value of L_o/d (between the limits $0.2 \leq L_o/d < 2.0$) can be calculated, using the above polynomial functions. The concrete stresses at Node 1 and 45 are taken as zero when $L_o/d < 0.2$ (see Fig. 7.3).

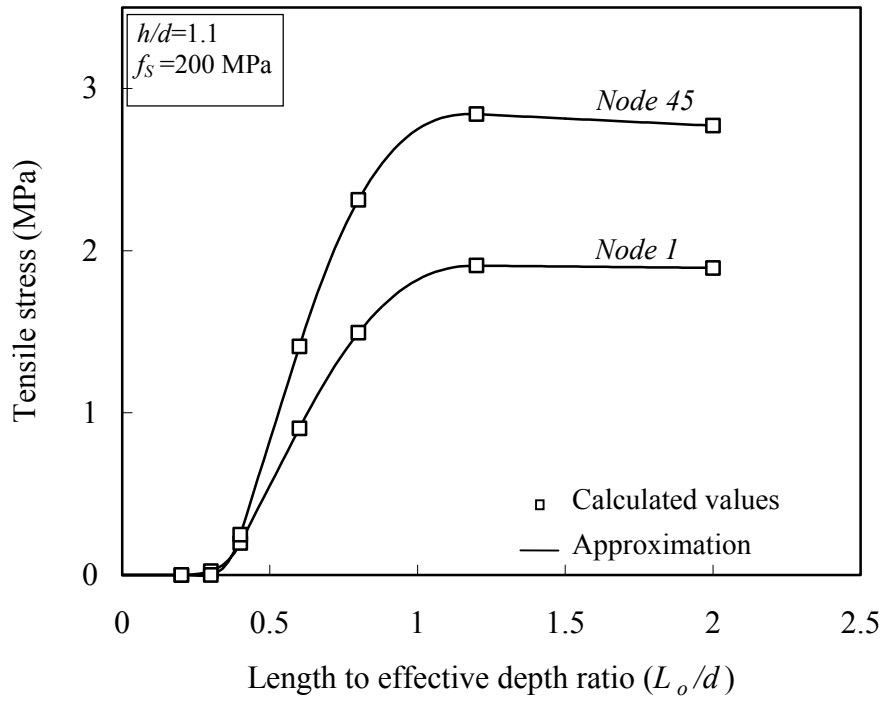

Fig. 7.3 Concrete stresses at Node 1 and 45 due to load case 1 (compressive force on transverse section)

The polynomial coefficients for each of the above four segments are determined using the calculated stress values that fall within each range. A *Microsoft Excel* Spreadsheet was prepared to determine these coefficients. When the stresses calculated for the seven L_o/d ratios (Table 7.1) are entered, the spreadsheet determines the above coefficients *a* to *h*. (A copy of this Spreadsheet is given in *Appendix E32*.) As an example, coefficients calculated for the polynomial function corresponding to the stress at Node 45 in Fig. 7.3 are shown in Table 7.2.

Table 7.2 Polynomial coefficients for stress at Node 45 (f_s =200MPa and h/d =1.1)

a	*b*	*c*	*d*	*e*	*f*	*g*	*h*
45.25	-10.225	0.57	1.91	2.1065	-2.463	-0.8917	1.91

Fig. 7.4 shows the calculated concrete extensions at Nodes 50 and 55 for the above typical case (f_S =200 MPa and h/d=1.1). As for the concrete stresses, a smooth curve is fitted to match the calculated values of concrete extensions. This curve comprises of the following four segments of polynomials.

$0.2 \le L_o/d < 0.3$,	linear function (aR)
$0.3 \le L_o/d < 0.6$,	fourth order polynomial ($bR^4 + cR^3 + dR^2 + eR$)
$0.6 \le L_o/d < 0.8$,	linear function (fR)
$0.8 \le L_o/d < 1.2$,	linear function (gR)
$1.2 \le L_o/d < 2.0$,	linear function (hR)

where a to h are the polynomial coefficients determined as described previously, and R is the length to effective depth ratio of the concrete block analysed $R=L_o/d$ (see Fig. 7.1). The concrete extensions at Node 50 and 55 are taken as zero when L_o/d <0.2 (see Fig. 7.4).

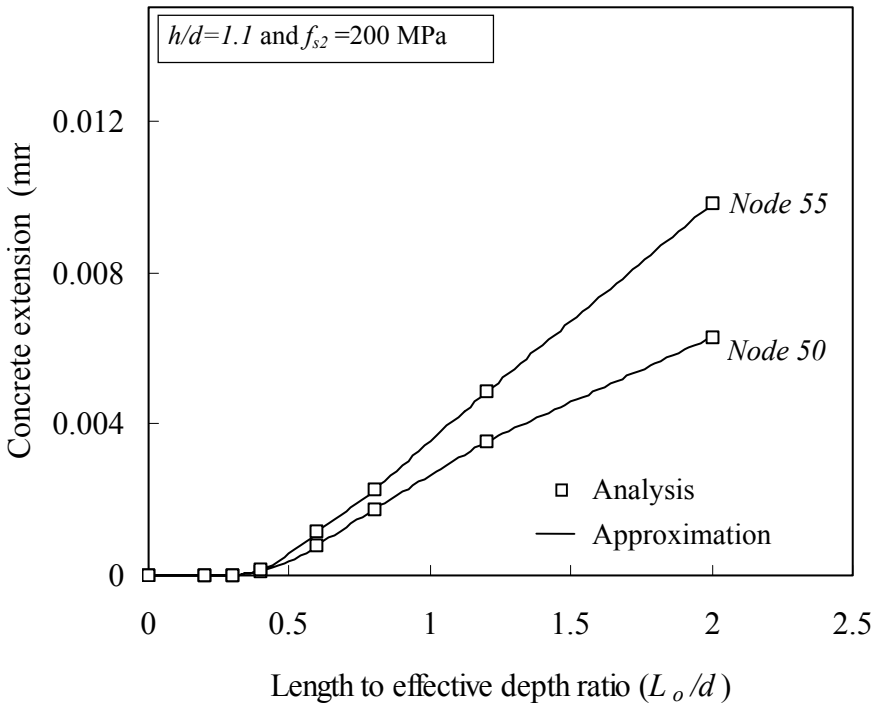

Fig. 7.4 Concrete extensions at Node 50 and 55 due to load case 1 (compressive force on transverse section)

As already mentioned, Figs. 7.3 and 7.4 show the concrete stresses and extensions, and the accompanying approximate polynomial curves for a typical case of f_s=200MPa and h/d=1.1. Similar analyses are carried out for other values of f_s and h/d ratios shown in Table 7.1, and the corresponding polynomial coefficients are determined. This has produced 112 sets (56 sets for stresses at Nodes 1 and 45; and 56 sets for extensions at Nodes 50 and 55) of polynomial coefficients, which are shown in *Appendix D1* to *D3*. These coefficients are stored in a computer data file by the name *APP-COEF.CSV*.

(*b*) *Analysis of base model*-2 *(load case* 2*)*

Analysis of *base model*-2 (L_o=100mm) indicated that the concrete stresses and extensions at the selected nodes (Nodes 1, 45, 50 and 55) due to the unit bond force (f_{bo}=1MPa and p=1) are not significantly affected by different block heights selected. This is because the calculation of stresses and extensions as well as the application of loads are at the bottom part of the concrete block, thereby making the influence of the top portion insignificant. Therefore, a constant effective depth (d=200mm) is selected for *base model*-2.

It was found that the calculated concrete stresses and extensions at the selected nodes vary with the concrete cover c, and the reduced thickness at reinforcement level t, (see Fig. 4.17). Consequently, the analysis is carried out for various values of c and t shown in Table 7.3. As seen in this Table, the concrete cover c is represented as a fraction of the bar diameter ϕ for convenience. As an example, the calculated stresses and extensions for various values of t are shown in Fig. 7.5 for a typical case of c/ϕ=1.

Table 7.3. Variables used to analyse *base model*-2

Variable	Values
Ratio of clear concrete cover to bar diameter (c/ϕ)	1, 1.25, 1.5, 2 and 2.5
Reduced thickness at reinforcement level (t)	1, 0.9, 0.8, 0.7, 0.6 and 0.5

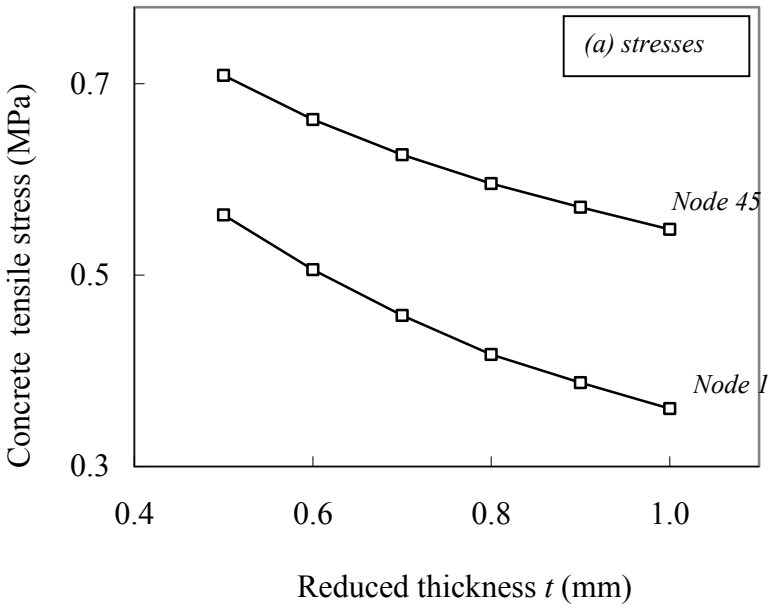

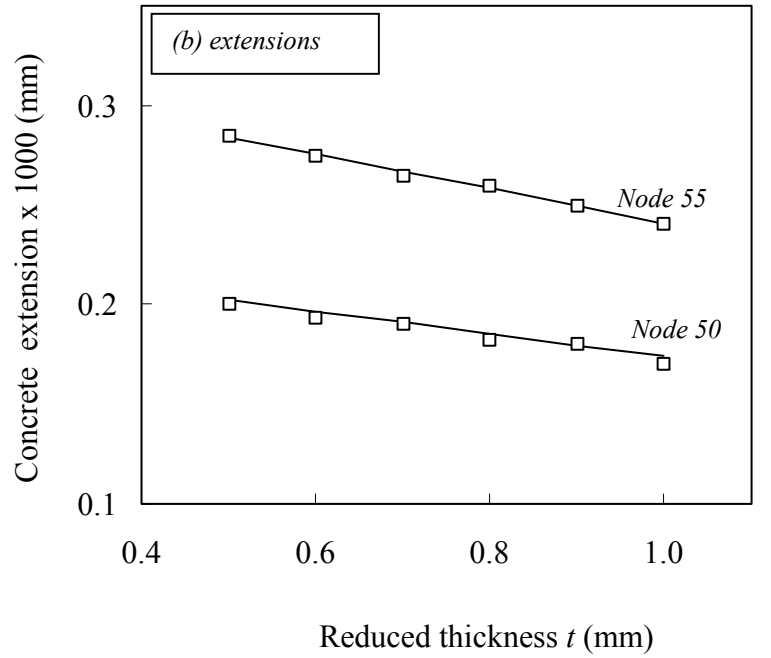

Fig. 7.5 Concrete stresses and extensions due to unit bond force (f_{bo}=1MPa, p=1) for a typical case of c/ϕ=1

The variations of concrete stresses at Nodes 1 and 45 shown in Fig. 7.5*a* for *base model*-2 are approximated as sixth order polynomials of the reduced thickness ($at^6 + bt^5 + ct^4 + dt^3 + et^2 + ft$) to facilitate the calculation of concrete stresses for all t values between $0.5 \leq t < 1.0$. As shown in this figure, the concrete extension is approximated as a linear function of the reduced thickness ($a + bt$).

Concrete stresses and extensions shown in Fig. 7.5 have been calculated for a typical case of $c/\phi=1$. Similar analyses are carried out to determine concrete stresses and extensions for all the values of c/ϕ shown in Table 7.3, and the corresponding polynomial coefficients are evaluated (see *Appendix D3*). These coefficients are stored in a data file (file name = *COEF-TH.CSV*) for using in the simplified method.

It must be noted that the *base model*-2 need not be analysed for various values of f_s, ϕ and m although these are taken as parameters in the calculation of the critical spacing and crack width (Section 7.3). This is because the analysis of *base model*-2 is carried out for a unit peak bond stress (f_{bo}=1MPa and perimeter of bars per unit beam width p=1). The resulting concrete stresses and extensions due to load case 2 are later multiplied by the actual values of f_{bo} and p, which depend on f_s, ϕ, m and b, as already described in Chapter 6.

7.3. Simplified Method of Calculating Critical Crack Spacing and Crack Width

Using the polynomial coefficients calculated in the previous Section, critical crack spacing l_c and maximum crack width W_s are determined for a series of beams to investigate the effects of different variables. Table 7.4 shows the list of variables and their ranges used. It may be seen that h/d ratio is not taken as a variable in this investigation, although it has been included in the development of polynomial coefficients described in previous Section. This is because the overall height h can be calculated using some of the other variables considered (*viz.* $h=d+\phi/2+c$).

It may be seen that the concrete strength f'_c is also taken as a variable, although a constant value f'_c=32MPa has been used in analysing the base models. While the force acting at the cracked section is not significantly affected by the concrete strength, it has some influence on the crack spacing and crack width results because the calculated concrete stress is compared with the flexural strength of concrete f_t (Note that $f_t = 0.62\sqrt{f'_c}$ as given in Eq. 4.11).

Table 7.4 Different variables used to calculate l_c and W_s

Variable	Range
Concrete strength f'_c	20 to 50 MPa in steps of 10 MPa
Steel stress at the cracked section f_s	100 to 400 MPa in steps of 50 MPa
Effective depth, d	100 to 500 mm in steps of 50 mm
Width of the member, b	200 to 1000 mm
Number of bars, m	2, 3, 4, 5,6 and 7
Ratio of clear concrete cover to bar diameter, c/ϕ	1 to 2, in steps of 0.25
Bar diameter, ϕ	10 to 32mm in steps of 4mm
Ratio of beam width/number of bars, b/m	40- 140

In selecting different values for b, m and ϕ, certain limitations are applied to ensure that a sufficient clear gap between bars is maintained, and to limit the distance between adjacent bars. Table 7.5 shows the upper and lower limits of m and ϕ used for various selected values of the effective depth d and beam width b.

Table 7.5 Minimum beam widths for different combinations of d, m and ϕ

Category	d (mm)		m		ϕ (mm)		Minimum width b (mm)
	Lower	Upper	Lower	Upper	Lower	Upper	
Beam	300	350	2	3	12	20	200
Beam	400	500	2	4	16	28	300
Beam	500	600	3	6	20	32	400
Slab	100	300	3	8	10	20	1000

Each of the variables listed in Table 7.4, except the b/m ratio, is varied one at a time and the critical crack spacing and the resulting crack width are calculated to assess the relative significance of their effects. To investigate the effect of b/m, the number of bars m is varied and the beam width b is chosen as required subjected to the constraints given in Table 7.5.

7.3.1 Method of calculating critical crack spacing and crack width

The procedure used for the calculation of critical crack spacing in the simplified method is similar to that described for the rigorous method (Chapter 6). The only difference is that in the simplified method, the concrete stresses and extensions are computed using the polynomial coefficients stored in data files, instead of carrying out the finite element analysis. This procedure is described below.

To calculate the critical crack spacing and crack width in the simplified method, a trial crack spacing is first selected and the resulting concrete stresses (at Nodes 1 and 45) and extensions (at Nodes 50 and 55) are determined using the polynomial coefficients. The peak bond stress f_{bo} corresponding to the selected parameters is then computed using the procedure described in Section 6.5.1, and the final stresses and extensions are determined using Eqs. 6.7 and 6.8. The trial crack spacing is changed and the calculation procedure is repeated until the resulting maximum concrete stress reaches

the flexural strength. When this condition is reached the trial crack spacing is taken as the critical crack spacing. The resulting maximum crack width is then calculated using the procedure described in Section 6.5.2.

A computer program written in BASIC language (program name = *CRACK.BAS*) is used for the above calculation. (The source program of *CRACK.BAS* is shown in *Appendix E18*). This program first reads the polynomial coefficients relating to concrete stresses (at Nodes 1 and 45) and extensions (at Nodes 50 and 55) stored in data files. It then selects a set of parameters (Table 7.4) to define a particular beam and, determines the critical crack spacing l_c and maximum crack width W_s using the procedure described in the previous paragraph. Results obtained from this calculation are used to investigate the effects of various variables on critical crack spacing and maximum crack width. This investigation is described in the next Section.

7.4 Effects of Different Variables on the Spacing and Width of Cracks

7.4.1 Effect of concrete strength, f'_c

The results indicate that the concrete strength has no significant effect on the spacing and width of cracks when other variables are kept constant. Fig. 7.6 presents the critical crack spacing and maximum crack width values calculated for a typical beam at different steel stress levels. The properties of the beam are: d=300 mm, b=200 mm, c=25 mm, ϕ=20 mm and m=2, which gives a reinforcement ratio ρ=1%.

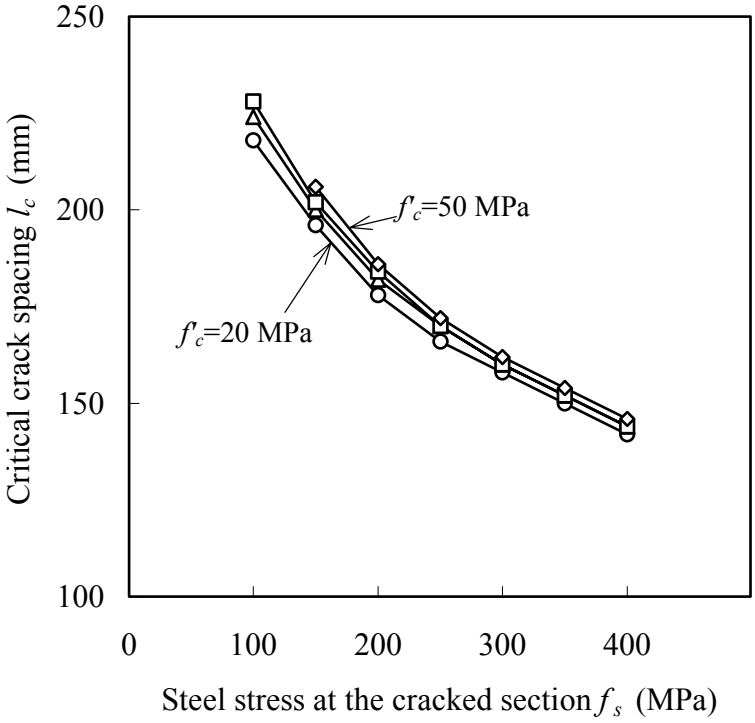

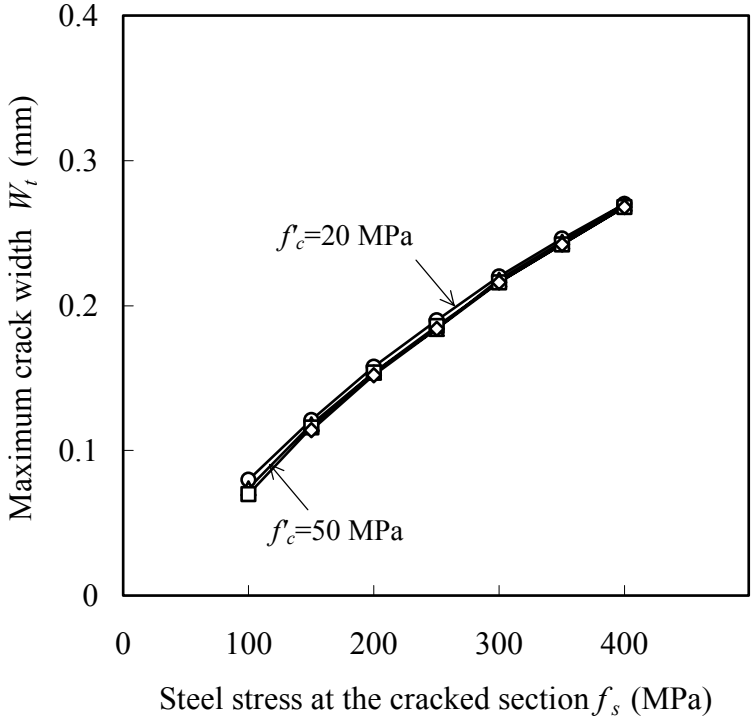

Fig. 7.6 Effect of concrete strength on critical crack spacing and crack width (d=300 mm, b=200 mm, ϕ=20, m=2, c=25 mm).

7.4.2 Effect of steel stress at the cracked section, f_s

The crack spacing decrease at a decreasing rate, while the crack width increases almost linearly with the steel stress at the cracked section, as seen in Fig. 7.6.

7.4.3 Effect of effective depth, d

Fig. 7.7 depicts the critical crack spacing and crack width values calculated for various effective depths ranging from 100 mm to 500 mm, for a typical beam where b=200 mm, c=24 mm, ϕ=16 mm and m=2. The calculation has been carried out for a steel stress of f_S=250 MPa. It is seen in this figure that the effective depth d does not influence the spacing and width of cracks if $d \geq 300$ mm. It is also seen that the spacing and width of cracks increase with the effective depth if d<300mm.

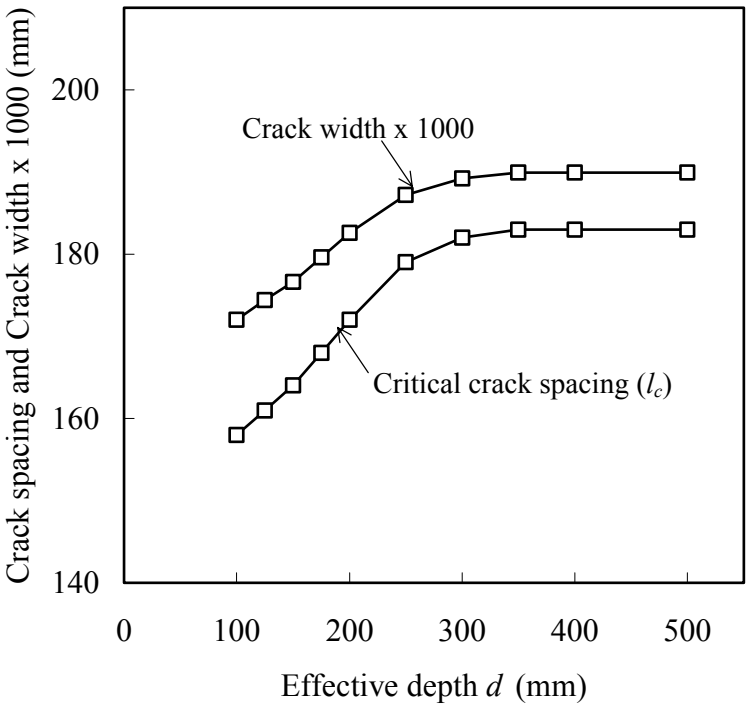

Fig. 7.7 Variation of spacing and width of cracks with the effective depth (f'_c=32 MPa, b=200 mm, ϕ=16 mm, c=24 mm, m=2, f_S=250 MPa)

This behaviour can be correlated to Fig. 7.3, which shows that the concrete tensile stresses at Nodes 1 and 45 due to *load case 1* are very small for large *d* values (small L_o/d values). For beams with d>300mm, the L_o/d ratio is generally less than 0.3 and the resulting tensile stress due to load case 1 is negligible. For this reason, the concrete tensile stresses at the above nodes are solely developed due to load case 2 (bond force). It was also mentioned in Section 7.2.2*b* that at the above nodes the resulting concrete stresses due to bond force are not affected by the beam height. Therefore, the critical crack spacing and crack width are not influenced by the effective depth if d>300mm.

7.4.4 Effect of width of the member, b and number of bars, m

Calculated values indicate that an increase in width of the member, and a decrease in number of bars have similar effects on spacing and width of cracks, if other variables are kept constant. Further, if both the values of *b* and *m* are changed in such a way that the ratio *b/m* is the constant, the resulting spacings and width of cracks remain the same. Increases in both critical crack spacing and crack width are observed when the effective width per one bar (*b/m*) is increased as seen in Fig. 7.8.

7.4.5 Effect of concrete cover, c

Both the crack width and crack spacing increase, as seen in Fig. 7.9, if the concrete cover is increased while keeping all other variables unchanged.

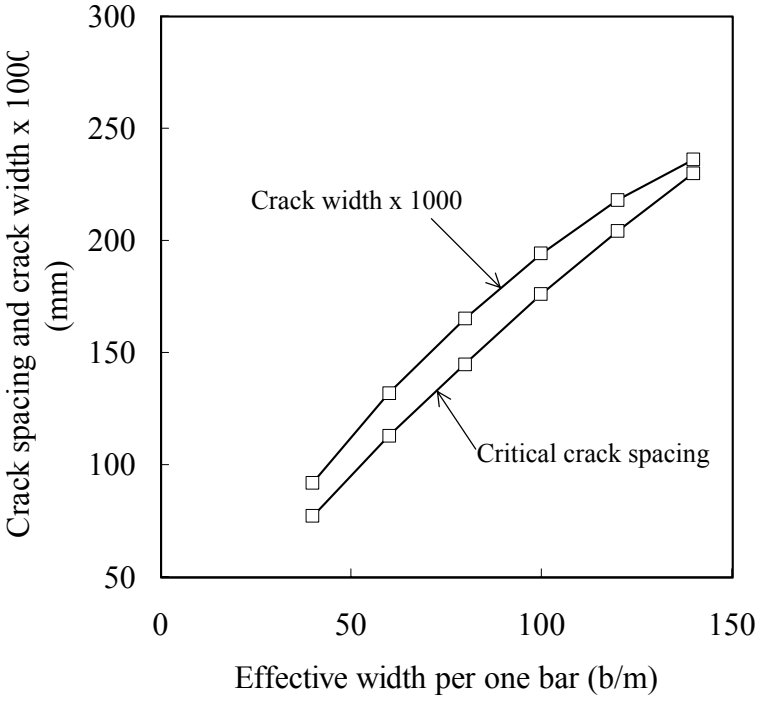

Fig. 7.8 Variation of spacing and width of cracks with effective width per one bar (f'_c=32 MPa , ϕ=20 mm, c=30 mm, , f'_S=200 MPa, d =300mm)

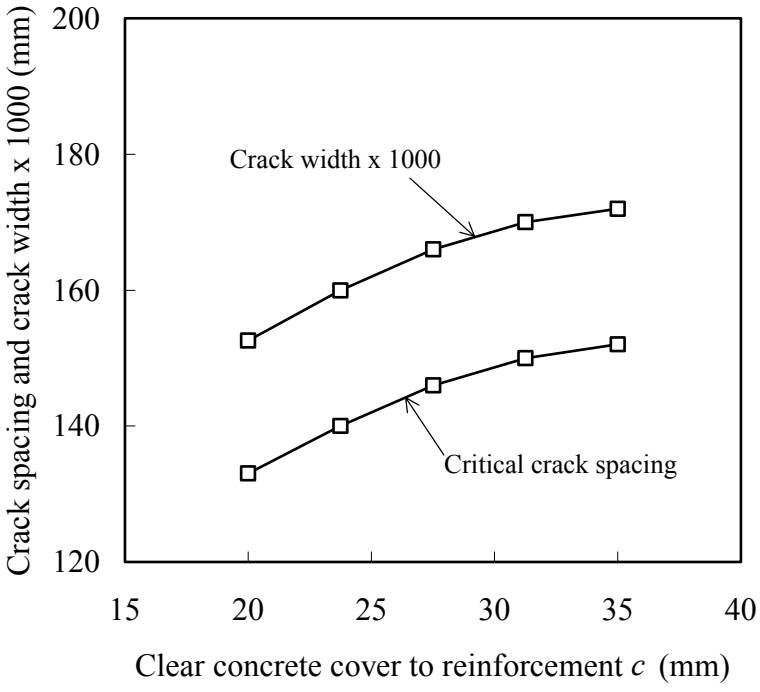

Fig. 7.9 Variation of crack spacing and crack width with concrete cover (f'_c=32 MPa, ϕ=20, b=160 mm, m=2, f'_S=250 MPa, d=300mm)

7.4.6 Effect of bar diameter, ϕ

Fig. 7.10 shows a typical variation of spacing and width of cracks with bar diameter. It may be seen that there is no significant change in spacing or width of cracks when the bar diameter is varied while keeping all other variables constant. It must be noted however that in normal practice, a change in bar diameter ϕ is associated with a change in the number of bars, *m*. This occurs when the area of reinforcement required for the design is known, and there is a choice for the selection of bar diameter. The effect of varying bar diameter ϕ, selected to provide a constant area of reinforcement by changing the number of bars, *m* is investigated below.

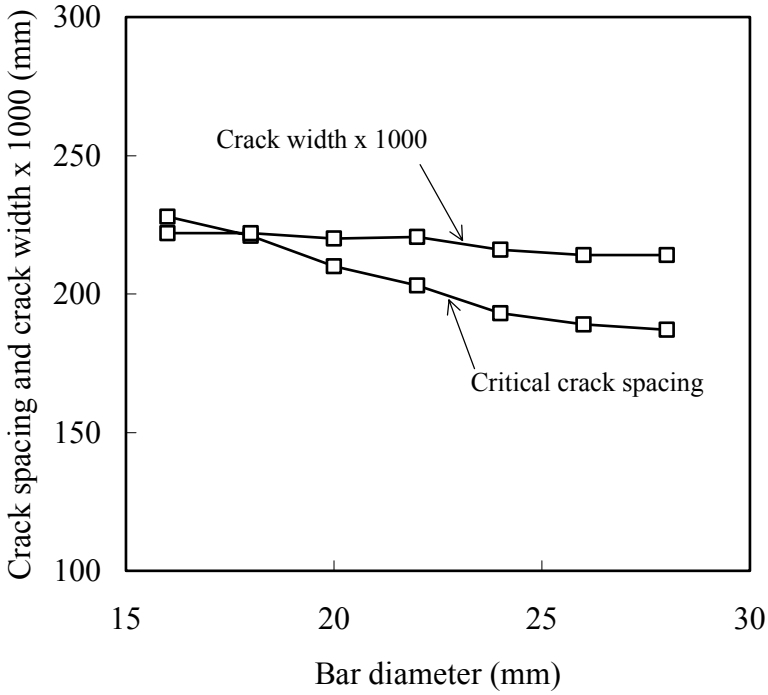

Fig. 7.10 Variation of crack spacing and crack width with bar diameter (f'_c=32 MPa, c/ϕ=1, b=250, m=2, f'_s=250 MPa)

Beam Nos. 5.4, 5.5 and 5.6 considered in Chapter 5 (see Table 5.5 for details) are selected to investigate the effect of bar diameter on the spacing and width of cracks. The area of reinforcement required for the ultimate strength of these beams are 600, 1260

and 1970 mm^2, respectively (using f_y=400MPa). For each beam, bar diameters are calculated for all possible numbers of bars, to have a minimum of two bars, and a maximum of 5 bars for *Beam-5.4* and 6 bars for others. It may be seen that some of the bar diameters calculated may not be available commercially, but they are included in the evaluation of crack width for comparison purposes.

Variations of the calculated spacing and width of cracks with bar diameter is shown in Fig. 7.11, for the above three beams, when the number of bars is changed accordingly to provide the necessary area of reinforcement. It may be seen in this figure that both spacing and width of cracks increase with bar diameter. In this calculation the clear cover to reinforcement is taken equal to the bar diameter, in all cases (c/ϕ=1).

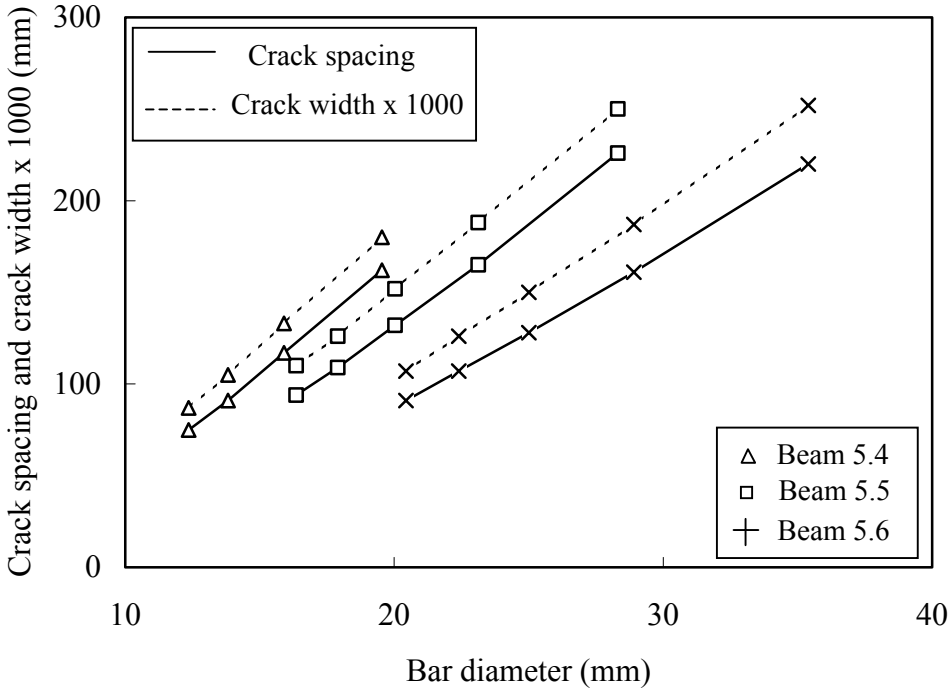

Fig. 7.11 Variation of spacing and width of cracks with bar diameter (f'_c=32 MPa, c/ϕ=1, f_s=250 MPa)

7.5 Parametric Study and Prediction Formulas for Spacing and Width of Cracks

To develop new prediction formulas, spacing and width of cracks are re-calculated for a series of beams using the simplified method (Section 7.4), by changing only those variables that were identified to have the most significant effects. Using the results described in Section 7.4, the variables shown in Table 7.6 are considered the most significant, and used in this parametric study within the ranges shown.

Table 7.6 Variables used in the parametric study and their ranges

Parameter	Range
steel stress at the cracked section, f_s	100 - 400 MPa
bar diameter, ϕ	10 - 36 mm
effective depth, d (d has no effect when d>300 mm)	100 to 300 mm
ratio of clear concrete cover/bar diameter, $c'=c/\phi$	1.0 - 2.5
ratio of effective width per one bar/bar diameter, $e=b/(m\phi)$	2 - 16

7.5.1 Effects of concrete cover and effective width per one bar

An inspection of Figs. 7.8 and 7.9 indicates that an increase (or decrease) in the effective width per one bar, e ($e=b/m$) and the concrete cover ratio c' ($c'=c/\phi$) have similar effects on spacing and width of cracks. Therefore, it is possible to combine c' and e, thereby reducing the number of parameters involved in prediction formulas. The results indicated that c' can be taken as unity ($c'=1$) in the calculation, if the parameter e is modified to include the effect of c', using the following formula.

$$e' = (0.8+0.2c')e \qquad (7.1)$$

where e' is the modified value of e, which takes into account the effect of c'. Fig. 7.12 shows the correlation between spacing and width of cracks calculated using the actual values of c' and e, and those computed using e' (with $c' = 1$). This correlation suggests that the use of e' evaluated by Eq. 7.1 together with $c'=1$ is acceptable for the calculation of spacing and width of cracks. This procedure is adopted in the present parametric study.

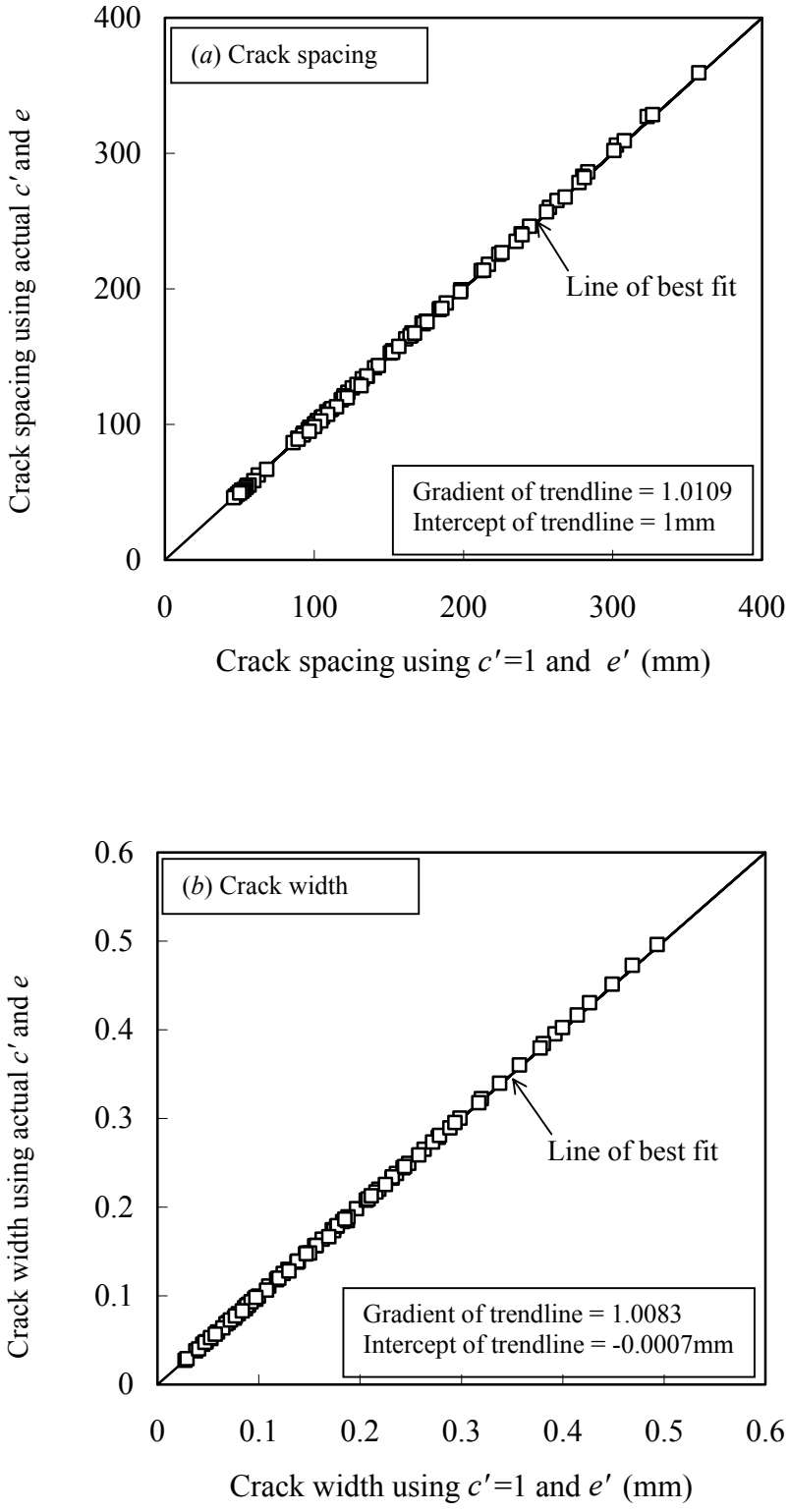

Fig. 7.12 Crack spacing and crack width calculated using modified value of *e*

7.5.2 Approximate formula for crack spacing in beams (d>300mm)

The critical crack spacing l_c values calculated in the parametric study were used in a linear regression analysis to develop the following empirical formula.

$$l_c = \left(\frac{200}{f_s} + 0.5 \right) l_f \qquad (7.2a)$$

and, $$l_f = 8e' + (0.65 + 0.35e')(\phi - 10) \qquad (7.2b)$$

where f_s = steel stress at the cracked section in MPa and ϕ is in mm ($\phi \geq 10$ mm).

A comparison of the critical crack spacing values calculated using Eq. 7.2 and those obtained in the parametric study is shown in Fig. 7.13. The results indicate good correlation.

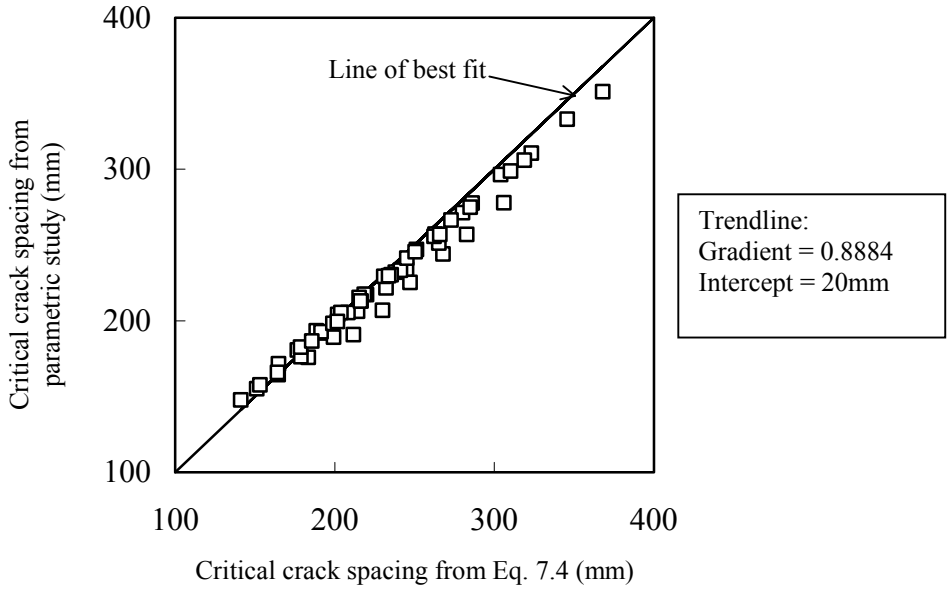

Fig. 7.13 Comparison of critical crack spacings obtained from the parametric study and those computed using Eq. 7.2 (e=6 and 8; c= 1.5 and 2; ϕ= 16, 20 and 24 mm; f_S=100 to 400 MPa)

7.5.3 Approximate formula for crack width in beams (d>300mm)

Calculated values of the maximum crack width at the tension face W_t have been used in a linear regression analysis to develop the following empirical formula.

$$W_t = W_f \left\{ 1 - \frac{400 - f_s}{400 + 500 W_f} \right\} \qquad (7.3a)$$

and $$W_f = 0.007\left\{ e' + 0.2\phi\left(1 + 0.4e'\right)\right\} \qquad (7.3b)$$

where W_t and ϕ are in millimetres and f_s in MPa ($400 \geq f_s$). Comparison of the crack width values calculated using Eq. 7.3 and those obtained in the parametric study is shown in Fig. 7.14. The results indicate very good correlation.

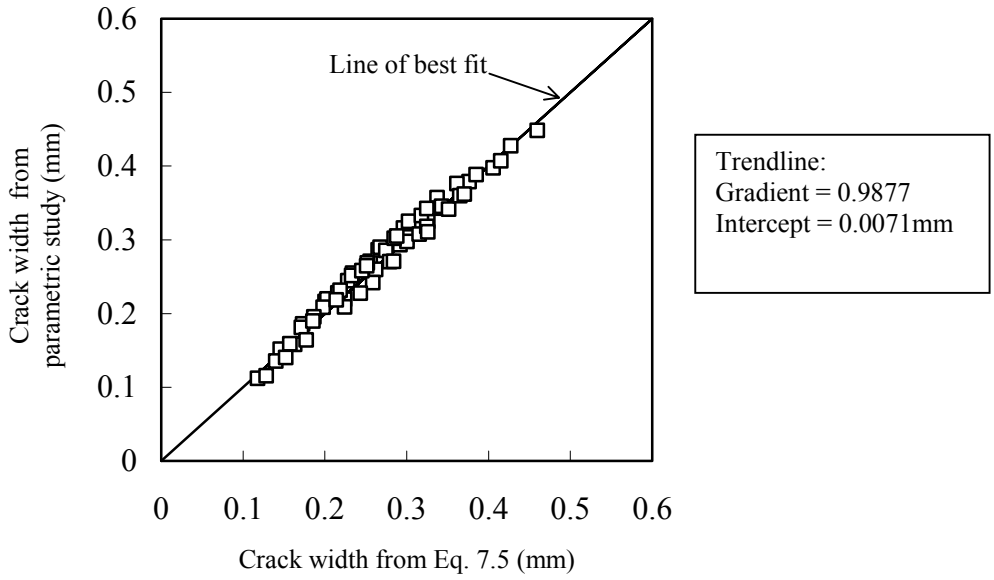

Fig. 7.14 Comparison of maximum crack width obtained from the parametric study and those computed using Eq. 7.3 (e=6 and 8; c= 1.5 and 2; ϕ= 16, 20 and 24 mm; f_S=100 to 400 MPa)

7.5.4 Crack spacing and crack width in slabs

As mentioned previously, the spacing and width of cracks increase with the effective depth d up to d=300mm. For beams with d > 300mm, the spacing and width of cracks are not affected when d is increased (see Fig. 7.7). Prediction formulas presented in Sections 7.5.2 and 7.5.3 are applicable for all members, which have effective depths larger than 300 mm. Values obtained from these formulas can be multiplied with suitable modification factors to determine the spacing and width of cracks for members if d<300 mm. The results obtained from the parametric study have been used in a linear regression analysis to develop the following formulas for these modification factors.

Modification factor for crack spacing:

$$F_{SP} = 1.1 - \frac{e'}{6 - 0.22d} \leq 1 \qquad (7.4a)$$

and, modification factor for crack width

$$F_{WD} = 1.05 - \frac{2e'}{d} \leq 1 \qquad (7.4b)$$

where F_{SP} and F_{WD} are the modification factors for crack spacing and crack width, respectively. A comparison of the modification factors determined using the results of the parametric study and those calculated using Eq. 7.4 is presented in Fig. 7.15.

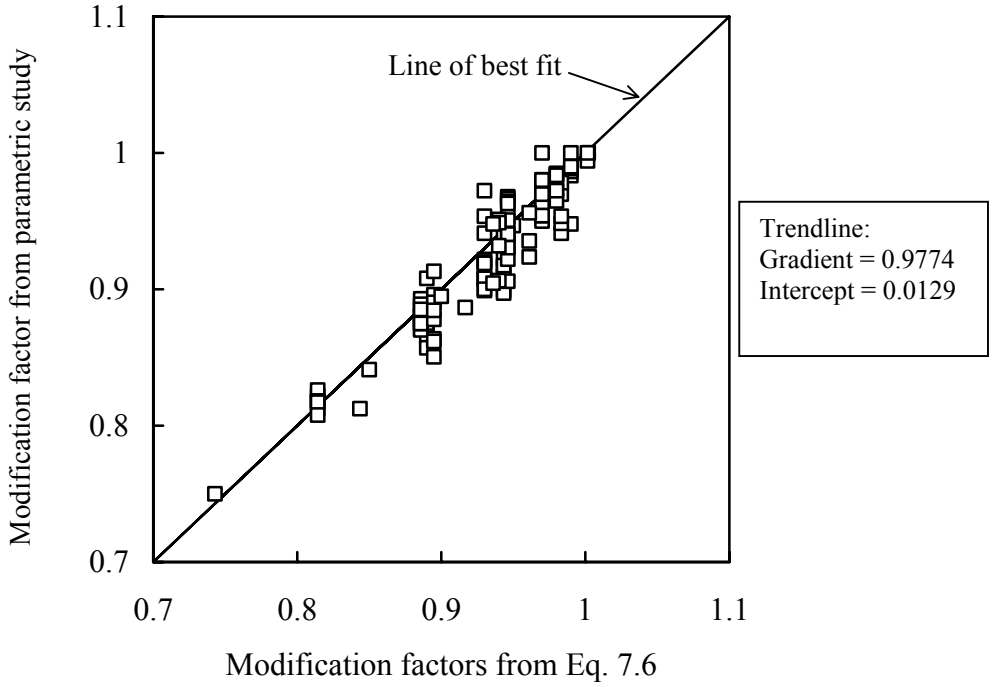

Fig. 7.15 Comparison of modification factors computed using approximate formula (e=6 and 8; c= 1.5 and 2; ϕ= 12 and 16; f_S=200 MPa; d=100-300mm)

7.5.5 Verification of new prediction formulas

As described in Chapter 6, the maximum, minimum and the average crack spacing in a constant moment region of a beam are expressed in terms of the critical crack spacing l_c (*viz.,* $S_{max}=l_c$, $S_{min}=0.5l_c$ and $S_{ave\text{-}pred} = 0.75l_c$; see Eq. 6.5). The value of l_c is calculated using the new empirical formulas developed in this Chapter (Eqs. 7.2 and 7.4*a*). To verify the accuracy of these equations, the predicted average crack spacings are compared with those measured by Clark (1956) and Chi & Kirstein (1958) on 70 test beams at seven steel stress levels. These 70 beams are the same test beams considered in Chapter 6 to verify the accuracy of the rigorous method of computing the spacing and width of cracks. Ranges of the variables included in these test beams have already been outlined in Section 6.6.

Comparison of the measured and predicted crack spacings for the above 70 beams is shown in Fig. 7.16. The *x*-axis in this figure represents the predicted average crack spacing $S_{ave\text{-}pred} = 0.75l_c$ where l_c is calculated using Eqs. 7.2 and 7.4*a* for various steel stress levels ranging from 103 to 310 MPa. The *y*-axis represents the corresponding measured average crack spacing at the same steel stress level.

It must be mentioned that for some of the above test beams, crack spacing measurements are not available for certain lower steel stress values. In total only 420 crack spacing measurements are available for the 70 beams tested at seven steel stress levels.

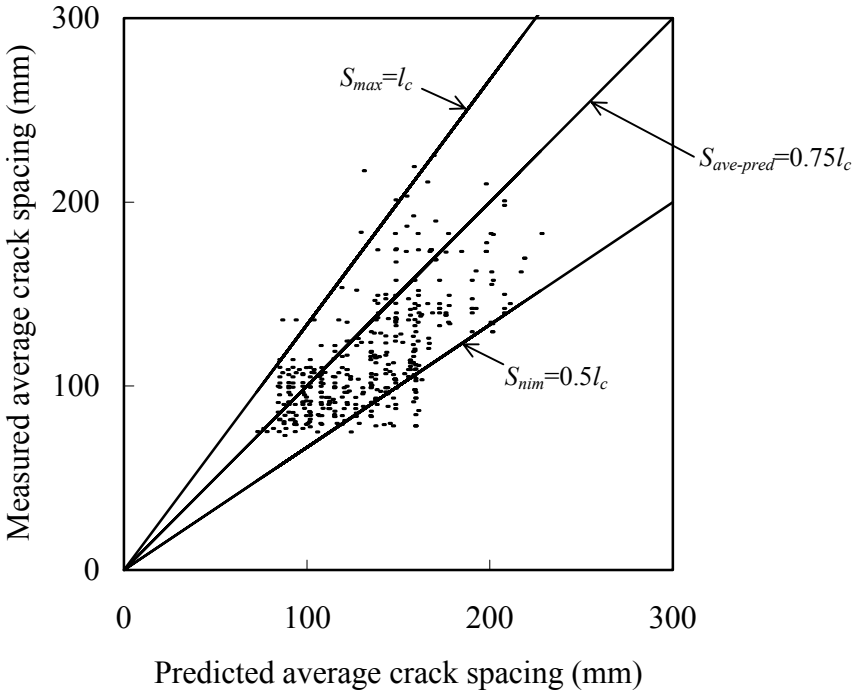

Fig. 7.16 Comparison of measured average crack spacing and those calculated using Eqs. 7.2 and 7.4*a*

Out of the 420 crack spacing measurements shown in Fig. 7.16, only 44 are smaller than the predicted lower limit of $0.5l_c$ while 13 measurements are larger than the upper limit l_c. This means that 363 measurements (86.4 %) lie within the predicted range of $0.5l_c$ and l_c (See Eq. 6.5). This amount is slightly lower than the 94 % of the measurements

lying within the range predicted by the rigorous method (Chapter 6). Considering the random nature of the locations of cracks formed in constant moment regions of beams, the accuracy of the proposed prediction formulas can be considered acceptable.

Maximum crack widths predicted by the proposed formulas (Eqs. 7.3 and 7.4*b*), are also compared with measured values for the same 70 beams at seven load levels, mentioned above. This comparison is shown in Fig. 7.17. It is seen that only 18 measurements (4%) are larger than 150% of the predicted values and 73 measurements (17%) are smaller than 50% of the predicted crack widths. These percentages are slightly larger than the corresponding values (3% and 6%) when the crack width is calculated using the rigorous method (Fig. 6.9). Considering the large scatter normally encountered in crack width measurements, the comparison shown in Fig. 7.17 is considered satisfactory.

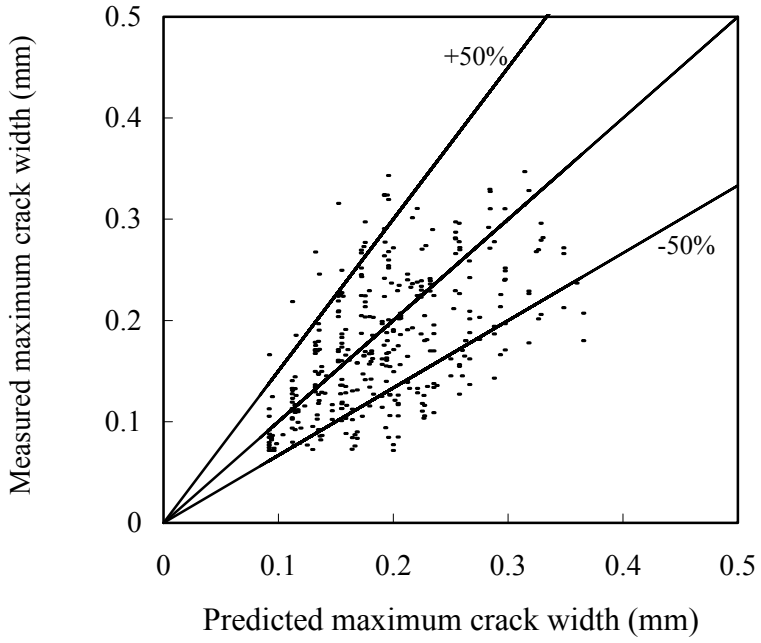

Fig. 7.17 Comparison of measured maximum crack width and those calculated using Eqs. 7.3 and 7.4*b*

7.5.6 Comparison with existing prediction formulas

In this Section, crack spacings and crack widths are calculated using the existing prediction formulas that were discussed in Chapter 2, and the results are compared with the measured values. The test results of Clark (1956) and Chi & Kirstein (1958), which were used to verify the new prediction formulas (Section 7.5.5), are used for this comparison.

It must be noted that some of the formulas predict the average crack width instead of the maximum crack width. In such cases, the corresponding maximum crack width is determined by multiplying the calculated average crack width by a factor of 1.5, which is close to the ratio observed by Clark (1956) and Chi & Kirstein (1958). Likewise, when the prediction formula evaluates the crack width at reinforcement level, the calculated value is multiplied by the factor (1.43h/d-0.43) to determine the crack width at the tension face (see Eq. 5.2b). This follows from the assumption that the depth of compression zone is equal to 0.3 times the effective depth, as described in Section 5.2.6.2. It must also be mentioned that some prediction methods calculate the crack width, with no reference to the crack spacing. Consequently, only 6 crack spacing comparisons are available for the 10 prediction procedures mentioned in Chapter 2.

The above comparisons are shown in Figs. 7.18 and 7.19. Inspection of these figures indicates that the accuracies of various methods are different. To evaluate the validity of different prediction procedures, percentages of measured crack width values lying between $\pm$ 50% of the predicted values are examined. These values are shown in Table 7.7, together with the corresponding percentage applicable for the present method. It can be seen that the accuracy of the proposed method is acceptable.

Table 7.7. Comparison of the accuracy of different crack width prediction procedures

Prediction method	Eq. No	Predicted crack width	Predicted location	Percentage of measured data lying within ± 50% of predicted crack width
Kaar & Muttock (1963)	2.11	maximum	reinforcement level [2]	86%
Oh & Kang (1987)	2.5*b*	maximum	tension face	85% [3]
Venkateswaralu & Gesund (1972)	2.4*b*	maximum	tension face	85%
Present method	**7.3**	**maximum**	**tension face**	**79%**
Chi & Kirstein (1958)	2.1*b*	average[1]	reinforcement level [2]	78%
Clark (1956)	2.10	average[1]	tension face	75%
Gergeley & Lutz (1968)	2.12	maximum	tension face	68%
Beeby (1970)	2.9	maximum	tension face	61% [3]
Broms & Lutz (1965)	2.3	maximum	tension face	57%
Chowdhury & Loo (2001)	2.13*d*	maximum	tension face	51% [4]
Lang & Ding (1992)	2.13*b*	maximum	tension face	51%

Notes:

(1) Average crack width was multiplied by a factor of 1.5 to calculate the maximum crack width

(2) Crack width at reinforcement level was multiplied by (1.43h/d -0.43) to calculate the crack width at tension face (see Eq. 5.2*b*)

(3) For the calculation of crack width, the depth of compression zone was assumed to be 0.3 times the effective depth; $x = 0.3d$ (see Section 5.2.6.2).

(4) In the test beams included in the present comparison, the spacing of reinforcing bars was not available. Estimations were made to determine this parameter, which may have affected the accuracy of the prediction.

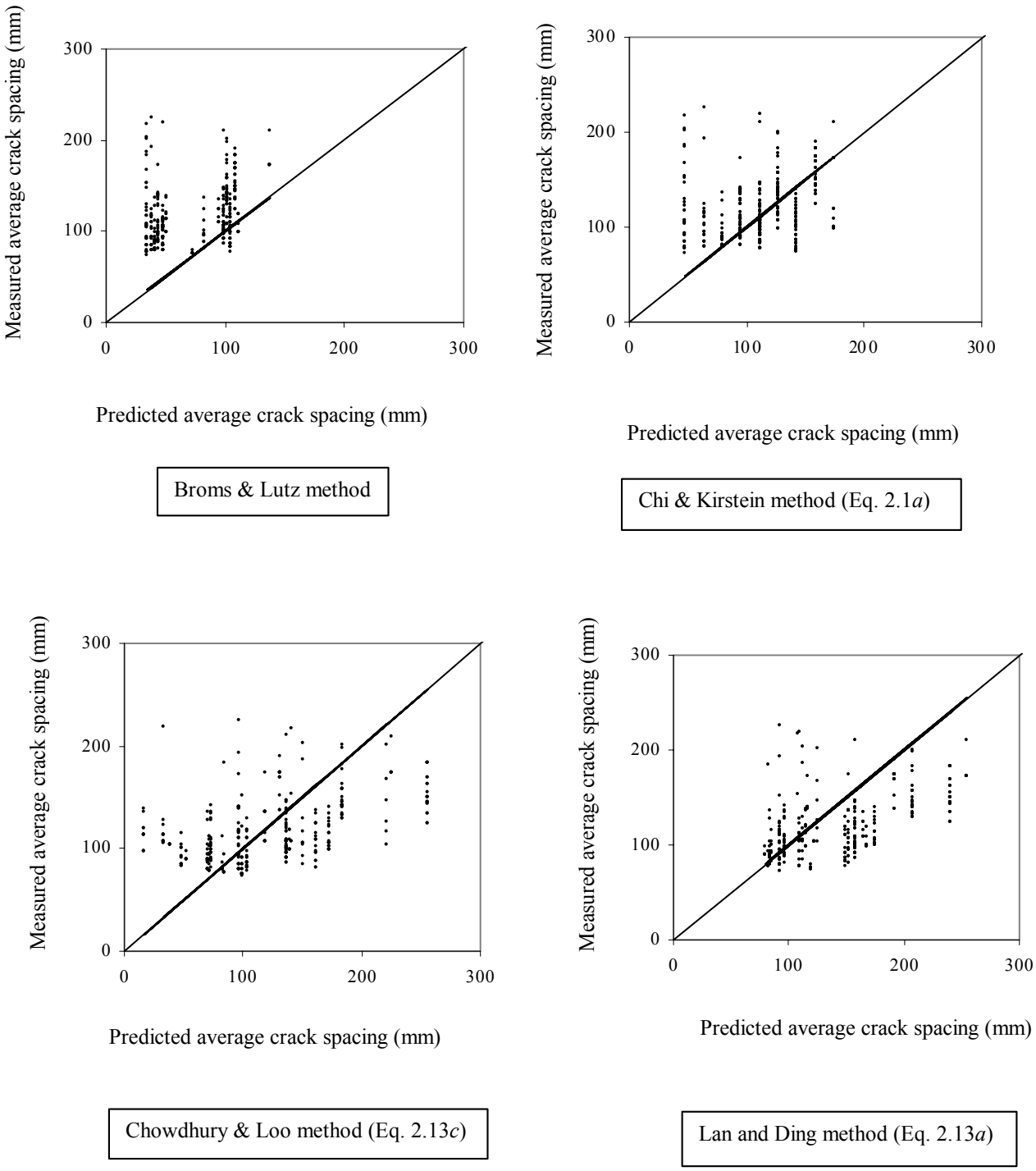

Fig. 7.18*a* Comparison of crack spacings predicted by different methods

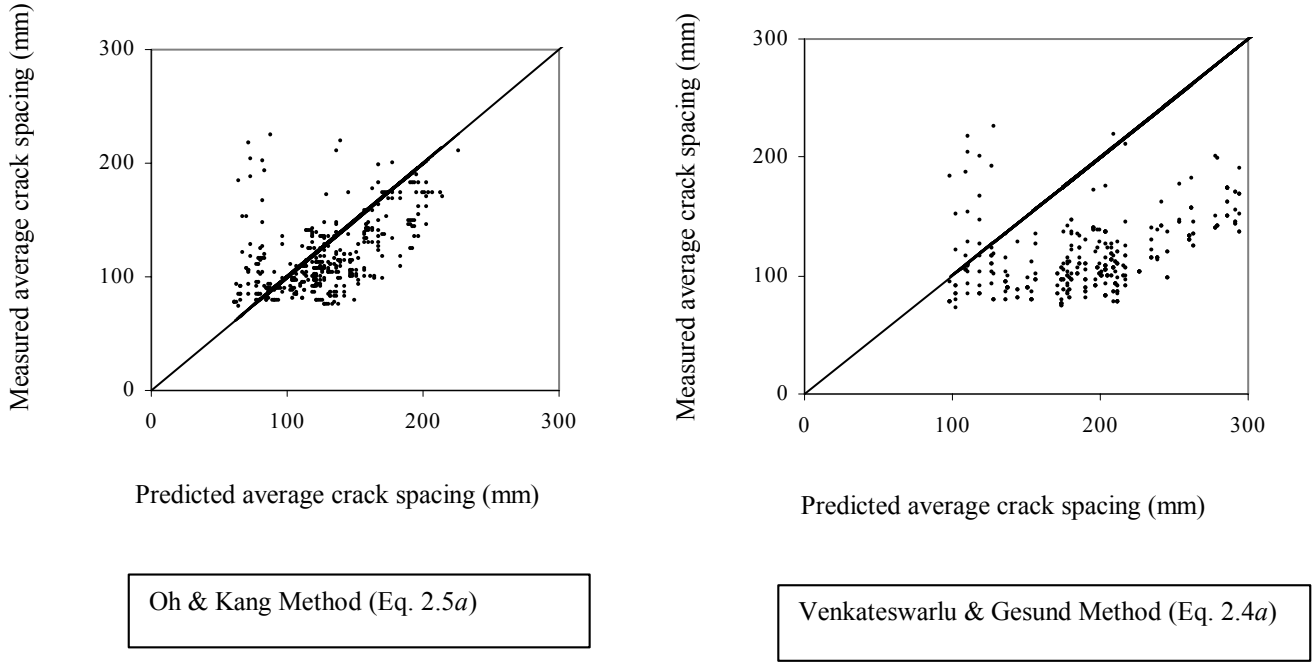

Fig. 7.18*b* Comparison of crack spacings predicted by different methods

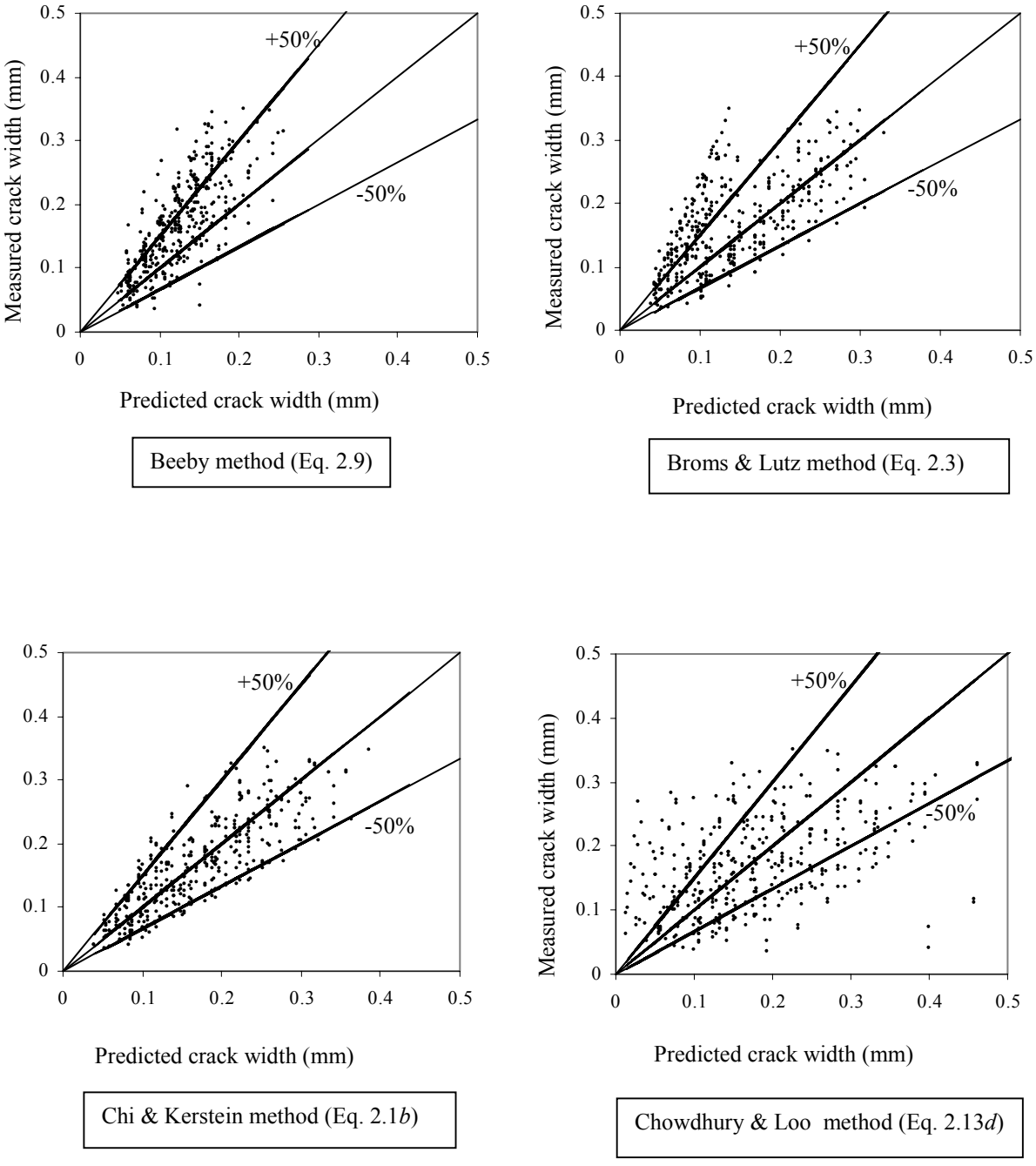

Fig. 7.19*a* Comparison of crack widths predicted by different methods

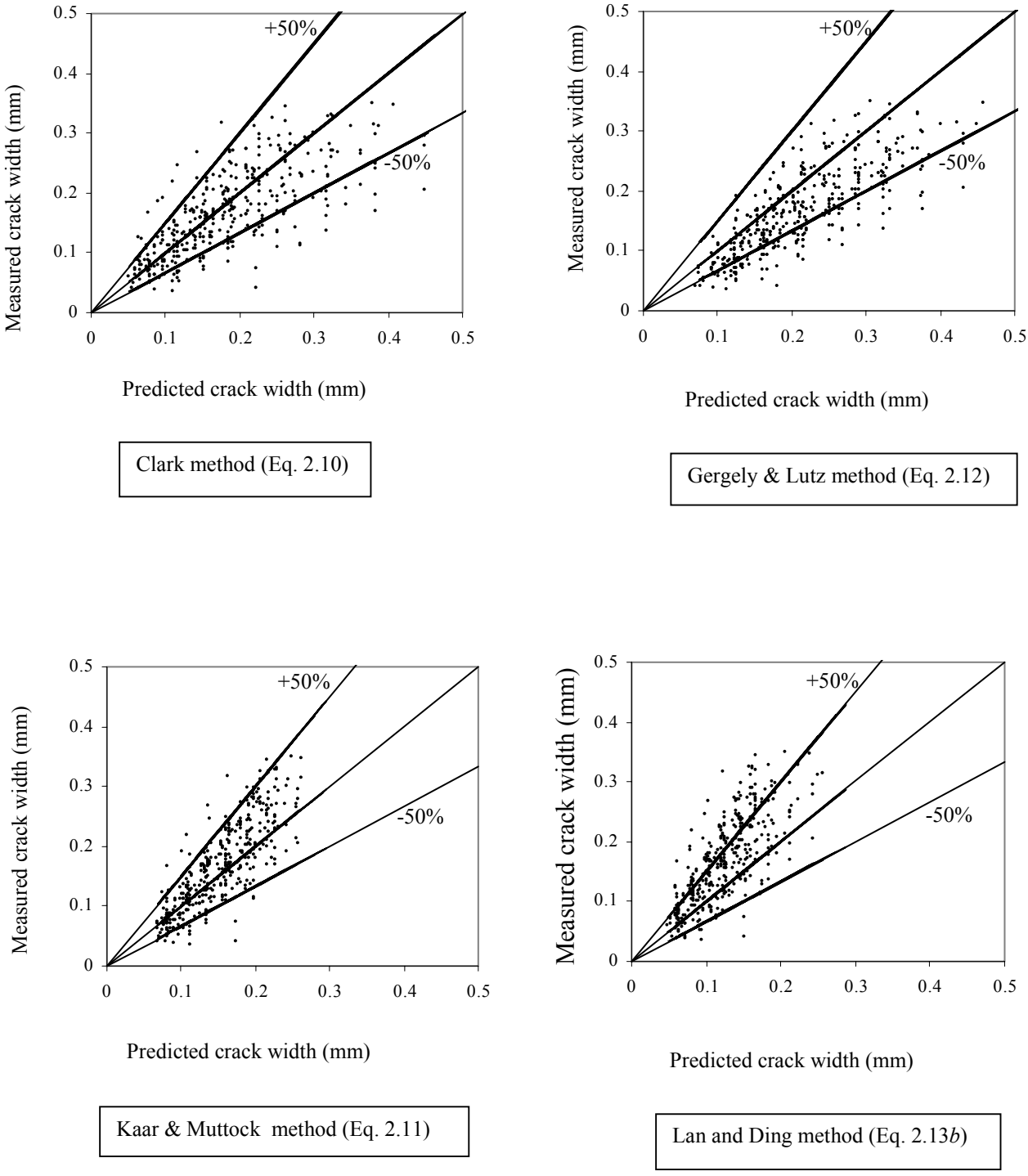

Fig. 7.19*b* Comparison of crack widths predicted by different methods

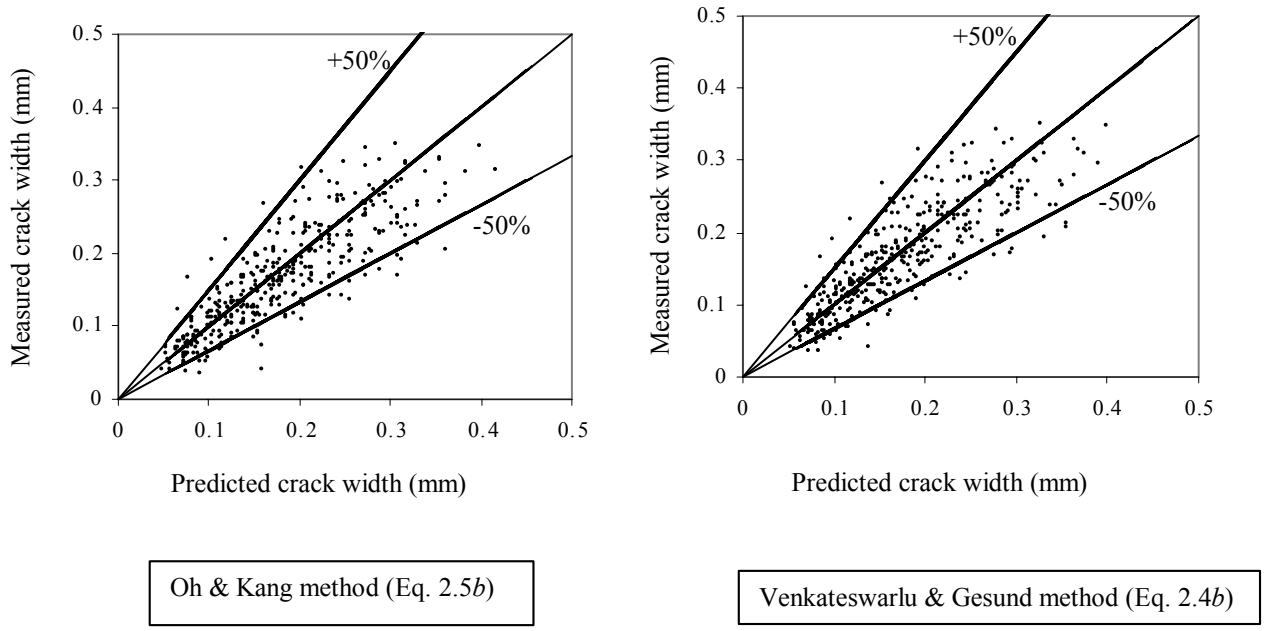

Fig. 7.19*c* Comparison of crack widths predicted by different methods

7.6 Summary

A simplified method is developed in the first part of this Chapter to calculate the critical crack spacing and the maximum crack width in reinforced concrete beams and one-way slabs. In this method, stresses and extensions in a concrete block between adjacent cracks are determined by using the previously stored data of finite element analyses. Spacing and width of cracks calculated by the simplified method are subsequently used to evaluate the relative significance of different variables.

The above evaluation reveals that the concrete cover c, bar diameter ϕ, effective width per one bar (b/m) and effective depth d (only if d<300mm) are the most significant parameters affecting the spacing and width of cracks. A parametric study was then carried out by re-calculating the spacing and width of crack using the simplified method, based on the above significant parameters. The calculated values were then used in a linear regression analysis to develop simplified formulas for predicting the average crack spacing and the maximum crack width.

A comparison of the spacing and width of cracks calculated using the proposed prediction formulas with those measured by other investigators indicates that the new formulas are acceptable. In particular, these formulas have nearly the same accuracy as using the rigorous method described in Chapter 6.

CHAPTER 8

TENSION STIFFENING EFFECT IN DEFLECTION CALCULATION

8.1 General Remarks

In this Chapter, a new method of incorporating the tension stiffening effect in deflection calculation is presented for beams and one-way slabs. The deflection is determined using curvature values calculated at a large number of sections along the beam. Curvature values at sections between adjacent cracks are determined using an empirical formula incorporating the bond force acting between the two cracks.

To develop the above formula, curvature values at sections between adjacent cracks are calculated for a number of beams using the strain distribution across the height of the member. The concrete strain is evaluated using the finite element analytical results, while the corresponding steel strain is based on the steel stress at the nearest cracked section and the associated bond force.

Short-term deflections are calculated using the curvature values determined by the empirical formula and compared with measured values for 37 flexural members tested by various investigators. These flexural members include one-way slabs as well as rectangular, T- and Box-shaped beams (both simply supported and continuous), tested under uniform and concentrated loads. The comparison indicates that the proposed method of incorporating the tension stiffening effect is acceptable.

8.2 Curvature at a Cracked Section

Calculation of curvature at a cracked section assumes that the plane sections before cracking remain plane after cracking. As a result, the strain distribution at the section is linear, as shown in Fig. 8.1, where ε_c is the concrete strain at the extreme compression fibre and ε_s is the steel strain. The depth of the compression zone is *kd* as shown, where *d* is the effective depth.

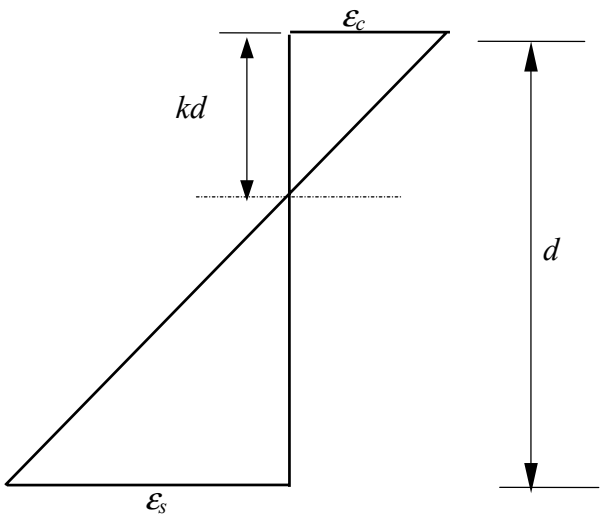

Fig. 8.1 Strain distribution at a cracked section

The curvature, κ at the section can be calculated as

$$\kappa = \frac{\varepsilon_c + \varepsilon_s}{d} \tag{8.1}$$

The values of ε_c and ε_s corresponding to a given bending moment *M* are determined by considering the translational and rotational equilibrium of the section, as described in Chapter 4 (Section 4.6.1).

8.3 Curvature at Sections Between Cracks

Calculation of curvature values at sections between adjacent cracks requires the strain distribution across the height of the beam at each section. The concrete strains at various sections are evaluated by analysing the concrete block between adjacent cracks using the finite element method described in Chapter 4 (Section 4.11). The corresponding steel strain is determined by considering the equilibrium of part of the steel bar between a section and the nearest cracked section as described in Section 4.7.1. As an example, strain distributions calculated at various sections between adjacent cracks in the constant moment region of a typical slab are presented in Fig. 8.2. The properties of this slab are as follows:

overall height h	= 170 mm,
effective depth d	= 150 mm,
reinforcement ratio ρ	= 0.0075
bar diameter ϕ	= 12 mm
steel stress at the crack f_s	= 200 MPa
concrete strength f'_c	= 32 MPa
crack spacing S	= 140 mm

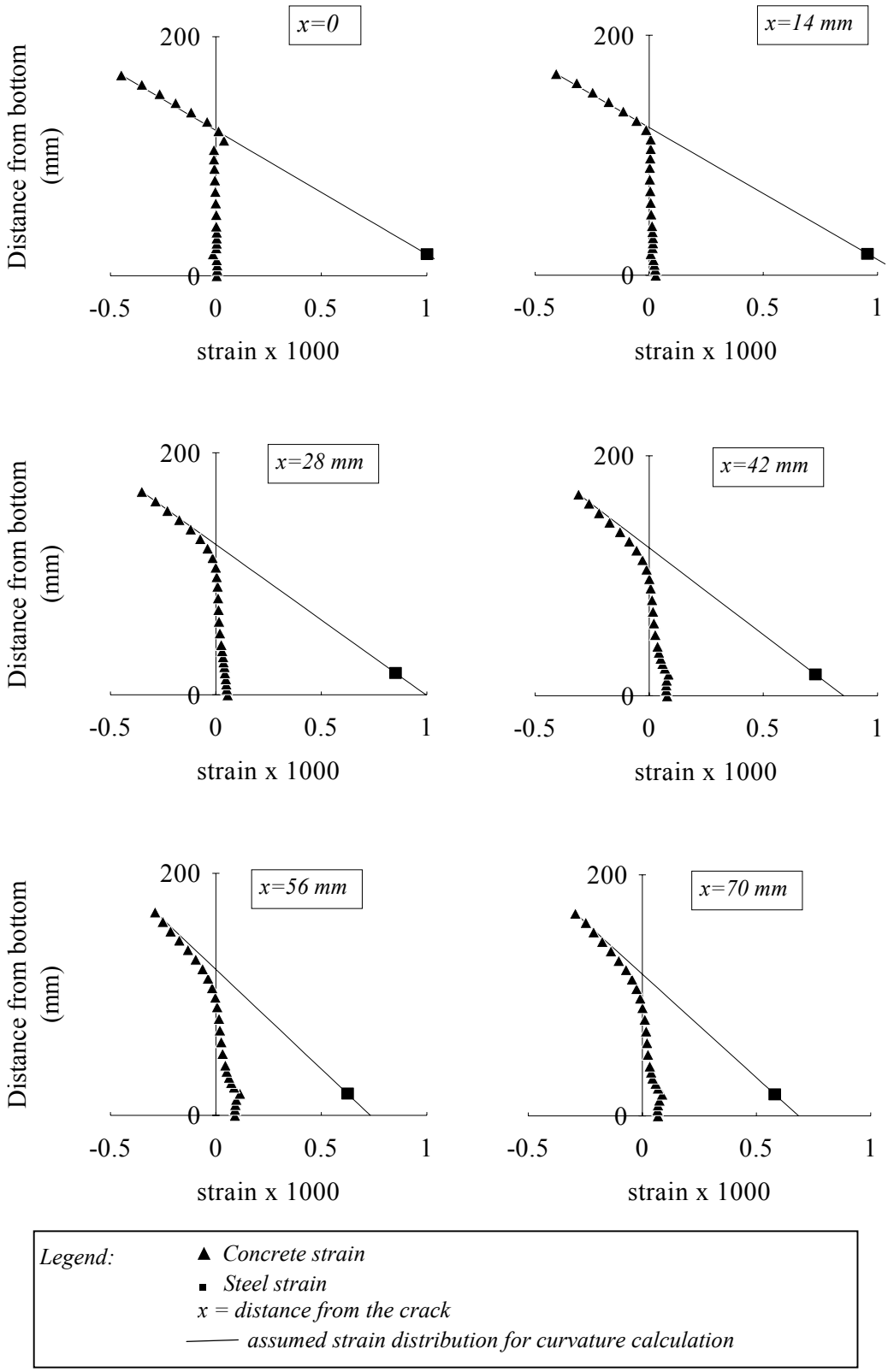

Fig. 8.2 Strain distribution across the depth of a typical slab (d=150 mm, f'_c=32 MPa, ρ=0.0075, crack spacing S=140mm, steel stress at the cracked section f_s =200MPa).

It can be seen in Fig. 8.2 that the strain distribution at the cracked section represents a linear variation within the compression zone as expected, while at sections away from the crack the concrete strain becomes non-linear. It is also seen that this non-linearity increases and the corresponding steel strain (and the steel stress) decreases with the distance from the crack.

It is deduced that the reduction in steel stress is the largest contributing factor to the increased bending stiffness at sections between cracks. Consequently, the curvature is based on the reduced steel stress at each section. For this calculation, a linear strain distribution defined by the reduced steel strain and the maximum concrete strain at the section is considered (see Fig. 8.2). The resulting curvature is then calculated using Eq. 8.1, as for a cracked section.

To demonstrate the variation of curvature between adjacent cracks, the procedure described in the previous paragraph is used to calculate the curvature for four typical crack spacings in the typical slab presented. These crack spacings are taken as S=80, 100, 120 and 140 mm, S=140 mm being the critical crack spacing corresponding to the selected variables. For each crack spacing, the curvature is calculated at 20 intermediate sections and the results are shown in Fig. 8.3.

Fig. 8.3 indicates that the curvature κ at sections between adjacent cracks decreases gradually with the distance from the nearest crack. For the case of constant moment region considered above, the lowest value of κ occurs at the mid section between the cracks (zero-slip section). In varying moment regions however, the lowest curvature value (the zero-slip section) occurs at a section closer to the crack having the lower bending moment (Section 5.3.2).

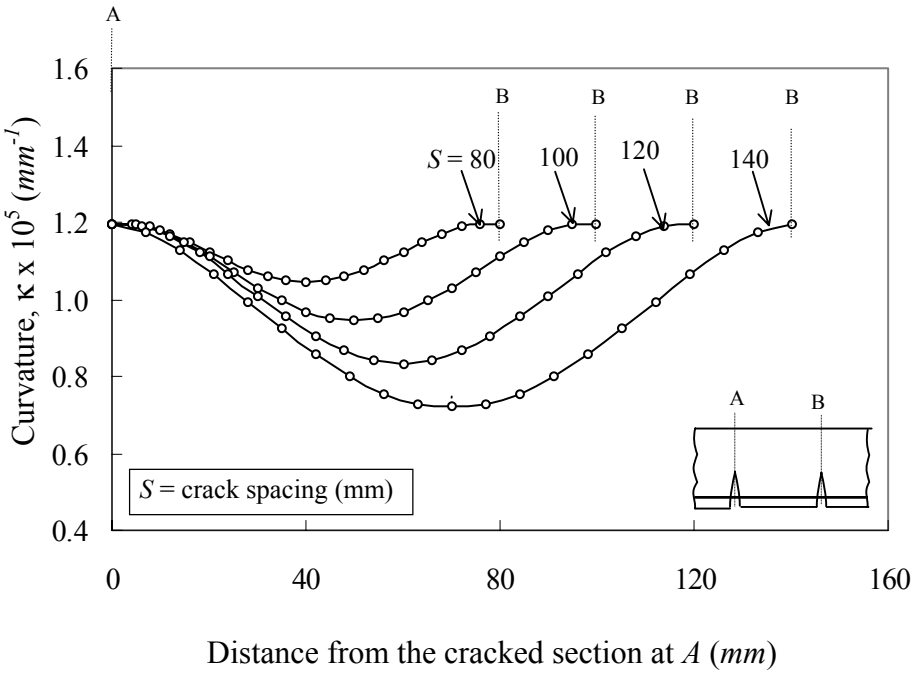

Fig. 8.3 Variation of curvature between adjacent cracks.

8.3.1 Approximation for the variation of curvature between cracks

For the calculation of deflections, the gradual variation of curvature between adjacent cracks is approximated as a tri-linear variation. As shown in Fig. 8.4, the curvature is assumed to be constant over distances of $0.2S_x$ and $0.2S_y$ near the two cracks and near the zero-slip section, where S_x and S_y are the distances from the zero-slip section to the nearest crack. For the remaining lengths, the curvature is assumed to be varying linearly as shown. Using this approximation, the curvature value at any section between the two cracks can be determined in terms of κ_1, κ_2 and κ_3 where κ_1 is the minimum curvature at the zero-slip section, and κ_2 and κ_3 are the two curvature values at the adjacent cracked sections (Fig. 8.4). Note that Fig. 8.4 shows calculated curvature values for two cracks in a constant moment region where $\kappa_2 = \kappa_3$ and $S_x = S_y$. The same approximation is used for calculating the curvature between adjacent cracks in varying moment regions, where κ_2 and κ_3 as well as S_x and S_y are different.

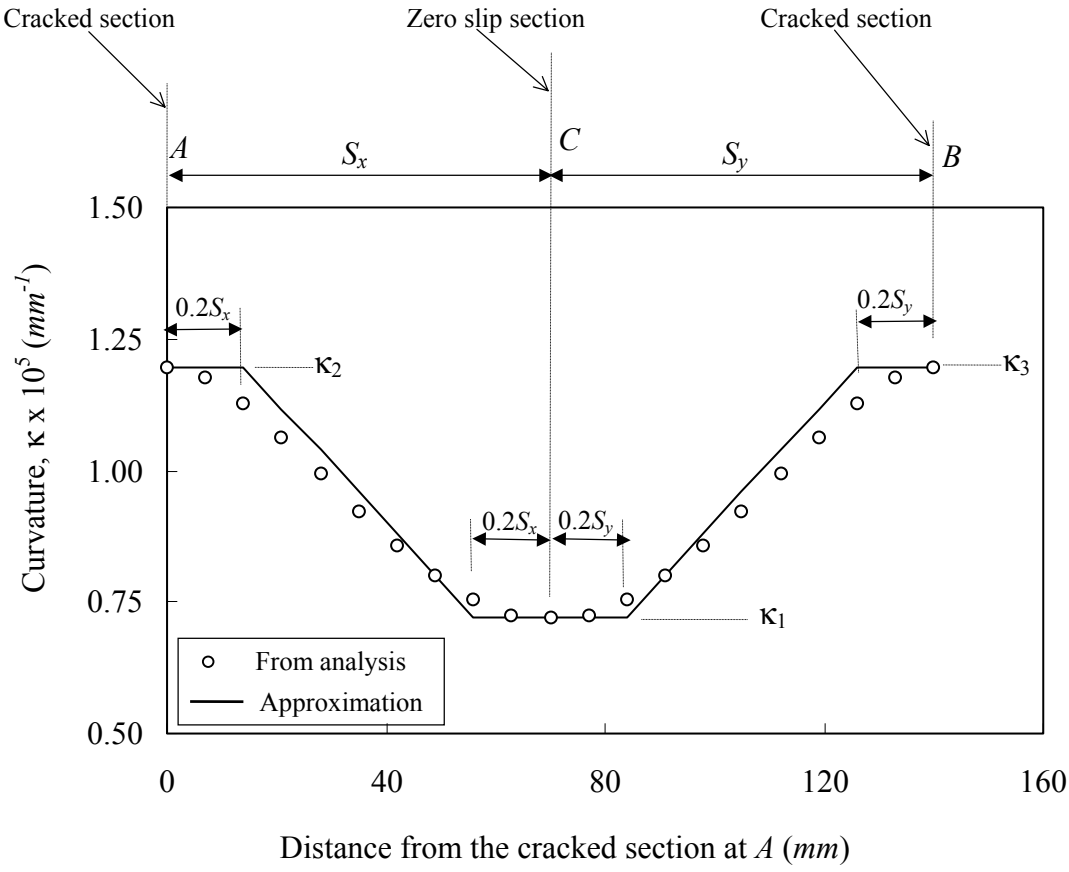

Fig. 8.4 Approximation for the variation of curvature between adjacent cracks (data from Fig. 8.3; *S*=140mm).

8.3.2 Empirical formula for the curvature κ_1 at zero-slip section

To determine the curvature at intermediate sections between adjacent cracks, the values of κ_1, κ_2 and κ_3 need to be evaluated first. The calculation of κ_2 and κ_3 is simple because it is based on the conditions of equilibrium, as described in Section 8.2. However, the evaluation of κ_1 was based on the concrete strain at the zero-slip section, ε_c, which was calculated by the finite element method. To make the deflection calculation simpler, an empirical formula will be developed to calculate κ_1 as described below.

To develop the empirical formula, curvature values at the zero-slip section κ_1 are calculated for the following flexural members.

effective depth d	= 100 mm :	crack spacing S= 90, 120, 140, 160 mm
effective depth d	= 150 mm :	crack spacing S= 80, 100, 120, 140 mm
effective depth d	= 300 mm :	crack spacing S= 120, 140, 180, 200 mm
reinforcement ratio ρ	= 0.0075	
Steel stress at the crack f_s	= 200 MPa	
Concrete strength f'_c	= 32 MPa	

The crack spacings S shown above have been selected between the two limits S_{max} and S_{min} for the selected variables. Note that $S_{max} = l_c$ and $S_{min} = 0.5l_c$ (Eq. 6.5).

Effective depths larger than 300mm need not be considered for this calculation because the concrete stresses are not affected by larger d, as indicated in Section 7.4.3. Also, the use of different reinforcement ratios and concrete strengths are not required for the above calculation, since the concrete stresses are not significantly affected by these variables (Section 7.2.2).

Calculated curvature values at the zero-slip section κ_1 suggest that κ_1 can be related to the curvature κ_2 (or κ_3) at the nearest cracked section via the steel stresses at the respective sections. Fig. 8.5 shows the relationship between κ_2/κ_1 and f_{s1}/f_{s2} where f_{s1} is the steel stress at the zero-slip section, and f_{s2} is the steel stress at the nearest cracked section. Note that f_{s1} is the minimum stress in the steel bar between the two cracked sections (Fig. 4.10).

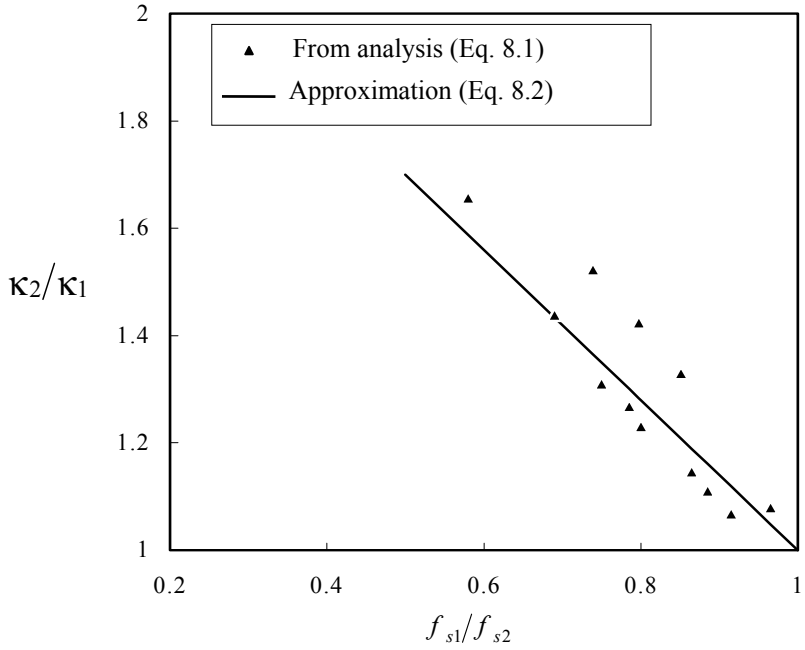

Fig. 8.5 Relationship between κ_2/κ_1 and f_{s1}/f_{s2}

Using a linear regression analysis of the calculated data, the following empirical formula is proposed to determine the curvature at the zero-slip section, κ_1.

$$\frac{\kappa_2}{\kappa_1} = 2.5 - 1.5\frac{f_{s1}}{f_{s2}} \tag{8.2}$$

In using the above equation, κ_2 is determined using Eq. 8.1, with ε_c and ε_s calculated by considering the equilibrium of the cracked section (Section 4.6.1). The resulting steel stress at the nearest cracked section f_{s2} is calculated as $f_{s2} = E_s\varepsilon_s$. Finally, the corresponding steel stress at the zero-slip section f_{s1} is evaluated by substituting S_x for S_o in Eq. 4.16*f*, which leads to the following formula.

$$f_{s1} = f_{s2} - \frac{8 f_{bo} S_x}{3\phi} \tag{8.3}$$

where f_{bo} is the peak bond stress determined using the procedure described in Chapter 4 (Section 4.7.2).

8.4 Calculation of Deflection

8.4.1 Location of flexural cracks

Before calculating the deflection under a particular load, the locations of flexural cracks within the cracked region are determined using the prediction procedure developed in previous Chapters. In Chapter 6, it was concluded that all cracks in a varying moment region are developed at a regular spacing of S_o (Section 6.4). The value of S_o can be determined using the empirical formula developed in Chapter 5 (Eq. 5.5). Also, as mentioned in Chapter 7, the average crack spacing in a constant moment region is calculated as $l_{ave\text{-}pred} = 0.75l_c$, where l_c is determined using Eq. 7.4.

In determining the location of cracks, the bending moment along the length of the beam due to the applied load is first evaluated. Regions in which the bending moment has exceeded the cracking moment are then established. Cracks are introduced in these regions such that the spacing of adjacent cracks is equal to either S_o or $0.75l_c$, depending on whether the region is in a varying or constant moment region. A schematic diagram showing the locations of cracks determined using this procedure is shown in Fig. 8.6.

8.4.2 Curvature along the length of the beam

After cracks are located, the procedures described in Sections 8.2 and 8.3 are used for curvature calculation. Note that curvature values at sections within the uncracked region are also calculated using Eq. 8.1, assuming that the plane sections remain plane while bending.

As a typical example, curvature values are calculated using the procedure described above for Beam Number B-H-13 tested by Al-Shaikh and Al-Zaid (1993). The calculated curvatures are plotted along the length of the beam and are presented in Fig. 8.7.

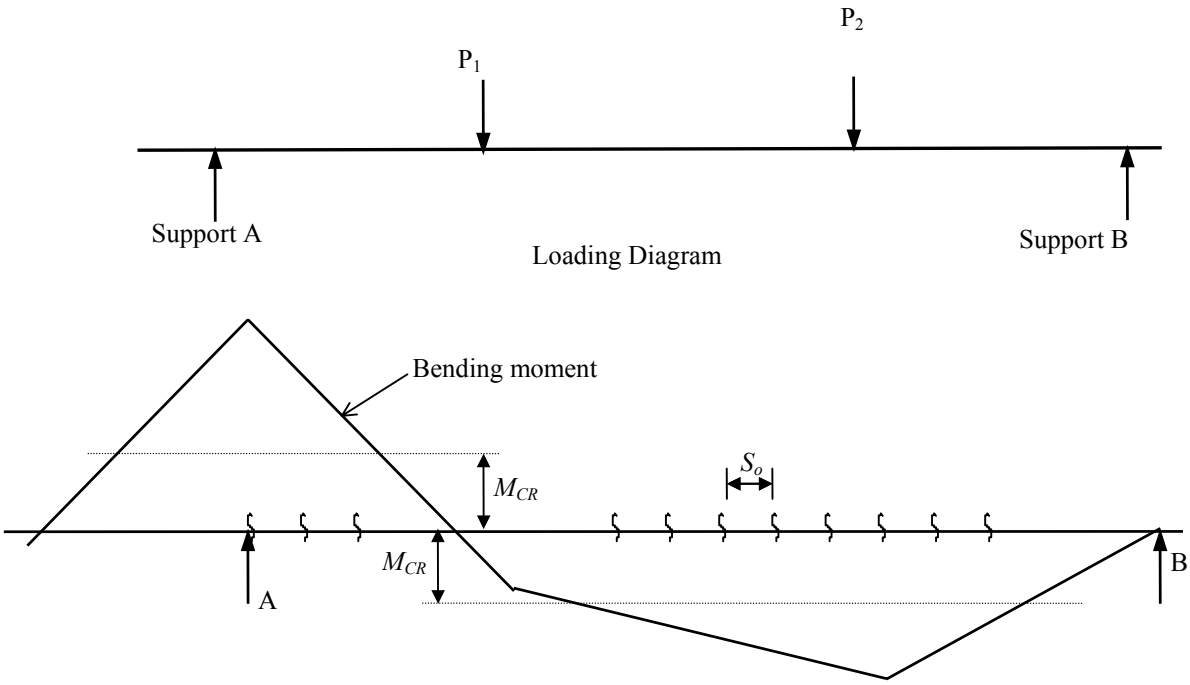

(a) Varying moment regions in a continuous beam (all crack spacings =S_o)

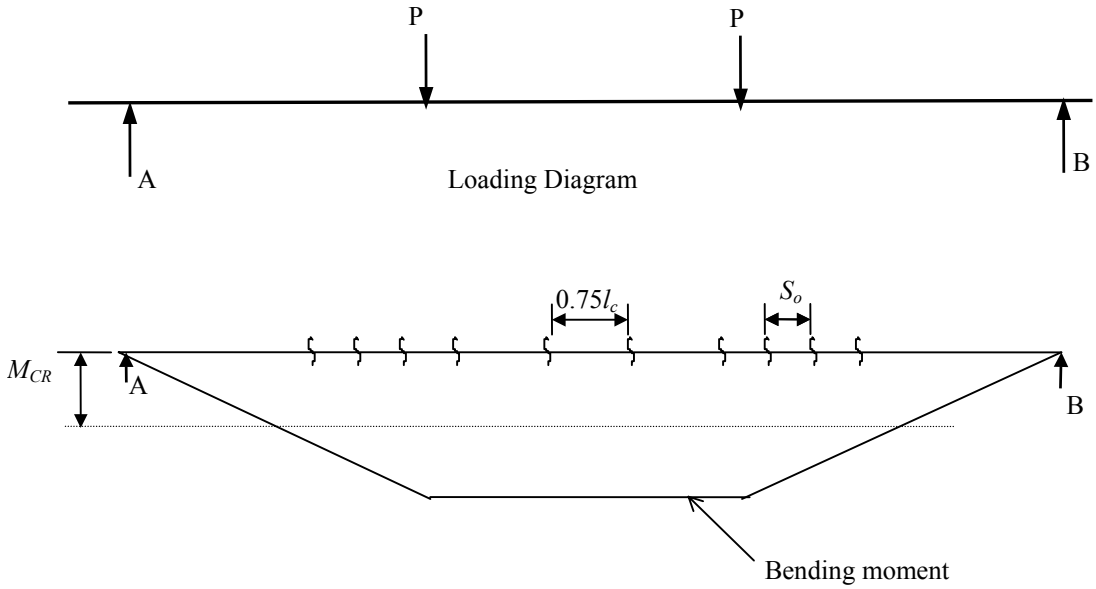

(b) Constant and varying moment regions in a simply supported beam

(crack spacings: constant moment region = $0.75l_c$; varying moment region = S_o)

Fig. 8.6 Locations of flexural cracks used in deflection calculation

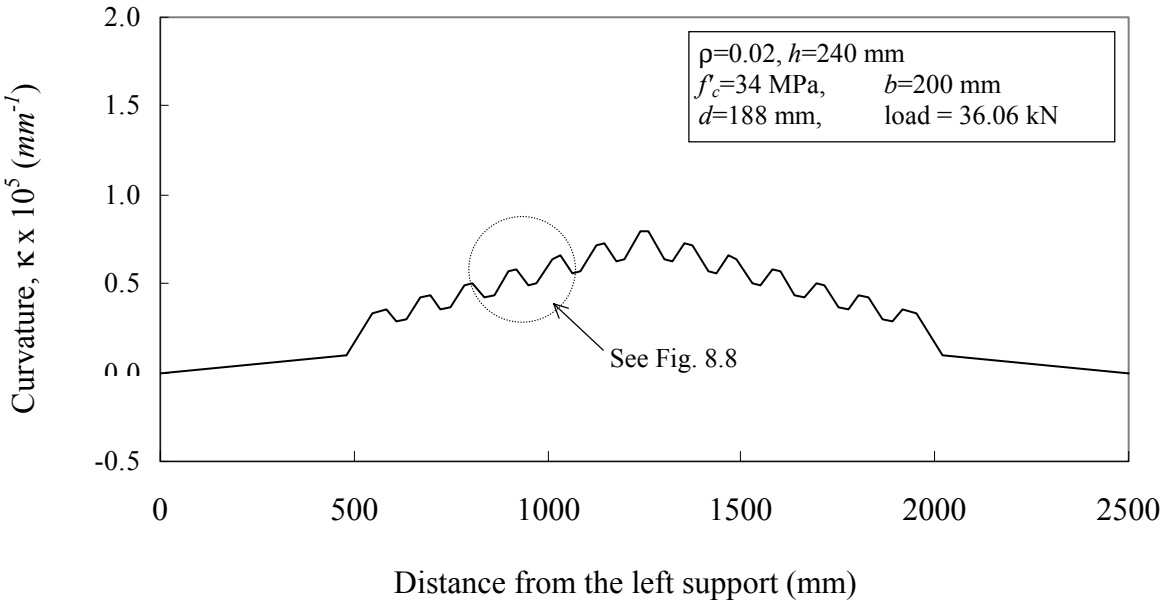

Fig. 8.7 Variation of curvature along the length of a typical beam (Beam No. B-H-13 tested by Al-Shaikh and Al-Zaid (1993); simply supported beam under central point load).

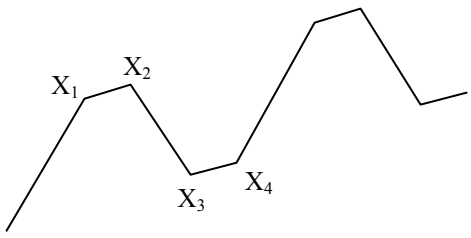

Fig. 8.8 Enlarged portion of Fig. 8.7

8.4.3 Calculation of the Deflection

After curvature values at various sections along the length of a particular span are evaluated, the deflection δ is calculated as

$$\delta = \int_{A}^{C} \kappa x dx \qquad (8.4)$$

where κ is the curvature at a section a distance x away from the point C where the deflection is calculated. In a simply supported beam subjected to symmetrical loading, the point C is taken at the mid-span. In a continuous beam, the maximum deflection within a span is determined by calculating the deflection at various points until the calculated value reaches the maximum.

The integration given in Eq. 8.4 is carried out numerically. Each segment of the beam that has a linear variation of κ (such as the segments X_1X_2, X_2X_3, X_3X_4 etc. in Fig. 8.8) is divided in to 50 equal divisions of Δx. The values of κ and x at the centre of the each division are determined, and the integration given in Eq. 8.4 is computed as

$$\delta = \sum \kappa x \Delta x \qquad (8.5)$$

8.4.4 Computer program to calculate deflection

As the calculation procedure described above requires a considerable amount of repetitions, a computer program written in BASIC language (program name: *DEFLECT.BAS*) is used for the evaluation of deflections. Source program of *DEFLECT.BAS* is given in *Appendix E20* to *E32*. The structure of this program is outlined below.

The program needs the input of beam cross sectional properties first. The following types of cross sectional shapes are acceptable.

(i) Rectangular sections
(ii) T-sections
(iii) Box sections

The deflection is calculated for a single span at a time. For this calculation, the program needs the input of support condition of the particular span, which should be selected from the following types.

(i) Simply supported span
(ii) End span of a continuous beam
(iii) Internal span of a continuous beam

Note that for continuous spans, the ratio(s) of the support moment(s) to the maximum span moment need to be input (See Fig. 8.9). These values represent the loading and span lengths of the adjoining spans. The program then needs the input of the span length and the loading for deflection calculation. The following three types of loading are acceptable.

(i) Uniform loading
(ii) Single point load at mid span
(iii) Two point loads at nominated distances

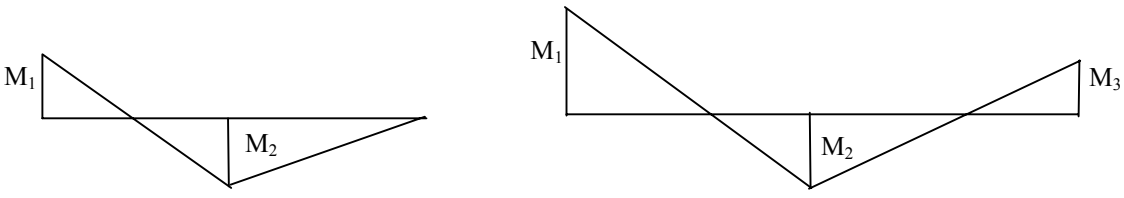

End span of a continuous beam
(Input data: M_1/M_2)

Internal span of a continuous beam
(Input data: M_1/M_2 and M_3/M_2)

Fig. 8.9 Bending moment ratios required for deflection calculation in continuous beams

Once the above data for a particular span are input, they can be stored in a computer data file for future use. The program then calculates the maximum deflection within the span, either for a single load level or for a series of load levels. The step by step procedure used for calculating the deflection is as follows.

(*a*) determine the bending moment within the span for the particular load level and find the locations of the flexural cracks as described in Section 8.4.1;

(*b*) calculate the concrete strain ε_c and the steel strain ε_s at all cracked sections using the procedure described in Chapter 4 (Section 4.6.1);

(*c*) calculate the curvature at all cracked sections using Eq. 8.1;

(*d*) determine the position of the zero-slip section and the associated peak bond stresses for each of the segments between adjacent cracks, using the procedure described in Section 4.7.2. Then calculate the steel stress f_{s1} at the zero-slip section using Eq. 8.3;

(*e*) calculate the curvature at the zero slip section between each pair of adjacent cracks using Eqs. 8.2. Use the tri-linear approximation shown in Fig. 8.4 to determine the curvature along the length of the cracked region;

(*f*) determine the maximum deflection δ using Eq. 8.5. (Note that for continuous beams, the maximum deflection is determined by calculating the deflections at various points, until the calculated value reaches the maximum).

While the computation is in progress, the program displays the following calculated values on the computer screen:

(i) curvature at each cracked section

(ii) peak bond stress between each pair of adjacent cracks

(iii) curvature at zero slip section between each pair of adjacent cracks

(iv) maximum deflection and the location where it occurs.

8.5 Comparison With Experimental Results

To verify the accuracy of the procedure described for determining the curvature between adjacent cracks, the short-term deflections are calculated for 37 flexural members tested by Yu & Winter (1960), Washa & Fluck (1952), Swamy & Anand (1974), Dilger & Abele (1974), Al-Shaik & Al-Zaid (1991), Mathey & Watstein (1960) and Stewart (1997). These flexural members comprise of the following types:

Simply supported members:

(i) one way solid slabs (uniform load)
(ii) rectangular beams (uniform, two-point and central point load)
(iii) T- beams (uniform load)
(iv) Box beams (two-point load)

Two-span continuous members:

(i) Box beams (two-point load)

Out of the 37 members included in this comparison, load deflection relationships are available for 16 members at various load levels. For these members, calculated deflections are plotted against the applied load and shown in Figs. 8.10 and 8.11, together with the corresponding measured values. For the rest of the members where only one deflection measurement is available, the measured deflections are plotted against calculated values in Fig. 8.12.

Inspection of Figs. 8.10 and 8.11 reveal that the computed deflections are in good agreement with measured values for all beams. Comparison shown in Fig. 8.12, which contains 21 measurements, shows that all the measured values fall within 20% of the calculated deflections. These figures indicate that the proposed method of computing the curvature in cracked beams and one-way slabs is acceptable.

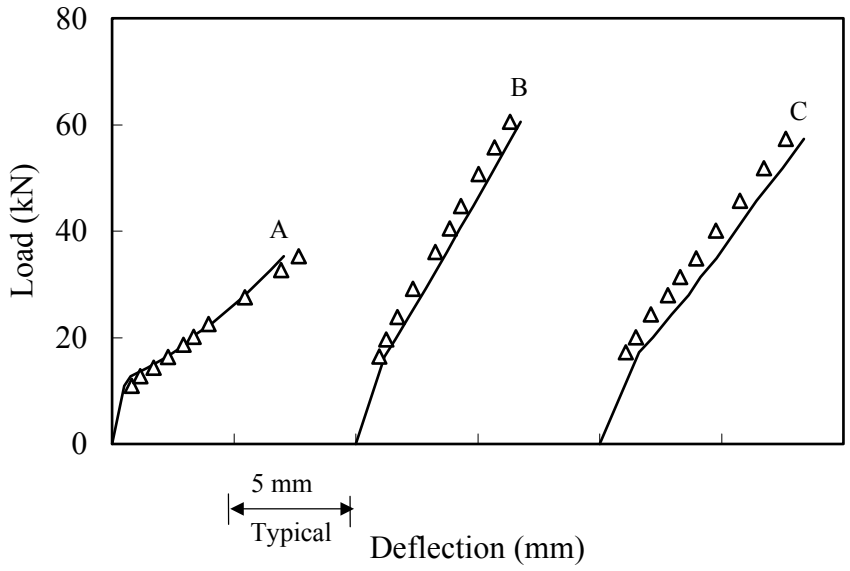

A: Beam No: BL-11
B: Beam No. BN-12
C: Beam No. BH-13

data from tests by Al-Shaik & Al-Zaid (1991) (simply supported rectangular beams with central point loads)

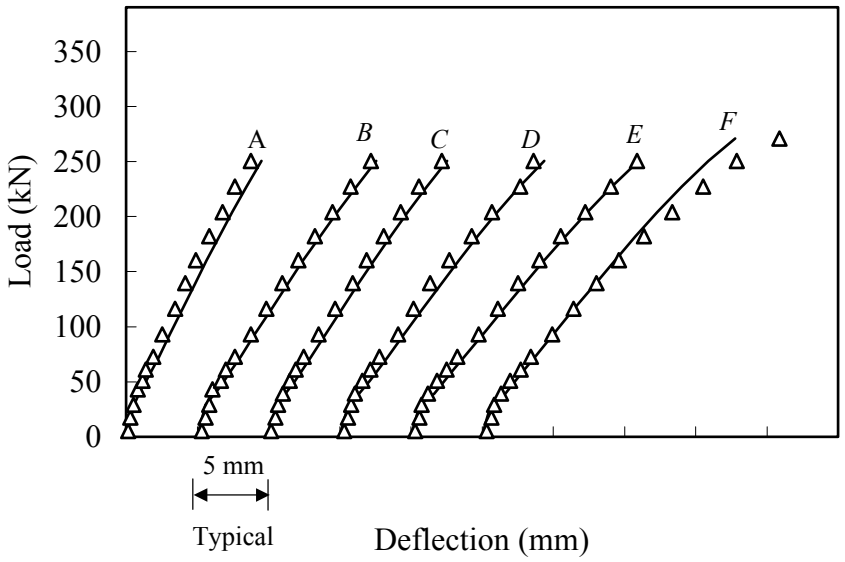

A: Beam No: I-22/23
B: Beam No. II-7/12
C: Beam No. III-8/13
D: Beam No. IV-20/21
E: Beam No. V-17/19
F: Beam No. VI-9/18

data from tests by Mathey & Watstein (1960) (simply supported rectangular beams with two-point loading)

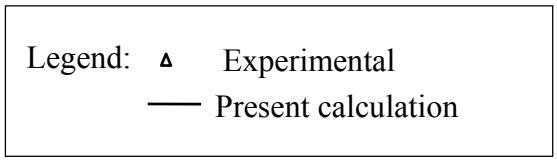

Fig. 8.10 Comparison of calculated and measured deflections

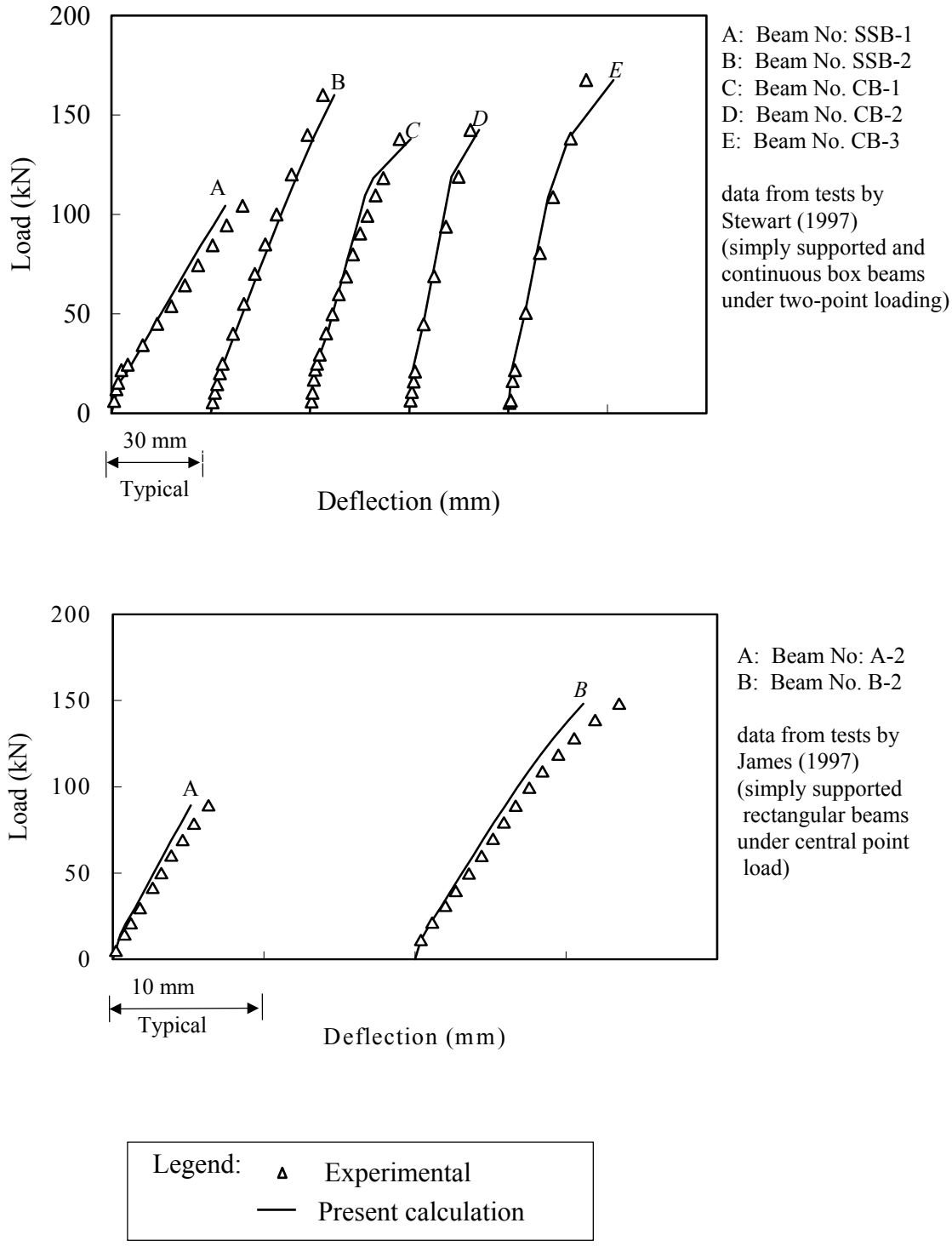

Fig. 8.11 Comparison of calculated and measured deflections

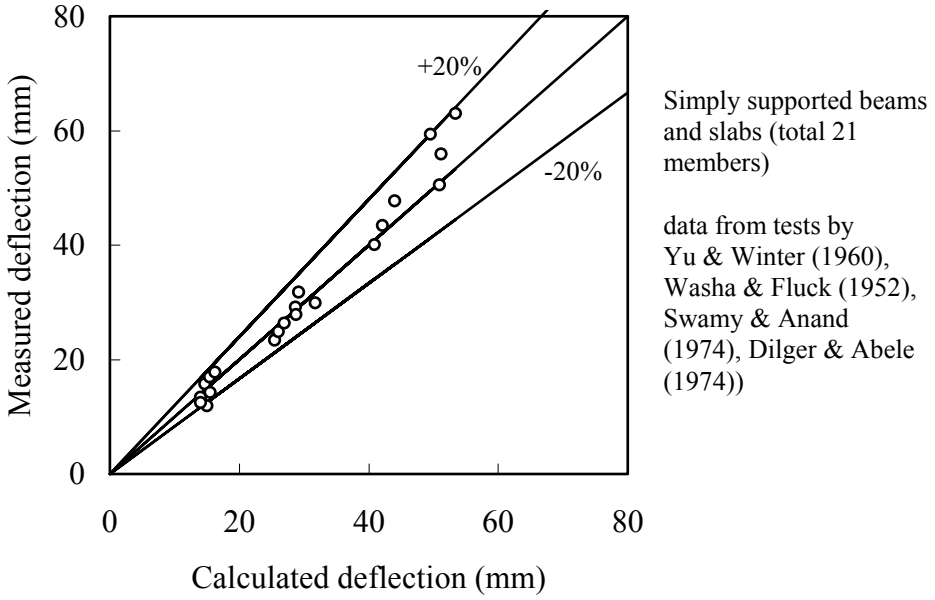

Fig. 8.12 Comparison of calculated and measured deflections

8.6 Summary

In this Chapter, a new method of incorporating the tension stiffening effect in deflection calculations is presented. The deflection is determined using the curvature values calculated at a large number of sections along the length of the beam. The curvature values at intermediate sections between adjacent cracks are evaluated using an empirical formula developed in this Chapter. For the calculation of deflections, the crack locations are determined by using the prediction formulas developed in Chapter 4 and Chapter 7.

After the curvature along the length of the beam is evaluated, the resulting maximum deflection within the span is determined by numerical integration. A computer program written in BASIC language is used for the calculations.

Using the proposed method of computing the curvature, short-term deflections are calculated for 37 flexural members tested by others. These members include beams and one-way slabs (both simply supported and continuous) with rectangular, T-shaped and box-shaped cross sections subjected to uniform loading, single point loading and two point loadings. A comparison of the calculated and measured deflections indicates that the new method of incorporating the tension stiffening effect in deflection calculations is acceptable.

CHAPTER 9

CONCLUSIONS

9.1 Outcomes of the Research

Spacing and width of cracks in reinforced concrete members were determined using the calculated concrete stress distributions near flexural cracks. To calculate the stresses, a free body concrete block bounded by top and bottom faces and two transverse sections of the member was isolated and analysed using the finite element method. The analysis was carried out using a standard finite element software package incorporating two-dimensional rectangular plane stress elements. Two types of concrete blocks were analysed. They are: (*i*) concrete block adjacent to the first flexural crack, and (*ii*) concrete block between successive cracks. The concrete block between successive cracks was analysed for various crack spacings under different load levels, to investigate their effects on the maximum tensile stress within the concrete block. Results of the analysis yield the following outcomes.

9.1.1 Primary cracks

The formation of the first crack affects the concrete and steel stresses for a certain distance, S_o, on either side of the crack. This distance is governed by bond characteristics of reinforcement and the increase in steel stress due to the formation of the crack. The concrete stress at the tension face of the member increases gradually from zero at the crack to the maximum at the end of the distance S_o. Consequently, the spacing of *primary cracks* is predicted as follows:

1. regular spacing S_o in a varying moment region, and
2. any value between S_o and $2S_o$ in a constant moment region.

An empirical formula was presented in Section 5.4 to calculate the value of S_o for a given flexural member.

It was also shown that the formation of primary cracks in a constant moment region will be completed within a short load increment whereas in a varying moment region it continues for the full loading stage.

9.1.2 Secondary cracks

The results showed that the maximum concrete tensile stress between successive cracks in a constant moment region occurs at the mid section between the cracks, while in a varying moment region its location is closer to the crack having the smaller moment. The magnitude of this maximum stress increases with the crack spacing as well as the load level on the beam. When the maximum concrete stress between adjacent cracks reaches the flexural strength of concrete, a *secondary crack* develops between the two cracks.

9.1.3 Crack spacing and crack width in constant moment region

Crack spacing that produces a maximum tensile stress equal to the flexural strength of concrete is taken as the maximum possible crack spacing l_c for the particular loading. The minimum crack spacing for the given load was found to be half of the maximum spacing ($0.5l_c$). Consequently, due to the random occurrences of primary cracks, the measured average crack spacing in a member will fall between the calculated values of two extremes l_c and $0.5l_c$. The theoretical average crack spacing at this load level is taken as $0.75l_c$. The resulting maximum crack width is determined as the relative difference in extensions of steel and surrounding concrete calculated for the maximum crack spacing l_c. Validity of this procedure was verified by comparing the calculated and measured values of average crack spacing and maximum crack widths for 70 flexural members tested by others.

9.1.4 Average crack spacing in varying moment region

It was shown that the formation of secondary cracks is more frequent in constant moment regions because of the possibility of having larger primary crack spacings closer to $2S_o$. This will result in a reduction of the average crack spacing with the increase of the applied load. However, in varying moment regions, the formation of secondary cracks is very rare because all the primary cracks are formed at a smaller spacing equal to S_o. Another reason for this rare formation of secondary cracks is that high steel stresses occur within a small length of the beam (near the mid span), compared to a constant moment region. As a result, the average crack spacing in a varying moment region remains almost constant at S_o during the full loading stage. It was also shown that, by comparing with experimental results, this constant spacing of cracks in a varying moment region has no correlations to the stirrup spacing.

9.1.5 Height of secondary cracks in transverse direction

The analysis showed that the height of secondary cracks in a constant moment region is less than the height of adjacent primary cracks for beams with effective depth larger than 300 mm. This difference increases with the beam height. As concluded in Section 9.1.4, secondary cracks do not exist in varying moment regions.

9.1.6 Factors influencing spacing and width of cracks

An investigation in to the effects of various variables on the spacing and width of cracks revealed the following:

1. An increase in the width of the member or the concrete cover increases both crack spacing and crack width if other variables are kept unchanged.
2. For shallow members with an effective depth less than 300 mm, the spacing and width of cracks increases with the effective depth.
3. Concrete strength has no appreciable effect on the crack spacing and crack width, if other variables remain unchanged.

4. An increase in the number of bars, by reducing the bar diameter to have the same reinforcement ratio, will reduce both spacing and width of cracks.
5. The steel stress at the cracked section will reduce the crack spacing while it increases the crack width.

Based on the results of a parametric study, simplified formulas were developed in Section 7.5 for the prediction of average crack spacings and maximum crack width. A comparison of predicted crack spacings and crack widths for the same 70 flexural members mentioned in Section 9.1.3 and the measured values reveals that the proposed formulas perform adequately. In particular, the predictions of these formulas have almost the same accuracy as the results of the finite element analysis.

9.1.7 Tension stiffening and deflection

A new method of incorporating the tension stiffening effect in deflection calculations was developed in Chapter 8. In this method, the curvature values at sections between adjacent cracks are calculated using an empirical formula. Development of this formula is based on the curvature values calculated using the concrete and steel strains at various sections between successive cracks, for a number of beams. Using the curvature values evaluated by the proposed formula, short-term deflections were determined for a large number of flexural members and the results were compared with those measured by other investigators. This comparison indicated that the present method of incorporating the tension stiffening effect in deflection calculations is acceptable.

9.2 Recommendations for Future Research

1. Analytical results of crack spacings and crack widths are greatly influenced by the assumed bond stress distribution and bond stress-bond slip relationship. As pointed out in Section 3.3.3, constitutive relationships proposed by different investigators vary considerably. Further research in to the measurement of bond stress and bond slip is proposed.

2. It was shown in Section 7.4.5 that the crack width increases with concrete cover. In spite of this, provision of a large cover is considered to be the most practical means of protecting the reinforcement against corrosion. Further research in to the effect of varying concrete cover on the crack width is proposed.

3. The analytical method presented in this thesis is based on the forces applied on a concrete section calculated using the conditions of equilibrium. Therefore, this method can be extended to include partially prestressed beams by incorporating the axial force due to prestress in the equilibrium equations.

4. The proposed analytical procedure can also be extended to determine the increase in the crack width with time by incorporating the creep and shrinkage effects in the calculation of concrete and steel strains.

5. The empirical method of calculating the curvature between adjacent cracks presented in this thesis may be used in a parametric study to develop a relationship for the average curvature in terms of the maximum bending moment within the span. This relationship may then be used to determine the deflections in two-way slabs.

REFERENCES

ACI Committee 224 (1972), *Control of Cracking in Concrete Structures*, ACI Journal, Proceedings, Vol. 69, No. 12.

ACI Committee 318 (1989), *Building Code Requirements for Reinforced Concrete (ACI 318-95*), American Concrete Institute.

ACI Committee 435 (1973), *Deflection of Continuous Concrete Beams*, American Concrete Institute, ACI Journal, pp 781-787.

ACI Committee 435 (1978), *Proposed Revisions By Committee 435 to ACI Building Code and Commentary - Provisions on Deflections*, ACI Journal, pp 229-238.

ACI-ASCE Committee 426 (1973), *Shear Strength of Reinforced Concrete Members*, Proceedings, American Society of Civil Engineers, Vol. 99, No. ST6, pp 1091-1187.

Al-Shaikh, A. H. and Al-Zaid, R. Z. (1993), *Effect of Reinforcement Ratio on the Effective Moment of Inertia of Reinforced Concrete Beams*, ACI Structural Journal, Vol. 90, No. 2, pp 144-149.

Al-Zaid, R. Z., Al-Shaikh, A. H. and Abu-Hussein, M. M. (1991), *Effect of Loading Type on the Effective Moment of Inertia of Reinforced Concrete Beams*, ACI Structural Journal, Vol. 88, No. 2, pp 184-190.

Ayoub, A. and Filippou, F. C. (1999), *Mixed Formulation of Bond-Slip Problems Under Cyclic Loads*, Journal of Structural Engineering, American Society of Civil Engineers, Vol. 125, No. 6, pp 661 - 671.

Base G. D. (1978), *Short Course on Design of Concrete Structures for Serviceability*, Lecture Notes, Concrete Institute of Australia, Sydney.

Base G. D., Read J. B., Beeby A. W. and Taylor H. P. J. (1966), *An Investigation of the Crack Control Characteristics of Various Types of Bar in Reinforced Concrete Beams*, Research Report No 18, Part 1, Cement and Concrete Association, London, 44 pp.

Bazant, Z. P. (1972), *Prediction of Concrete Creep Effects Using Age-adjusted Effective Modulus Method*, ACI Journal, Proceedings, Vol. 69, No. 4, pp 212 – 217.

Bazant, Z. P. and Oh, B. H. (1983), *Spacing of Cracks in Reinforced Concrete*, Journal of the Structural Engineering, American Society of Civil Engineers, Vol. 109, No. 9, pp 2066-2085.

Bazant, Z. P. and Oh, B. H. (1984), *Deformation of progressively Cracking reinforced Concrete Beams*, ACI Structural Journal, Vol. 81, No. 3, pp 268 - 278.

Beeby, A. W. (1970), *An Investigation of Cracking in Slabs Spanning One Way,* Cement and Concrete Association, Technical Report 42.433, London.

Beeby, A. W. (1971*a*), *Prediction and Control of Flexural Cracking in Reinforced Concrete Members*, Cracking, Deflection and Ultimate Load of Concrete Slab Systems, SP-20, American Concrete Institute.

Beeby, A. W. (1971*b*), *An Investigation of Cracking on the Side Faces of Beams*, Cement and Concrete Association, Technical Report 42.466, London.

Beeby, A. W. (1979), *The Prediction of Crack Widths in Hardened Concrete,* The structural Engineer, Vol. 57A, No. 1, pp 9-17.

Behfarnia, K., Barzegar, F. and Gilbert, R. I. (1995), *Three Dimensional Finite Element Model for Reinforced and Prestressed Concrete Structures*, Proceedings of the 14th Australasian Conference on the Mechanics of Structures and Materials", Hobart, Australia, pp 278 - 283.

Branson, D. E. (1963), *Instantaneous and Time-Dependent Deflections of Simple and Continuous Reinforced Concrete Beams*, HPR Report No. 7, Part 1, Alabama Highway Department, Bureau of Public Roads, pp 1-78.

Branson, D. E. (1968), *Design Procedures for Computing Deflections*, ACI Journal, Proceedings, Vol. 65, No.9, pp 730-742.

Branson, D. E. (1971), *Compression Steel Effect on Long-Time Deflections*, ACI Journal, Vol. 68, No. 8, pp 555-560.

Broms, B. B. (1965), *Crack Width and Crack Spacing in Reinforced Concrete Members*, ACI Journal, Proceedings, Vol. 62, No. 10, pp 1237-1255.

Broms, B. B. (1965*a*), *Stress Distribution in Reinforced Concrete Members with Tension Cracks*, ACI Journal, Proceedings, Vol. 62, No. 9, pp 1095-1108.

Broms, B. B. (1965*b*), *Technique for Investigation of Internal Cracks in Reinforced Concrete Members*, ACI Journal, Proceedings, Vol. 62, No. 1, January 1965, pp 35-44.

Broms, B. B. and Lutz L. A. (1965), *Effects of Arrangement of Reinforcement on Crack Width and Spacing of Reinforced Concrete Members*, ACI Journal, Proceedings, Vol. 62, No. 11, pp 1395-1410.

British Standard Institute (1997), *Structural Use of Concrete: Code of Practice for Design and Construction, BS 8110: Part 1*, British Standard Institute.

British Standard Institute (1985), *Structural Use of Concrete: Code of Practice for Special Circumstances, BS 8110: Part 2*, British Standard Institute.

Carreira, D. J. and Chu, K. (1986*a*), *Stress-Strain Relationship for Reinforced Concrete in Tension*, ACI Journal, Proceedings, Vol. 83, No. 1, pp 21 -28.

Carreira, D. J. and Chu, K. (1986*b*), *The Moment-Curvature Relationship of Reinforced Concrete members*, ACI Journal, Proceedings, Vol. 83, No. 2, pp 191 - 198.

Chi, M. and Kirstein, A. F. (1958), *Flexural Cracks in Reinforced Concrete Beams*, ACI Journal, Proceedings, Vol. 54, No. 10, pp 865-878.

Chowdhury, S.H. and Loo, Y. C. (2001), *A New Formula for Prediction of Crack Widths in Reinforced and Partially Prestressed Concrete Beams,* Advances in Structural Engineering, Vol. 4, No. 2, pp 101-109.

Clark, A. P. (1949), *Bond of Concrete and Reinforcing Bars*, ACI Journal, Proceedings, Vol. 46, No. 3, pp 161-184.

Clark, A. P. (1956), *Cracking in Reinforced Concrete Flexural Members*, ACI Journal, Proceedings, Vol. 52, No. 8, pp 851-862.

Clough, R. W. and Felippa, C. A. (1968), *A Refined Quadrilateral Element for Analysis of Plate Bending*, Proceedings of the Second Conference on Matrix Methods in Structural Mechanics, Wright-Patterson Air Force Base, Ohio, AFFSL-TR-68-150.

Comite Euro-International du Beton (CEB) (1993), *CEB-FIP Model Code 1990:CEB Bulletin d'Information 213-214*, Thomas Telford Service Ltd., London, England.

Cook, R. D., Malkus, D. S. and Plesha, M. E. (1989), *Concepts and Applications of Finite Element Analysis,* Third Edition, J. Willey.

Dilger, W.H. and Abele, G. (1974), *Initial and Time Dependent Shear Deflection of Reinforced Concrete T-Beams*, Proceedings, Symposium on Deflections of Structures, American Concrete Institute, pp 487-513.

Dilger, W. H. and Ghali, A (1976), *Time-dependent Stress in Continuous Precast Bridges,* Journal of Structural Division, American Society of Civil Engineers, Vol. 102, No. 1, pp 239 – 252.

Edwards, A. D. and Yannopoulos, P. J. (1979), *Local Bond-Stress to Slip Relationship for Hot Rolled Deformed Bars and Mild Steel Plain Bars*, ACI Journal, Proceedings, Vol. 76, No. 3, pp 405-420.

Eligehausen, R., Bertero, V. V. and Popov, E. P. (1983), *Local Bond Stress-slip Relationships of Deformed Bars Under Generalised Excitation: Tests and Analytical Model,* Report No. UCB/EERC-83, Earthquake Engineering Research Centre, University of California, Berkeley, California.

Esfahani, M. R. and Rangan, B. V. (1998), *Local Bond Strength of Reinforcing Bars in Normal Strength and High-Strength Concrete (HSC),* ACI Structural Journal, Vol. 95, No. 2, pp 96 - 106.

Evans R. H. and Kong F. K. (1967), *Shear Design and British Code CP 114*, The Structural Engineer, Vol. 45, No. 4, pp 153-158.

Fantilli, A. P., Ferretti, D., Iori, I. and Vallini, P. (1998), *Flexural Deformability of Reinforced Concrete Beams*, Journal of Structural Engineering, American Society of Civil Engineers, Vol. 124, No. 9, pp 1041 – 1049.

Favre, R. and Charif, H. (1994), *Basic Model and Simplified Calculations of Deformations According to the CEB-FIP Model Code 1990*, ACI Structural Journal, Vol. 91, No. 2, pp 169 – 177.

Frosch R. (1999), *Another Look at Cracking and Crack Control in Reinforced Concrete*, ACI Structural Journal, Vol. 96, No. 3, pp 437 – 442.

Gambarova, P. G. and Karakok, C. (1982), *Shear-confinement Interaction at the Bar-to-concrete Interface,* Bond in Concrete, P. Bartos, ed., Applied Science Publishers, London, England, pp 82 – 98.

Gambarova, P. G., Rosati, G. P. and Zasso, B, (1989), *Steel-to-concrete Bond After Concrete Splitting: Test Results*, Materials and Structures, Vol 22, No. 127, pp 35 – 47.

Gergely, P. and Lutz, L. A. (1968), *Maximum Crack Width in Reinforced Concrete Flexural Members*, Causes, Mechanism, and Control of Cracking Concrete, SP-20, American Concrete Institute, pp 87-117.

Ghali, A. and Azarnejad, A. (1999), *Deflection Prediction of Members of Any Concrete Strength*, ACI Structural Journal, Vol. 96, No. 5, pp 807 - 816.

Ghali, A. and Favre, R. (1986), *Concrete Structures: Stress and Deformation, J. W. Arrowsmith Ltd., Bristol, United Kingdom.*

Gilbert, R. I. and Warner, R. F. (1978), *Tension Stiffening in Reinforced Concrete Slabs*, Journal of Structural Engineering, American Society of Civil Engineers, Vol. 104, No. 12, pp 1885-1900.

Gilbert, R. I. (1998), *Deflection Calculation and Control for Reinforced Concrete Structures*, Australasian Structural Engineering Conference, Auckland, pp 269-274.

Gilbert, R. I. (1998), *Serviceability Considerations and Requirements for High Performance Reinforced Concrete Slabs*, Proceedings, Int. Conference on High Performance High Strength Concrete, Curtain University of Technology, Perth, Australia.

Gilbert, R. I. (1999), *Flexural Crack Control for Concrete Beams and Slabs: An Evaluation of Design Procedures*, Proceedings of the 16th Australasian Conference on the Mechanics of Structures and Materials, Sydney, Australia, pp175 – 180.

Giuriani, E., Plizzari, G. and Schumm, C. (1991), *Role of Stirrups and residual Tensile Strength of Cracked Concrete on Bond*, Journal of the Structural Engineering, American Society of Civil Engineers, Vol. 117, No. 1, pp 1-18.

Giuriani, E. and Plizzari, G. A. (1998), *Interrelation of Splitting and Flexural Cracks in RC Beams*, Journal of the Structural Engineering, American Society of Civil Engineers, Vol. 124, No. 9, pp 1032 - 1040.

Gravina, R. J. and Warner, R. F. (1999), *Modelling of High-Moment Plastification Regions in Concrete Structures*, Proceedings of the 16th Australasian Conference on the Mechanics of Structures and Materials, Sydney, Australia, pp 103 – 108.

Goto, Y. (1971), *Cracks Formed in Concrete Around Deformed Tension Bars*, ACI Structural Journal, Vol. 68, No. 4, pp 244-251.

Grossman, J. S. (1981), *Simplified Computations for Effective Moment of Inertia I_e and Minimum Thickness to Avoid Deflection Computations*, Proceedings, ACI Journal, Vol. 78, No. 6, pp 423-439.

Hand, F. R., Pecknold, D. A. and Schnobrich, W. C. (1973), *Nonlinear Layered Analysis of RC Plates and Shells,* Journal of the Structural Division, American Society of Civil Engineers, Vol. 99, No. ST7, Proc. Paper 98060, pp 1491 –1505.

Hognestad, E. (1951) *A study of Combined Bending and Axial Load in Reinforced Concrete Members*, University of Illinois, Eng Expt Station Bull No 399.

Husain, S. I. and Ferguson, P. M. (1968), *Flexural Crack Width at the Bars in Reinforced Concrete Beams*, Research Report No 102-1F, Centre for Highway Research, Univ. of Texas, Austin.

Hwang, S., Leu, Y. and Hwang, H. (1996), *Tensile Bond Strengths of Deformed Bars of High-Strength Concrete*, ACI Structural Journal, Vol. 93, No. 1, pp 11 - 20.

Jiang, D. H., Shah, S. P. and Andonian, A. T. (1984), *Study of the Transfer of Tensile Forces by Bond*, ACI Structural Journal, Vol. 81, No 3, pp 251-259.

Kaar, H. P. (1968), *An Approach to the Control of Cracking in Reinforced Concrete*, Causes, Mechanism, and Control of Cracking Concrete, SP-20, American Concrete Institute, pp 141-157.

Kaar, P. H. and Muttock, A. H. (1963), *High Strength Bars as Concrete Reinforcement-Part 4 Control of Cracking*, Journal of Portland Cement Association Research and Development Laboratories, Vol. 7, No 1, pp 42-53.

Kaklauskas, G. and Ghaboussi, J. (2001), *Stress-Strain Relations for Cracked Tensile Concrete from RC Beam Tests*, Journal of Structural Engineering, American Society of Civil Engineers, Vol. 127, No. 1, pp 64 - 73.

Kankam, C. K. (1997), *Relationship of Bond Stress, Steel Stress, and Slip in Reinforced Concrete*, Journal of Structural Engineering, American Society of Civil Engineers, Vol. 123, No. 1, pp 79 – 85.

Kong F. K. and Evans, R. H. (1987), *Reinforced and Prestressed Concrete*, Third Edition, Chapman and Hall.

Lahnert, B. J., Houde, J. and Gerstle, K. H. (1986), *Direct Measurement of Slip Between Steel and Concrete*, ACI Structural Journal, Proceedings, Vol. 83, No. 86, pp 974-982.

Lan, Z. and Ding, D. (1992), *Crack Width in Reinforced Concrete Members*, International Journal of Structures, Vol. 12, No. 2, pp 137-163.

Leonhardt, F. (1977) *Crack Control in Concrete Structures*, IABSE Surveys, S-4/77, pp 1-26.

Limkatanyu, S. and Spacone, E. (2002), *Reinforced Concrete Frame Element with Bond Interfaces. I: Displacement-Based, Force-Based, and Mixed Formulations*, Journal of the American Concrete Institute, proceedings Vol. 128, No. 3, pp 346 – 355.

Lin, C. and Scordelis, A. C. (1975), *Nonlinear Analysis of RC Shells of General Form*, Journal of the American Concrete Institute, Proceedings, Vol. 101, No. ST3, pp 523 – 538.

Loo, Yew-Chaye, (1990), *Reinforced Concrete Analysis and Design with Emphasis on the Application of AS3600 –1988*, University of Wollongong Press, Wollongong, Australia

Lutz, L. A. and Gergely, P. (1967), *Mechanics of Bond and Slip of Deformed Bars in Concrete*, ACI Structural Journal, Proceedings, Vol. 64, No. 11, pp 711-721.

Lutz, L. A. (1970), *Analysis of Stresses in Concrete Near Reinforcing Bar Due to Bond and Transverse Cracking*, ACI Structural Journal, Vol. 67, No. 10, pp 778-787.

Mains R. M. (1951), *Measurement of the Distribution of Tensile and Bond Stresses Along Reinforcing Bars*, ACI Journal, Proceedings, Vol. 48, No. 3, pp 225-252.

Makhlouf, H. M. and Malhas, F. A. (1996), *The Effect of Thick Concrete Cover on the Maximum Flexural Crack Width Under Service Load*, ACI Structural Journal, Vol. 93, No. 3, pp 257-265.

Mathey, R. G. and Watstein, D. (1960), *Effect of Tensile Properties of Reinforcement on the Flexural Characteristics of Beams*, ACI Journal, Proceedings, Vol. 56 No. 12, pp 1253-1273.

Mirza, S. M. and Houde, J. (1979), *Study of Bond Stress-Slip Relationships in Reinforced Concrete, Symposium on Interaction between Concrete and Steel*, American Concrete Institute, Proceedings, Vol. 76, No. 1, pp19-46.

Monti, G., Filippou, C. F. and Spacone, E. (1997), *Finite Element for Anchored Bars Under Cyclic Load Reversal*, Journal of Structural Engineering, American Society of Civil Engineers, Vol. 123, No. 5, pp 614 - 623.

Nawy, E. G. (1968), *Crack Control in Reinforced Concrete Structures*, ACI Journal, Proceedings, Vol. 65, No. 10, pp 825-836.

Nie, J. and Cai, C. S. (2000), *Deflection of Cracked RC Beams Under Sustained Loading*, Journal of Structural Engineering, American Society of Civil Engineers, Vol. 126, No. 6, pp 708 - 716.

Nilson, A. H. (1972), *Internal Measurement of Bond Slip*, ACI Journal, Proceedings, Vol. 69, No. 7, pp 439-441.

Nilson, A. H. (1968), *Nonlinear Analysis of Reinforced Concrete by the Finite Element Method*, ACI Journal, Proceedings, Vol. 65, No. 9, pp 757-766.

Oh, B. H. and Kang, Y. (1987), *New Formulas for Maximum Crack Width and Crack Spacing in Reinforced Concrete Flexural Members*, ACI Structural Journal, Vol. 84, No. 2, pp 103-112.

Ouyang C., Wollrab, E., Kulkarni, S. M. and Shah, S. P. (1997), *Prediction of Cracking Response of Reinforced Concrete Tensile Members*, Journal of Structural Engineering, American Society of Civil Engineers, Vol. 123, No. 1, pp 70 – 78.

Park, R. and Paulay, T. (1975), *Reinforced Concrete Structures,* John Wiley and Sons, New York.

Perry, S. E. and Thompson, J. N. (1966), *Bond Stress Distribution on Reinforcing Steel in Beams and Pullout Specimens*, ACI Journal, Proceedings, Vol. 63, No. 8, pp 865 – 874.

Polak, M. A. and Blackwell, K. G. (1998), *Modelling Tension in Reinforced Concrete Members Subjected to Bending and Axial Load*, Journal of Structural Engineering, American Society of Civil Engineers, Vol. 124, No. 9, pp 1018 – 1024.

Prakhya, G. K. V. and Morley, C. T. (1990), *Tension-Stiffening and Moment-Curvature Relations of Reinforced Concrete Elements*, ACI Structural Journal, Vol. 87, No. 5, pp 597-605.

Raab, A. R. (1966), *A Discussion on 'Stress Distribution in Reinforced Concrete Members with Tension Cracks' - Discussion of the Paper by Bengt B. Broms'*, ACI Journal, Proceedings, Vol. 63, No. 3, p 1743.

Rangan, B. V. (1982), *Control of Beam Deflections by Allowable Span-Depth Ratios*, ACI Journal, Proceedings, Vol. 79, No. 5, pp 372-377.

Samra, R. S. (1997), *Time-Dependent Deflections of Reinforced Concrete Beams Revisited*, Journal of Structural Engineering, American Society of Civil Engineers, Vol. 123, No. 6, pp 823 - 830.

Scanlon, A. and Choi, B. (1999), *Evaluation of ACI 318 Minimum Thickness requirements for One-Way Slabs*, ACI Structural Journal, Vol. 96, No. 4, pp 616 – 622.

Soroushian, P. and Choi, K. (1989), *Local Bond of Deformed Bars with Different Diameters in Confined Concrete*, ACI Structural Journal, Vol. 86, No. 2, pp 217 - 222.

Soroushian, P. and Choi, K. (1991), *Analytical Evaluation of Straight Bar Anchorage Design in Exterior Joints*, ACI Structural Journal, Vol. 88, No. 2, pp 161 - 168.

Spacone, E. and Limkatanyu, S. (2000), *Responses of Reinforced Concrete members Including Bond-Slip effects*, ACI Structural Journal, Vol. 97, No. 6, pp 831 - 839.

Standards Australia (AS 3600) (2001), *Concrete Structures*, Standards Association of Australia, Sydney, Australia.

STAND6 (1993), *Finite Element Analysis System*, G+D Computing Pty Ltd, New South Wales, Australia.

Stewart, R. A. (1997), *Crack Widths and Cracking Characteristics of Simply Supported and Continuous Reinforced Concrete Box Beams*, B. Eng Thesis, School of Engineering, Griffith University, Gold Coast, Australia

Swamy, R. N. and Anand, K. L. (1974), *Influence of Steel Stress and Concrete Strength on the Deflection Characteristics of Reinforced and Prestressed Beams*, Proceedings, Symposium on Deflections of Structures, American Concrete Institute, pp 443-471.

Tassios, T. P. and Koronoes, E. G. (1984), *Local Bond-Slip Relationships by Means of the Moire Method*, ACI Journal, Proceedings, Vol. 81, No. 4, pp 27-35.

Tassios, T. P. and Yannopoulos, P. J. (1981), *Analytical Studies on Reinforced Concrete Members Under Cyclic Loading Based on Bond Stress-Slip Relationships*, ACI Journal, Proceedings, Vol. 78, No. 3, pp 206-216.

Taylor, H. P. J. (1974), *The Fundamental Behaviour of Reinforced Concrete Beams in Bending and Shear, Proceedings*, ACI-ASCE Shear Symposium, Ottawa, (ACI Special Publication SP42), American Concrete Institute, Detroit, pp 43-77.

Youssef, M. and Ghobarah, A. (1999), *Strength Deterioration Due to Bond Slip and Concrete Crushing in Modelling of Reinforced Concrete Members*, ACI Journal, Proceedings, Vol. 96, No. 6, pp 956 - 966.

Venkateswarlu, B. and Gesund, H. (1972), *Cracking and Bond Slip in Concrete Beams*, Journal of the Structural Division, Proceedings, American Society of Civil Engineers, Vol. 98, No. ST11, pp 2663-2885.

Wanchoo, M. K. and May, G. W. (1975), *Cracking Analysis of Reinforced Concrete Plates*, Journal of the Structural Division, American Society of Civil Engineers, Vol. 101, No. ST1, Proc. Paper 11059, pp 201 – 215.

Warner, R. F., Rangan B. V., Hall A. S. and Faulkes, K.A. (1998), *Concrete Structures*, Addison Wesley Longman Australia Pty. Ltd., South Melbourne, Australia.

Washa, G. W. and Fluck, P.G. (1952), *Effect of Compressive Reinforcement on the Plastic Flow of Reinforced Concrete Beams*, ACI Journal, Proceedings, Vol. 49, No. 8, pp 89-108.

Watstein, D. and Parsons, D. E. (1943), *Width and Spacing of Tensile Cracks in Axially Reinforced Concrete Cylinders*, Journal of Research, National Bureau of Standards, Vol. 31, No. RP1545, pp 1-24.

Watstein, D. and Mathey, R. G. (1959), *Width of Cracks in Concrete at the Surface of Reinforcing Steel Evaluated by Means of Tensile Bond Specimens*, ACI Journal, Proceedings, Vol. 56, No. 1, pp 47-56.

Watstein, D. and Seese, N. A. Jr. (1945), *Effect of Type of Bar on Width of Cracks in Reinforced Concrete Subjected to Tension*, ACI Journal, Proceedings, Vol. 41, No. 4, pp 293-304.

Yu, W. and Winter, G. (1960), *Instantaneous and Long-Time Deflections of Reinforced Concrete Beams Under Working Loads*, ACI Journal, Proceedings, Vol. 57, No. 1, pp 29-50.

Zienkiewicz, O. C. (1977), *The Finite Element Method*, Third Edition, McGraw-Hill.

Zuo, J. and Darwin, D. (2000), *Bond Slip of High Relative Rib Area Bars Under Cyclic Loading*, ACI Structural Journal, Vol. 97, No. 2, pp 331 - 334.

Appendix A

CALCULATED FORCES

ON CONCRETE SECTIONS

For typical members

```
Beam Name = rect


File name = rect.pro

Beam properties
---------------

Beam width b =               300
Effective depth d =          500
Overall heighth (h) =        600

Tensile Steel :Bar diameter   =            25
               Number of bars =            4
Concrete strength =          40
```

```
Beam Name = flange


File name = flange.pro

Beam properties
---------------

Top flange width =           800
Top flange depth =           250
Bottom flange width =        750
Bottom flange depth =        200
Web width (b) =              300
Overall height (h) =         600
Effective depth d =          500

Tensile Steel :Bar diameter   =            25
               Number of bars =            8
Comp. Steel :Bar diameter   =              20
             Number of bars =              3
             Depth to steel =              50
Concrete strength =          50
```

```
================================================================================
=====
```

```
File name = rect.301

------------------------------------------------
Beam Name = rect  (Rectangular section)

Solution Mode =  3   (Forces on transverse section for a given moment)

------------------------------------------------
 Mcr =  77 kNm
 Mu  =  364 kNm
------------------------------------------------
Input data:
Sectional properties: Read from data file
Bending moment at the section =  60  kNm
Stress in tensile steel =  9  MPa
Nodal forces on transverse section:

Node No       Force (N/mm)
-------       ------------
 275          -103
 264          -119
 253          -98
 242          -77
 231          -57
 220          -36
 209          -14
 198          -2
 187           5
 176           15
 165           24
 154           34
 143           37
 132           37
 121           43
 110           48
 99            35
 88            18
 77            19
 66            19
 55            20
 44            20
 33            21
 22            22
 11            11
-----------------------------------
Check equilibrium:
Sum of nodal forces = -65  (N/mm)
Force in steel bars/beam width =  64  (N/mm)
-----------------------------------
```

```
File name = flange.301

------------------------------------------------
Beam Name = flange  (Flanged section)

Solution Mode =  3   (Forces on transverse section for a given moment)

------------------------------------------------
 Mcr =  152 kNm
 Mu  =  751 kNm
------------------------------------------------
Input data:
Sectional properties: Read from data file
Bending moment at the section =  140  kNm
Stress in tensile steel =  10  MPa
Nodal forces on transverse section:

Node No       Force (N/mm)
-------       ------------
 275          -267
 264          -203
 253          -354
 242          -284
 231          -214
 220          -143
 209          -53
 198          -2
 187           13
 176           25
 165           47
 154           122
 143           131
 132           131
 121           147
 110           164
 99            119
 88            62
 77            64
 66            66
 55            67
 44            69
 33            71
 22            73
 11            37
-----------------------------------
Check equilibrium:
Sum of nodal forces = -101  (N/mm)
Force in steel bars/beam width =  99  (N/mm)
-----------------------------------
```

```
 File name = rect.302

------------------------------------------------
Beam Name = rect  (Rectangular section)

Solution Mode =  3   (Forces on transverse section for a given moment)

------------------------------------------------
 Mcr =  77 kNm
 Mu  =  364 kNm
------------------------------------------------
Input data:
Sectional properties: Read from data file
Bending moment at the section =  200  kNm
Stress in tensile steel =  226  MPa
Nodal forces on transverse section:

Node No       Force (N/mm)
-------       ------------
 275          -389
 264          -618
 253          -391
 242          -143
 231           57
-----------------------------------
Check equilibrium:
Sum of nodal forces = -1481  (N/mm)
Force in steel bars/beam width =  1479  (N/mm)
-----------------------------------
```

```
File name = flange.302

------------------------------------------------
Beam Name = flange  (Flanged section)

Solution Mode =  3   (Forces on transverse section for a given moment)

------------------------------------------------
 Mcr =  152 kNm
 Mu  =  751 kNm
------------------------------------------------
Input data:
Sectional properties: Read from data file
Bending moment at the section =  500  kNm
Stress in tensile steel =  277  MPa
Nodal forces on transverse section:

Node No       Force (N/mm)
-------       ------------
 275          -1122
 264          -1625
 253          -732
 242           18
-----------------------------------
Check equilibrium:
Sum of nodal forces = -3460  (N/mm)
Force in steel bars/beam width =  3461  (N/mm)
-----------------------------------
```

```
File name = rect.701

------------------------------------------------
Beam Name = rect  (Rectangular section)

Solution Mode =  7   (Forces on transverse section for a given steel
stress)

------------------------------------------------
 Fs1 =  12 MPa
 Fs2 =  80 MPa
------------------------------------------------
Input data:
Sectional properties: Read from data file
Stress in tensile steel =  200  MPa
----------------------------------
Output results:
Bending moment at the section =  227  kNm
Nodal forces on transverse section:

Node No       Force (N/mm)
-------       ------------
 275          -349
 264          -553
 253          -347
 242          -126
 231           65
----------------------------------
Check equilibrium:
Sum of nodal forces = -1309  (N/mm)
Force in steel bars/beam width =  1308  (N/mm)
----------------------------------
Elastic Moduli
_____________________
Row - 1    35653
Row - 2    36644
Row - 3    37965
Row - 4    39285
Row - 5    39973
----------------------------------
```

```
File name = flange.701

------------------------------------------------
Beam Name = flange  (Flanged section)

Solution Mode =  7   (Forces on transverse section for a given steel
stress)

------------------------------------------------
 Fs1 =  11 MPa
 Fs2 =  80 MPa
------------------------------------------------
Input data:
Sectional properties: Read from data file
Stress in tensile steel =  250  MPa
---------------------------------
Output results:
Bending moment at the section =  569  kNm
Nodal forces on transverse section:

Node No       Force (N/mm)
-------       ------------
 275          -1020
 264          -1471
 253          -657
 242           28
---------------------------------
Check equilibrium:
Sum of nodal forces = -3118  (N/mm)
Force in steel bars/beam width =  3117  (N/mm)
---------------------------------
```

```
File name = rect.101

-----------------------------------
Beam Name = rect  (Rectangular section)

Solution Mode =  1   (Forces on transverse section just before
cracking)

-----------------------------------
 M = Mcr : Just before cracking
-----------------------------------
Input data:
Sectional properties: Read from data file
-----------------------------------
Output results:
Bending moment (Mcr) =  77  (kNm)
Steel stress just before cracking =  12  (MPa)
Nodal forces on transverse section:

Node No       Force (N/mm)
-------       ------------
 275          -134
 264          -153
 253          -127
 242          -100
 231          -73
 220          -46
 209          -18
 198          -2
 187           7
 176           19
 165           31
 154           44
 143           48
 132           49
 121           56
 110           62
 99            45
 88            24
 77            24
 66            25
 55            26
 44            27
 33            27
 22            28
 11            14
-----------------------------------
Check equilibrium:
Sum of nodal forces = -84  (N/mm)
Force in steel bars/beam width =  83  (N/mm)
-----------------------------------
```

```
File name = flange.101

-----------------------------------
Beam Name = flange  (Flanged section)

Solution Mode =  1   (Forces on transverse section just before
cracking)

-----------------------------------
 M = Mcr : Just before cracking
-----------------------------------
Input data:
Sectional properties: Read from data file
-----------------------------------
Output results:
Bending moment (Mcr) =  152  (kNm)
Steel stress just before cracking =  11  (MPa)
Nodal forces on transverse section:

Node No       Force (N/mm)
-------       ------------
 275          -292
 264          -221
 253          -385
 242          -309
 231          -233
 220          -156
 209          -58
 198          -2
 187           14
 176           27
 165           51
 154           133
 143           143
 132           142
 121           161
 110           179
 99            129
 88            67
 77            69
 66            72
 55            74
 44            76
 33            78
 22            80
 11            40
-----------------------------------
Check equilibrium:
Sum of nodal forces = -110  (N/mm)
Force in steel bars/beam width =  108  (N/mm)
-----------------------------------
```

```
File name = rect.201

-----------------------------------
Beam Name = rect  (Rectangular section)

Solution Mode =  2   (Forces on transverse section just after
cracking)

-----------------------------------
 M = Mcr : Just after cracking
-----------------------------------
Input data:
Sectional properties: Read from data file
-----------------------------------
Output results:
Bending moment (Mcr) =  77  (kNm)
Steel stress just after cracking =  80  (MPa)
Nodal forces on transverse section:

Node No       Force (N/mm)
-------       ------------
 275          -166
 264          -265
 253          -172
 242          -77
 231           21
 220           119
 209           13
-----------------------------------
Check equilibrium:
Sum of nodal forces = -525  (N/mm)
Force in steel bars/beam width =  525  (N/mm)
-----------------------------------
```

```
File name = flange.201

-----------------------------------
Beam Name = flange  (Flanged section)

Solution Mode =  2   (Forces on transverse section just after
cracking)

-----------------------------------
 M = Mcr : Just after cracking
-----------------------------------
Input data:
Sectional properties: Read from data file
-----------------------------------
Output results:
Bending moment (Mcr) =  152  (kNm)
Steel stress just after cracking =  80  (MPa)
Nodal forces on transverse section:

Node No       Force (N/mm)
-------       ------------
 275          -373
 264          -537
 253          -253
 242           2
 231           125
 220           28
-----------------------------------
Check equilibrium:
Sum of nodal forces = -1006  (N/mm)
Force in steel bars/beam width =  1005  (N/mm)
-----------------------------------
```

```
File name = rect.401

------------------------------------------------------------
Beam Number: rect  (Rectangular section)

Solution mode  4   (Slip length and bond force near the first flexural
crack)

------------------------------------------------------------
Input data:
Sectional properties: Read from data file
------------------------------------------------------------
Output results:
Bending moment at the first crack (Mcr) =  77  (kNm)
Steel stress at the first crack =  80  (MPa)
Steel stress at the zero-slip section =  12  (MPa)
Peak bond stress  =  3.93  (MPa)
Slip length =  162  (mm)
Bond forces at nodes:

 Node No.    Bond force (N/mm)
 --------    -----------------
    45          3.2
    46          23.8
    47          42.5
    48          55.8
    49          63.8
    50          66.5
    51          63.8
    52          55.8
    53          42.5
    54          23.8
    55          3.2
------------------------------------------------------------
Check equilibrium:
Total bond force =  445  N/mm
Difference in force in steel bars/beam width = 445
------------------------------------------------------------
```

```
File name = flange.401

------------------------------------------------------------
Beam Number: flange  (Flanged section)

Solution mode  4   (Slip length and bond force near the first flexural
crack)

------------------------------------------------------------
Input data:
Sectional properties: Read from data file
------------------------------------------------------------
Output results:
Bending moment at the first crack (Mcr) =  152  (kNm)
Steel stress at the first crack =  80  (MPa)
Steel stress at the zero-slip section =  11  (MPa)
Peak bond stress  =  4.2  (MPa)
Slip length =  153  (mm)
Bond forces at nodes:

 Node No.    Bond force (N/mm)
 --------    -----------------
    45          6.5
    46          48.3
    47          86.2
    48          113.3
    49          129.6
    50          135
    51          129.6
    52          113.3
    53          86.2
    54          48.3
    55          6.5
------------------------------------------------------------
Check equilibrium:
Total bond force =  903  N/mm
Difference in force in steel bars/beam width = 903
------------------------------------------------------------
```

```
File name = rect.501

------------------------------------------------------------
Beam Number: rect  (Rectangular section)

Solution mode  5   (Bond force between cracks -Constant moment region)

------------------------------------------------------------
Input data:
Sectional properties: Read from data file
Steel stress at the cracked section =  200  MPa
Half crack spacing =  100  mm
------------------------------------------------------------
Output results:
Steel stress at the zero-slip section =  163  MPa
Peak bond stress =  3.45  MPa
Bond forces at nodes:

 Node No.    Bond force (N/mm)
 --------    -----------------
    45          1.7
    46          12.9
    47          23
    48          30.2
    49          34.6
    50          36
    51          34.6
    52          30.2
    53          23
    54          12.9
    55          1.7
------------------------------------------------------------
Check equilibrium:
Total bond force =  241  N/mm
Difference in force in steel bars/beam width = 241
------------------------------------------------------------
```

```
File name = flange.501

------------------------------------------------------------
Beam Number: flange  (Flanged section)

Solution mode  5   (Bond force between cracks -Constant moment region)

------------------------------------------------------------
Input data:
Sectional properties: Read from data file
Steel stress at the cracked section =  180  MPa
Half crack spacing =  90  mm
------------------------------------------------------------
Output results:
Steel stress at the zero-slip section =  148  MPa
Peak bond stress =  3.25  MPa
Bond forces at nodes:

 Node No.    Bond force (N/mm)
 --------    -----------------
    45          2.9
    46          21.8
    47          39
    48          51.3
    49          58.6
    50          61.1
    51          58.6
    52          51.3
    53          39
    54          21.8
    55          2.9
------------------------------------------------------------
Check equilibrium:
Total bond force =  408  N/mm
Difference in force in steel bars/beam width = 408
------------------------------------------------------------
```

```
File name = rect.601

------------------------------------------------------------
Beam Number: rect  (Rectangular section)

Solution mode  6   (Bond force between cracks -Varying moment region)

------------------------------------------------------------
Input data:
Sectional properties: Read from data file
Steel stress at the cracked section =  200  MPa
Steel stress at the adjacent cracked section =  180  MPa
Crack spacing  =  150  mm
------------------------------------------------------------
Output results:
Zero-slip section is 91 mm from the crack that has steel stress =  200
MPa
steel stress at the zero-slip section =  169  MPa
Peak bond stresses: fb1 =  3.12  MPa : fb2 =  1.71  MPa
Bond forces at nodes:

 Node No.    Bond force (N/mm)
 --------    -----------------
    45           3.7
    46           26.3
    47           42.6
    48           48.5
    49           44
    50           29
    51           4.2
    52          -18.2
    53          -26.3
    54          -20.1
    55          -3.2
------------------------------------------------------------
Check equilibrium:
Total bond force =  131  N/mm
Difference in force in steel bars/beam width = 130
------------------------------------------------------------
```

```
File name = flange.601

------------------------------------------------------------
Beam Number: flange  (Flanged section)

Solution mode  6   (Bond force between cracks -Varying moment region)

------------------------------------------------------------
Input data:
Sectional properties: Read from data file
Steel stress at the cracked section =  180  MPa
Steel stress at the adjacent cracked section =  160  MPa
Crack spacing  =  130  mm
------------------------------------------------------------
Output results:
Zero-slip section is 84 mm from the crack that has steel stress =  180
MPa
steel stress at the zero-slip section =  153  MPa
Peak bond stresses: fb1 =  3  MPa : fb2 =  1.41  MPa
Bond forces at nodes:

 Node No.    Bond force (N/mm)
 --------    -----------------
    45           5.9
    46           42
    47           69.1
    48           80.6
    49           76.4
    50           56.6
    51           21.1
    52          -18.8
    53          -36.8
    54          -30.2
    55          -5
------------------------------------------------------------
Check equilibrium:
Total bond force =  261  N/mm
Difference in force in steel bars/beam width = 261
------------------------------------------------------------
□
============================================================
====
```

Appendix B

CALCULATED FORCES

ON CONCRETE SECTIONS

For members analysed

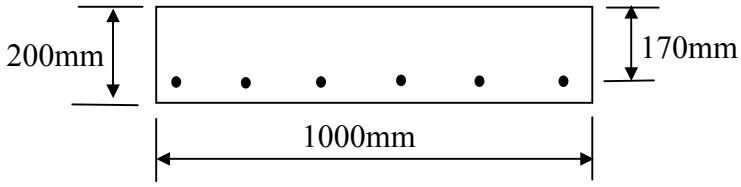

Cross section of *Slab 5.1* and *Slab 5.2*

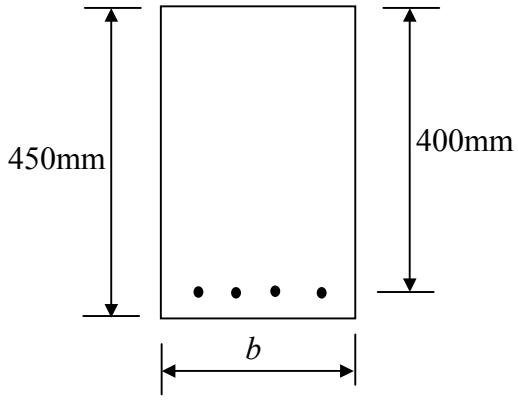

Cross section of *Beam* 5.1 and *Beam 5.2*

b=200mm for *Beam 5.1* and *b*=325mm for *Beam 5.2*

Details of slab and beam cross sections for *Slab5.1, Slab 5.2, Beam 5.1* and *Beam 5.2*

```
File name = slab51.401

------------------------------------------------------------
Beam Number: slab51  (Rectangular section)

Solution mode  4   (Slip length and bond force near the first flexural
crack)

------------------------------------------------------------
Input data:
Sectional properties: Read from data file
------------------------------------------------------------
Output results:
Bending moment at the first crack (Mcr) =  24  (kNm)
Steel stress at the first crack =  219  (MPa)
Steel stress at the zero-slip section =  15  (MPa)
Peak bond stress  =  4.97  (MPa)
Slip length =  184  (mm)
Bond forces at nodes:

 Node No.    Bond force (N/mm)
 --------    -----------------
    45          1
    46          7.4
    47          13.2
    48          17.3
    49          19.8
    50          20.6
    51          19.8
    52          17.3
    53          13.2
    54          7.4
    55          1
------------------------------------------------------------
Check equilibrium:
Total bond force =  138  N/mm
Difference in force in steel bars/beam width = 138
------------------------------------------------------------
```

```
File name = slab52.401

------------------------------------------------------------
Beam Number: slab52  (Rectangular section)

Solution mode  4   (Slip length and bond force near the first flexural
crack)

------------------------------------------------------------
Input data:
Sectional properties: Read from data file
------------------------------------------------------------
Output results:
Bending moment at the first crack (Mcr) =  25  (kNm)
Steel stress at the first crack =  126  (MPa)
Steel stress at the zero-slip section =  15  (MPa)
Peak bond stress  =  4.39  (MPa)
Slip length =  151  (mm)
Bond forces at nodes:

 Node No.    Bond force (N/mm)
 --------    -----------------
    45          .9
    46          7.1
    47          12.7
    48          16.8
    49          19.2
    50          20
    51          19.2
    52          16.8
    53          12.7
    54          7.1
    55          .9
------------------------------------------------------------
Check equilibrium:
Total bond force =  133  N/mm
Difference in force in steel bars/beam width = 133
------------------------------------------------------------
```

```
File name = beam51.401

------------------------------------------------------------
Beam Number: beam51  (Rectangular section)

Solution mode  4   (Slip length and bond force near the first flexural
crack)

------------------------------------------------------------
Input data:
Sectional properties: Read from data file
------------------------------------------------------------
Output results:
Bending moment at the first crack (Mcr) =  26  (kNm)
Steel stress at the first crack =  109  (MPa)
Steel stress at the zero-slip section =  16  (MPa)
Peak bond stress  =  4.41  (MPa)
Slip length =  126  (mm)
Bond forces at nodes:

 Node No.    Bond force (N/mm)
 --------    -----------------
    45          2
    46          15
    47          26.7
    48          35.2
    49          40.2
    50          41.9
    51          40.2
    52          35.2
    53          26.7
    54          15
    55          2
------------------------------------------------------------
Check equilibrium:
Total bond force =  280  N/mm
Difference in force in steel bars/beam width = 280
------------------------------------------------------------
```

```
File name = beam52.401

------------------------------------------------------------
Beam Number: beam52  (Rectangular section)

Solution mode  4   (Slip length and bond force near the first flexural
crack)

------------------------------------------------------------
Input data:
Sectional properties: Read from data file
------------------------------------------------------------
Output results:
Bending moment at the first crack (Mcr) =  46  (kNm)
Steel stress at the first crack =  55  (MPa)
Steel stress at the zero-slip section =  16  (MPa)
Peak bond stress  =  2.67  (MPa)
Slip length =  136  (mm)
Bond forces at nodes:

 Node No.    Bond force (N/mm)
 --------    -----------------
    45          1.7
    46          12.6
    47          22.5
    48          29.5
    49          33.8
    50          35.2
    51          33.8
    52          29.5
    53          22.5
    54          12.6
    55          1.7
------------------------------------------------------------
Check equilibrium:
Total bond force =  235  N/mm
Difference in force in steel bars/beam width = 235
------------------------------------------------------------
```

```
File name = slab51.101

-----------------------------------
Beam Name = slab51  (Rectangular section)

Solution Mode =  1   (Forces on transverse section just before
cracking)

-----------------------------------
 M = Mcr : Just before cracking
-----------------------------------
Input data:
Sectional properties: Read from data file
-----------------------------------
Output results:
Bending moment (Mcr) =  24  (kNm)
Steel stress just before cracking =  15  (MPa)
Nodal forces on transverse section:

Node No       Force (N/mm)
-------       ------------
 265          -32
 254          -45
 243          -37
 232          -30
 221          -22
 210          -14
 199          -6
 188          -1
 177           2
 166           6
 155           10
 144           13
 133           14
 122           14
 111           16
 100           18
 89            13
 78            7
 67            7
 56            7
 45            7
 34            8
 23            8
 12            8
 1             4
-----------------------------------
Check equilibrium:
Sum of nodal forces = -11  (N/mm)
Force in steel bars/beam width =  10  (N/mm)
-----------------------------------
```

```
File name = slab51.201

-----------------------------------
Beam Name = slab51  (Rectangular section)

Solution Mode =  2   (Forces on transverse section just after
cracking)

-----------------------------------
 M = Mcr : Just after cracking
-----------------------------------
Input data:
Sectional properties: Read from data file
-----------------------------------
Output results:
Bending moment (Mcr) =  24  (kNm)
Steel stress just after cracking =  219  (MPa)
Nodal forces on transverse section:

Node No       Force (N/mm)
-------       ------------
 275          -62
 264          -84
 253          -28
 242           23
-----------------------------------
Check equilibrium:
Sum of nodal forces = -150  (N/mm)
Force in steel bars/beam width =  149  (N/mm)
-----------------------------------
```

```
File name = slab52.101

-----------------------------------
Beam Name = slab52  (Rectangular section)

Solution Mode =  1   (Forces on transverse section just before
cracking)

-----------------------------------
 M = Mcr : Just before cracking
-----------------------------------
Input data:
Sectional properties: Read from data file
-----------------------------------
Output results:
Bending moment (Mcr) =  25  (kNm)
Steel stress just before cracking =  15  (MPa)
Nodal forces on transverse section:

Node No       Force (N/mm)
-------       ------------
 265          -37
 254          -46
 243          -38
 232          -30
 221          -22
 210          -14
 199          -6
 188          -1
 177           2
 166           6
 155           9
 144           13
 133           14
 122           14
 111           16
 100           18
 89            13
 78            7
 67            7
 56            7
 45            7
 34            8
 23            8
 12            8
 1             4
-----------------------------------
Check equilibrium:
Sum of nodal forces = -19  (N/mm)
Force in steel bars/beam width =  18  (N/mm)
-----------------------------------
```

```
File name = slab52.201

-----------------------------------
Beam Name = slab52  (Rectangular section)

Solution Mode =  2   (Forces on transverse section just after
cracking)

-----------------------------------
 M = Mcr : Just after cracking
-----------------------------------
Input data:
Sectional properties: Read from data file
-----------------------------------
Output results:
Bending moment (Mcr) =  25  (kNm)
Steel stress just after cracking =  126  (MPa)
Nodal forces on transverse section:

Node No       Force (N/mm)
-------       ------------
 275          -53
 264          -81
 253          -46
 242          -10
 231           28
 220           7
-----------------------------------
Check equilibrium:
Sum of nodal forces = -153  (N/mm)
Force in steel bars/beam width =  152  (N/mm)
-----------------------------------
```

```
File name = beam51.101

-----------------------------------
Beam Name = beam51  (Rectangular section)

Solution Mode =  1   (Forces on transverse section just before
cracking)

-----------------------------------
 M = Mcr : Just before cracking
-----------------------------------
Input data:
Sectional properties: Read from data file
-----------------------------------
Output results:
Bending moment (Mcr) =  26  (kNm)
Steel stress just before cracking =  16  (MPa)
Nodal forces on transverse section:

Node No       Force (N/mm)
-------       ------------
 265          -87
 254          -102
 243          -85
 232          -67
 221          -49
 210          -31
 199          -12
 188          -1
 177           5
 166           13
 155           21
 144           29
 133           32
 122           33
 111           37
 100           42
 89            30
 78            16
 67            16
 56            17
 45            17
 34            18
 23            18
 12            19
 1             9
-----------------------------------
Check equilibrium:
Sum of nodal forces = -51  (N/mm)
Force in steel bars/beam width =  50  (N/mm)
-----------------------------------
```

```
File name = beam51.201

-----------------------------------
Beam Name = beam51  (Rectangular section)

Solution Mode =  2   (Forces on transverse section just after
cracking)

-----------------------------------
 M = Mcr : Just after cracking
-----------------------------------
Input data:
Sectional properties: Read from data file
-----------------------------------
Output results:
Bending moment (Mcr) =  26  (kNm)
Steel stress just after cracking =  109  (MPa)
Nodal forces on transverse section:

Node No       Force (N/mm)
-------       ------------
 275          -111
 264          -174
 253          -107
 242          -39
 231           32
 220           65
-----------------------------------
Check equilibrium:
Sum of nodal forces = -331  (N/mm)
Force in steel bars/beam width =  330  (N/mm)
-----------------------------------
```

```
File name = beam52.101

-----------------------------------
Beam Name = beam52  (Rectangular section)

Solution Mode =  1   (Forces on transverse section just before
cracking)

-----------------------------------
 M = Mcr : Just before cracking
-----------------------------------
Input data:
Sectional properties: Read from data file
-----------------------------------
Output results:
Bending moment (Mcr) =  46  (kNm)
Steel stress just before cracking =  16  (MPa)
Nodal forces on transverse section:

Node No       Force (N/mm)
-------       ------------
 265          -115
 254          -106
 243          -87
 232          -69
 221          -51
 210          -32
 199          -12
 188           1
 177           11
 166           19
 155           28
 144           31
 133           32
 122           37
 111           41
 100           30
 89            16
 78            16
 67            17
 56            17
 45            18
 34            18
 23            19
 12            9
-----------------------------------
Check equilibrium:
Sum of nodal forces = -102  (N/mm)
Force in steel bars/beam width =  100  (N/mm)
-----------------------------------
```

```
File name = beam52.201

-----------------------------------
Beam Name = beam52  (Rectangular section)

Solution Mode =  2   (Forces on transverse section just after
cracking)

-----------------------------------
 M = Mcr : Just after cracking
-----------------------------------
Input data:
Sectional properties: Read from data file
-----------------------------------
Output results:
Bending moment (Mcr) =  46  (kNm)
Steel stress just after cracking =  55  (MPa)
Nodal forces on transverse section:

Node No       Force (N/mm)
-------       ------------
 275          -95
 264          -161
 253          -121
 242          -80
 231          -39
 220           4
 209           36
 198           50
 187           69
 176           0
-----------------------------------
Check equilibrium:
Sum of nodal forces = -333  (N/mm)
Force in steel bars/beam width =  332  (N/mm)
-----------------------------------
```

```
File name = slab53.301

------------------------------------------------
Beam Name = slab53  (Rectangular section)

Solution Mode =  3   (Forces on transverse section for a given moment)

------------------------------------------------
 Mcr =  24 kNm
 Mu  =  66 kNm
------------------------------------------------
Input data:
Sectional properties: Read from data file
Bending moment at the section =  32.5  kNm
Stress in tensile steel =  200  MPa
Nodal forces on transverse section:

Node No       Force (N/mm)
-------       ------------
 275          -70
 264          -103
 253          -51
 242           5
 231           14
-----------------------------------
Check equilibrium:
Sum of nodal forces = -204  (N/mm)
Force in steel bars/beam width =  203  (N/mm)
-----------------------------------
```

```
File name = slab53.501

------------------------------------------------------------
Beam Number: slab53  (Rectangular section)

Solution mode  5   (Bond force between cracks -Constant moment region)

------------------------------------------------------------
Input data:
Sectional properties: Read from data file
Steel stress at the cracked section =  200  MPa
Half crack spacing =  60  mm
------------------------------------------------------------
Output results:
Steel stress at the zero-slip section =  156  MPa
Peak bond stress =  3.27  MPa
Bond forces at nodes:

 Node No.    Bond force (N/mm)
 --------    -----------------
    45           .3
    46          2.3
    47          4.2
    48          5.5
    49          6.3
    50          6.6
    51          6.3
    52          5.5
    53          4.2
    54          2.3
    55           .3
------------------------------------------------------------
Check equilibrium:
Total bond force =  44  N/mm
Difference in force in steel bars/beam width = 44
------------------------------------------------------------
```

```
File name = slab53.502

------------------------------------------------------------
Beam Number: slab53  (Rectangular section)

Solution mode  5   (Bond force between cracks -Constant moment region)

------------------------------------------------------------
Input data:
Sectional properties: Read from data file
Steel stress at the cracked section =  200  MPa
Half crack spacing =  80  mm
------------------------------------------------------------
Output results:
Steel stress at the zero-slip section =  120  MPa
Peak bond stress =  4.44  MPa
Bond forces at nodes:

 Node No.    Bond force (N/mm)
 --------    -----------------
    45          .5
    46          4.3
    47          7.6
    48          10
    49          11.5
    50          12
    51          11.5
    52          10
    53          7.6
    54          4.3
    55          .5
------------------------------------------------------------
Check equilibrium:
Total bond force =  80  N/mm
Difference in force in steel bars/beam width = 80
------------------------------------------------------------
```

```
File name = slab53.503

------------------------------------------------------------
Beam Number: slab53  (Rectangular section)

Solution mode  5   (Bond force between cracks -Constant moment region)

------------------------------------------------------------
Input data:
Sectional properties: Read from data file
Steel stress at the cracked section =  200  MPa
Half crack spacing =  110  mm
------------------------------------------------------------
Output results:
Steel stress at the zero-slip section =  72  MPa
Peak bond stress =  5.23  MPa
Bond forces at nodes:

 Node No.    Bond force (N/mm)
 --------    -----------------
    45           .9
    46          6.9
    47          12.4
    48          16.3
    49          18.6
    50          19.4
    51          18.6
    52          16.3
    53          12.4
    54          6.9
    55           .9
------------------------------------------------------------
Check equilibrium:
Total bond force =  130  N/mm
Difference in force in steel bars/beam width = 130
------------------------------------------------------------
```

```
File name = slab53.301

------------------------------------------------
Beam Name = slab53  (Rectangular section)

Solution Mode =  3   (Forces on transverse section for a given moment)

------------------------------------------------
 Mcr =  24 kNm
 Mu  =  66 kNm
------------------------------------------------
Input data:
Sectional properties: Read from data file
Bending moment at the section =  25  kNm
Stress in tensile steel =  150  MPa
Nodal forces on transverse section:

Node No       Force (N/mm)
-------       ------------
 275          -56
 264          -83
 253          -42
 242           0
 231           26
-----------------------------------
Check equilibrium:
Sum of nodal forces = -153  (N/mm)
Force in steel bars/beam width =  152  (N/mm)
-----------------------------------
```

```
File name = slab53.302

------------------------------------------------
Beam Name = slab53  (Rectangular section)

Solution Mode =  3   (Forces on transverse section for a given moment)

------------------------------------------------
 Mcr =  24 kNm
 Mu  =  66 kNm
------------------------------------------------
Input data:
Sectional properties: Read from data file
Bending moment at the section =  48  kNm
Stress in tensile steel =  300  MPa
Nodal forces on transverse section:

Node No       Force (N/mm)
-------       ------------
 275          -100
 264          -147
 253          -72
 242           10
----------------------------------
Check equilibrium:
Sum of nodal forces = -308  (N/mm)
Force in steel bars/beam width =  307  (N/mm)
----------------------------------
```

```
File name = slab53.501

------------------------------------------------------------
Beam Number: slab53  (Rectangular section)

Solution mode  5   (Bond force between cracks -Constant moment region)

------------------------------------------------------------
Input data:
Sectional properties: Read from data file
Steel stress at the cracked section =  150  MPa
Half crack spacing =  90  mm
------------------------------------------------------------
Output results:
Steel stress at the zero-slip section =  59  MPa
Peak bond stress =  4.51  MPa
Bond forces at nodes:

 Node No.    Bond force (N/mm)
 --------    -----------------
    45          .6
    46          4.9
    47          8.7
    48          11.5
    49          13.1
    50          13.7
    51          13.1
    52          11.5
    53          8.7
    54          4.9
    55          .6
------------------------------------------------------------
Check equilibrium:
Total bond force =  91  N/mm
Difference in force in steel bars/beam width = 91
------------------------------------------------------------
```

```
File name = slab53.502

------------------------------------------------------------
Beam Number: slab53  (Rectangular section)

Solution mode  5   (Bond force between cracks -Constant moment region)

------------------------------------------------------------
Input data:
Sectional properties: Read from data file
Steel stress at the cracked section =  200  MPa
Half crack spacing =  90  mm
------------------------------------------------------------
Output results:
Steel stress at the zero-slip section =  100  MPa
Peak bond stress =  4.96  MPa
Bond forces at nodes:

 Node No.    Bond force (N/mm)
 --------    -----------------
    45          .7
    46          5.4
    47          9.600001
    48          12.6
    49          14.5
    50          15.1
    51          14.5
    52          12.6
    53          9.600001
    54          5.4
    55          .7
------------------------------------------------------------
Check equilibrium:
Total bond force =  101  N/mm
Difference in force in steel bars/beam width = 101
------------------------------------------------------------
```

```
File name = slab53.503

------------------------------------------------------------
Beam Number: slab53  (Rectangular section)

Solution mode  5   (Bond force between cracks -Constant moment region)

------------------------------------------------------------
Input data:
Sectional properties: Read from data file
Steel stress at the cracked section =  300  MPa
Half crack spacing =  90  mm
------------------------------------------------------------
Output results:
Steel stress at the zero-slip section =  182  MPa
Peak bond stress =  5.87  MPa
Bond forces at nodes:

 Node No.    Bond force (N/mm)
 --------    -----------------
    45          .8
    46          6.3
    47          11.4
    48          15
    49          17.1
    50          17.8
    51          17.1
    52          15
    53          11.4
    54          6.3
    55          .8
------------------------------------------------------------
Check equilibrium:
Total bond force =  119  N/mm
Difference in force in steel bars/beam width = 119
------------------------------------------------------------
```

```
File name = beam53.301

------------------------------------------------
Beam Name = beam53  (Rectangular section)

Solution Mode =  3   (Forces on transverse section for a given moment)

------------------------------------------------
 Mcr =  42 kNm
 Mu  =  187 kNm
------------------------------------------------
Input data:
Sectional properties: Read from data file
Bending moment at the section =  91.7  kNm
Stress in tensile steel =  200  MPa
Nodal forces on transverse section:

Node No       Force (N/mm)
-------       ------------
 275          -207
 264          -332
 253          -217
 242          -94
 231           37
 220           12
-----------------------------------
Check equilibrium:
Sum of nodal forces = -799  (N/mm)
Force in steel bars/beam width =  799  (N/mm)
-----------------------------------
```

```
File name = beam53.501

------------------------------------------------------------
Beam Number: beam53  (Rectangular section)

Solution mode  5   (Bond force between cracks -Constant moment region)

------------------------------------------------------------
Input data:
Sectional properties: Read from data file
Steel stress at the cracked section =  200  MPa
Half crack spacing =  40  mm
------------------------------------------------------------
Output results:
Steel stress at the zero-slip section =  193  MPa
Peak bond stress =  1.25  MPa
Bond forces at nodes:

 Node No.    Bond force (N/mm)
 --------    -----------------
    45          .1
    46          1.4
    47          2.5
    48          3.3
    49          3.8
    50          3.9
    51          3.8
    52          3.3
    53          2.5
    54          1.4
    55          .1
------------------------------------------------------------
Check equilibrium:
Total bond force =  26  N/mm
Difference in force in steel bars/beam width = 26
------------------------------------------------------------
```

```
File name = beam53.502

------------------------------------------------------------
Beam Number: beam53  (Rectangular section)

Solution mode  5   (Bond force between cracks -Constant moment region)

------------------------------------------------------------
Input data:
Sectional properties: Read from data file
Steel stress at the cracked section =  200  MPa
Half crack spacing =  60  mm
------------------------------------------------------------
Output results:
Steel stress at the zero-slip section =  183  MPa
Peak bond stress =  2.04  MPa
Bond forces at nodes:

 Node No.    Bond force (N/mm)
 --------    -----------------
    45          .4
    46          3.4
    47          6.2
    48          8.1
    49          9.3
    50          9.7
    51          9.3
    52          8.1
    53          6.2
    54          3.4
    55          .4
------------------------------------------------------------
Check equilibrium:
Total bond force =  65  N/mm
Difference in force in steel bars/beam width = 65
------------------------------------------------------------
```

```
File name = beam53.503

------------------------------------------------------------
Beam Number: beam53  (Rectangular section)

Solution mode  5   (Bond force between cracks -Constant moment region)

------------------------------------------------------------
Input data:
Sectional properties: Read from data file
Steel stress at the cracked section =  200  MPa
Half crack spacing =  80  mm
------------------------------------------------------------
Output results:
Steel stress at the zero-slip section =  169  MPa
Peak bond stress =  2.89  MPa
Bond forces at nodes:

 Node No.    Bond force (N/mm)
 --------    -----------------
    45          .8
    46          6.5
    47          11.7
    48          15.4
    49          17.6
    50          18.4
    51          17.6
    52          15.4
    53          11.7
    54          6.5
    55          .8
------------------------------------------------------------
Check equilibrium:
Total bond force =  123  N/mm
Difference in force in steel bars/beam width = 123
------------------------------------------------------------
```

```
File name = beam53.301

------------------------------------------------
Beam Name = beam53  (Rectangular section)

Solution Mode =  3   (Forces on transverse section for a given moment)

------------------------------------------------
 Mcr =  42 kNm
 Mu  =  187 kNm
------------------------------------------------
Input data:
Sectional properties: Read from data file
Bending moment at the section =  45  kNm
Stress in tensile steel =  90  MPa
Nodal forces on transverse section:

Node No       Force (N/mm)
-------       ------------
 275          -110
 264          -178
 253          -120
 242          -61
 231           0
 220           62
 209           41
----------------------------------
Check equilibrium:
Sum of nodal forces = -361  (N/mm)
Force in steel bars/beam width =  360  (N/mm)
----------------------------------
```

```
File name = beam53.302

------------------------------------------------
Beam Name = beam53  (Rectangular section)

Solution Mode =  3   (Forces on transverse section for a given moment)

------------------------------------------------
 Mcr =  42 kNm
 Mu  =  187 kNm
------------------------------------------------
Input data:
Sectional properties: Read from data file
Bending moment at the section =  135.65  kNm
Stress in tensile steel =  300  MPa
Nodal forces on transverse section:

Node No       Force (N/mm)
-------       ------------
 275          -293
 264          -477
 253          -319
 242          -142
 231           29
----------------------------------
Check equilibrium:
Sum of nodal forces = -1199  (N/mm)
Force in steel bars/beam width =  1199  (N/mm)
----------------------------------
```

```
File name = beam53.501

------------------------------------------------------------
Beam Number: beam53  (Rectangular section)

Solution mode  5   (Bond force between cracks -Constant moment region)

------------------------------------------------------------
Input data:
Sectional properties: Read from data file
Steel stress at the cracked section =  90  MPa
Half crack spacing =  70  mm
------------------------------------------------------------
Output results:
Steel stress at the zero-slip section =  70  MPa
Peak bond stress =  2.04  MPa
Bond forces at nodes:

 Node No.    Bond force (N/mm)
 --------    -----------------
    45          .5
    46          4
    47          7.2
    48          9.5
    49          10.9
    50          11.4
    51          10.9
    52          9.5
    53          7.2
    54          4
    55          .5
------------------------------------------------------------
Check equilibrium:
Total bond force =  76  N/mm
Difference in force in steel bars/beam width = 76
------------------------------------------------------------
```

```
File name = beam53.502

------------------------------------------------------------
Beam Number: beam53  (Rectangular section)

Solution mode  5   (Bond force between cracks -Constant moment region)

------------------------------------------------------------
Input data:
Sectional properties: Read from data file
Steel stress at the cracked section =  200  MPa
Half crack spacing =  70  mm
------------------------------------------------------------
Output results:
Steel stress at the zero-slip section =  177  MPa
Peak bond stress =  2.46  MPa
Bond forces at nodes:

 Node No.    Bond force (N/mm)
 --------    -----------------
    45          .6
    46          4.9
    47          8.7
    48          11.5
    49          13.1
    50          13.7
    51          13.1
    52          11.5
    53          8.7
    54          4.9
    55          .6
------------------------------------------------------------
Check equilibrium:
Total bond force =  91  N/mm
Difference in force in steel bars/beam width = 91
------------------------------------------------------------
```

```
File name = beam53.503

------------------------------------------------------------
Beam Number: beam53  (Rectangular section)

Solution mode  5   (Bond force between cracks -Constant moment region)

------------------------------------------------------------
Input data:
Sectional properties: Read from data file
Steel stress at the cracked section =  300  MPa
Half crack spacing =  70  mm
------------------------------------------------------------
Output results:
Steel stress at the zero-slip section =  273  MPa
Peak bond stress =  2.84  MPa
Bond forces at nodes:

 Node No.    Bond force (N/mm)
 --------    -----------------
    45          .7
    46          5.6
    47          10.1
    48          13.2
    49          15.1
    50          15.8
    51          15.1
    52          13.2
    53          10.1
    54          5.6
    55          .7
------------------------------------------------------------
Check equilibrium:
Total bond force =  105  N/mm
Difference in force in steel bars/beam width = 105
------------------------------------------------------------
```

Appendix C

FINITE ELEMENT MESH

Node numbers at which loads are applied

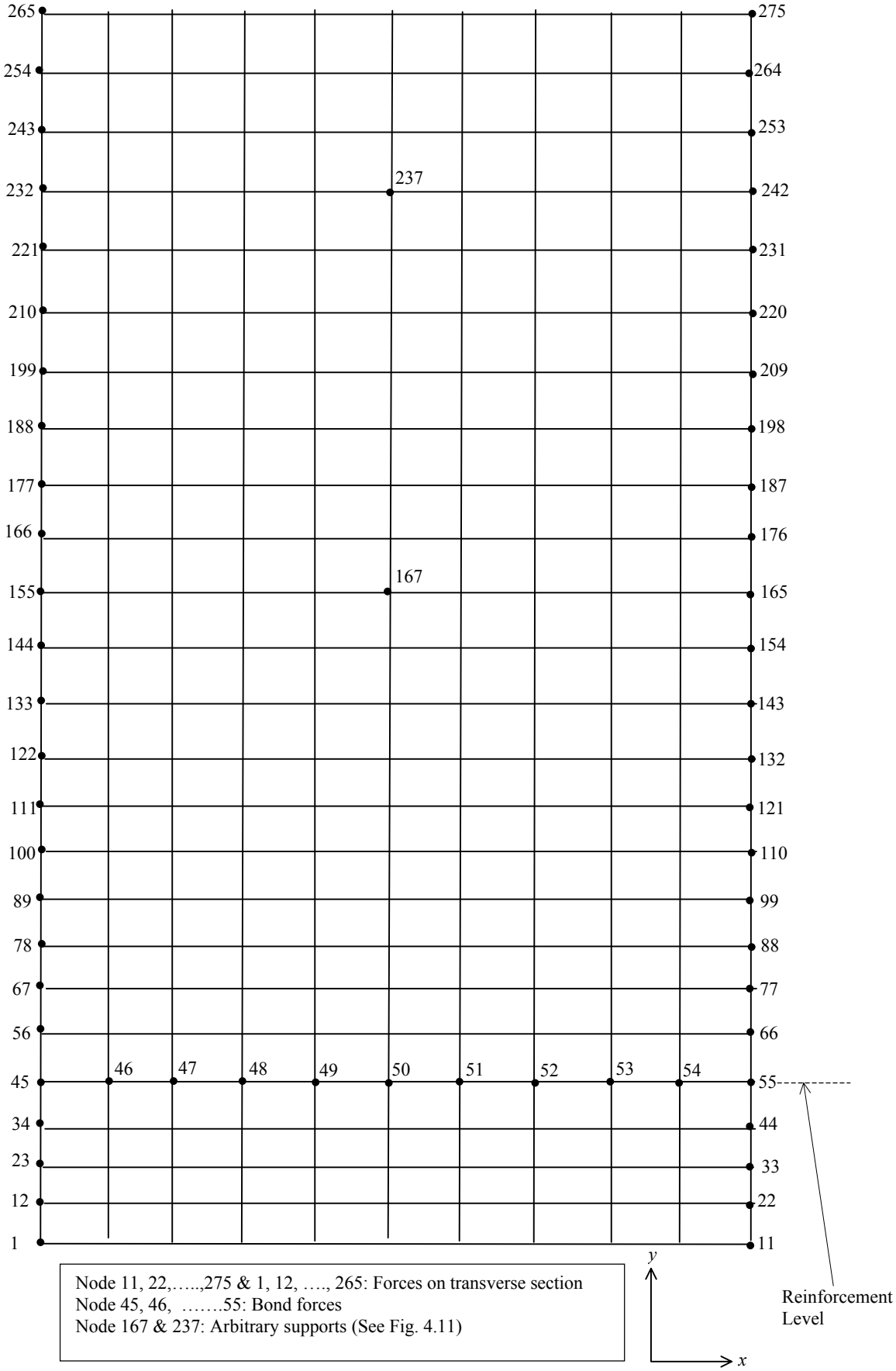

Node numbers at which loads are applied
(Not to scale; see Fig. 4.17 for dimensions of the mesh)

Appendix D

POLYNOMIAL COEFFICIENTS

For calculating concrete stress and extension

Poilynomial coefficients for STRESS at Nodes 1 and 45: LOAD CASE 1

a	*b*	*c*	*d*	*e*	*f*	*g*	*h*
45.2500	-10.2250	0.5700	1.9100	2.1065	-2.4630	-0.8917	1.9100
33.0000	-4.1500	0.0850	2.3850	2.1296	-2.3009	-1.4500	2.3850
43.3500	-6.8150	0.4740	2.9500	1.8519	-1.7037	-2.2583	2.9500
52.5000	-8.2000	0.5750	3.5950	2.2396	-2.0625	-2.7521	3.5950
60.7500	-9.2250	0.6450	4.2450	2.5984	-2.3634	-3.2813	4.2450
71.0000	-10.9500	0.7850	4.9250	2.8819	-2.5556	-3.8792	4.9250
78.7500	-11.9750	0.8800	5.5400	2.9630	-2.5093	-4.4917	5.5400
22.0000	-3.4000	0.1200	1.4000	1.1516	-1.6782	-0.4854	1.4000
22.7500	-2.8750	0.1500	1.7300	1.3831	-1.9745	-0.6604	1.7300
26.2500	-3.3250	0.3000	2.1200	1.4641	-2.0532	-0.9729	2.1200
31.0000	-3.7000	0.3400	2.5800	1.9734	-2.7384	-1.1063	2.5800
36.7500	-4.4500	0.4175	3.0475	2.1065	-2.9421	-1.4083	3.0475
41.7500	-4.8750	0.4700	3.5300	2.5289	-3.5162	-1.5979	3.5300
46.5000	-5.3500	0.5300	3.9700	2.7431	-3.8194	-1.8458	3.9700
5.5000	1.6000	-0.2150	1.0850	-0.9433	1.0532	-1.1729	1.0850
5.0000	2.1500	-0.1650	1.2950	-0.5961	0.6088	-1.1979	1.2950
7.2500	1.7250	-0.0050	1.5550	-0.6539	0.6412	-1.4021	1.5550
8.2500	2.3250	-0.0250	1.8950	-0.8796	0.8843	-1.7417	1.8950
9.9000	2.6400	-0.0090	2.2350	-1.0648	1.0880	-2.0750	2.2350
11.2000	3.1200	-0.0070	2.5850	-1.1632	1.1597	-2.3604	2.5850
11.5000	3.8500	-0.0200	2.9000	-1.3426	1.3519	-2.6667	2.9000
-5.5000	5.0000	-0.4450	0.8950	-2.5058	3.5116	-2.1021	0.8950
-6.5000	5.4500	-0.3700	1.0300	-2.7604	3.8125	-2.3021	1.0300
-8.0000	6.1500	-0.2950	1.2050	-3.4201	4.6736	-2.7479	1.2050
-9.2500	7.2750	-0.3350	1.4650	-4.0799	5.5764	-3.3021	1.4650
-11.2500	8.6750	-0.3950	1.7250	-4.8148	6.5880	-3.9000	1.7250
-14.5000	10.5500	-0.4900	1.9900	-5.5845	7.6273	-4.5021	1.9900
-15.5000	11.5000	-0.5050	2.2350	-6.4526	8.8218	-5.1563	2.2350
122.2500	-34.7250	2.2500	3.0300	3.9410	-3.7569	-1.9813	3.0300
97.7500	-22.9750	1.3200	3.8600	3.0208	-1.9583	-3.6292	3.8600
83.7500	-14.6750	0.6700	4.8500	1.6725	0.5301	-5.7229	4.8500
102.2500	-17.9750	0.8350	5.9150	2.0139	0.6806	-6.9917	5.9150
119.0000	-20.6000	0.9500	6.9900	2.2569	0.9861	-8.3375	6.9900
135.7500	-23.0750	1.0500	8.1100	2.5231	1.2870	-9.7333	8.1100
151.7500	-25.6750	1.2000	9.1400	2.3206	2.1505	-11.2229	9.1400
124.2500	-36.7750	2.4350	2.6350	7.9572	-10.0810	1.1479	2.6350
112.0000	-29.6000	1.8400	3.4400	7.8993	-9.5903	0.0771	3.4400
107.7500	-24.8750	1.4100	4.3900	7.6157	-8.7315	-1.2833	4.3900
130.5000	-30.0000	1.6950	5.3550	9.3171	-10.6759	-1.5625	5.3550
152.7000	-34.8700	1.9600	6.3360	10.6401	-12.1218	-2.0313	6.3360
175.2500	-39.7250	2.2200	7.3600	12.0891	-13.7199	-2.4896	7.3600
193.7500	-43.3750	2.4000	8.3000	13.3796	-15.0926	-2.9667	8.3000
110.7500	-33.2250	2.2150	2.2150	11.5567	-15.8634	4.1104	2.2150
117.5000	-33.0000	2.1250	3.0250	11.6319	-15.7222	3.2542	3.0250
122.7500	-31.9750	1.9700	3.9100	12.6447	-16.8310	2.7854	3.9100
149.5000	-38.9000	2.3950	4.7750	15.3183	-20.3866	3.3396	4.7750
175.2500	-45.4250	2.7900	5.6500	17.8530	-23.7477	3.8104	5.6500
202.5000	-52.3500	3.2100	6.5700	20.6424	-27.4097	4.3313	6.5700
225.2500	-57.8750	3.5350	7.4150	22.7951	-30.2569	4.6396	7.4150
90.0000	-27.0000	1.8000	1.8000	14.4734	-20.7384	6.7438	1.8000
114.7500	-33.3750	2.1900	2.6100	14.5602	-20.7870	6.0500	2.6100
127.7500	-35.4250	2.2650	3.4250	16.5509	-23.4769	6.3583	3.4250
155.8500	-43.1850	2.7600	4.1880	19.9583	-28.3167	7.6250	4.1880
183.2500	-50.6750	3.2350	4.9550	23.6169	-33.4838	9.0021	4.9550
211.7500	-58.4250	3.7250	5.7650	27.1296	-38.4676	10.2833	5.7650
237.2500	-65.2750	4.1550	6.5150	30.4225	-43.0949	11.4521	6.5150

Poilynomial coefficients for EXTENSION x 1000 at Nodes 50 and 55: LOAD CASE 1

a	*b*	*c*	*d*	*e*	*f*	*g*
0.0000	-12.7778	7.9444	3.0333	2.5850	2.4200	1.8538
0.0000	-0.5556	-1.4444	6.1500	3.2400	3.0175	2.3125
0.0900	14.4444	-11.2778	8.9833	3.9950	3.7125	2.8475
0.1200	15.1852	-12.1852	10.6667	4.8700	4.5250	3.4713
0.1400	21.0185	-16.3519	12.9250	5.7500	5.3425	4.0963
0.1700	23.1482	-18.3148	14.9000	6.6650	6.1925	4.7500
0.2000	26.4815	-20.9815	16.8333	7.4950	6.9625	5.3413
0.0000	4.4444	-2.9444	3.8500	1.9950	1.9200	1.4975
0.0000	11.1111	-7.7778	5.6667	2.5000	2.3825	1.8550
0.1000	16.0185	-10.8519	6.9250	3.0550	2.9175	2.2725
0.1200	24.8148	-16.6481	9.0167	3.7150	3.5600	2.7700
0.1400	31.0185	-20.8519	10.8750	4.3850	4.1975	3.2688
0.1700	35.8333	-24.0000	12.5417	5.0850	4.8650	3.7888
0.2000	43.1482	-27.9815	14.0667	5.7450	5.4700	4.2588
0.0000	10.6482	-8.1482	4.3083	1.5350	1.4775	1.1700
0.0300	13.7037	-10.3704	5.3000	1.8900	1.8100	1.4313
0.0900	25.9259	-18.4259	7.2833	2.2850	2.1975	1.7388
0.1200	31.2037	-21.8704	8.6750	2.7900	2.6800	2.1200
0.1500	32.1296	-23.2963	9.9083	3.2750	3.1625	2.5000
0.1730	40.7778	-29.2444	11.8567	3.7950	3.6625	2.8950
0.2000	46.2963	-33.1296	13.3500	4.2650	4.1125	3.2525
0.0000	11.5741	-10.5741	4.6417	1.1800	1.0900	0.8738
0.0400	17.2222	-14.7222	5.8000	1.4050	1.3075	1.0425
0.1000	21.0185	-17.8519	6.8750	1.6750	1.5600	1.2450
0.1200	28.6111	-23.6111	8.6750	2.0400	1.9000	1.5175
0.1500	31.0185	-26.0185	9.8917	2.4100	2.2375	1.7875
0.1700	39.0741	-32.2407	11.8333	2.7850	2.5900	2.0700
0.2000	42.4074	-35.2407	13.1000	3.1250	2.9050	2.3213
0.0000	-12.5926	9.0926	3.7167	3.3250	3.4600	3.3238
0.0000	18.7963	-11.9630	9.0083	4.2050	4.3550	4.1650
0.1100	23.5185	-15.3519	11.2000	5.2250	5.3925	5.1463
0.1400	25.5556	-16.7222	13.3167	6.3750	6.5750	6.2750
0.1700	30.6482	-20.1481	15.8083	7.5250	7.7650	7.4075
0.2000	51.5741	-30.4074	19.0250	8.9750	8.8800	8.5888
0.2400	41.2963	-27.2963	20.8167	9.8200	10.1300	9.6613
0.0000	8.6111	-4.1111	4.6250	2.5950	2.7600	2.6425
0.0000	38.5185	-23.1852	8.9333	3.2600	3.4450	3.2988
0.1000	29.5370	-18.0370	9.3083	4.0050	4.2450	4.0538
0.1400	35.1852	-20.6852	10.9167	4.9050	5.1750	4.9413
0.1500	48.7963	-29.1296	13.7250	5.7900	6.1100	5.8313
0.2000	48.2407	-28.4074	14.9583	6.7150	7.0825	6.7600
0.2300	56.3889	-33.3889	17.0750	7.5500	7.9650	7.6000
0.0000	18.6111	-11.7778	5.2917	2.0050	2.1600	2.0850
0.0500	17.9630	-11.4630	5.9667	2.4750	2.6600	2.5538
0.1200	35.0926	-21.7593	8.3250	3.0300	3.2500	3.1063
0.1500	40.0000	-24.8333	9.8833	3.6950	3.9600	3.7850
0.1800	46.4815	-28.9815	11.6333	4.3550	4.6725	4.4650
0.2100	57.3148	-35.6481	13.7917	5.0500	5.4075	5.1763
0.2400	65.0926	-40.5926	15.6083	5.6750	6.0825	5.8113
0.0000	21.8519	-15.8519	5.7667	1.5400	1.6450	1.5963
0.0500	28.0556	-19.8889	6.9083	1.8550	1.9800	1.9075
0.1200	34.1667	-24.0000	8.1583	2.2250	2.3850	2.2813
0.1500	41.6667	-29.1667	9.9000	2.7150	2.9025	2.7800
0.1800	47.9630	-33.7963	11.6000	3.1950	3.4250	3.2763
0.2100	56.4815	-39.6481	13.5000	3.7050	3.9650	3.7925
0.2400	64.3519	-45.1852	15.2750	4.1550	4.4500	4.2550

Poilynomial coefficients for STRESS at Nodes 1 and 45: LOAD CASE 2

a	*b*	*c*	*d*	*e*	*f*
-8.496	37.427	-68.128	65.231	-34.116	8.65
-7.135	32.968	-62.177	60.932	-32.248	8.195
-3.8826	20.8251	-44.1612	47.5169	-27.0997	7.31055
-7.4532	33.5654	-61.9143	59.4885	-30.8912	7.69186
-19.9777	80.78118	-131.993	110.5391	-49.0384	10.15704
-6.881	25.4503	-50.4147	57.40328	-22.6871	5.1035
-6.207	22.088	-36.6844	55.44812	-21.6384	4.548225
-2.95078	13.61962	-34.4457	26.9896	-24.3897	4.7811
-4.87439	25.67753	-54.4846	45.21126	-27.1843	5.37661
-15.3828	54.9312	-114.174	86.88373	-22.3615	9.141336

Poilynomial coefficients for EXTENSION x 1000 at Nodes 50 and 55: LOAD CASE 2

a	*b*
0.215	0.1
0.202	0.092
0.191	0.086
0.181	0.082
0.174	0.078
0.237	0.07
0.219	0.06
0.204	0.052
0.191	0.046
0.181	0.042

Appendix E

COMPUTER PROGRAMS

Developed for using in the thesis

PROGRAM TO CALCULATE FORCES ON CONCRETE SECTIONS

```
10 REM   ************************************************************
20 DIM
EXC(110),SLIP(110),BOND(110),BNDF(110),S(110),CONC(11),FORCE(11),EC(20)
30 DIM Y(25),F(25),ND(25),NP(25),MD(25),MP(25),FB(110),D(25),BF(25),BF1(15)
40 DIM
X(25),Z(25),X1(25),Y1(25),FX(25),BS(25),A(25),B(25),FT(25),FF(25),ECX(30)
50 REM ************************************************************
60 WR=1
70 CLS:PRINT:PRINT"       ------------------------------------------------"
80 PRINT"       Program to calculate forces acting on a RC section"
90 PRINT"       ------------------------------------------------"
100 PRINT:PRINT"       Sectional properties:"
110 PRINT:PRINT"       Read from data file            (1)   OR"
120 PRINT"       Input properties from Keyboard (2)"
130 'X$="1":'PRINT:PRINT:INPUT "       What option (1/2)
",X$:###############
131 PRINT:PRINT:INPUT "       What option (1/2)  ",X$
140 X=VAL (X$):IF X<1 OR X>2 THEN BEEP:GOTO 70
150 IF X=2 THEN GOSUB 3370:GOTO 200
160 'XP$="rect":'PRINT:INPUT "       File Name =
",XP$:######################
161 PRINT:INPUT "       File Name =  ",XP$
170 IF XP$="" THEN BEEP:GOTO 70
180 GOSUB 6790:IF XINP=1 THEN 200
190 GOSUB 3680
200 TOL1=.999:TOL2=1.001
210 PI=3.14159
220 'FC=50
230 BB=B:'B=300
240 'H=550
250 'D=500
260 'BX1=1:BX2=1
270 'HF1=.25
280 'HF2=.25
290 'DIA =25:NB=6
300 'DIA1 =20:NB1=2
310 'DD=.1
320 RO=PI/4*DIA^2*NB/(B*D)
330 ROD=PI/4*DIA1^2*NB1/(B*D)
340 MCR=2:MX=MXZ
350 E0=.002
360 EES=200000!
370 FR=.62*FC^.5
380 ECI=1000*FC
390 ER=FR/ECI
400 BE=H/D
410 MCR=0:MCS=0:ULT=0
420 CLS
430 PRINT "------------------------------------------------------------------"
440 PRINT "                 M A I N     M E N U
"
450 PRINT "------------------------------------------------------------------"
460 MCR=1:GOSUB 2000:MCR=0:STT1=INT(EST*EES)
470 PRINT "Cracking moment Mcr = ", MXX; "kNm":PRINT :MCRR=MXX
480 PRINT "Steel stress before cracking = ";STT1; "MPa"
490 MCR=2:MX=MXZ:GOSUB 2000:MCR=0:STT2=INT(EST*EES)
500 PRINT:PRINT "Steel stress after  cracking = ";STT2; "MPa"
510 PRINT "------------------------------------------------------------------"
520 ULT=1:GOSUB 2000:ULT=0
530 PRINT "Ultimate moment Mu  = ", MXX; "kNm":MU=MXX
```

```
540 PRINT "-----------------------------------------------------------------"
550 PRINT "    Select one of the following calculation modes":PRINT
560 PRINT "    1. Forces on transverse section just before cacking (M=Mcr)"
570 PRINT "    2. Forces on transverse section just after  cacking (M=Mcr)"
580 PRINT "    3. Forces on transverse section for any bending moment (M)"
590 PRINT "    4. Bond force near first crack and slip length (M=Mcr)"
600 PRINT "    5. Bond force between cracks (Constant moment region)"
610 PRINT "    6. Bond force between cracks (Varying  moment region)"
620 PRINT "    7. Forces on transverse section for any steel stress (Fs2)"
625 PRINT "    8. EXIT":PRINT
630 PRINT "-----------------------------------------------------------------"
640 'X$="1":'INPUT "Input Option No:
(1/2/3/4/5/6/7/8)",X$:X=VAL(X$):###########
641 INPUT "Input Option No: (1/2/3/4/5/6/7/8)",X$:X=VAL(X$)
650 J=VAL(X$):IF J<1 OR J>8 THEN BEEP:GOTO 640
660 IF J=8 THEN 1640
670 IF R$="R" THEN R$="  (Rectangular section)"
680 IF R$="F" THEN R$="  (Flanged section)"
690 INPUT "File identification number = ",ID$
700 IF ID$="" THEN BEEP:GOTO 690
710 IF LEN(ID$)>2 THEN BEEP:PRINT:PRINT "Invalid ID number...!":PRINT:GOTO
690
720 IF LEN(ID$)<2 THEN ID$="0"+ID$
730 J$=STR$(J):J$=RIGHT$(J$,1):ID$=J$+ID$
740 IF J>1 THEN 800
750 CLS:PRINT:PRINT"-----------------------------------"
760 PRINT" M = Mcr : Just before cracking"
770 PRINT"-----------------------------------"
780 M$="  (Forces on transverse section just before cracking)"
790 MCR=1:MCS=1:GOSUB 2000:GOTO 940
800 IF J>2 THEN 860
810 M$="  (Forces on transverse section just after cracking)"
820 CLS:PRINT:PRINT"-----------------------------------"
830 PRINT" M = Mcr : Just after cracking"
840 PRINT"-----------------------------------"
850 MCR=2:MCS=1:GOSUB 2000:GOTO 940
860 IF J>3 THEN 1060
870 CLS:PRINT
880 PRINT "-----------------------------------------------------------------"
890 PRINT" Mcr = ";MCRR; "kNm"
900 PRINT" Mu  = ";MU  ; "kNm"
910 PRINT "-----------------------------------------------------------------"
920 M$="  (Forces on transverse section for a given moment)"
930 GOSUB 2190
940 PRINT"End of Solution"
950 PRINT "-----------------------------------------------------------------"
960 IF J<>2 AND J<>3 AND J<>7 THEN 970:'PRINT FZ,FZ1
961 INPUT "Press RETURN Key",X$
962 PRINT "Elastic Modulii":PRINT "_____________________":PRINT
963 FOR I=1 TO N3:PRINT "Row -";I;"  ";ECX(I):NEXT
970 INPUT "Press RETURN Key",X$:XINP=1
980 IF J<3 THEN GOSUB 7430:GOTO 1030
990 IF J=3 THEN GOSUB 7770:GOTO 1030
991 IF J=7 THEN GOSUB 8750:GOTO 1030
1000 IF J>3 THEN GOSUB 8070:GOTO 1030
1010 REM:GOSUB 8900
1020 GOSUB 7660:STOP:REM
1030 'GOTO 180
1031 RUN
1040 PRINT:INPUT "Option (1/2/3) ",X$
1050 X=VAL(X$):IF X<1 OR X>3 THEN BEEP:GOTO 1040
1060 IF J>4 THEN 1140
1070 CLS
1080 PRINT "-----------------------------------------------------------------"
1090 PRINT"Steel stress before cracking = ";STT1; "  (MPa)"
1100 PRINT"Steel stress after  cracking = ";STT2; "  (MPa)"
1110 PRINT "-----------------------------------------------------------------"
```

```
1120 M$="  (Slip length and bond force near the first flexural crack)"
1130 BND=0:S1=STT1:S2=STT2:GOSUB 4090: GOTO 1240
1140 IF J>5 THEN 1250
1150 M$="  (Bond force between cracks -Constant moment region)"
1160 PRINT:INPUT "Steel stress at the cracked section (MPa) = ",X$
1170 X=VAL(X$):IF X<=0 THEN BEEP : GOTO 1160
1180 STT=X
1190 PRINT:INPUT "Half crack spacing  (mm)           = ",X$:PRINT
1200 X=VAL(X$):IF X<=0 THEN BEEP : GOTO 1190
1210 LL=X:S2=STT
1220 BND=1:GOSUB 4090
1230 REM
1240 PRINT:GOTO 940
1250 IF J>6 THEN 1640
1260 M$="  (Bond force between cracks -Varying moment region)"
1270 'BND=3:LL=200:S2=200:S3=190:GOSUB 8500:STOP
1280 PRINT:INPUT "Steel stress at the first cracked section (MPa) = ",X$
1290 X=VAL(X$):IF X<=0 THEN BEEP : GOTO 1280
1300 S1=X
1310 PRINT:INPUT "Steel stress at the second cracked section (MPa) = ",X$
1320 X=VAL(X$):IF X<=0 THEN BEEP : GOTO 1310
1330 S2=X
1340 PRINT:INPUT "Crack spacing  (mm)           = ",X$
1350 X=VAL(X$):IF X<=0 THEN BEEP : GOTO 1340
1360 PRINT "-------------------------------------------------------"
1370 PRINT "Crack spacing  (mm)  =", X
1380 LLX=X
1390 S3=S2:IF S3<S1 THEN S3=S1
1400 S4=S2:IF S4>S1 THEN S4=S1
1410 S1=S3:S2=S4
1420 BNDX=1:LMIN=10:LMAX=LLX
1430 BND=1:LX=LLX/2
1440 S2=S3
1450 LL=LX:GOSUB 4190:SX=S1:FBX=(INT(FB*10000))/10000
1460 LY=LLX-LX
1470 S2=S4
1480 LL=LY:GOSUB 4190:SY=S1:FBY=(INT(FB*10000))/10000
1490 FAC=SX/SY:'PRINT SX,SY,FAC:STOP
1500 IF FAC<TOL1 THEN LMAX=LX:GOTO 1530
1510 IF FAC>TOL2 THEN LMIN=LX:GOTO 1530
1520 GOTO 1550
1530 LX=(LMIN+LMAX)/2:GOTO 1440
1540 PRINT LX,LY,SX,SY:STOP
1550 SX=INT(S1)
1560 PRINT "S1 = ";S3; "(MPa)";":  S2 = ";S4;"(MPa)";": S-min = ";SX;
"(MPa)"
1570 PRINT "Zero-slip point is "; INT(LX); "mm away from the crack that"
1580 PRINT "has the steel stress of";S3;" MPa"
1590 PRINT "Bond stresses: Fb1 = ";FBX;" MPa  : Fb2 = "; FBY;" MPa"
1600 PRINT "-------------------------------------------------------"
1610 NX=LX/LLX*10:N1=INT(NX)
1620 FB=FBX:L=LX:GOSUB 4760
1630 'STOP
1640 IF J>7 THEN 1990
1641 M$="  (Forces on transverse section for a given steel stress)"
1650 CLS:PRINT
1660 PRINT "-------------------------------------------------------"
1670 PRINT" Fs1 = ";STT1; "MPa"
1680 PRINT" Fs2 = ";STT2; "MPa"
1690 PRINT "-------------------------------------------------------"
1700 M$="  (Forces on transverse section for a given moment)"
1710 PRINT:INPUT "Steel stress at the cracked section (MPa) = ",X$
1720 X=VAL(X$):IF X>400 THEN 1710
```

```
1721 EAX=X/EES
1730 F1MAX=1
1740 F1MIN=.01
1750 F1=F1MIN
1760 GOSUB 2610
1770 FAC=LH/RH:'PRINT FAC
1780 IF FAC>TOL2 THEN F1MAX=F1:GOTO 1810
1790 IF FAC<TOL1 THEN F1MIN =F1:GOTO 1810
1800 GOSUB 5210:GOTO 940
1810 F1=(F1MIN+F1MAX)/2:GOTO 1760
1990 CLS:SYSTEM:END
2000 REM ************************************************************
2010 E2MAX=.01
2020 E2MIN=ER
2030 E2=E2MIN
2040 IF MCR=1 THEN E2=ER
2050 IF MCR=2 THEN E2=.003
2060 'IF ULT=1 THEN E2=.0035
2070 F1MAX=1
2080 F1MIN=.01
2090 F1=F1MIN
2100 GOSUB 2610
2110 FAC=LH/RH
2120 IF FAC>TOL2 THEN F1MAX=F1:GOTO 2550
2130 IF FAC<TOL1 THEN F1MIN=F1:GOTO 2550
2140 GOSUB 3050
2150 MXY=MM*BB*D*D*FC/1000000!:MXX=INT(MXY):IF MCR=1 THEN MXZ=MXY
2160 IF MCR=2 THEN M0=MX*1000000!/(BB*D*D*FC):GOTO 2340
2170 IF MCS=1 THEN 5210:REM 60
2180 RETURN
2190 INPUT "bending moment (kNm) = ", MX
2200 IF MX>.9*MU THEN TOL1=.99:TOL2=1.01
2210 IF MX>MU THEN TOL1=.9:TOL2=1.1
2220 PRINT "-----------------------------------------------------------"
2230 M0=MX*1000000!/(BB*D*D*FC):'PRINT M0:STOP
2240 IF MX=0 THEN BEEP:GOTO 2190
2250 'IF MX>MCRR/2 THEN 1790
2260 IF MX>0 THEN 2300
2270 BEEP:PRINT:PRINT"Moment too small ....! ":PRINT
2280 INPUT "Press RETURN KEY  ",X$:PRINT:PRINT
2290 GOTO 2190
2300 IF MX<MU THEN 2340
2310 BEEP:PRINT:PRINT"Moment too large ....! ":PRINT
2320 INPUT "Press RETURN KEY  ",X$:PRINT:PRINT
2330 GOTO 2190
2340 IF MX<=MCRR THEN E2MAX=ER:E2MIN=0:E2=E2MAX
2350 IF MX>MCRR THEN E2MAX=.004:E2MIN=ER:E2=E2MAX
2360 F1MAX=1
2370 F1MIN=.1
2380 F1=F1MIN
2390 GOSUB 2610
2400 FAC=LH/RH:'PRINT FAC
2410 IF FAC>TOL2 THEN F1MAX=F1:GOTO 2480
2420 IF FAC<TOL1 THEN F1MIN=F1:GOTO 2480
2430 GOSUB 3050:FAC1=MM/M0:'PRINT E2,E2MAX,FAC1:IF MX>390 THEN STOP
2440 IF FAC1<TOL1 THEN E2MIN=E2:GOTO 2470
2450 IF FAC1>TOL2 THEN E2MAX=E2:GOTO 2470
2460 GOTO 2570
2470 E2=(E2MIN+E2MAX)/2:GOTO 2360
2480 F1=(F1MIN+F1MAX)/2
2490 GOTO 2390
2500 FAC1=MM/M0:STOP:'GOTO 5390
2510 IF FAC1<TOL1 THEN E2MIN=E2:GOTO 2540
2520 IF FAC1>TOL2 THEN E2MAX=E2:GOTO 2540
2530 GOTO 2570
2540 E2=(E2MIN+E2MAX)/2:GOTO 2070
2550 F1=(F1MIN+F1MAX)/2
2560 GOTO 2100
```

```
2570 'PRINT MM:STOP:GOTO 1040
2580 IF MCR=2 AND MCS=0 THEN RETURN
2590 'GOTO 60
2600 GOTO 5210
2610 REM ************************************************************
2620 K2=F1
2630 K1=BE-K2
2640 E1=K2/K1*E2
2650 IF ULT=1 THEN E1=.0035:E2=K1/K2*E1
2660 IF J<7 THEN 2690
2670 E2=EAX*(BE-K2)/(1-K2)
2680 E1=EAX*K2/(1-K2)
2690 Z=E1/E0
2700 K3=K2-HF1
2710 X0=K2/Z
2720 K4=K1-HF2
2730 IF E1>E0 THEN 2800
2740 FC1=K2*(Z-Z^2/3)
2750 FC2=0:IF BX1=1 THEN 2780
2760 IF K2<=HF1 THEN FC1=FC1*BX1:GOTO 2780
2770 FC2=(BX1-1)*(Z/K2*(K2^2-K3^2)-Z^2*(K2^3-K3^3)/(3*K2^2))
2780 FCC=FC1+FC2
2790 GOTO 2920
2800 FC11=2*K2/(3*Z)
2810 FC12=K2*(1-1/Z)*(1-41*(E1-E0))
2820 FC1=FC11+FC12
2830 FC2=0:IF BX1=1 THEN 2910
2840 IF K2<=HF1 THEN FC1=FC1*BX1:GOTO 2910
2850 IF X0<K3 THEN 2900
2860 FC21=(BX1-1)*(Z/K2*(X0^2-K3^2)-Z^2/(3*K2^2)*(X0^3-K3^3))
2870 FC22=(BX1-1)*K2*(1-1/Z)*(1-41*(E1-E0))
2880 FC2=FC21+FC22
2890 GOTO 2910
2900 FC2=(BX1-1)*(1-41*(E1*(1+K3/K2)-2*E0))*HF1
2910 FCC=FC1+FC2
2920 FRX=FR:A=(ER/E2)*K1:IF A>K1 THEN FRX=FR/A*K1:A=K1
2930 FT1=(A/2)*(FRX/FC)
2940 FT2=0:IF A<=K4 THEN 2970
2950 IF BX2=1 THEN 2970
2960 FT2=(BX2-1)*(A-K4)*(K4/A+1)*FRX/(2*FC)
2970 FT=FT1+FT2
2980 ESD=(E1/K2)*(K2-DD):IF ESD>.002 THEN ESD=.002
2990 FSD=ROD*(EES/FC)*ESD
3000 EST=E2*(1-K2)/K1:IF EST>.002 THEN EST=.002
3010 FST=RO*(EES/FC)*EST
3020 RH=FT+FST
3030 LH=FCC+FSD
3040 RETURN
3050 IF E1>E0 THEN 3110
3060 MC1=K2^2*(2*Z/3-Z^2/4)
3070 MC2=0:IF BX1=1 THEN 3100
3080 IF K2<=HF1 THEN MC1=MC1*BX1:GOTO 3100
3090 MC2=(BX1-1)*(2*Z/(3*K2)*(K2^3-K3^3)-Z^2/(4*K2^2)*(K2^4-K3^4))
3100 MC=MC1+MC2:GOTO 3270
3110 MC11=5*K2^2/(12*Z^2)
3120 MC121=(1-83*(E1-E0))*(K2-X0)*(K2+X0)/2
3130 MC122=41.5*(E1-E0)*(K2-X0)*(K2/3+2*X0/3)
3140 MC1=MC11+MC121+MC122
3150 MC2=0:IF BX1=1 THEN 3260
3160 IF K2<=HF1 THEN MC1=MC1*BX1:GOTO 3260
3170 IF X0<K3 THEN 3230
3180 MC21=(BX1-1)*(2*Z/(3*K2)*(X0^3-K3^3)-Z^2/(4*K2^2)*(X0^4-K3^4))
3190 MC221=(BX1-1)*(1-83*(E1-E0))*(K2-X0)*(K2+X0)/2
3200 MC222=41.5*(BX1-1)*(E1-E0)*(K2-X0)*(K2/3+2*X0/3)
3210 MC2=MC21+MC221+MC222
3220 GOTO 3260
3230 MC21=(BX1-1)*(1-83*(E1-E0))*(K2-HF1/2)*HF1
3240 MC22=41.5*(BX1-1)*(E1-E1*K3/K2)*(K3+HF/3)*HF1
3250 MC2=MC21+MC22
```

```
3260 MC=MC1+MC2
3270 MT1=(A^2/3)*(FRX/FC)
3280 MT2=0:IF BX2=1 THEN 3320
3290 IF A<=K4 THEN 3320
3300 MT21=(BX2-1)*(FRX/FC)*(K4/A)*(A-K4)*(A+K4/2)
3310 MT22=(BX2-1)*(FRX/FC)*(1-K4/A)*(A-K4)*(2*A/3+K4/3)/2
3320 MT=MT1+MT2
3330 MSD=FSD*(K2-DD)
3340 MST=FST*(1-K2)
3350 MM=MC+MT+MSD+MST
3360 RETURN
3370 REM ************************************************************
3380 PI=3.14159
3390 CLS:PRINT:PRINT "Input Beam properties":PRINT
3400 INPUT "Flanged beam or rectangular beam (F/R)", X$
3410 IF X$="F" OR X$="f" THEN R$="F": GOTO 3440
3420 IF X$="R" OR X$="r" THEN R$="R": GOTO 3550
3430 BEEP:GOTO 3400
3440 INPUT "Top flange width = ",XBX1:IF XBX1=0 THEN BEEP:GOTO 3440
3450 INPUT "Top flange depth = ",XHF1:IF XHF1=0 THEN BEEP:GOTO 3450
3460 INPUT "Bottom flange present (Y/N) ",X$
3470 IF X$ =  "y" OR X$ = "Y" THEN 3500
3480 IF X$ = "n" OR X$ = "N" THEN 3520
3490 BEEP:GOTO 3460
3500 INPUT "Bottom flange width = ",XBX2:IF XBX2=0 THEN BEEP:GOTO 3500
3510 INPUT "Bottom flange depth = ",XHF2:IF XHF2=0 THEN BEEP:GOTO 3510
3520 INPUT "Web width (b) = ",BB:IF BB=0 THEN BEEP:GOTO 3520
3530 GOTO 3560
3540 'CLS:PRINT:PRINT "Input Beam properties":PRINT
3550 INPUT "Beam width (b) = ",BB:IF BB=0 THEN BEEP: GOTO 3550
3560 INPUT "Effective depth (d) = ",D:IF D=0 THEN BEEP: GOTO 3560
3570 INPUT "Overall height (h) = ",H:IF H=0 THEN BEEP: GOTO 3570
3580 INPUT "Tensile Steel :Bar diameter   = ",DIA:IF DIA=0 THEN BEEP:GOTO
3580
3590 INPUT "               Number of bars = ",NB:IF NB=0 THEN BEEP:GOTO
3590
3600 INPUT "Compression steel present (y/n) ",X$
3610 IF X$ =  "y" OR X$ = "Y" THEN 3640
3620 IF X$ = "n" OR X$ = "N" THEN 3670
3630 BEEP: GOTO 3600
3640 INPUT "Comp. Steel :Bar diameter   = ",DIA1:IF DIA1=0 THEN BEEP:GOTO
3640
3650 INPUT "             Number of bars = ",NB1:IF NB1=0 THEN BEEP:GOTO
3650
3660 INPUT "             Depth to steel = ",XDD:IF XDD=0 THEN BEEP:GOTO
3660
3670 INPUT "Concrte Strength = ",FC:IF FC=0 THEN BEEP:GOTO 3670
3680 CLS:PRINT:PRINT "Beam properties":PRINT
3690 IF XBX1=0 THEN 3720
3700 PRINT "Top flange width = ",XBX1
3710 PRINT "Top flange depth = ",XHF1
3720 IF XBX2=0 THEN 3780
3730 PRINT "Bottom flange width = ",XBX2
3740 PRINT "Bottom flange depth = ",XHF2
3750 PRINT "Web width (b) = ",BB
3760 PRINT "Overall height (h) = ",H
3770 GOTO 3790
3780 PRINT "Beam width b = ",BB
3790 PRINT "Effective depth d = ",D
3800 PRINT "Overall heighth (h) = ",H
3810 PRINT
3820 PRINT "Tensile Steel :Bar diameter   = ",DIA
3830 PRINT "               Number of bars = ",NB
3840 IF DIA1=0 THEN 3880
3850 PRINT "Comp. Steel :Bar diameter   = ",DIA1
3860 PRINT "             Number of bars = ",NB1
3870 PRINT "             Depth to steel = ",XDD
3880 PRINT "Concrete strength = ",FC
```

```
3890 'X$="y":'PRINT:PRINT:INPUT"Accept above data (Y/N) ",
X$:##################
3891 PRINT:PRINT:INPUT"Accept above data (Y/N) ", X$
3900 IF X$="y" OR X$="Y" THEN 3930
3910 IF X$="n" OR X$="N" THEN RUN
3920 BEEP:GOTO 3890
3930 XQ$="":'PRINT:INPUT "File name to save data (RETURN - no save) :",
XQ$:###
3940 IF XQ$="" THEN XQ$="Temp"
3950 XP$=XQ$
3960 GOSUB 6730
3970 IF XBX1=0 THEN BX1=1
3980 IF XBX1>0 THEN BX1=XBX1/BB
3990 IF XBX2=0 THEN BX2=1
4000 IF XBX2>0 THEN BX2=XBX2/BB
4010 HF1=XHF1/D
4020 HF2=XHF2/D
4030 DD=XDD/D
4040 B=BB
4050 AT=PI/4*DIA^2*NB:RO=AT/(BB*D)
4060 AC=PI/4*DIA1^2*NB1:ROD=AC/(BB*D)
4070 GOSUB 6850
4080 RETURN
4090 REM ************************************************************
4100 LMIN=10
4110 LMAX=1000
4120 L=LMIN
4130 IF BND<3 THEN 4190
4140 L=LL-10:S1=0:SMIN=S1:SMAX=S2
4150 GOSUB 4410
4160 IF FAC>TOL2 THEN SMIN=S1:GOTO 4290
4170 IF FAC<TOL1 THEN SMAX=S1:GOTO 4290
4180 'STOP
4190 IF BND=1 THEN L=LL:S1=0:SMIN=S1:SMAX=S2
4200 GOSUB 4410
4210 IF BND=1 THEN 4250
4220 IF FAC>TOL2 THEN LMIN=L:GOTO 4280
4230 IF FAC<TOL1 THEN LMAX=L:GOTO 4280
4240 GOTO 4320
4250 IF FAC>TOL2 THEN SMIN=S1:GOTO 4290
4260 IF FAC<TOL1 THEN SMAX=S1:GOTO 4290
4270 GOTO 4320
4280 L=(LMIN+LMAX)/2:GOTO 4310
4290 S1=(SMIN+SMAX)/2:IF S1<1 THEN 5170
4300 IF BND=3 THEN 4150
4310 GOTO 4200
4320 IF BNDX=1 THEN RETURN
4330 IF BND=1 THEN 4360
4340 PRINT USING "Slip Length   (mm) = ####";L
4350 GOSUB 4560:RETURN
4360 PRINT "-----------------------------------------------------------"
4370 PRINT USING "Half crack spacing  (mm) = ####";L
4380 PRINT USING "Steel stress at cracked section = ####";S2
4390 PRINT USING "Steel stress at zero-slip point = ####";S1
4400 GOSUB 4560:RETURN
4410 REM
************************************************************
4420 FB=(S2-S1)*DIA*3/(8*L)
4430 ES0=S2*L/(2*EES)-13*FB*L^2/(12*EES*DIA):'PRINT FB,L:STOP
4440 ECC0=(2.5*L/D-.5)*D/100
4450 ECB0=(1.3*L/D-.5)*L/100*FB*4*RO*D/DIA
4460 EC0=ECC0+ECB0:EC0=EC0/1000:IF EC0<0 THEN EC0=0
4470 S0=ES0-EC0:IF S0<0 THEN S0=0
4480 IF S0<.004 THEN FBS=150*S0:GOTO 4510
4490 IF S0>.01 THEN FBS=.71+9*S0:GOTO 4510
4500 FBS=.47+33*S0
4510 FBS=FBS*(FC^.5):RED=1:IF .5*L<4*DIA THEN RED=.5*L/(4*DIA)
4520 FBS=FBS*RED:IF FBS=0 THEN FBS=.001
4530 FAC=FB/FBS
```

```
4540 RETURN
4550 REM ************************************************************
4560 PRINT USING "Peak bond stress   (MPa)  = ##.##";FB
4570 PRINT "-------------------------------------------------------"
4580 PRINT" Node No.    Bond force (N/mm)
4590 PRINT" --------    ----------------
4600 FOR I = 1 TO 11:LL=L/10
4610 A=(I-1.5)*LL
4620 B=(I-.5)*LL
4630 IF I =1 THEN A=0
4640 IF I=11 THEN B=L
4650 BF(I)=4*FB*PI*DIA*((B^2-A^2)/(2*L)-(B^3-A^3)/(3*L^2))
4660 NEXT
4670 FOR I=1 TO 11:PRINT USING "   ###        ";44+I;
4680 BF(I)=BF(I):PRINT USING " ####.#";BF(I)*NB/BB
4690 NEXT:'BF(I)=INT(BF(I)):NEXT
4700 FBB=O:FOR K=1 TO 11:FBB=FBB+BF(K):NEXT:'PRINT FBB
4710 FBB=2/3*PI*DIA*FB*L:'PRINT FBB
4720 RETURN
4730 REM ************************************************************
4740 NZ=NX-N:PRINT NZ:STOP
4750 PRINT "-------------------------------------------------------"
4760 PRINT:PRINT" Node No.    Bond force (N/mm)
4770 PRINT" --------    ----------------
4780 'GOSUB 9000:STOP
4790 S=LLX/10:LY=LLX-LX
4800 M0=LX/S:N0=INT(M0):X0=(M0-N0)*S
4810 IF M0>1 THEN 4850
4820 IF X0>.5*S THEN 4840
4830 N1=1:A(1)=0:B(1)=LX:GOTO 4920
4840 N1=2:A(1)=0:B(1)=.5*S:A(2)=B(1):B(2)=LX:GOTO 4920
4850 N1=1:A(1)=0:B(1)=.5*S
4860 FOR I=2 TO N0:A(I)=B(I-1):B(I)=A(I)+S:NEXT
4870 N1=N0+1:A(N1)=B(N1-1)
4880 IF X0<.5*S THEN B(N1)=LX:GOTO 4920
4890 B(N1)=A(N1)+S
4900 N1=N1+1:A(N1)=B(N1-1)
4910 B(N1)=LX:'PRINT N1,A(N1),B(N1)
4920 'PRINT "Length = ";LLX; "  : Lx = ";LX
4930 'FOR I =1 TO N1:PRINT I,A(I),B(I):NEXT
4940 FOR I=1 TO N1:A=A(I):B=B(I)
4950 BF(I)=4*FBX*PI*DIA*((B^2-A^2)/(2*LX)-(B^3-A^3)/(3*LX^2)):NEXT
4960 REM ************************************
4970 Y0=S-X0
4980 IF M0>9.5 THEN X(11)=0:Y(11)=LY:GOTO 5050
4990 IF Y0>.5*S THEN Z0=Y0-.5*S
5000 IF M0>9 THEN X(10)=0:Y(10)=Z0:X(11)=Y(10):Y(11)=LY:GOTO 5050
5010 IF Y0<.5*S THEN X(N1)=0:Y(N1)=Y0+S/2:GOTO 5030
5020 X(N1)=0:Y(N1)=Z0
5030 FOR I=N1+1 TO 10:X(I)=Y(I-1):Y(I)=X(I)+S:NEXT
5040 X(11)=Y(10):Y(11)=X(11)+S/2
5050 'FOR I=N1 TO 11:PRINT I,X(I),Y(I):NEXT
5060 I=N1:A=X(I):B=Y(I)
5070 BF(I)=BF(I)-4*FBY*PI*DIA*((B^2-A^2)/(2*LY)-(B^3-A^3)/(3*LY^2))
5080 FOR I=N1+1 TO 11:A=X(I):B=Y(I)
5090 BF(I)=-4*FBY*PI*DIA*((B^2-A^2)/(2*LY)-(B^3-A^3)/(3*LY^2)):NEXT
5100 'PRINT "*************************"
5110 BF(I)=BF(I)*NB/BB
5120 FF=0:FOR I=1 TO 11
5130 PRINT 44+I,INT(BF(I)*NB/BB*10)/10:FF=FF+BF(I)*NB/BB:NEXT:PRINT
5140 FG=2/3*PI*DIA*(FBX*LX-FBY*LY)*NB/BB:'PRINT INT(FG*10)/10
5150 'RETURN
5160 GOTO 940
5170 BEEP:PRINT:REM ************************************************
5180 PRINT "-------------------------------------------------------"
5190 PRINT "Crack specing is too large for the selected steel stress..!"
5200 PRINT:INPUT "Press RETURN Key ",X$: GOTO 1640
```

```
5210 REM ***************************************************
5220 K1=A:K1=K1/BE:K2=K2/BE:K11=K1:K22=K2
5230 FOR I=1 TO 6:S(I)=.075:NEXT
5240 FOR I=7 TO 12:S(I)=.05:NEXT
5250 S=.075
5260 IF K2<=.5*S THEN N3=1:A(1)=0:B(1)=K2:GOTO 5420
5270 IF K2<S THEN N3=2:A(1)=0:B(1)=K2-S/2:A(2)=B(1):B(2)=K2:GOTO 5420
5280 IF K2<=.45 THEN M0=K2/.075:N0=INT(M0):X0=(M0-N0)*.075:GOTO 5310
5290 IF K2<=.75 THEN M0=(K2-.45)/.05:N0=INT(M0):X0=(M0=N0)*.05:N0=N0+6:GOTO
5310
5300 PRINT:PRINT "Unacceptable k2.......!":STOP
5310 SA=S(N0+1): SB=S(N0)
5320 IF X0>SA/2 THEN 5390
5330 N3=1:A(N3)=0:B(N3)=X0+SB/2
5340 IF B(N3)>K2-.075 THEN N3=N3+1:A(N3)=B(N3-1):B(N3)=K2:GOTO 5420
5350 N3=N3+1:N0=N0-1
5360 SA=S(N0+1):SB=S(N0)
5370 A(N3)=B(N3-1):B(N3)=A(N3)+SA/2+SB/2
5380 GOTO 5340
5390 N3=1:A(1)=0:B(1)=X0-SA/2
5400 N3=N3+1:A(N3)=B(N3-1):B(N3)=A(N3)+SA/2+SB/2
5410 GOTO 5340
5420 REM
5430 REM ***********************************************************
5440 PRINT:PRINT"Node No       Force (N/mm)
5450 PRINT"-------       ------------"
5460 IF BX1=1 THEN HF1=.2
5470 IF BX2=1 THEN HF2=.1
5480 IC=0:FF=0:FOR I=1 TO N3:A=A(I):B=B(I):IC=IC+1
5490 EA=E1/K2*A:EB=E1/K2*B
5491 EEX=(EA+EB)/2
5492 EE=EEX/E0
5493 IF EE<1 THEN FCX=FC*(2*EE-EE^2)
5494 IF EE>=1 THEN FCX=FC*(1-83*(EE-1))
5495 ECX(N3+1-IC)=FCX/EEX:'PRINT ECX:STOP
5500 HF11=HF1/BE:HF21=HF2/BE
5510 K3=K2-HF11:K4=1-K2-HF21:'STOP
5520 Z=E1/(E0*K2)
5530 IF EA>E0 THEN 5660
5540 IF EB>E0 THEN 5770
5550 IF K2<=HF11 THEN B1=BX1:GOTO 5590
5560 IF B<=K3 THEN B1=1:GOTO 5590
5570 IF A>=K3 THEN B1=BX1:GOTO 5590
5580 GOTO 5610
5590 F=Z*(B^2-A^2)-Z^2*(B^3-A^3)/3:'PRINT F:STOP
5600 F=F*B1:GOTO 5980
5610 C=K3
5620 F1=Z*(C^2-A^2)-Z^2*(C^3-A^3)/3
5630 F2=Z*(B^2-C^2)-Z^2*(B^3-C^3)/3
5640 F=F1+F2*BX1
5650 GOTO 5980
5660 IF K2<=HF11 THEN B1=BX1:GOTO 5700
5670 IF B<=K3 THEN B1=1:GOTO 5700
5680 IF A>=K3 THEN B1=BX1:GOTO 5700
5690 GOTO 5720
5700 F=(B-A)*(1-41.5*(EA+EB-2*E0))
5710 F=F*B1:GOTO 5980
5720 EC=K2/E1*E0
5730 C=K3
5740 F1=(C-A)*(1-41.5*(EA+EC-2*E0))
5750 F2=(B-C)*(1-41.5*(EC+EB-2*E0))
5760 F=F1+F2*BX1:GOTO 5980
5770 C=K2/E1*E0
5780 IF K2<=HF11 THEN B1=BX1:GOTO 5820
5790 IF B<=K3 THEN B1=1:GOTO 5820
5800 IF A>=K3 THEN B1=BX1:GOTO 5820
5810 GOTO 5860
```

```
5820 F1=Z*(C^2-A^2)-Z^2*(C^3-A^3)/3
5830 F2=(B-C)*(1-41.5*(E0+EB-2*E0))
5840 F=F1+F2
5850 F=F*B1:GOTO 5980
5860 C1=K3:C2=E0/E1*K2
5870 IF C2>C1 THEN 5930
5880 F1=Z*(C2^2-A^2)-Z^2*(C2^3-A^3)/3
5890 EC1=K3/K2*E1
5900 F21=(C1-C2)*(1-41.5*(EC1+E0-2*E0))
5910 F22=(B-C1)*(1-41.5*(EC1+EB-2*E0))
5920 F=F1+F21+F22*BX1:GOTO 5980
5930 EC1=K3/K2*E1
5940 F11=Z*(C1^2-A^2)-Z^2*(C1^3-A^3)/3
5950 F12=Z*(C2^2-C1^2)-Z^2*(C2^3-C1^3)/3
5960 F2=(B-C2)*(1-41.5*(EB+E0-2*E0))
5970 F=F11+(F12+F2)*BX:GOTO 5980
5980 F(I)=F*FC*D*BE:FF=FF+F(I):NEXT:'PRINT I,F(I):FF=FF+F(I):NEXT
5990 FFX=Z*(B(N3))^2-Z^2*(B(N3))^3/3:IF E1<=E0 THEN 6040
6000 X=E0/E1*K2
6010 FFX1=Z*X^2-Z^2*X^3/3
6020 FFX2=(K2-X)*(1-41.5*(E1-E0))
6030 FFX=FFX1+FFX2
6040 FFX=FFX*FC*D*BE:'PRINT "***";FFX,FF
6050 N1=M1+M2+M3+M4:'PRINT N1:STOP
6060 FOR I=1 TO 6:S(I)=.075:NEXT
6070 FOR I=7 TO 12:S(I)=.05:NEXT
6080 FOR I=13 TO 16:S(I)=.0375:NEXT
6090 FOR I=17 TO 24:S(I)=.0125:NEXT
6100 FOR I=1 TO 20:A(I)=0:B(I)=0:NEXT
6110 REM
6120 IF K2<.45 THEN M0=K2/.075:N0=INT(M0):X0=(M0-N0)*.075
6130 IF K2>.45 THEN M0=(K2-.45)/.05:N0=INT(M0):X0=(M0-N0)*.05:N0=N0+6
6140 SA=S(N0+1):SB=S(N0+2)
6150 IF X0>.5*SA THEN 6260
6160 XZ1=.5*SA-X0
6170 IF X0+K11<=.5*SA THEN N1=1:A(1)=0:B(1)=11:GOTO 6360
6180 N1=1:A(1)=0:B(1)=XZ1
6190 N1=N1+1:A(N1)=B(N1-1)
6200 XP=A(N1)+.5*SA+.5*SB
6210 IF N0=23 THEN B(N1)=K11:GOTO 6360
6220 IF XP>K11 THEN B(N1)=K11:GOTO 6360
6230 B(N1)=XP
6240 N0=N0+1
6250 SA=S(N0+1):SB=S(N0+2):GOTO 6190
6260 N1=1:A(1)=0:X1=SA-X0
6270 IF X1+.5*SB>K11 THEN B(1)=K11:GOTO 6360
6280 B(1)=X1+.5*SB
6290 N1=N1+1:A(N1)=B(N1-1)
6300 N0=N0+1:SA=S(N0+1):SB=S(N0+2)
6310 XP=A(N1)+.5*SA+.5*SB
6320 IF N0=23 THEN B(N1)=K11:GOTO 6360
6330 IF XP>K11 THEN B(N1)=K11:GOTO 6360
6340 B(N1)=XP
6350 GOTO 6290
6360 NN=N1:'GOTO 7610
6370 FOR I=1 TO NN:EX=E1/K2*A(I):EY=E1/K2*B(I)
6380 F1=EX/ER*FR:F2=EY/ER*FR:REM $$$$$$$$$$$$$$$$$$$$$$$$$$$$$
6390 A=A(I):B=B(I)
6400 IF B<K4 THEN B1=1:GOTO 6430
6410 IF A>K4 THEN B1=BX2:GOTO 6430
6420 GOTO 6460
6430 FZ=(F1+F2)/2*(B-A)*D*BE
6440 FT(I)=FZ*B1
6450 GOTO 6530
6460 C=K4
6470 EC=E1/K2*K4
6480 F3=EC/ER*FR
```

```
6490 FZ1=(F1+F3)/2*(C-A)
6500 FZ2=(F3+F2)/2*(B-C)
6510 FZ=FZ1+FZ2*BX2
6520 FT(I)=FZ*D*BE
6530 NEXT
6540 FTX=0:FOR I=1 TO NN:FTX=FTX+FT(I):NEXT
6550 FTY=E1/K2*(KA-K2)*FR/ER*(KA-K2)/2*D*BE:'PRINT
"&&&&";FTX,FTY:PRINT:'STOP
6560 NN0=275:IF J=1 THEN NN0=265
6570 FOR I=1 TO N3:ND(I)=NN0-11*(I-1):FF(I)=-F(N3+1-I):NEXT
6580 FF(N3)=FF(N3)+FT(1)
6590 FOR I=2 TO NN:ND(N3+I-1)=NN0-(N3+I-2)*11:FF(N3+I-1)=FT(I):NEXT
6600 FZ=0:FOR I=1 TO N3+NN-1:PRINT ND(I),INT(FF(I)*10/10)
6610 IF I=15 THEN INPUT "More...",X$
6620 FZ=FZ+FF(I)
6630 IF FF(I)<0 THEN F7=F7+FF(I):'PRINT "*****";F7:STOP
6640 IF FF(I)>0 THEN F8=F8+FF(I)
6650 NEXT:FZ1=PI/4*DIA*DIA*NB/BB*EST*EES:'PRINT FZ,FZ1:'STOP
6660 FZ1=FZ1-PI/4*DIA1*DIA1*NB1/BB*ESD*EES:'PRINT FZ,FZ1:'STOP
6670 'PRINT FCC*FC*D/F7,FT*FC*D/F8:STOP:GOTO 630
6680 RETURN:'STOP:GOTO 940
6690 F=RO*BB*D*400
6700 X=F/(.85*FC*BB*BX1)
6710 Z=D-X/2
6720 M=F*Z/1000000!
6730 X$=XQ$+".dat"
6740 OPEN "o" ,1, X$
6750 WRITE #1, "beam Name = ";XQ$,R$
6760 B=BB:BX1=XBX1/BB:HF1=XHF1/D:BX2=XBX2/BB:HF2=XHF2/D:DD=XDD/D
6770 WRITE#1, B,H,D,BX1,HF1,BX2,HF2,DIA,NB,DIA1,NB1,DD,FC
6780 CLOSE:RETURN
6790 X$=XP$+".dat"
6800 OPEN "i" ,1, X$
6810 INPUT #1, X$,X$,R$
6820 INPUT#1, B,H,D,BX1,HF1,BX2,HF2,DIA,NB,DIA1,NB1,DD,FC
6830 BB=B:XBX1=BX1*BB:XHF1=HF1*D:XBX2=BX2*BB:XHF2=HF2*D:XDD=DD*D
6840 CLOSE:RETURN
6850 IF WR=0 THEN RETURN
6860 XR$=XP$+".pro"
6870 OPEN "o",1, XR$
6880 PRINT #1, "Beam Name = ";XP$:PRINT  #1, ""
6890 PRINT #1, "":PRINT #1, "File name = ";XR$:PRINT #1,""
6900 PRINT #1,"Beam properties"
6910 PRINT #1,"---------------"
6920 PRINT #1,""
6930 IF XBX1=0 THEN 6960
6940 PRINT #1,"Top flange width = ",XBX1
6950 PRINT #1,"Top flange depth = ",XHF1
6960 IF XBX2=0 THEN 7020
6970 PRINT #1,"Bottom flange width = ",XBX2
6980 PRINT #1,"Bottom flange depth = ",XHF2
6990 PRINT #1,"Web width (b) = ",BB
7000 'PRINT #1,"Overall height (h) = ",H
7010 GOTO 7030
7020 PRINT #1,"Beam width b = ",BB
7030 PRINT #1,"Effective depth d = ",D
7040 PRINT #1,"Overall heighth (h) = ",H
7050 PRINT #1, ""
7060 PRINT #1,"Tensile Steel :Bar diameter   = ",DIA
7070 PRINT #1,"               Number of bars = ",NB
7080 IF DIA1=0 THEN 7120
7090 PRINT #1,"Comp. Steel :Bar diameter   = ",DIA1
7100 PRINT #1,"             Number of bars = ",NB1
7110 PRINT #1,"             Depth to steel = ",XDD
7120 PRINT #1,"Concrete strength = ",FC
7130 CLOSE:RETURN
7140 IF WR=0 THEN RETURN
7150 XR$=XP$+".rp"
7160 OPEN "o",1, XR$
```

```
7170 PRINT #1, "Beam Name = ";XP$:PRINT  #1, ""
7180 PRINT #1, "":PRINT #1, "File name = ";XR$:PRINT #1,""
7190 PRINT #1,"Beam properties"
7200 PRINT #1,"---------------"
7210 PRINT #1,""
7220 IF XBX1=0 THEN 7250
7230 PRINT #1,"Top flange width = ",XBX1
7240 PRINT #1,"Top flange depth = ",XHF1
7250 IF XBX2=0 THEN 7310
7260 PRINT #1,"Bottom flange width = ",XBX2
7270 PRINT #1,"Bottom flange depth = ",XHF2
7280 PRINT #1,"Web width (b) = ",BB
7290 'PRINT #1,"Overall height (h) = ",H
7300 GOTO 7320
7310 PRINT #1,"Beam width b = ",BB
7320 PRINT #1,"Effective depth d = ",D
7330 PRINT #1,"Overall heighth (h) = ",H
7340 PRINT #1, ""
7350 PRINT #1,"Tensile Steel :Bar diameter   = ",DIA
7360 PRINT #1,"               Number of bars = ",NB
7370 IF DIA1=0 THEN 7410
7380 PRINT #1,"Comp. Steel :Bar diameter   = ",DIA1
7390 PRINT #1,"             Number of bars = ",NB1
7400 PRINT #1,"             Depth to steel = ",XDD
7410 PRINT #1,"Concrete strength = ",FC
7420 CLOSE:RETURN
7430 IF WR=0 THEN RETURN
7440 'IF MCR=1 THEN X$=XP$+"."+ID$
7450 'IF MCR=2 THEN X$=XP$+".r2"
7460 X$=XP$+"."+ID$
7470 OPEN "o", #1, X$
7480 PRINT #1, "":PRINT #1, "File name = ";X$:PRINT #1,""
7490 PRINT #1, "-----------------------------------"
7500 PRINT #1, "Beam Name = "; XP$;R$:PRINT #1, ""
7510 PRINT #1, "Solution Mode = "; J;M$:PRINT #1, ""
7520 PRINT #1, "-----------------------------------"
7530 IF J=1 THEN PRINT #1, " M = Mcr : Just before cracking"
7540 IF J=2 THEN PRINT #1, " M = Mcr : Just after cracking"
7550 PRINT #1, "-----------------------------------"
7560 PRINT #1, "Input data:"
7570 PRINT #1, "Sectional properties: Read from data file"
7580 PRINT #1, "-----------------------------------"
7590 PRINT #1, "Output results:"
7600 PRINT #1, "Bending moment (Mcr) = ";INT(MX);" (kNm)"
7610 X$="before":IF J=2 THEN X$="after"
7620 PRINT #1, "Steel stress just " ;X$; " cracking = ";INT(EST*EES);"
(MPa)"
7630 PRINT #1, "Nodal forces on transverse section:"
7640 PRINT #1, ""
7650 PRINT #1, "Node No       Force (N/mm)"
7660 PRINT #1, "-------       ------------"
7670 FX=0:FOR I=1 TO N3+NN-1:PRINT #1,
ND(I),INT(FF(I)*10/10):FX=FX+FF(I):NEXT
7680 PRINT #1, "-----------------------------------"
7690 PRINT #1, "Check equilibrium:"
7700 PRINT #1, "Sum of nodal forces = ";INT(FX);" (N/mm)"
7710 FY=PI/4*DIA*DIA*EST*EES*NB/BB
7720 FY=FY-PI/4*DIA1*DIA1*ESD*EES*NB1/BB
7730 PRINT #1, "Force in steel bars/beam width = ";INT(FY);" (N/mm)"
7740 PRINT #1, "-----------------------------------"
7741 PRINT #1, "Elastic Modulii":PRINT #1, "____________________"
7742 FOR I=1 TO N3:PRINT #1, "Row -";I;"  ";INT(ECX(I)):NEXT
7743 PRINT #1, "-----------------------------------"
7750 'GOSUB 8550
7760 CLOSE:RETURN
7770 IF WR=0 THEN RETURN
7780 'X$=XP$+".r3"
7790 X$=XP$+"."+ID$
7800 OPEN "o", #1, X$
```

```
7810 PRINT #1, "":PRINT #1, "File name = ";X$:PRINT #1,""
7820 PRINT #1, "-------------------------------------------------"
7830 PRINT #1, "Beam Name = "; XP$;R$:PRINT #1, ""
7840 PRINT #1, "Solution Mode = "; J;M$:PRINT #1, ""
7850 PRINT #1, "-------------------------------------------------"
7860 PRINT #1, " Mcr = ";MCRR; "kNm"
7870 PRINT #1, " Mu  = ";MU  ; "kNm"
7880 PRINT #1, "-------------------------------------------------"
7890 PRINT #1, "Input data:"
7900 PRINT #1, "Sectional properties: Read from data file"
7910 PRINT #1, "Bending moment at the section = "; MX; " kNm"
7911 PRINT #1, "---------------------------------"
7912 PRINT #1, "Output results:"
7920 PRINT #1, "Stress in tensile steel = "; INT(EST*EES); " MPa"
7930 PRINT #1, "Nodal forces on transverse section:"
7940 PRINT #1, ""
7950 PRINT #1, "Node No       Force (N/mm)"
7960 PRINT #1, "-------       ------------"
7970 FX=0:FOR I=1 TO N3+NN-1:PRINT #1,
ND(I),INT(FF(I)*10/10):FX=FX+FF(I):NEXT
7980 PRINT #1, "---------------------------------"
7990 PRINT #1, "Check equilibrium:"
8000 PRINT #1, "Sum of nodal forces = ";INT(FX);" (N/mm)"
8010 FY=PI/4*DIA*DIA*EST*EES*NB/BB
8020 FY=FY-PI/4*DIA1*DIA1*ESD*EES*NB1/BB
8030 PRINT #1, "Force in steel bars/beam width = ";INT(FY);" (N/mm)"
8040 PRINT #1, "---------------------------------"
8050 'GOSUB 8550
8051 IF J<>2 AND J<>3 AND J<>7 THEN 8060
8053 PRINT #1, "---------------------------------"
8054 PRINT #1, "Elastic Modulii for compression zone"
8055 FOR I=1 TO N3:PRINT #1,"Row - ";I;" ";INT(ECX(N3+1-I)):NEXT
8056 PRINT #1, "---------------------------------"
8060 CLOSE:RETURN
8070 IF WR=0 THEN RETURN
8080 J$=STR$(J):J$=RIGHT$(J$,1)
8090 'X$=XP$+".r"+J$
8100 X$=XP$+"."+ID$
8110 OPEN "o", #1, X$
8120 PRINT #1, "":PRINT #1, "File name = ";X$:PRINT #1,""
8130 PRINT #1, "-------------------------------------------------------------
"
8140 PRINT #1, "Beam Number: ";XP$;R$:PRINT #1, ""
8150 PRINT #1, "Solution mode "; J;M$:PRINT #1, ""
8160 PRINT #1, "-------------------------------------------------------------
"
8170 PRINT #1, "Input data:"
8180 PRINT #1, "Sectional properties: Read from data file"
8190 IF J=4 THEN 8270
8200 IF J=6 THEN 8240
8210 PRINT #1, "Steel stress at the cracked section = ";S2;" MPa"
8220 PRINT #1, "Half crack spacing = ";L;" mm"
8230 GOTO 8270
8240 PRINT #1, "Steel stress at the cracked section = ";S3;" MPa"
8250 PRINT #1, "Steel stress at the adjacent cracked section = ";S2;" MPa"
8260 PRINT #1, "Crack spacing  = ";LLX; " mm"
8270 PRINT #1, "-------------------------------------------------------------
"
8280 PRINT #1, "Output results:"
8290 IF J>4 THEN 8360
8300 PRINT #1, "Bending moment at the first crack (Mcr) = ";INT(MX);"
(kNm)"
8310 PRINT #1, "Steel stress at the first crack = ";INT(S2);" (MPa)"
8320 PRINT #1, "Steel stress at the zero-slip section = ";INT(S1);" (MPa)"
8330 PRINT #1, "Peak bond stress  = ";INT(FB*100)/100;" (MPa)"
8340 PRINT #1, "Slip length = ";INT(L);" (mm)"
8350 GOTO 8450
8360 IF J>5 THEN 8400
8370 PRINT #1, "Steel stress at the zero-slip section = ";INT (S1);" MPa"
```

```
8380 PRINT #1, "Peak bond stress = ";INT(FB*100)/100;" MPa"
8390 GOTO 8450
8400 PRINT #1, "Zero-slip section is";INT(L);"mm from the crack";
8410 PRINT #1, " that has steel stress = ";S3;" MPa"
8420 PRINT #1, "steel stress at the zero-slip section = ";INT (S1);" MPa"
8430 PRINT #1, "Peak bond stresses: fb1 = ";INT(FBX*100)/100;" MPa";
8440 PRINT #1, " : fb2 = ";INT(FBY*100)/100;" MPa"
8450 PRINT #1, "Bond forces at nodes:"
8460 PRINT #1, ""
8470 GOTO 8620
8480 GOTO 8600
8490 IF J>5 THEN 8550
8500 PRINT #1, "Half crack spacing  (mm) = ";L
8510 PRINT #1, "Steel stress at cracked section = ";S2
8520 PRINT #1, "Steel stress at zero-slip point = ";S1
8530 PRINT #1, "Peak bond stress   (MPa)  = ";FB
8540 GOTO 8600
8550 PRINT #1, "Crack spacing  = ";LLX
8560 PRINT #1,"S1 = ";S3; "(MPa)";":  S2 = ";S4;"(MPa)";": S-min = ";SX;
"(MPa)"
8570 PRINT #1,"Zero-slip point is "; INT(LX); "mm away from the crack that"
8580 PRINT #1,"has the steel stress of";S3;" MPa"
8590 PRINT #1, "Bond stresses: Fb1 = ";FBX;" MPa  : Fb2 = "; FBY;" MPa"
8600 PRINT #1, "-------------------------------------------------------------
"
8610 PRINT #1,""
8620 PRINT #1, " Node No.    Bond force (N/mm)"
8630 PRINT #1, " --------    -----------------"
8640 FBF=0:FOR I=1 TO 11:BF(I)=BF(I)*NB/BB
8650 PRINT #1,"   ";44+I;"        ";INT(BF(I)*10)/10:FBF=FBF+BF(I)
8660 NEXT
8670 PRINT #1, "-------------------------------------------------------------
"
8680 PRINT #1, "Check equilibrium:"
8690 PRINT #1, "Total bond force = ";INT(FBF);" N/mm
8700 FSX=PI/4*DIA*DIA*(S2-S1)*NB/BB
8710 IF J=6 THEN FSX=PI/4*DIA*DIA*(S3-S2)*NB/BB
8720 PRINT #1, "Difference in force in steel bars/beam width
=";INT(FSX)'"MPa"
8730 PRINT #1, "-------------------------------------------------------------
"
8740 CLOSE:RETURN
8750 IF WR=0 THEN RETURN
8760 'X$=XP$+".r3"
8770 X$=XP$+"."+ID$
8780 OPEN "o", #1, X$
8790 PRINT #1, "":PRINT #1, "File name = ";X$:PRINT #1,""
8800 PRINT #1, "-----------------------------------------------"
8810 PRINT #1, "Beam Name = "; XP$;R$:PRINT #1, ""
8820 PRINT #1, "Solution Mode = "; J;M$:PRINT #1, ""
8830 PRINT #1, "-----------------------------------------------"
8840 PRINT #1, " Fs1 = ";STT1; "MPa"
8850 PRINT #1, " Fs2 = ";STT2; "MPa"
8860 PRINT #1, "-----------------------------------------------"
8870 PRINT #1, "Input data:"
8880 PRINT #1, "Sectional properties: Read from data file"
8890 'PRINT #1, "Bending moment at the section = "; MX; " kNm"
8900 PRINT #1, "Stress in tensile steel = "; INT(EST*EES); " MPa"
8901 PRINT #1, "---------------------------------"
8902 PRINT #1, "Output results:"
8910 PRINT #1, "Nodal forces on transverse section:"
8911 PRINT #1, ""
8912 PRINT #1, "Node No       Force (N/mm)"
8913 PRINT #1, "-------       ------------"
8914 FX=0:FOR I=1 TO N3+NN-1:PRINT #1,
ND(I),INT(FF(I)*10/10):FX=FX+FF(I):NEXT
8915 PRINT #1, "---------------------------------"
8916 PRINT #1, "Check equilibrium:"
8917 PRINT #1, "Sum of nodal forces = ";INT(FX);" (N/mm)"
```

```
8920 FY=PI/4*DIA*DIA*EST*EES*NB/BB
8921 FY=FY-PI/4*DIA1*DIA1*ESD*EES*NB1/BB
8922 PRINT #1, "Force in steel bars/beam width = ";INT(FY);" (N/mm)"
8923 PRINT #1, "-----------------------------------"
8930 PRINT #1, "Elastic Modulii":PRINT #1, "_____________________"
8940 FOR I=1 TO N3:PRINT #1, "Row -";I;"  ";INT(ECX(I)):NEXT
8941 PRINT #1, "-----------------------------------"
8950 CLOSE:RETURN
```

PROGRAM TO CALCULATE CONCRETE STRESS

```
10 REM ******************************************************
20 REM                 P r o g r a m STRESS
30 REM ******************************************************
40 REM Program to calculate maximum concrete stress in the mesh
50 REM ******************************************************
60 CLS:PRINT:INPUT " Beam number = ",X$
70 PRINT:INPUT " Half-crack spacing (Lo/2) = ",L
80 PRINT:INPUT " Steel stress = ",FS
90 ES=200000!
100 OPEN "i" ,1, X$:BN$=X$
110 INPUT #1, B,H,D,DIA,NB,FC,FSX
120 CLOSE:PRINT
130 Y=2
140 Y$=STR$(Y):Y$=RIGHT$(Y$,1)
150 X$="displ"
160 OPEN "i" ,1, X$
170 INPUT #1, C1,C2,D1,D2
180 CLOSE
190 XR$="stres"
200 OPEN "i",1, XR$
210 FOR I=1 TO 6:INPUT #1,S1(I),S2(I):NEXT
220 CLOSE
230 PI=3.14159
240 P=PI*DIA*NB/B
250 FBN=0:FBX=10
260 FB=.01
270 ES0=FS*L/(4*ES)-13*FB*L^2/(48*ES*DIA)
280 EC0=C1+C2*FB*P*L/100
290 S0=ES0-EC0:'PRINT ES0,EC0,S0:STOP
300 IF S0<=.004 THEN FBX=150*S0*FC^.5:GOTO 330
310 IF S0<=.01 THEN FBX=(.47+33*S0)*FC^.5:GOTO 330
320 FBX=(.71+9*S0)*FC^.5
330 FAC=FBX/FB:'PRINT FAC:'STOP
340 IF FAC>1.001 THEN FBN=FB:GOTO 370
350 IF FAC<.999 THEN FBX=FB:GOTO 370
360 GOTO 380
370 FB=(FBN+FBX)/2:GOTO 270
380 FOR I=1 TO 6:S(I)=S1(I)+FB*L/100*P*S2(I):NEXT
390 SMAX=0:FOR I=1 TO 6
400 IF SMAX<S(I) THEN SMAX=S(I):J=I
410 NEXT
420 JJ=(J-1)*11+1
430 FT=.62*FC^.5:FTX=INT(FT*1000)/1000
440 ES1=FS*L/ES-4*FB*L^2/(3*ES*DIA)
450 EC1=D1+D2*FB*P*L/100
460 WS=ES1-EC1
470 WT=(1.43*(H/B)-.67)*WS*2
480 WT = INT(WT*1000)/1000
490 PRINT "  ------------------------------------"
500 PRINT "  Half- crack spacing = ";L
510 PRINT
520 PRINT "  Maximum steel stress = ";SMAX
530 PRINT "  ------------------------------------"
540 PRINT:PRINT
550 CLS
560 PRINT:PRINT
```

```
570 PRINT "   ----------------------------------------"
580 PRINT "   Input data:"
590 PRINT "   Beam Number = ";BN$
600 PRINT "   Half-crack spacing (mm) = ";L
610 PRINT "   Steel stress at the crack (MPa) = ";FS
620 PRINT "   ----------------------------------------"
630 PRINT "   Output data:"
640 PRINT "   Peak bond stress (MPa) = "; INT (FB*100)/100
650 PRINT "   Maximum concrete stress (MPa) = ";INT(SMAX*100)/100;
660 PRINT "   (at Node Number = ";JJ;")"
670 PRINT ""
680 PRINT "   Flexural strength of concrete (MPa) = ";FTX
690 PRINT "   ----------------------------------------"
700 PRINT "   Crack width = ";WT;" (mm)"
710 PRINT "   ----------------------------------------"
720 PRINT:PRINT
730 OPEN "o", #1, "stress.out"
740 PRINT #1,"   ----------------------------------------"
750 PRINT #1,"   Input data:"
760 PRINT #1,"   Beam Number = ";BN$
770 PRINT #1,"   Half-crack spacing (mm) = ";L
780 PRINT #1,"   Steel stress at the crack (MPa) = ";FS
790 PRINT #1,"   ----------------------------------------"
800 PRINT #1,"   Output data:"
810 PRINT #1,"   Peak bond stress (MPa) = "; INT (FB*100)/100
820 PRINT #1,"   Maximum concrete stress (MPa) = ";INT(SMAX*100)/100;
830 PRINT #1,"   (at Node Number = ";JJ;")"
840 PRINT #1,""
850 PRINT #1,"   Flexural strength of concrete (MPa) = ";FTX
860 PRINT #1,"   ----------------------------------------"
870 PRINT #1,"   Crack width = ";WT;" (mm)"
880 PRINT #1,"   ----------------------------------------"
890 CLOSE
```

SAMPLE OUTPUT FROM PROGRAM STRESS

```
 ----------------------------------------
  Input data:
  Beam Number = beam.1
  Half-crack spacing (mm) =  65
  Steel stress at the crack (MPa) =  250
  ----------------------------------------
  Output data:
  Peak bond stress (MPa) =  4.64
  Maximum concrete stress (MPa) =  3.01    (at Node Number =  45 )

  Flexural strength of concrete (MPa) =  3.507
  ----------------------------------------
  Crack width =  .194  (mm)
  ----------------------------------------
```

PROGRAM TO CALCULATE CRACK SPACING AND CRACK WIDTH IN PARAMETRIC STUDY

```
5 REM ****** CRACK
10 WR=0
20 CF0=1:DX0=1:ZZ0=4:FFX0=8
30 'DIM LZ(CF0,ZZ0,DX0,FFX0),CRZ(CF0,ZZ0,DX0,FFX0)
40 DIM LZ(DX0,FFX0),CRZ(DX0,FFX0)
50 OPEN "i", #1, "coef-th.csv"
60 FOR I=1 TO 5:FOR J=1 TO 6:INPUT #1, X:A(I,J)=X:NEXT:NEXT
70 FC=30:EES=200000!:X0=30:LG0=10:LG=LG0:'CLOSE
80 FR=.62*(FC)^.5:PRINT "Fr = ";FR:'STOP
90 'X=.7:FOR K=1 TO 6:Y=Y+A(5,K)*X^(7-K):NEXT:PRINT Y:STOP
100 FOR I=1 TO 2:FOR J=1 TO 6:INPUT #1, X:B(I,J)=X:NEXT:NEXT
110 FOR I=1 TO 2:FOR J=1 TO 6:INPUT #1, X:C(I,J)=X:NEXT:NEXT:CLOSE
111 IF WR=1 THEN OPEN "o", #1,"cr1-4.dat": REM ******* cr1-1,1-2,1-3 and 1-
4
120 CF=3:REM    *********************: CF= 1, 3 and 5
130 ZZ=1:REM    *********************:  ZZ=1
140 Z=2*ZZ:REM    ********************* :Z=2.2*ZZ, 2.4*ZZ and 2*ZZ
150 DX=1:REM  *********************: DX =1 and 5
160 DIA=12+(DX-1)*4:REM  *********************
170 FFX=1:REM  *********************
180 FF=50+(FFX-1)*50::REM  *********************
190 LL=30
200 CF$=STR$(CF):L=LEN(CF$)-1:CF$=RIGHT$(CF$,L)
210 ZZ$=STR$(ZZ):L=LEN(ZZ$)-1:ZZ$=RIGHT$(ZZ$,L)
220 PRINT:PRINT "Cf = ";CF;" : Z = ";Z;" : Dia = ";DIA;" : Fs = ";FF
230 LX=Z*DIA
240 FG=1:X(1)=1-(3.142/4)/Z:'PRINT X(1):STOP
250 X=X(1):SX=0:FOR K=1 TO 6:SX=SX+A(CF,K)*X^(7-K):NEXT:'PRINT "S-1 =
";SX:'STOP
260 SY=SX
270 E1=B(1,CF)+C(1,CF)*(1-X):'PRINT "E-1 = ";E1:'STOP
280 E2=B(2,CF)+C(2,CF)*(1-X):'PRINT "E-2 = ";E2:'STOP
290 SX=SX*X0/10:'PRINT "S-1 = ";SX:'STOP
300 F0=.01:DXX=3.142*DIA/LX:'PRINT DXX:'STOP
310 E1BNX=E1*DXX*F0*(LL/10):E2BNX=E2*DXX*F0*(LL/10)
320 S1=FF-8*F0*LL/(3*DIA):SOX=S1:'PRINT S1
330 E1ST=1000*(S1*LL/2+F0*LL*LL/(4*DIA))/EES
340 E2ST=1000*(S1*LL+4*F0*LL*LL/(3*DIA))/EES
350 S=E1ST-E1BNX:IF S<0 THEN FFX=FFX+1:LL=0:GOTO 580:'IF S<0 THEN S=0
360 SLIP=S:SS=S/1000
370 IF SLIP<=4 THEN F00=SS*150:GOTO 400
380 IF SLIP<=10 THEN F00=.47+SS*33:GOTO 400
390 F00=.71+SS*9
400 F00=F00*FC^.5
410 IF LL<8*DIA THEN F00=F00*LL/(8*DIA)
420 IF F00>F0 THEN F0=F0+FG:GOTO 310
430 IF FG<.01 THEN 450
440 F0=F0-FG:FG=FG/10:F0=F0+FG:GOTO 310
450 'PRINT USING "Fo = ###.####";F0:PRINT:'STOP
460 SZ=SX*F0*DXX:'PRINT"S-1 = ";SX:STOP
470 IF SZ>FR THEN 490
480 LL=LL+LG:GOTO 240
490 IF LG<1 THEN 510
500 LL=LL-LG:LG=LG/10:GOTO 480
510 PRINT "L/2 = ";LL:'STOP
520 CRW=E2ST-E2BNX:PRINT "Crw = ";CRW
530 'LZ(CF,ZZ,DX,FFX)=LL
```

```
540 'CRZ(CF,ZZ,DX,FFX)=CRW
550 'LZ(DX,FFX)=LL
560 'CRZ(DX,FFX)=CRW
570 LG=LG0:FFX=FFX+1
580 IF WR=1 THEN WRITE #1,LL,CRW
581 IF FFX<FFX0+1 THEN 180
590 DX=DX+1:IF DX<DX0+1 THEN 160
600 'ZZ=ZZ+1:IF ZZ<ZZ0+1 THEN 140
610 'CF=CF+1:IF CF<CF0+1 THEN 120
620 GOTO 661:IF WR=0 THEN 661
630 OPEN "o", #1,"crsw-"+CF$+ZZ$+".dat"
640 FOR K=1 TO FFX0
650 WRITE #1,
LZ(1,K),LZ(2,K),LZ(3,K),LZ(4,K),LZ(5,K),LZ(6,K),LZ(7,K),X$,CRZ(1,K),CRZ(2,K
),CRZ(3,K),CRZ(4,K),CRZ(5,K),CRZ(6,K),CRZ(7,K):NEXT
660 CLOSE
661 ZZ=ZZ+1:IF ZZ<ZZ0+1 THEN 140
662 CF=CF+1:IF CF<CF0+1 THEN 130
670 CLOSE:END
```

PROGRAM TO CALCULATE DEFLECTION

```
3 CLS
4 OPEN "i",#1,"CASES.DAT":INPUT #1,CAS:CLOSE
5 CA$=STR$(CAS):LX=LEN(CA$)-1:CA$=RIGHT$(CA$,LX)
6 BN$="Beam -1 "
7 OPEN "o", #1, BN$+".def"
8 WR=1
10 DIM
L(90),IX(90),X(90),L00(30),M00(30),PP(30),MMX(30),ICR(30),SX(30),S1X(30)
20 DIM FCX(30),FCY(30),ICM(30),LCX(30),LCY(30),LOD(20),DELTA(20),DEFL(20)
21 DIM RO(20):K0=.6
22 RO(1)=.003:RO(2)=.004:RO(3)=.005:RO(4)=.006:RO(5)=.007
23 RO(6)=8.000001E-03:RO(7)=8.999999E-03:RO(8)=.01:RO(9)=.0125:RO(10)=.015
24 RO(11)=.003:RO(12)=.0175:RO(13)=.02:RO(14)=.0325
25 L=4000:H=440:B=300:D=400:FC=20:DIA=15:BE=H/D:COMPR=1:ROD=0:DD=.25
26 FL=1:BX=1:GX=.324
27 LO$= "t":LOT=1000:LOD=1:LOD(1)=3.8:DELTA(1)=50:EEE=.002:EES=200000!
30 PXX=.05:CASE=CAS:INDIC=1
40 KK=1:WR=1
90 IF LO$="p" OR LO$="P" THEN LO1$="Point Load":LOS=1:GOTO 160
100 IF LO$="u" OR LO$="U" THEN LO1$="Uniform Load":LOS=2:GOTO 160
110 IF LO$="t" OR LO$="T" THEN LO1$="Two Point Loads":LOS=3:GOTO 160
120 BEEP:CLS:PRINT:PRINT "Invalid Loading type ...!":PRINT:END
160 IF GX>.45 THEN PRINT "GX too big..":END
170 PRINT:PRINT "Case - ";CASE:PRINT "Beam No. ";BN$;" : ";LO1$:PRINT
171 IF WR=0 THEN 180
172 PRINT #1,"":PRINT #1,"Case - ";CASE:PRINT #1,"Beam No. ";BN$;" : ";LO1$
173 PRINT #1, ""
180 'INPUT "Press <ENTER> Key to continue",X$
190 LODX=1:FCC=0:RO=RO(CAS)
192 ROX=RO
193 AS=ROX*B*D/5:DIAX=4*AS/3.14159:DIAX=(DIAX)^.5:IF DIAX>DIA THEN DIA=DIAX
200 YY=0:GOSUB 2000:MCR=MOMT:IG=MI:REM *** Uncracked - Mcr and Ig
210 S1X=ES*EES
220 PRINT:PRINT:'PRINT "Load = ";LOD(LODX):PRINT
230 PRINT "Mcr = ";MCR;"  : Ig = ";IG;
231 IF WR=0 THEN 240
232 PRINT #1,"":PRINT #1,"":'PRINT "Load = ";LOD(LODX):PRINT
233 PRINT #1,"Mcr = ";MCR;
240 YY=2 :GOSUB 2000:MU=MOMT:                  :REM **** Ultimate M = Mu
250 PRINT "  :   Mu = ";MU;
251 IF WR=1 THEN PRINT #1, "  :   Mu = ";MU;
260 MIU=MI
270 PU=2*MU*1000/(L/2):IF LOS=2 THEN PU=8*MU*1000*1000/(L^2)
280 IF LOS=3 THEN PU=2*MU*1000/LOT
281 PRINT "   : Pu = ";PU:PRINT
282 IF WR=1 THEN PRINT #1,"   : Pu = ";PU:PRINT #1,""
290 P=2*MCR*1000/(L/2):IF LOS=2 THEN P=8*MCR*1000*1000/(L^2)
300 IF LOS=3 THEN P=2*MCR*1000/LOT
310 PCR=P:II=1:L00(II)=0:LX=0:PP(II)=P
320 IF LOS=3 THEN 340
330 PRINT "Crack -";II;": at x = ";L/2-LX;", when load = ";PP(II):GOTO 350
331 IF WR=1 THEN PRINT #1,"Crack -";II;": at x = ";L/2-LX;", when load =
";PP(II):GOTO 350
340 PRINT "Cracks within constant moment region when load = ";PP(II)
```

```
341 IF WR=1 THEN PRINT #1, "Cracks within constant moment region when load
= ";PP(II)
350 YY=1:GOSUB 2000:STT=ES*EES             :REM **** Cracked  M = Mcr - S2
360 IF LOS<3 THEN 390
370 SS=STT:NU=0:GOSUB 6000:PRINT
380 PRINT "Cracks outside this region:":PRINT
381 IF WR=1 THEN PRINT #1,"Cracks outside this region:":PRINT #1,""
390 ZZ=0:ST0=S1X:ST1=STT:GOSUB 4000:S1Z=S1X:LLP=LL:REM ** Slip length
400 LY=0:FOR K=1 TO II:LY=LY+L00(K):NEXT:IF LOS=3 THEN LY=LY+(L/2-LOT-
LMIN2)
410 LX=LY+LLP
420 P=2*MCR*1000/(L/2-LX):IF LOS=2 THEN P=2*MCR*1000*1000/(L^2/4-LX^2)
430 IF P<0 THEN 550
440 MX=P*(L/2-LY)/2000:IF LOS=2 THEN MX=P*(L^2/4-LY^2)/(2000*1000)
450 IF P>K0*PU THEN 550
460 'IF P>LOD(LOD) THEN 550
470 FAC=MX/MCR:YY=4:GOSUB 2000:STT=ES*EES
480 ZZ=0:ST0=S1X:ST1=STT:GOSUB 4000:IF LL-LLP<1 THEN 500
490 LX=LX+(LL-LLP):LLP=LL:GOTO 420
500 II=II+1:L00(II)=LL:PP(II)=P:IIJ=II:IF LOS=3 THEN IIJ=II-1
510 PRINT "Crack -";IIJ;": at x = ";L/2-LX;", when load = ";PP(II)
511 IF WR=1 THEN PRINT #1,"Crack -";IIJ;": at x = ";L/2-LX;", when load =
";PP(II)
520 LX=0:FOR K=1 TO II:LX=LX+L00(K):NEXT
530 PX=2*MCR*1000/(L/2-LX):IF LOS=2 THEN PX=2*MX*1000*1000/(L^2/4-LX^2)
540 IF PX<PU THEN P=PX:GOTO 390
550 I00=II
560 P=LOD(LODX):P=K0*PU:PRINT:PRINT "Load = ";P:PRINT
570 'L00=LL
580 'PRINT "S2-(M=Mcr) =";STT;"  :  Lo = ";L00:PRINT
590 GOTO 690
600 MX=13.18:YY=3 :GOSUB 2000:             :REM **** S2 and Ic for any M>Mcr
610 STX=ES*EES:ICR=MI
620 PRINT "For M = ";MX;" : S2 = ";STX;"  :  Icr = ";ICR:PRINT
621 IF WR=1 THEN PRINT #1, "For M = ";MX;" : S2 = ";STX;"  :  Icr =
";ICR:PRINT  #1,""
630 ZZ=1:LXY=L00:ST1=130:ST2=100:GOSUB 4000 :REM **** Fo and Lx, Ly for
ST1,ST2
640 F01=F0X:L01=L0X:F02=F0Y:L02=L0Y
650 PRINT "For St1 = ";ST1; "  and St2 = ";ST2
651 IF WR=1 THEN PRINT #1, "For St1 = ";ST1; "  and St2 = ";ST2
660 PRINT "     Fo1 = ";F0X;"  :  Lo1 = ";L0X
661 IF WR=1 THEN PRINT #1, "     Fo1 = ";F0X;"  :  Lo1 = ";L0X
670 PRINT "     Fo2 = ";F0Y;"  :  Lo2 = ";L0Y
671 IF WR=1 THEN PRINT #1, "     Fo2 = ";F0Y;"  :  Lo2 = ";L0Y
680 M=(P*L/4)/1000:IF LOS=2 THEN M=(P*L*L/8)/1000000!
690 IF P>PCR THEN 740
691 DEFL=0:GOTO 1411
700 DEFL=P*L^3/(48*EC*IG*100000!):IF LOS=1 THEN 730
710 DEFL=5*P*L^4/(384*EC*IG*1E+08):IF LOS =2 THEN 730
720 DEFL=P*LOT*(3*L^2-4*LOT^2)/(48*EC*IG*100000!)
730 PRINT:PRINT "Deflection = ";DEFL:STOP:GOTO 1420
731 IF WR=1 THEN PRINT #1,"":PRINT #1,"Deflection = ";DEFL:STOP:GOTO 1420
740 IF P>=PP(I00) THEN KC=I00:GOTO 780
750 K=1
760 IF P>PP(K) THEN K=K+1:GOTO 760
770 KC=K-1
780 IF LOS<3 THEN PRINT "No. of cracks on half-span = ";KC:GOTO 800
781 IF WR=1 THEN IF LOS<3 THEN PRINT #1,"No. of cracks on half-span =
";KC:GOTO 800
790 PRINT "No. of cracks outside constant mom region =";KC-1
```

```
791 IF WR=1 THEN PRINT #1,"":PRINT #1,"No. of cracks outside constant mom
region =";KC-1
800 PRINT:PRINT
801 IF WR=1 THEN PRINT #1,"":PRINT #1,""
810 IF LOS=3 THEN L00(1)=L/2-LOT-LMIN2
820 FOR I=1 TO KC:LX=0:JJ=KC-I+1:FOR J=1 TO JJ:LX=LX+L00(J):NEXT
830 MMX(I)=P*(L/2-LX)/2000:IF LOS=2 THEN MMX(I)=P*(L^2/4-LX^2)/(2000*1000)
840 IF LOS=3 AND LX<(L/2-LOT) THEN MMX(I)=P*LOT/2000
850 NEXT
860 FOR KX=1 TO KC:MX=MMX(KX):IF MX<MU THEN 880
870 SX(KX)=EEE*EES:ICR(KX)=MIU:GOTO 900
880 YY=3:GOSUB 2000
890 SX(KX)=ES*EES:ICR(KX)=MI
900 CUR=MMX(KX)*1000/(EC*ICR(KX))
905 PRINT "Mom = ";MMX(KX);"  :  Cur = "; CUR;"  :S2 = ";SX(KX);
906 IF WR=1 THEN PRINT #1,"Mom = ";MMX(KX);"  :  Cur = "; CUR;"  :S2 =
";SX(KX);
910 PRINT "Es = ";ESS*1000:'PRINT
911 IF WR=1 THEN PRINT #1, "Es = ";ESS*1000:'PRINT
912 NEXT
920 IF LOS<3 THEN 980
930 SS=SX(KC):NU=1:GOSUB 6000:'PRINT NV,LAV
940 FOR KX=1 TO NX:KY=KC+KX:MMX(KY)=MMX(KY-1):ICR(KY)=ICR(KY-
1):SX(KY)=SX(KY-1)
950 CUR=MMX(KY)*1000/(EC*ICR(KY))
955 PRINT "Mom = ";MMX(KY);"  :  Cur = "; CUR;"  :S2 = ";SX(KY);
956 IF WR=1 THEN PRINT #1,"Mom = ";MMX(KY);"  :  Cur = "; CUR;"  :S2 =
";SX(KY);
960 PRINT "Es = ";ESS*1000
961 IF WR=1 THEN PRINT #1,"Es = ";ESS*1000
962 NEXT
970 PRINT:PRINT "No. of cracks in the constant mom region = ";NVM+1
971 IF WR=1 THEN PRINT #1,"":PRINT #1, "No. of cracks in the constant mom
region = ";NVM+1
980 PRINT:IF WR=1 THEN PRINT #1,""
981 ZZ=0:ST0=S1X:ST1=SX(1):GOSUB 4000:L01=LL
990 IF LOS<3 THEN 1040
1000 M00(1)=0:IF NUV=1 THEN M00(1)=LAV/2
1010 FOR K=2 TO NX+1:M00(K)=LAV:NEXT
1020 FOR K=1 TO KC-1:KX=NX+1+K:M00(KX)=L00(K+1):NEXT
1030 FOR K=1 TO KC+NX:L00(K)=M00(K):NEXT
1040 KC1=KC-1:IF LOS=3 THEN KC1=KC
1050 FOR KX=1 TO KC1:KY=KC-KX+1+NX:L00=L00(KY):IF KX=KC THEN L00=LAV
1060 ZZ=1:LXY=L00:ST2=SX(KX):ST1=SX(KX+1):GOSUB 4000
1070 LCX(KX)=L0X:FCX(KX)=F0X:FCY(KX)=F0Y:S1X(KX)=S1
1080 PRINT "Crack ";KX;"-";KX+1;" : Lx=";L00-LCX(KX);"  :Ly=";LCX(KX)
1081 IF WR=1 THEN PRINT #1, "Crack ";KX;"-";KX+1;" : Lx=";L00-LCX(KX);"
:Ly=";LCX(KX)
1090 PRINT "              : Fx=";FCY(KX);"  :Fy=";FCX(KX)
1091 IF WR=1 THEN PRINT #1,"              : Fx=";FCY(KX);"  :Fy=";FCX(KX)
1100 PRINT "              : Mid Stress = ";S1X(KX)
1101 IF WR=1 THEN PRINT #1, "              : Mid Stress = ";S1X(KX)
1110 NEXT
1120 FOR KX=1 TO KC1:KY=KC-KX+1:L00=L00(KY):IF KX=KC THEN L00=LAV
1130 MX=MMX(KX)+(MMX(KX+1)-MMX(KX))*(L00-LCX(KX))/L00
1140 IF INDIC=2 THEN 1190
1150 SXX=SX(KX)+(SX(KX+1)-SX(KX))*(L00-LCX(KX))/L00
1160 RATIO=SXX/S1X(KX):RO=ROX*RATIO
1161 IF S1X(KX)<=S1Z*1.1 THEN ICM(KX)=IG:GOTO 1210
1170 YY=3:GOSUB 2000:ICM(KX)=MI:IF ICM(KX)>IG THEN ICM(KX)=IG
1180 GOTO 1210
```

```
1190 YY=5:SMX=S1X(KX):GOSUB 2000:ICM(KX)=MI*MX/MOMT
1200 'ICM(KX)=(ICR(KX)+ICR(KX+1))/2*RATIO:ICM(KX)=IG/2
1210 CUR=MX*1000/(EC*ICM(KX))
1215 PRINT "Cur-o";KX;"  = ";CUR;"(stress = ";ES*EES;")"
1216 IF WR=1 THEN PRINT #1,"Cur-o";KX;"  = ";CUR;"(stress = ";ES*EES;")"
1217 NEXT
1220 IF LOS<3 THEN 1250
1230 FOR KX=1 TO NX-1:KY=KC+KX:ICM(KY)=ICM(KY-
1):FCX(KY)=LAV/2:LCX(KY)=LCX(KY-1)
1240 CUR=MX*1000/(EC*ICM(KY))
1245 PRINT "Cur-o";KY;"  = ";CUR;"(stress = ";ES*EES;")"
1246 IF WR=1 THEN PRINT #1,"Cur-o";KY;"  = ";CUR;"(stress = ";ES*EES;")"
1247 NEXT:KC=KC+NX
1250 PX1=0:IF ROX<.025 THEN 1280
1260 PX1=L01/2:IF ROX>.02 THEN 1280
1270 PX1=L01/((ROX-.015)*400)
1280 PX2=L01*.5:IF ROX<.01 THEN 1310
1290 PX2=5:IF ROX<.025 THEN 1310
1300 PX2=L01/((ROX-.01)*400)
1310 LX=0:FOR K=1 TO KC:LX=LX+L00(K):NEXT
1320 N=3*KC:L(1)=L/2-LX-L01+PX1:L(2)=L01-PX1-PX2:L(3)=PX2
1330 FOR K=1 TO KC-1:L00=L00(KC+1-K):KK=3*K+1:L(KK)=(L00-LCX(K))*(1-PXX)
1340 L(KK+1)=L00*PXX:L(KK+2)=L00-L(KK)-L(KK+1)
1350 NEXT
1360 IX(1)=IG:IX(2)=ICR(1):FOR K=1 TO KC-1:IX(3*K)=ICR(K)
1370 IX(3*K+1)=ICM(K):IX(3*K+2)=ICM(K):NEXT:IX(3*KC)=ICR(KC)
1380 X=0:FOR K=1 TO N:X=X+L(K):NEXT:IF L/2-X<5 THEN 1401
1390 IX(N+1)=IX(N-1):IX(N+2)=IX(N+1)
1400 L(N+1)=LAV*(1-PXX(1))/2:L(N+2)=LAV*PXX/2:N=N+2
1401 PRINT:PRINT "Case = ";CAS;"   : Fc = ";FC;"  : Ro =";ROX
1402 IF WR=1 THEN PRINT #1, "":PRINT #1,"Case = ";CAS;"   : Fc = ";FC;"  :
Ro =";ROX
1410 EC=1000*FC:GOSUB 5000:CLOSE:STOP
1411 FCC=FCC+1:DEFL(FCC)=DEFL
1412 FCC(FCC)=FC:ROX(FCC)=ROX
1420 DEFL(FCC)=DEFL:PRINT:'PRINT ".Delta =";DELTA(LODX):PRINT
1430 'PRINT "Ratio = ";DELTA(LODX)/DEFL(LODX);"**********"
1440 RO=ROX:LODX=LODX+1:IF LODX<=LOD THEN 560
1442 FD=FC:FC=FC+5:IF FC=55 THEN PRINT "Fc = ";FC:GOTO 1445
1443 RO=ROX*(FC/FD)^.5:GOTO 192
1445 IF WR=0 THEN 1470
1450 OPEN "o",#1, "def-"+LO$+"-"+CA$+".DAT"
1451 WRITE #1, "L =",L,"  :h =",H,"  : b = ",B,"  : d =",D,"  : Dia ="'dia
1452 WRITE #1, "Compr =",COMPR,"  :Ro' =",ROD;"  : d'= ",DD
1453 WRITE #1, "Fl =",FL,"  :Bx' =",BX;"  : Gx= ",GX
1454 WRITE #1, "Loading =",LO$:IF LOS=3 THEN WRITE #1, "Distance = ",LOT
1460 FOR K=1 TO FCC:WRITE #1,FCC(K),ROX(K),DEFL(K):NEXT:CLOSE
1461 CAS=CAS+1
1462 IF CAS=14 THEN 1470
1463 OPEN "O",#1,"CASES.DAT":WRITE #1,CAS:CLOSE
1464 RUN "P-DEF-T.BAS"
1470 END
1480 REM ************************************************************
2000 G1=.1:GOTO 2050:       REM ******************* check G1 for
accuracy..!
2010 CLS:PRINT:PRINT:PRINT "Fc = ";FC;"MPa"
2020 PRINT "Ro =";RO
2030 PRINT "d  =";D; "mm"
2040 PRINT:PRINT:INPUT "Press Return Key",PR$
2050 FY=410
2060 'EES=197000!
```

```
2070 W=2400
2080 E0=.002:E00=.001:       REM ****************** check Eoo for
accuracy..!
2090 ECI=2*FC/E0
2100 FR=.6*(FC^.5)
2110 EC=.043*W^1.5*(FC^.5)
2120 ER =FR/ECI
2130 LA=ER/E0
2140 N=EES/EC
2150 M=EC/FC
2160 IF YY=0 OR YY=1 THEN E2=ER
2170 IF YY=2 THEN E1=.0035
2180 IF YY=3 OR YY=4 OR YY=5 THEN E2=ER
2190 G1=.01:F1=BE/2:IF FL=1 THEN F1=.05
2200 IF YY=0 OR YY=1 OR YY=3 OR YY=4 OR YY=5 THEN E1=E2*F1/(BE-F1):GOTO
2220
2210 IF YY=2 THEN E2=E1*(BE-F1)/F1
2220 K=BE*E1/(E1+E2)
2230 A=(BE-K)*ER/E2
2240 ES=(1-K)*E1/K
2250 ESS=ES
2260 'IF ES>.002 THEN ES=.002
2270 IF ES>EEE THEN ES=EEE:REM ************* c h e c k *********
2280 RH=N*M*RO*ES
2290 P1=(8*LA*A*K*K*K-3*LA*LA*K*K*K*K)/(4*(3*A*LA*K*K-LA*LA*K*K*K))
2300 P2=(3*A*LA*K*K-LA*LA*K*K*K)/(3*A*A)
2310 P3=A*FR/(2*FC):IF E2<=ER THEN P3=P3*(E2/ER)^2
2320 IF E1>E0 THEN JJ=1:GOTO 2340
2330 LH=LA*K*K/A-LA*LA*K*K*K/(3*A*A)-P3:GOTO 2380
2340 LL=A/LA
2350 P5=41*ER*(K-LL)/A:P5=0
2360 P6=2*(K-LL)*(3/4-P5)/(3*(1-P5))
2370 LH=2*A/(3*LA)+(1-P5)*(K-LL)-P3
2380 IF FL=1 THEN GOSUB 2900:IF COMPR=1 THEN GOSUB 3430
2390 'PRINT LH*1000,RH*1000,K
2400 IF LH>RH THEN 2430
2410 F1=F1+G1
2420 GOTO 2200
2430 IF G1<.0001 THEN 2450
2440 F1=F1-G1:G1=G1/10:GOTO 2410
2450 MOX=P3*(1-K-2*A/3):IF E2<=ER THEN MOX=P3*((BE-K)/3-(BE-1))
2460 IF E1>E0 THEN 2480
2470 MOM=P2*(1-K+P1)-MOX:GOTO 2490
2480 MOM=2*A/(3*LA)*(1-K+5*LL/8)+(1-P5)*(K-LL)*(1-K+LL+P6)-MOX
2490 IF FL=1 THEN GOSUB 3130:IF COMPR=1 THEN GOSUB 3460
2500 MOMT=MOM*B*D*D*FC/1000000!
2510 MI=MOM*B*D*D*K*D/(E1*1E+11)
2520 'IF YY=1 AND MOM=MCR/(FC*B*D*D/1000000!) THEN STOP:MX=MCR:GOTO 1690
2530 IF YY=4 OR YY=5 THEN 2710
2540 MZ=MCR/(FC*B*D*D/1000000!):MZ=MZ/MOM*1000
2550 IF YY=1 AND CINT(MZ)=1000 THEN MX=MCR:GOTO 2790
2560 IF YY=2 THEN EE0=E2
2570 IF YY=1 OR YY=3 THEN 2710
2580 X$="Mu = ":IF YY=0 THEN X$="Mcr = "
2590 IF YY=1 THEN X$="Ic x E+08 just after cracking = "
2600 'PRINT:PRINT "k1 = ";:PRINT USING "##.####";A;
2610 'PRINT ":   k2 = ";:PRINT USING "##.####";K;
2620 'PRINT ":   e1 x 1000= ";:PRINT USING "##.####";E1*1000
2630 'IF YY=0 OR YY=2 THEN PRINT:PRINT X$;MOMT
2640 'IF YY=0 THEN PRINT "Ig x E+08 = ";MI
2650 IF YY=0 OR YY=2 THEN 2860
```

```
2660 'IF YY=1 THEN PRINT:PRINT X$;MI:GOTO 930
2670 IF YY=1 THEN 2860
2680 'PRINT:PRINT "Steel stress =";ES*200000!
2690 'PRINT:PRINT "Ic = ";MI:GOTO 930
2700 GOTO 2860
2710 'PRINT MOMT,MX,E2*1000:REM ************** %%%%% *******
2720 IF YY=5 THEN 2760
2730 IF YY<4 THEN 2780
2740 IF MOMT>MCR*FAC THEN 2820
2750 GOTO 2790
2760 IF ES*EES>SMX THEN 2820
2770 GOTO 2790
2780 IF MOMT>MX THEN 2820
2790 E2=E2+E00
2800 IF E2<ER THEN 2840
2810 GOTO 2190
2820 IF E00<.00001 THEN 2590
2830 E2=E2-E00:E00=E00/10:GOTO 2790
2840 IF MOMT/(MCR*FAC)<1.2 THEN 2590
2841 IF YY<>3 THEN 2850
2842 IF MOMT/MX<1.2 THEN 2590
2850 PRINT "Unusual reinforcement ratio...!":STOP:END
2860 'END
2870 'IF YY=0 THEN MCR=MOM*FC*B*D*D/1000000!
2880 IF YY=1 THEN EX0=E2
2890 RETURN
2900 LL=A/LA
2910 IF GX>K THEN 3050
2920 IF E1<E0 THEN 3020
2930 IF GX>K-LL THEN 2980
2940 PK=1:CX=(1-41*ER/A*(2*K-2*LL-GX))*BX*GX
2950 CY=(1-41*ER/A*(K-LL-GX))*(K-LL-GX)
2960 C1=2/3*LL
2970 LH=C1+CX+CY-P3:GOTO 3110
2980 PK=2:C2=BX*(1-41*ER/A*(K-LL))*(K-LL)
2990 KGX=K-GX:CX=BX*LL*(2/3-KGX*KGX/(LL*LL)*(1-KGX/(3*LL)))
3000 C1=KGX*KGX/LL*(1-KGX/(3*LL))
3010 LH=C1+C2+CX-P3:GOTO 3110
3020 PK=3:KGX=K-GX:C1=KGX*KGX*LA/A*(1-LA*KGX/(3*A))
3030 C2=BX*LA/A*(K*K*(1-LA*K/(3*A))-KGX*KGX*(1-LA*KGX/(3*A)))
3040 LH=C1+C2-P3:GOTO 3110
3050 PK=4:IF E1<=E0 THEN LH=LA*K*K/A-LA*LA*K*K*K/(3*A*A)
3060 IF E1>E0 THEN LL=A/LA:LH=2*A/(3*LA)+(1-P5)*(K-LL)
3070 IF GX>K+A THEN LH=LH-P3:LH=LH*BX:GOTO 3110
3080 XP=GX-K:P3X=P3*XP*XP/(A*A)
3090 P3Y=P3-P3X
3100 LH=LH*BX-P3X*BX-P3Y
3110 RETURN
3120 REM ************************************************
3130 LL=A/LA
3140 IF GX>K THEN 3340
3150 IF E1<E0 THEN 3290
3160 IF GX>K-LL THEN 3230
3170 MOM=5*LL*LL/12
3180 KLG=K-LL-GX:MOM=MOM+CY*(K-GX)-KLG*KLG/6*(2+83*ER/A*KLG)
3190 MOM=MOM+CX*K-GX*BX/6*(3-83*ER/A*(3*K-2*GX-3*LL))
3200 MOX=P3*2*A/3:IF E2<=ER THEN MOX=P3*2*(BE-K)/3
3210 MOM=MOM+MOX
3220 GOTO 3410
3230 KG=K-GX:MOM=KG*KG*KG*(8*LL-3*KG)/(12*LL*LL)
3240 MOM=MOM+BX*(5*LL*LL/12-KG*KG*KG*(8*LL-3*KG)/(12*LL*LL))
```

```
3250 KL=K-LL:MOM=MOM+C2*K-BX*KL*KL*(2+83*ER/A*KL)/6
3260 MOX=P3*2*A/3:IF E2<=ER THEN MOX=P3*2*(BE-K)/3
3270 MOM=MOM+MOX
3280 GOTO 3410
3290 LL=A/LA:KG=K-GX:MOM=KG*KG*KG*(8*LL-3*KG)/(12*LL*LL)
3300 MOM=MOM+BX*(K*K*K*(8*LL-3*K)/(12*LL*LL)-KG*KG*KG*(8*LL-
3*KG)/(12*LL*LL))
3310 MOX=P3*2*A/3:IF E2<=ER THEN MOX=P3*2*(BE-K)/3
3320 MOM=MOM+MOX
3330 GOTO 3410
3340 IF E1<=E0 THEN MOM=BX*K*K*K*(8*LL-3*K)/(12*LL*LL):M1=MOM:GOTO 3380
3350 MOM=BX*5*LL*LL/12
3360 KL=K-LL:C2=BX*KL*(1-41*ER/A*KL)
3370 MOM=MOM+C2*K-BX*KL*KL*(2+83*ER/A*KL)/6:M1=MOM
3380 IF GX>K+A THEN MOM=MOM+BX*P3*2*A/3:M2=MOM-M1:GOTO 3410
3390 XP=GX-K:P3X=(BX-1)*P3*XP*XP/(A*A)
3400 MOM=MOM+(P3*2*A/3)+(P3X*2*XP/3):M2=MOM-M1
3410 MOM=MOM+N*M*RO*ES*(1-K):M3=MOM-M1-M2:'PRINT K,A,E2*1000,MOM:STOP
3420 RETURN
3430 IF DD<K THEN ES1=E1/K*(K-DD):FRDD=N*M*ROD*ES1
3440 IF DD>K THEN ES1=ER/A*(DD-K):FRDD=-N*M*ROD*ES1
3450 LH=LH+FRDD:RETURN
3460 IF K>DD THEN MOM=MOM+FRDD*(K-DD)
3470 IF K<DD THEN MOM=MOM+FRDD*(DD-K)
3480 RETURN
4000 REM
*****************************************************************
4010 FACT0=1.5:LLZ=200:EES=200000!
4020 SY=400:LG1=50:LG=10:'LXY=200:ZZ=1
4030 Z=0
4040 ST=ST1
4050 LL=LG1:IF ZZ=1 THEN LL=LXY/2
4060 FG=1:F0=0:DX=4*RO*D/DIA
4070 EBX=3
4080 S1=ST-8*F0*LL/(3*DIA):S10=S1
4090 E1ST=1000*(S1*LL/2+F0*LL*LL/(4*DIA))/EES
4100 EX11=EBX
4110 S=E1ST-EX11:IF S<0 THEN S=0
4120 SLIP=S:SS=S/1000
4130 IF SLIP<40 THEN F00=208330!*SS^4+12500*SS^3-3520*SS^2+189*SS
4140 IF SLIP>=40 THEN F00=2.928+8.333*SS
4150 F00=F00*1.5:FACT=FACT0:IF LL<LLZ THEN FACT=FACT0*LL/LLZ
4160 F00=F00*FACT:F00=F00*((FC/50)^.5)
4170 IF F00>F0 THEN 4200
4180 IF FG<.01 THEN 4210
4190 F0=F0-FG:FG=FG/10
4200 F0=F0+FG:GOTO 4080
4210 IF ZZ=0 THEN 4300
4220 'PRINT "Fo = ";F0,LL:PRINT
4230 IF Z=0 THEN F0X=F0:L0X=LL
4240 IF Z=1 THEN F0Y=F0:L0Y=LL
4250 'PRINT SY,S1:STOP
4260 IF Z=0 THEN ST=ST2:LY=LL:LL=LXY-LL:SY=S1:Z=1:GOTO 4060
4270 IF SY-S1>2 THEN LL=LY+1:Z=0:ST=ST1:GOTO 4060
4280 'PRINT:PRINT F0X,L0X:PRINT F0Y,L0Y:GOTO 1900
4290 GOTO 4350
4300 IF S1>ST0 THEN LL=LL+LG:GOTO 4060
4310 IF LG<10 THEN 4330
4320 LL=LL-LG:LG=LG/10:LL=LL+LG:GOTO 4060
4330 'PRINT S1,ST0,ST,LL
4340 IF ZZ=0 THEN 4350
```

```
4350 IF LOX<0 OR LOY<0 THEN STOP
4352 RETURN
5000 REM Deflection ***************************************************
5010 DIV=50:IF LOS=1 OR LOS=3 THEN P=P*1000
5020 'READ N:FOR I=1 TO N:READ L(I):NEXT
5030 X(0)=0:FOR K=1 TO N:X(K)=X(K-1)+L(K):NEXT
5040 'FOR I=1 TO N:READ IX(I):IX(I)=IX(I)*1E+08:NEXT:IX(0)=IX(1)
5050 FOR I=1 TO N:IX(I)=IX(I)*1E+08:NEXT:IX(0)=IX(1)
5060 DEFL=0:FOR I=1 TO N
5070 X1=X(I-1):X2=X(I)
5080 I1=IX(I-1):I2=IX(I)
5090 AXX=(I1*X2-I2*X1)/(X2-X1):BXX=(I2-I1)/(X2-X1)
5100 GOSUB 5140
5110 DEFL=DEFL+MM/EC
5120 NEXT
5130 PRINT:PRINT "Deflection  =  ";DEFL:REM **********************
5131 IF WR=1 THEN PRINT #1,"":PRINT #1,"Deflection  =  ";DEFL:REM
*************
5132 RETURN
5140 DX=(X2-X1)/DIV:MM=0
5150 FOR K=1 TO DIV
5160 Y1=X1+DX*(K-1):Y2=Y1+DX
5170 LOX1=1:LOX2=1:IF LOS=2 THEN LOX1=L-Y1:LOX2=L-Y2
5180 Z1=(Y1/2)*LOX1/(AXX+BXX*Y1):IF LOS<3 THEN 5210
5190 IF Y1<LOT THEN Z1=(Y1/2)/(AXX+BXX*Y1):GOTO 5210
5200 Z1=(LOT/2)/(AXX+BXX*Y1)
5210 Z2=(Y2/2)*LOX2/(AXX+BXX*Y2):IF LOS<3 THEN 5240
5220 IF Y2<LOT THEN Z2=(Y2/2)/(AXX+BXX*Y2):GOTO 5240
5230 Z2=(LOT/2)/(AXX+BXX*Y2)
5240 DA=(Z1+Z2)/2*DX
5250 DM=DA*(Y1+Y2)/2
5260 MM=MM+DM*P
5270 NEXT
5280 RETURN
6000 ALP=1.5-1/(400*RO)
6010 NETA=D^.5/DIA
6020 BETA=5+D/(15*(1+NETA)):IF D>=350 THEN BETA=5+23/(1+NETA)
6030 LMIN=10000/(SS^ALP)-1/(90*RO)^4+75-40*NETA+BETA*(1/(RO)^.5-6.32)
6040 LMIN=INT(LMIN):LMIN2=INT(LMIN/2):LAV=INT(1.5*LMIN)
6050 IF NU=1 THEN 6070
6060 GOTO 6120
6070 LX=L-2*(LOT+LMIN2):NUM=LX/LAV:NVM=INT(NUM)
6080 IF NUM-NVM>.5 THEN NVM=NVM+1
6090 LAV=INT(LX/NVM)
6100 NW=NVM/2:NX=INT(NW)
6110 NUV=0:IF NW>NX THEN NUV=1
6120 RETURN
7000 REM*********************  DATA  ****************************
7010 REM ******* Case - 1 *******
7020 DATA Beam=,BL-11,dia=,14,Ro=,0.008188
7030 DATA L=,3000,h=,240,b=,200,d=,188,Fc=,34
7040 DATA Compr=,1,Ro'=,0.002,d'=,0.15
7050 DATA Fl=,1,Bx=,1,Gx=,.3
7060 DATA Loading =,p,No of loads=,10
7070 DATA Loads
=,10.97,12.70,14.29,16.36,18.64,20.13,22.51,27.52,32.73,35.27
7080 DATA Deltas=,0.81,1.16,1.71,2.30,2.93,3.34,3.96,5.44,6.94,7.66
7090 DATA Eo = ,0.002,Es = ,200000
7100 REM ******* Case - 2 *******
7110 DATA Beam=,BN-12,dia=,18,Ro=,0.014
7120 DATA L=,2500,h=,240,b=,200,d=,188,Fc=,34
```

```
7130 DATA Compr=,1,Ro'=,0.002,d'=,0.15
7140 DATA Fl=,1,Bx=,1,Gx=,.3
7150 DATA Loading =,p,No of loads=,10
7160 DATA
Loads=,17.22,20.06,24.35,28.02,31.39,34.88,40.09,45.69,51.86,57.39
7170 DATA Deltas=,1.07,1.48,2.11,2.81,3.31,3.95,4.77,5.75,6.73,7.63
7180 DATA Eo = ,0.002,Es = ,200000
7190 REM ******* Case - 3 *******
7200 DATA Beam=,BM-13,dia=,18,Ro=,0.02
7210 DATA L=,2500,h=,240,b=,200,d=,188,Fc=,34
7220 DATA Compr=,1,Ro'=,0.002,d'=,0.15
7230 DATA Fl=,1,Bx=,1,Gx=,.3
7240 DATA Loading =,p,No of loads=,10
7250 DATA
Loads=,16.43,19.62,23.81,29.18,36.06,40.55,44.70,50.68,55.74,60.60
7260 DATA Deltas=,0.96,1.25,1.70,2.35,3.27,3.85,4.31,5.04,5.68,6.32
7270 DATA Eo = ,0.002,Es = ,200000
7280 REM ******* Case - 4 *******
7290 DATA Beam=,I-22-23,dia=,28.575,Ro=,0.02596
7300 DATA L=,3048,h=,381,b=,152.4,d=,325,fc=,24.5
7310 DATA Compr=,1,Ro'=,0.0,d'=,0.154
7320 DATA Fl=,1,Bx=,1,Gx=,.0323
7330 DATA Loading =,t,Distance=,762,No of loads=,15
7340 DATA Loads=,5.24,17.47,29.12,39.31,50.95,61.15,72.80,93.18
7350 DATA 116.47,139.77,160.15,182.00,203.83,227.12,250.42
7360 DATA Deltas=,0.134,0.301,0.543,0.835,1.170,1.387,1.905,2.540,3.440
7370 DATA 4.144,4.896,5.849,6.785,7.637,8.773
7380 DATA Eo = ,0.0015,Es = ,197000
7390 REM ******* Case - 5 *******
7400 DATA Beam=,II-7-12,Dia=,22.225,Ro=,0.015445
7410 DATA L=,3048,h=,381,b=,152.4,d=,325,Fc=,26.4
7420 DATA Compr=,1,Ro'=,0.0,d'=,0.154
7430 DATA Fl=,1,Bx=,1,Gx=,.0323
7440 DATA Loading =,t,Distance=,762,No of loads=,15
7450 DATA Loads=,5.24,17.47,29.12,39.31,50.95,61.15,72.80,93.18
7460 DATA 116.47,139.77,160.15,182.00,203.83,227.12,250.42
7470 DATA Deltas=,0.301,0.585,0.835,1.086,1.671,2.005,2.640,3.760,4.846
7480 DATA 5.982,7.102,8.272,9.483,10.778,12.199
7490 DATA Eo = ,0.0024,Es = ,199000
7500 REM ******* Case - 6 *******
7510 DATA Beam=,III-8-13,Dia=,22.225,Ro=,0.01559
7520 DATA L=,3048,h=,381,b=,152.4,d=,325,Fc=,25.2
7530 DATA Compr=,1,d'=,0.0,Ro'=,0.154
7540 DATA Fl=,1,Bx=,1,Gx=,.0323
7550 DATA Loading = ,t,Distance =,762,No of loads =,15
7560 DATA Loads=,5.24,17.47,29.12,39.31,50.95,61.15,72.80,93.18
7570 DATA 116.47,139.77,160.15,182.00,203.83,227.12,250.42
7580 DATA Deltas=,0.200,0.501,0.685,1.003,1.504,1.922,2.456,3.509,4.679
7590 DATA 5.899,6.885,8.105,9.274,10.561,12.165
7600 DATA Eo = ,0.00232,Es = ,204800
7610 REM ******* Case - 7 *******
7620 DATA Beam=,IV-20-21,Dia=,22.2,Ro=,0.01564
7630 DATA L=,3048,h=,381,b=,152.4,d=,325,Fc=,23.62
7640 DATA Compr=,1,Ro'=,0.0,d'=,0.154
7650 DATA Fl=,1,Bx=,1,Gx=,.0323
7660 DATA Loading=,t,Distance=,762,No of loads =,15
7670 DATA Loads =,5.24,17.47,29.12,39.31,50.95,61.15,72.80,93.18
7680 DATA 116.47,139.77,160.15,182.00,203.83,227.12,250.42
7690 DATA Deltas=,0.334,0.585,0.819,1.053,1.588,2.172,2.807,4.094,5.180
7700 DATA 6.350,7.687,9.274,10.695,12.667,13.619
7710 DATA Eo = ,0.0027,Es = ,178000
```

```
7720 REM ******* Case - 8 *******
7730 DATA Beam=,V-17-19,Dia=,19.05,Ro=,0.01128
7740 DATA L=,3048,h=,381,b=,152.4,d=,325,Fc=,25.66
7750 DATA Compr=,1,Ro'=,0.0,d'=,0.154
7760 DATA Fl=,1,Bx=,1,Gx=,.0323
7770 DATA Loading=,t,Distance =,762,No of loads=,15
7780 DATA Loads=,5.24,17.47,29.12,39.31,50.95,61.15,72.80,93.18
7790 DATA 116.47,139.77,160.15,182.00,203.83,227.12,250.42
7800 DATA Deltas=,0.317,0.585,0.752,1.203,1.838,2.506,3.242,4.746,6.099
7810 DATA 7.520,9.023,10.528,12.249,14.037,15.875
7820 DATA Eo = ,0.00352,Es = ,194000
7830 REM ******* Case - 9 *******
7840 DATA Beam=,VI-9-18,Dia=,19.05,Ro=,0.0113
7850 DATA L=,3048,h=,381,b=,152.4,d=,325,Fc=,25.7
7860 DATA Compr=,1,Ro'=,0.0,d'=,0.154
7870 DATA Fl=,1,Bx=,1,Gx=,.0323
7880 DATA Loading= ,t,Distance =,762,No of loads =,16
7890 DATA Loads=,5.24,17.47,29.12,39.31,50.95,61.15,72.80,93.18
7900 DATA 116.47,139.77,160.15,182.00,203.83,227.12,250.42,270.80
7910 DATA Deltas=,0.334,0.668,0.835,1.337,1.972,2.715,3.426,4.930,6.433
7920 DATA 8.021,9.608,11.363,13.368,15.541,17.880,20.888
7930 DATA Eo = ,0.00369,Es = ,195000
7940 REM ******* Case - 10 ******
7950 DATA Beam=,A1-4,Dia=,19.05,Ro=,0.01633
7960 DATA L=,6096,h=,304,b=,203,d=,257,Fc=,25.9
7970 DATA Compr=,1,Ro'=,0.01633,d'=,0.179
7980 DATA Fl=,1,Bx=,1,Gx=,.0323
7990 DATA Loading= ,u,No of loads =,1
8000 DATA Loads=,5.518
8010 DATA Deltas=,13.46
8020 DATA Eo = ,0.002,Es = ,200000
8030 REM ******* Case - 11 ******
8040 DATA Beam=,A2-5,Dia=,19.05,Ro=,0.01633
8050 DATA L=,6096,h=,304,b=,203,d=,257,Fc=,25.9
8060 DATA Compr=,1,Ro'=,0.007667,d'=,0.179
8070 DATA Fl=,1,Bx=,1,Gx=,.0323
8080 DATA Loading= ,u,No of loads =,1
8090 DATA Loads=,5.518
8100 DATA Deltas=,15.75
8110 DATA Eo = ,0.002,Es = ,200000
8120 REM ******* Case - 12 ******
8130 DATA Beam=,A3-6,Dia=,19.05,Ro=,0.01633
8140 DATA L=,6096,h=,304,b=,203,d=,257,Fc=,25.9
8150 DATA Compr=,1,Ro'=,0.0,d'=,0.179
8160 DATA Fl=,1,Bx=,1,Gx=,.0323
8170 DATA Loading= ,u,No of loads =,1
8180 DATA Loads=,5.518
8190 DATA Deltas=,17.01
8200 DATA Eo = ,0.002,Es = ,200000
8210 REM ******* Case - 13 ******
8220 DATA Beam=,B1-4,Dia=,15.88,Ro=,0.01676
8230 DATA L=,6096,h=,203,b=,152,d=,157,Fc=,20.8
8240 DATA Compr=,1,Ro'=,0.01676,d'=,0.293
8250 DATA Fl=,1,Bx=,1,Gx=,.0323
8260 DATA Loading= ,u,No of loads =,1
8270 DATA Loads=,1.562
8280 DATA Deltas=,23.4
8290 DATA Eo = ,0.002,Es = ,200000
8300 REM ******* Case - 14 ******
8310 DATA Beam=,B2-5,Dia=,15.88,Ro=,0.01676
8320 DATA L=,6096,h=,203,b=,152,d=,157,Fc=,20.8
```

```
8330 DATA Compr=,1,Ro'=,0.008381,d'=,0.293
8340 DATA Fl=,1,Bx=,1,Gx=,.0323
8350 DATA Loading= ,u,No of loads =,1
8360 DATA Loads=,1.562
8370 DATA Deltas=,24.9
8380 DATA Eo = ,0.002,Es = ,200000
8390 REM ******* Case - 15 ******
8400 DATA Beam=,B3-6,Dia=,15.88,Ro=,0.01676
8410 DATA L=,6096,h=,203,b=,152,d=,157,Fc=,20.8
8420 DATA Compr=,1,Ro'=,0.0,d'=,0.293
8430 DATA Fl=,1,Bx=,1,Gx=,.0323
8440 DATA Loading= ,u,No of loads =,1
8450 DATA Loads=,1.562
8460 DATA Deltas=,26.4
8470 DATA Eo = ,0.002,Es = ,200000
8480 REM ******* Case - 16 ******
8490 DATA Beam=,C1-4,Dia=,12.7,Ro=,0.01659
8500 DATA L=,6340,h=,127,b=,305,d=,102,Fc=,20.3
8510 DATA Compr=,1,Ro'=,0.01659,d'=,0.25
8520 DATA Fl=,1,Bx=,1,Gx=,.0323
8530 DATA Loading= ,u,No of loads =,1
8540 DATA Loads=,1.197
8550 DATA Deltas=,40.1
8560 DATA Eo = ,0.002,Es = ,200000
8570 REM ******* Case - 17 ******
8580 DATA Beam=,C2-5,Dia=,12.7,Ro=,0.01659
8590 DATA L=,6340,h=,127,b=,305,d=,102,Fc=,20.3
8600 DATA Compr=,1,Ro'=,0.008295,d'=,0.25
8610 DATA Fl=,1,Bx=,1,Gx=,.0323
8620 DATA Loading= ,u,No of loads =,1
8630 DATA Loads=,1.197
8640 DATA Deltas=,43.43
8650 DATA Eo = ,0.002,Es = ,200000
8660 REM ******* Case - 18 ******
8670 DATA Beam=,C3-6,Dia=,12.7,Ro=,0.01659
8680 DATA L=,6340,h=,127,b=,305,d=,102,Fc=,20.3
8690 DATA Compr=,1,Ro'=,0.0,d'=,0.25
8700 DATA Fl=,1,Bx=,1,Gx=,.0323
8710 DATA Loading= ,u,No of loads =,1
8720 DATA Loads=,1.197
8730 DATA Deltas=,47.75
8740 DATA Eo = ,0.002,Es = ,200000
8750 REM ******* Case - 19 ******
8760 DATA Beam=,D1-4,Dia=,12.7,Ro=,0.01659
8770 DATA L=,3810,h=,127,b=,305,d=,102,Fc=,20.1
8780 DATA Compr=,1,Ro'=,0.01659,d'=,0.25
8790 DATA Fl=,1,Bx=,1,Gx=,.0323
8800 DATA Loading= ,u,No of loads =,1
8810 DATA Loads=,3.343
8820 DATA Deltas=,11.94
8830 DATA Eo = ,0.002,Es = ,200000
8840 REM ******* Case - 20 ******
8850 DATA Beam=,D2-5,Dia=,12.7,Ro=,0.01659
8860 DATA L=,3810,h=,127,b=,305,d=,102,Fc=,20.1
8870 DATA Compr=,1,Ro'=,0.008295,d'=,0.25
8880 DATA Fl=,1,Bx=,1,Gx=,.0323
8890 DATA Loading= ,u,No of loads =,1
8900 DATA Loads=,3.343
8910 DATA Deltas=,14.22
8920 DATA Eo = ,0.002,Es = ,200000
8930 REM ******* Case - 21 ******
```

```
8940 DATA Beam=,D3-6,Dia=,12.7,Ro=,0.01659
8950 DATA L=,3810,h=,127,b=,305,d=,102,Fc=,20.1
8960 DATA Compr=,1,Ro'=,0.0,d'=,0.25
8970 DATA Fl=,1,Bx=,1,Gx=,.0323
8980 DATA Loading= ,u,No of loads =,1
8990 DATA Loads=,3.343
9000 DATA Deltas=,17.78
9010 DATA Eo = ,0.002,Es = ,200000
9020 REM ******* Case - 22 ******
9030 DATA Beam=,E1-4,Dia=,9.5,Ro=,0.01578
9040 DATA L=,5334,h=,76,b=,305,d=,59,Fc=,20.6
9050 DATA Compr=,1,Ro'=,0.01578,d'=,0.25
9060 DATA Fl=,1,Bx=,1,Gx=,.0323
9070 DATA Loading= ,u,No of loads =,1
9080 DATA Loads=,0.5548
9090 DATA Deltas=,59.44
9100 DATA Eo = ,0.002,Es = ,200000
9110 REM ******* Case - 23 ******
9120 DATA Beam=,E2-5,Dia=,9.5,Ro=,0.01578
9130 DATA L=,5334,h=,76,b=,305,d=,59,Fc=,20.6
9140 DATA Compr=,1,Ro'=,0.00789,d'=,0.25
9150 DATA Fl=,1,Bx=,1,Gx=,.0323
9160 DATA Loading= ,u,No of loads =,1
9170 DATA Loads=,0.5548
9180 DATA Deltas=,55.9
9190 DATA Eo = ,0.002,Es = ,200000
9200 REM ******* Case - 24 ******
9210 DATA Beam=,E3-6,Dia=,9.5,Ro=,0.01578
9220 DATA L=,5334,h=,76,b=,305,d=,59,Fc=,20.6
9230 DATA Compr=,1,Ro'=,0.0,d'=,0.25
9240 DATA Fl=,1,Bx=,1,Gx=,.0323
9250 DATA Loading= ,u,No of loads =,1
9260 DATA Loads=,0.5548
9270 DATA Deltas=,63
9280 DATA Eo = ,0.002,Es = ,200000
9290 REM ******* Case - 25 ******
9300 DATA Beam=,A1,Dia=,15.9,Ro=,0.010134
9310 DATA L=,6096,h=,304,b=,152.4,d=,259,Fc=,25.4
9320 DATA Compr=,1,Ro'=,0.0,d'=,0.154
9330 DATA Fl=,1,Bx=,2,Gx=,.247
9340 DATA Loading= ,u,No of loads =,1
9350 DATA Loads=,6.42
9360 DATA Deltas=,31.75
9370 DATA Eo = ,0.002,Es = ,200000
9380 REM ******* Case - 26 ******
9390 DATA Beam=,B1,Dia=,15.9,Ro=,0.010134
9400 DATA L=,6096,h=,304,b=,152.4,d=,259,Fc=,26.8
9410 DATA Compr=,1,Ro'=,0.005067,d'=,0.154
9420 DATA Fl=,1,Bx=,2,Gx=,.247
9430 DATA Loading= ,u,No of loads =,1
9440 DATA Loads=,6.44
9450 DATA Deltas=,29.21
9460 DATA Eo = ,0.002,Es = ,200000
9470 REM ******* Case - 27 ******
9480 DATA Beam=,C1,Dia=,15.9,Ro=,0.010134
9490 DATA L=,6096,h=,304,b=,152.4,d=,259,Fc=,24.4
9500 DATA Compr=,1,Ro'=,0.010134,d'=,0.154
9510 DATA Fl=,1,Bx=,2,Gx=,.247
9520 DATA Loading= ,u,No of loads =,1
9530 DATA Loads=,6.41
9540 DATA Deltas=,27.91
```

```
9550 DATA Eo = ,0.002,Es = ,200000
9560 REM ******* Case - 28 ******
9570 DATA Beam=,D1,Dia=,22.2,Ro=,0.0207
9580 DATA L=,6096,h=,304,b=,152.4,d=,246,Fc=,25.4
9590 DATA Compr=,1,Ro'=,0.0,d'=,0.154
9600 DATA Fl=,1,Bx=,4,Gx=,.26
9610 DATA Loading= ,u,No of loads =,1
9620 DATA Loads=,11.74
9630 DATA Deltas=,29.92
9640 DATA Eo = ,0.002,Es = ,200000
9650 REM ******* Case - 30 ******
9660 DATA Beam=,E1,Dia=,15.9,Ro=,0.01053
9670 DATA L=,4267,h=,304,b=,152.4,d=,249.2,Fc=,29.4
9680 DATA Compr=,1,Ro'=,0.0,d'=,0.154
9690 DATA Fl=,1,Bx=,2,Gx=,.255
9700 DATA Loading= ,u,No of loads =,1
9710 DATA Loads=,12.29
9720 DATA Deltas=,12.45
9730 DATA Eo = ,0.002,Es = ,200000
9740 REM ******* Case - 30 ******
9750 DATA Beam=,F1,Dia=,15.9,Ro=,0.0167
9760 DATA L=,6096,h=,203,b=,152.4,d=,157.2,Fc=,29.4
9770 DATA Compr=,1,Ro'=,0.0,d'=,0.154
9780 DATA Fl=,1,Bx=,2,Gx=,.324
9790 DATA Loading= ,u,No of loads =,1
9800 DATA Loads=,3.8
9810 DATA Deltas=,50.55
9820 DATA Eo = ,0.002,Es = ,200000
9830 REM ******* Case - 31 ******
9840 DATA Beam=,XX,Dia=,15,Ro=,0.0047434
9850 DATA L=,4000,h=,440,b=,300,d=,400,Fc=,20
9860 DATA Compr=,1,Ro'=,0.00,d'=,0.25
9870 DATA Fl=,1,Bx=,1,Gx=,.324
9880 DATA Loading= ,u,No of loads =,1
9890 DATA Loads=,3.8
9900 DATA Deltas=,50.55
9910 DATA Eo = ,0.002,Es = ,200000
```

Input values of Y for X values from 0.2 to 1.20 (Line Number 145-151)
This worksheet calculates

a1, b1, and c1 for Curve-1 : Y = aX^3+bX^3+cX
m1 for Curve-2 : Y=mX + C
a2, b2, c2 and d2 for Curve-3 : Y = aX^4+bX^3+cX^2+dX
m2 for Curve-4 : Y=mX+C

Curve-1 : X from 0.2 to 0.4

Curve-2 : X from 0.4 to 0.6 (straight)

Curve-3 : X from 0.6 to 1.2

Curve-4 : X from 1.2 to 2.0 (straight)

x	y		y3	y4	y5
0.20	0		0.8343	0.5712	0.9653
0.30	0.0129				
0.40	0.1646				
0.60	0.8343	b1	b2	b4	b5
0.80	1.4055				
1.20	1.7996	0.1	0.2	0.2	0.6
2.00	1.7858				

Curve-2

a1	**b1**	**c1**	**m1**
143.13	**-14.69**	**1.3275**	**3.3485**

Curve-4

a2	**b2**	**c2**	**d2=m2**
3.5197	**-3.9081**	**-1.8217**	**-0.0172**

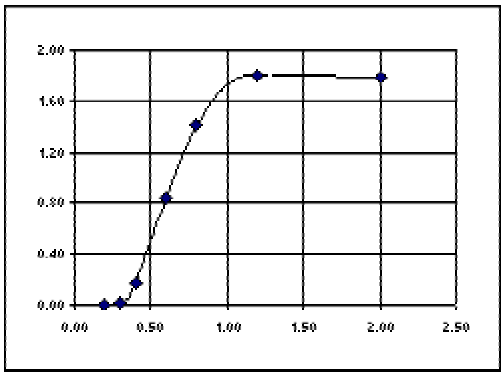

	0.2-0.4 curve	0.4-0.6 straight	0.6-1.2 curve	1.2-2..0 straight		
x	y1	y2	y3	y4	x	y
0.00	0.000	0.000	0.000	0.000	0.00	0.000
0.02	0.000	0.000	0.000	0.000	0.02	0.000
0.04	0.000	0.000	0.000	0.000	0.04	0.000
0.06	0.000	0.000	0.000	0.000	0.06	0.000
0.08	0.000	0.000	0.000	0.000	0.08	0.000
0.10	0.000	0.000	0.000	0.000	0.10	0.000
0.12	0.000	0.000	0.000	0.000	0.12	0.000
0.14	0.000	0.000	0.000	0.000	0.14	0.000
0.16	0.000	0.000	0.000	0.000	0.16	0.000
0.18	0.000	0.000	0.000	0.000	0.18	0.000
0.20	0.000	0.000	0.000	0.000	0.20 0	0.000
0.22	0.000	0.000	0.000	0.000	0.22	0.000

0.24	0.002	0.000	0.000	0.000	0.24		0.002
0.26	0.003	0.000	0.000	0.000	0.26		0.003
0.28	0.007	0.000	0.000	0.000	0.28		0.007
0.30	0.013	0.000	0.000	0.000	0.30	0.0129	0.013
0.32	0.023	0.000	0.000	0.000	0.32		0.023
0.34	0.041	0.000	0.000	0.000	0.34		0.041
0.36	0.068	0.000	0.000	0.000	0.36		0.068
0.38	0.108	0.000	0.000	0.000	0.38		0.108
0.40	0.165	0.000	0.000	0.000	0.40	0.16	0.165
0.42	0.000	0.232	0.000	0.000	0.42		0.232
0.44	0.000	0.299	0.000	0.000	0.44		0.299
0.46	0.000	0.366	0.000	0.000	0.46		0.366
0.48	0.000	0.432	0.000	0.000	0.48		0.432
0.50	0.000	0.499	0.000	0.000	0.50		0.499
0.52	0.000	0.566	0.000	0.000	0.52		0.566
0.54	0.000	0.633	0.000	0.000	0.54		0.633
0.56	0.000	0.700	0.000	0.000	0.56		0.700
0.58	0.000	0.767	0.000	0.000	0.58		0.767
0.60	0.000	0.834	0.000	0.000	0.60	0.8343	0.834
0.62	0.000	0.000	0.901	0.000	0.62		0.901
0.64	0.000	0.000	0.965	0.000	0.64		0.965
0.66	0.000	0.000	1.028	0.000	0.66		1.028
0.68	0.000	0.000	1.089	0.000	0.68		1.089
0.70	0.000	0.000	1.147	0.000	0.70		1.147
0.72	0.000	0.000	1.204	0.000	0.72		1.204
0.74	0.000	0.000	1.258	0.000	0.74		1.258
0.76	0.000	0.000	1.310	0.000	0.76		1.310
0.78	0.000	0.000	1.359	0.000	0.78		1.359
0.80	0.000	0.000	1.406	0.000	0.80	1.4055	1.406
0.82	0.000	0.000	1.449	0.000	0.82		1.449
0.84	0.000	0.000	1.491	0.000	0.84		1.491
0.86	0.000	0.000	1.529	0.000	0.86		1.529
0.88	0.000	0.000	1.565	0.000	0.88		1.565
0.90	0.000	0.000	1.598	0.000	0.90		1.598
0.92	0.000	0.000	1.628	0.000	0.92		1.628
0.94	0.000	0.000	1.656	0.000	0.94		1.656
0.96	0.000	0.000	1.680	0.000	0.96		1.680
0.98	0.000	0.000	1.703	0.000	0.98		1.703
1.00	0.000	0.000	1.722	0.000	1.00		1.722
1.02	0.000	0.000	1.739	0.000	1.02		1.739
1.04	0.000	0.000	1.754	0.000	1.04		1.754
1.06	0.000	0.000	1.766	0.000	1.06		1.766
1.08	0.000	0.000	1.777	0.000	1.08		1.777
1.10	0.000	0.000	1.785	0.000	1.10		1.785
1.12	0.000	0.000	1.791	0.000	1.12		1.791
1.14	0.000	0.000	1.795	0.000	1.14		1.795
1.16	0.000	0.000	1.798	0.000	1.16		1.798
1.18	0.000	0.000	1.799	0.000	1.18		1.799
1.20	0.000	0.000	1.800	0.000	1.20	1.7996	1.800
1.22	0.000	0.000	0.000	1.799	1.22		1.799
1.24	0.000	0.000	0.000	1.799	1.24		1.799
1.26	0.000	0.000	0.000	1.799	1.26		1.799
1.28	0.000	0.000	0.000	1.798	1.28		1.798

1.30	0.000	0.000	0.000	1.798	1.30		1.798
1.32	0.000	0.000	0.000	1.798	1.32		1.798
1.34	0.000	0.000	0.000	1.797	1.34		1.797
1.36	0.000	0.000	0.000	1.797	1.36		1.797
1.38	0.000	0.000	0.000	1.796	1.38		1.796
1.40	0.000	0.000	0.000	1.796	1.40		1.796
1.42	0.000	0.000	0.000	1.796	1.42		1.796
1.44	0.000	0.000	0.000	1.795	1.44		1.795
1.46	0.000	0.000	0.000	1.795	1.46		1.795
1.48	0.000	0.000	0.000	1.795	1.48		1.795
1.50	0.000	0.000	0.000	1.794	1.50		1.794
1.52	0.000	0.000	0.000	1.794	1.52		1.794
1.54	0.000	0.000	0.000	1.794	1.54		1.794
1.56	0.000	0.000	0.000	1.793	1.56		1.793
1.58	0.000	0.000	0.000	1.793	1.58		1.793
1.60	0.000	0.000	0.000	1.793	1.60		1.793
1.62	0.000	0.000	0.000	1.792	1.62		1.792
1.64	0.000	0.000	0.000	1.792	1.64		1.792
1.66	0.000	0.000	0.000	1.792	1.66		1.792
1.68	0.000	0.000	0.000	1.791	1.68		1.791
1.70	0.000	0.000	0.000	1.791	1.70		1.791
1.72	0.000	0.000	0.000	1.791	1.72		1.791
1.74	0.000	0.000	0.000	1.790	1.74		1.790
1.76	0.000	0.000	0.000	1.790	1.76		1.790
1.78	0.000	0.000	0.000	1.790	1.78		1.790
1.80	0.000	0.000	0.000	1.789	1.80		1.789
1.82	0.000	0.000	0.000	1.789	1.82		1.789
1.84	0.000	0.000	0.000	1.789	1.84		1.789
1.86	0.000	0.000	0.000	1.788	1.86		1.788
1.88	0.000	0.000	0.000	1.788	1.88		1.788
1.90	0.000	0.000	0.000	1.788	1.90		1.788
1.92	0.000	0.000	0.000	1.787	1.92		1.787
1.94	0.000	0.000	0.000	1.787	1.94		1.787
1.96	0.000	0.000	0.000	1.786	1.96		1.786
1.98	0.000	0.000	0.000	1.786	1.98		1.786
2.00	0.000	0.000	0.000	1.786	2.00	1.7858	1.786

x	y		
		143.125	a1
0.20	**0**	-14.688	b1
0.30	**0.0129**	1.328	c1
0.40	**0.1646**	3.349	m1
0.60	**0.8343**	3.520	a2
0.80	**1.4055**	-3.908	b2
1.20	**1.7996**	-1.822	c2
2.00	**1.7858**	-0.017	d2=m2

0.2	0.3	0.4	0.6	0.8	1.2	2.0
0.0000	0.0129	0.1646	0.8343	1.4055	1.7996	1.7858

a1	b1	c1	m1	a2	b2	c2	d2=m2
143.125	-14.6875	1.3275	3.3485	3.5197	-3.9081	-1.8217	-0.0172